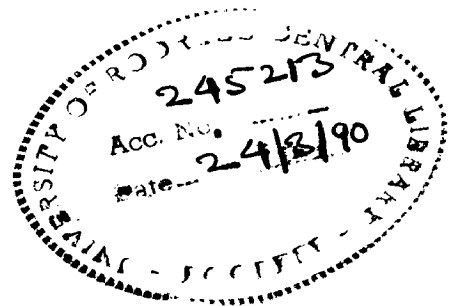# MODELLING AND ANALYSIS OF NEURONAL NETWORK

A DISSERTATION

Submitted in partial fulfilment of the
requirements for the award of the degree
of
MASTER OF ENGINEERING
in
ELECTRICAL ENGINEERING
(Measurement and Instrumentation)

By

GURULINGAPPA M. PATIL

DEPARTMENT OF ELECTRICAL ENGINEERING
UNIVERSITY OF ROORKEE
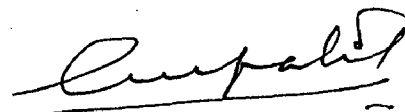**ROORKEE-247 667**
(INDIA)

JANUARY, 1990

DEDICATED TO

MY PARENTS

CANDIATE'S DECLARATION

I hereby certify that the work which is being presented in the Thesis entitled "MODELLING AND ANALYSIS OF NEURONAL NETWORK" in partial fulfilment of the requirements for the award of the degree of Master of Engineering in Electrical Engineering (MEASUREMENT AND INSTRUMENTATION) submitted in the Department of Electrical Engineering of the University is an aunthetic record of my own work, carried out during a period from July, 1989 to January, 1990 under the supervision of Dr. S.C.Saxena and Dr. D.S.Chitore.
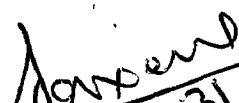
The matter embodied in this thesis has not been submitted by me for the award of any other degree.
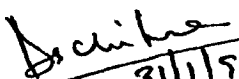
Candidate's Signature

(GURULINGAPPA M. PATIL)

This is to certify that the above statement made by the candidate is correct to the best of our knowledge.

Dr. S.C.SAXENA
Professor,
Electrical Engineering
Department,
University of Roorkee,
Roorkee.

Dr.D.S.CHITORE
Reader,
Electrical Engineering
Department,
University of Roorkee,
Roorkee.

ACKNOWLEDGEMENTS

The author expresses his deep sense of gratitude and indebtness to Dr. S.C.Saxena, Professor, Department of Electrical Engineering and Dr. D.S.Chitore, Reader, Department of Electrical Engineering for the constant encouragement, systematic guidance and keen interest throughout the completion of this dissertation work. The author will in particular, long cherish the fruitful and enjoyable discussions he had with them, on many varied aspects of this work. Also, he is highly indebted for all the help and expert guidance they had provided on the practical problems that came up from time to time.

The author is highly grateful to Dr. R.B.Saxena, Professor and Head of Electrical Engineering Department, for providing-adequate facilities to carryout the experimental work.
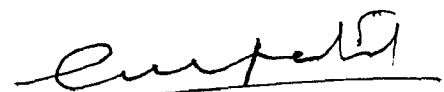
The author expresses his sincere thanks to Sri Harish and Sri Manju, for helping in many ways.

The author is thankful, for the efforts put in by the technicians of various laboratories, and workshops, particularly, Sri H.D.Sharma, Sri Sadiram of Biomedical Instrumentation Laboratory, and Sri C.P.Kansal, Sri Kapoor and Sri Bhattacharya.

The author is also thankful to Sri D.P.Tyagi for the neat typing.

ROORKEE

JANUARY   , 1990.

(GURULINGAPPA M. PATIL)

C O N T E N T S

*****

CHAPTER - I

INTRODUCTION

1.1 MODELLING :

Even though physicists believe that the physical world obeys the laws of physics, they are also aware that the mathematical descriptions of some physical situations are too complex to permit solutions. For example, if we tore a small corner off a page and let it fall to the floor, it would go through various gyrations. It's path would be determined by the laws of physics, but it would be almost impossible to write the equations describing this path.

Similarly, while the laws of physics are involved in all aspects of body functions, each situation is so complex that it is almost impossible to predict the exact behaviour from our knowledge of physics. Nevertheless, a knowledge of the laws of physics will help our understanding of physiology in health and diseases.

Sometimes in trying to understand a physical phenomenon we simplify it by selecting it's main features and ignoring those that we believe are less important. The engineer has been trained to make approximations until the essence of the system can be represented by a simplified Model. In trying to understand the physical aspects of the body, we often resort to analogies (i.e. Modelling). Just as philosophers teach their folloers by parables, physicist often teach and think by analogy. It is to be emphasized that analogies are never perfect. For example,

in many ways the eye is analogous to a camera; however, the analogy is poor when the film, which must be developed and replaced is compared to the retina, the light detector of the eye.

Many of the analogies used by physicists employ models. Model making is common in scientific activities. A famous nineteenth centuary physicist Lord Kelvin, said '' I never satisfy myself until I can make a model of a thing. If I can make a model I can understand it''. Naturally analogies have their limitations.

While many of the control mechanisms of the nervous system and of the body are not yet understood, various disceases have been found to be directly related to the failure of these mechanisms. For example as the body grows, it's cells keep increasing in number until it reaches adult size, and then the body remains more or less constant in size under some type of feedback control. Occasionally some cells do not respond to this control and become tumours. Hence it is hoped that modelling and analysis of human systems will help investigate and yield insight into the inner workings of the unsimplified organism.

Models could be of various types such as mathematical, chemical, electrical, electronic etc. Every type of modelling technique has some advantages and disadvantages and their selection depend upon the requirements and the objectives. Biological systems usually require complex equations for their representations in the mathematical format. Chemical models require large space,

more cost and also are not convenient in varying its parameters for observing their effects on overall systems. The electrical, electronic models are small in size, less costly and convenient in handling.Any type of nonlinearity can be included with reasonable accuracy. Hence electrical models are generally resorted to, for simulation of the complex human systems with very close correlation to the real.

1.2 STRUCTURE OF NERVOUS TISSUE :

In the nervous systems structure and function are so closely related that it is difficult to understand one without knowing some thing about the other. Before beginning a discussion of function, therefore, it will be necessary to develop some basic neuroanotomical concepts and terminology. We shall describe the basic element of the nervous system, the neuron, consider the anatomical relationships between neurons and discuss the overall scheme of organisation to which groups of neurons within a nervous system conform.

The humain brain contains a complicated network of perhaps ten billion highly specialized cells called neurons or nerve cells. The term neuron is used to describe the nerve cell (cell body, soma) and it's processes,the dendrites and the axon (axis cylinder, nerve fibre) [Fig. 1.1]. The nutrition of the axon and the preservation of it's structure depend on it's intact connection with it's cell body [3].

Neurons vary considerably in shape and size in different parts of the body. Although no two neurons have exactly the same

Dendrites

Cell body
Axon hillock

Axon
Axon collateral

Medullary sheath

Node of Ranvier

Nonmyelinated terminal
arborizations
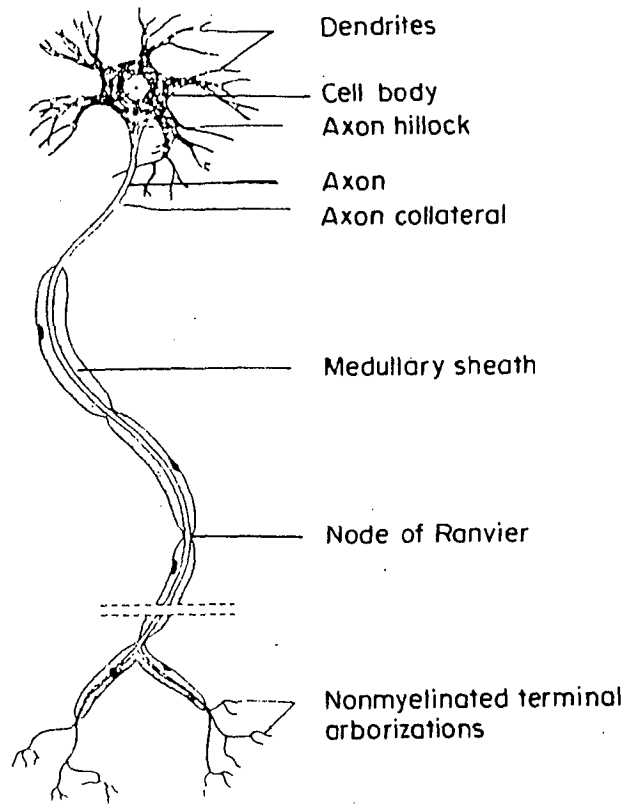
FIG.1·1 Schematic diagram of a neuron

Dendrites

Dendrites

Nucleus

Soma

Axon

Axon branch

Axo-dendritic
synapse

Axons

Axon

Axo-somatic
synapse

Nucleus

Soma

Dendrites

50 μ
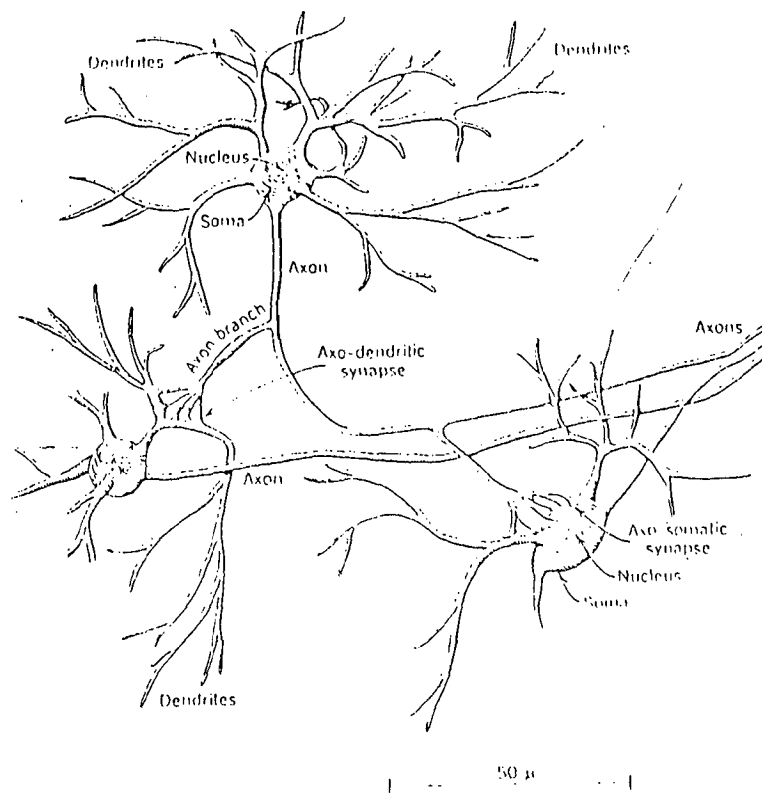
FIG.1·2 Three neurons interconnected

structure, fortunately they do share certain features that are significant for the neurophysiologist. Like other cells, the neuron is bounded by a thin membrane (the plasma membrane) and has a cell body (Soma). Projecting from the Soma are a number of extensions of the cell known as the dendrites and the axon. Figure 1.2 illustrates three neighbouring cells with important parts labeled. Generally only a single axon or nerve fibre arises from the part of the Soma (cell body), called the axon hillock, but as shown in the Figure 1.1, this axon may give off side branches and characteristically divides up into a number of smaller branches, referred to as terminal arborization just before terminating. As a rule, several or perhaps many dendrites arise from the cell body and then branch again and again to form a complicated tree like structure known, in fact, as the dendritic tree. The dimensions of a neuron vary greatly from one to the next, but, to give a general idea of size, the cell body is roughly 30 microns across (1 micron = 10^{-6} meter), and dendrites are perhaps 200 or 300 microns long. It is the length of the axon which is subject to the greatest variation from one nerve cell to the next, for axons may be from perhaps 50 microns to several meters long [5].

Nerve cells are not isolated but rather are interconnected in a very characteristic way. Special points of contact between neurons called synapses are of particular importance, for it is at the synapse that information flows from one nerve cells to the next. Also shown in Figure 1.2 is the way in which nerve cells

come into contact with each other. Typically, the axon of one nerve cell forms a synapse with either the cell body or dendrites of other neurons. Thus there are two principal types of synapses, axo-dendritic (axon with dendrite) and axo-somatic (axon with cell body) as shown in Fig. 1.2. Virtually all of the surface of a neuron's_Soma and dendrites is provided with axon terminals, so much so that the somatic and dendritic membranes are literally encrusted with synaptic endings [13]. Thus the anatomical basis for the main channels of communication between neurons is clear: and axon branch from one nerve cell makes synaptic contact with a dendrite or cell body of another neuron. A narrow space about 200 to 300 $\overset{o}{A}$ wide (1 $A^o = 10^{-10}$ meter) separates the presynaptic membrane (the axon terminal adjacent to the dendrite) from the postsynaptic membrane (dendritic part of the synapse) ; this space is known as the synaptic cleft [11].

Because neurons have synaptic connections with one another, they form neurol circuits, and the properties of these circuits determine the behaviour of the nervous system and thus of the organism. In addition to neurons, there are of course, other types of cells in the brain. As elsewhere, we find blood vessels and a certain amount of connective tissue, particularly on the brain surfaces; but the most conspicuous class of cells aside from the neurons is the neuroglia or glia cells. Nearly all the space in the nervous system which is not taken up by the nerve cells themselves is occupied by the glia. Neuroglia provides support, structural and metabolic for the extraordinarily diffuse

and delicate neurons. Because the entire functioning of the
nervous system depends on countless minute connections between
nerve cells, it is vital that the complicated neural circits
have some sort of metabolic protection and mechanical stabiliz-
ation, a role fulfilled admirably by the glia [4].

The brain then, is an immense number of spidery nerve
cells interconnected in a complex net and embedded in a suppor-
ting and protecting meshwork of neuroglia. Dendrites spring from
the neuron cell body, branch profusely, and along with the Soma
receive a large number of axon terminals making it possible for
a single nerve cell to gather information from hundreds of others.
Further more, cell bodies are collected into groups, the nuclei
and these in turn into clusters. Running back and forth between
nuclei or between collections of nuclei are fiber tracts, the
main channels of communications between one part of the brain
and another. Altogether, these structures are arranged in an
orderly way to form the brain of the animal and to provide the
anatomical basis for neural function [3].

1.3 FUNCTIONS OF NEURON :

Any nervous system, mammalian or otherwise, is composed
of discrete units called neurons. There are some 10^{10} neurons in
the human central nervous system consisting of the brain and
spinal cord. The nervous system can be divided into two parts-
the central nervous system and the autonomic nervous system.
The central nervous system consists of the brain, the spinal
cord and the paripheral nerves- nerve fibers (neurons) that

transmit sensory information to the brain or spinal cord (afferent nerves) and nerve fibers that transmit information from the brain or spinal cord to the appropriate museles and glands (efferent nerves) [8]. The autonomic nervous system controls various internal organs such as the heart, intestines, and glands. The control of the autonomic nervous system is essentially involuntary.

The basic structural unit of the nervous system is the neuron, a nerve cell specialized for the reception, interpretation, and transmission of electrical messages. There are many types of neurons. Basically, a neuron consists of a cell body that receives electrical messages from other neurons through contacts called synapses located on the dendtrites- axodendritic-synapses or on the cell body, axosomatic synapses.

A highly simplified representation of the five components of a typical neuron is shown in the Figure 1.3 below. The dendrites, axon, and out going collateral branches can be visualized as extremely fine insulated conductors that are immersed in salt water. The conductors carry electrical signals that are converted into chemical transmitters at the synaptic junction termination of each collateral branch. In figure all of the incoming junctions occur on dendrites ; (these are called axodendritic synapses). Incoming junctions can also occur directly on the neuron Soma ; (these are called axosomatic synapses). In either case the chemical transmitter diffuses across the synaptic junction, tending to excite (+ sign in Figure 1.3) or inhibit (- sign) an electrical
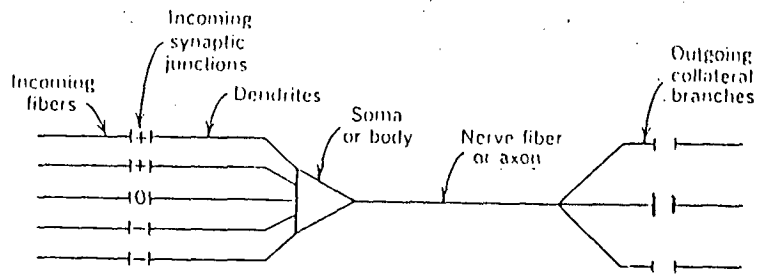
FIG. I·3 A highly simplified representatio of a neuron

(a)
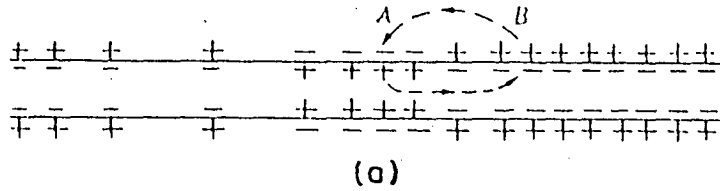
FIG. I·4 Local circuit propagation (unmyelinated nerve)

(b)
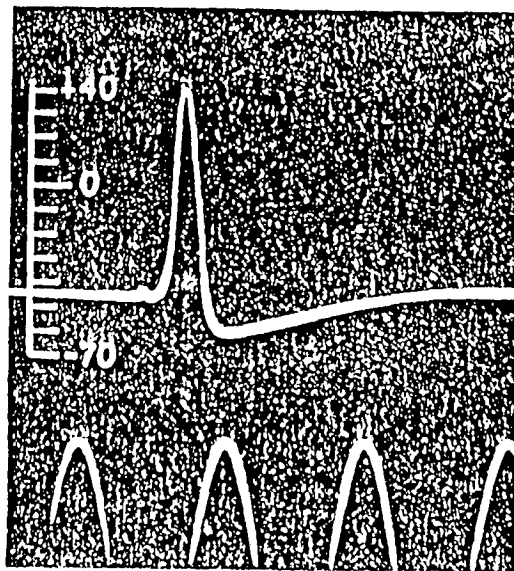
FIG. I·4 Action potential recorded between inside and outside of axon

[Hodgkin, A. L., and Huxley, A. F. (1945)]

discharge in the succeeding neuron. A hypothetical neural junction which has not been experimentally identified is indicated by the O sign. The effectiveness of the chemical transmitters is modified by chemical agents in the interstitial fluid [9].

The dendrites are the parts of the neuron specialized for receiving information from stimuli or from other cells. The dendrite has certain properties which specialize it for receiving the information transmitted along the axon; often, in fact, at the dendrite, nerve impulse frequency is translated back into a depolerization similar to the one which originally generated the axonal nerve impulses.

The Soma can integrate the information contained in arriving nerve impulses, and responds to the algebreic summation of incoming messages ; it is symbolized by a triangle that points in the direction of signal flow. If the stimuli are strong enough, the nerve impulse originates from axon hillock region of the Soma, and the neuron transmits an electrical signal outward along a fiber called an axon.

A nerve biber (axon) is simply the long process (is very long in man, from the toes to the base of the spinal cord) of a neurone; it's only function is to conduct the nerve impulse. Experimentally the fiber can be stimulated at any accessible point on it's course; the nerve impulse setup at the point of stimulation travels just as readily centrally as distally. Under natural conditions the nerve impulse is usually generated in the nerve cell and travels along the axon. The nerve impulse (also known

as the action-potential) propogates along the axon and is the major method of transmission of signals within the body. The stimulation may be caused by various physical and chemical stimuli, such as heat, cold, light, sound, and odours. If the stimulation is electrical, only about 20 mV across the membrane is needed to initiate the action potential [6].

1.4 CHARACTERISTICS OF NEURON :

1.4.1 Resting Nerve-Membrane Potential :

The surface membrane of the nerve cell and it's axon separates the intracellular fluid from the extracellular fluid which have widely different ionic compositions. Inside the neuron the cytoplasm is rich in potassium (110 - 170 mMol/litre) but low in chloride and sodium; the reverse obtains in extra-cellular fluid. The protoplasm of nerve cells contains between 30 and 50 times as many potassium ions, eight to ten times fewer sodium ions, and 50 times fewer chlorine ions as does the extra-cellular fluid.

In a state of rest there is a difference in potential of the order of 60 to 90 mV, due to the presence of more negative ions on the inside of the membrane then on the outside, the cell surface being electrically positive with respect to the proto-plasm. This potential difference is called the resting-membrane potential.

If a microelectrode is inserted through the cell membrane the potential of this electrode may be measured with reference to a second electrode in the external fluid medium. Such a procedure

has shown that the interior of the axon (or nerve cell body) is some 60 to 90 mV negative with respect to the exterior. The cell membrane is said to be polarized [11].

In the state of physiological rest the diffusion of positively charged potassium ions from protoplasm to the external fluid lends a possitive charge to the outer surface of the membrane, and a negative charge to the inner one.

It has also been established that an increased concentration of potassium ions in the external medium and consequently, a reduction of the difference in the concentration of these ions on both sides of the membrane lead to a drop of the resting potential, and it has been noted that within a certain range of concentrations the changes show a clear quantitative coincidence with those calculated from the formula.

The most important direct evidence in favour of these conjectures, however, was obtained by Hodgkin and his co-workers (1962) in experiments [24,6] with substituting saline solutions for protoplasm in the giant nerve fibres of squid. These experiments have shown that the concentration gradient of potassium ions is really the principal factor determining the value of the resting potential of a nerve fibre.

Apart from potassium ions, sodium ions diffusing into protoplasm from the extracellular fluid, where their concentration is high, also give rise to a resting potential. The diffusion is largely hampered by the low permeability of the membrane to sodium at rest. Nevertheless, in diffusing through the membrane sodium

ions transfer their positive charges into the protoplasm which somewhat reduces the value of the resting potential produced by the diffusion of potassium ions out of the cell,which is why the resting potential of most nerve cells and fibres is not 90 mV, as it would be expected if the potential were produced exclusively by potassium ions, but only between 60 and 70 mV.

Thus, the value of the resting potential of nerve fibres and cells is determined by the ratio between the positively charged potassium ions diffusing outward from the cell per unit time and the positively charged sodium ions diffusing in the opposite direction. The higher the ratio the greater is the resting potential,and vice versa.

The resting cell membrane is relatively impermeable to sodium. There is a sodium-pump mechanism whereby sodium which leaks into the cell is actively extruded by cellular metabollic processes which furnish the required energy. Because of the effective impermeability of the resting nerve fibre membrane to sodium and because the cell contains non diffusible protein anions the potassium and chloride ions which are diffusible arrange them-selves on either side of the cell membrane, according to the Donnan equilibrium [5] ;

$$\frac{[K^+]_i}{[K^+]_o} = \frac{[Cl^-]_o}{[Cl^-]_i}$$

where o and i stand for the ion concentrations outside and inside of the membrane.

In such a system the membrane potential is given by the Nernst's equation.

$$E = \frac{RT}{nF} \ln \frac{[K^+]_o}{[K^+]_i}$$

where, R = the 'gas' constant = 8.316 Joules/degree.

T = absolute temperature.

n = valency of the ion (unity in this case).

F = Faraday = 96, 500 coulombs.

At a temperature of $18^\circ C$ this equation simplifies to :

$$E_{(volts)} = \frac{8.316 \times 291}{96, 500} \times 2.3 \, \log_{10} \frac{[K^+]_o}{[K^+]_i}$$

$$E = 0.058 \, \log_{10} \frac{[K^+]_o}{[K^+]_i}$$

$$E = 58 \, \log_{10} \frac{[K^+]_o}{[K^+]_i} \quad mV.$$

at $38^\circ C$

$$E = 61.5 \, \log_{10} \frac{[K^+]_o}{[K^+]_i} \quad mV.$$

1.4.2   Excitation - The Spike or Action Potential and Impulse
Propagation :

The nerve impulse is a complicated physico-chemical event which is transmitted by nerve fibres. It involves an alteration in electrical state.

When a nerve is stimulated electrically it propogates a nerve impulse and the conduction of such a nerve impulse along the axon is associated with an action potential. This can be measured after suitable amplification as a potential difference longitudinally distributed along the nerve fibre. Using surface electrodes, it can be shown that as the action potential reaches any point on the axon the surface at that particular site becomes negative with respect to a resting part of the axon. We have seen that in resting conditions the external surface of the membrane is positive with respect to the interior of the fibre. Direct recording by intracellular electrodes (Hodgkin and Huxley) showed that the membrane potential is reversed in sign during the action potential [24,11], the interior of the fibre becoming positive with respect to the exterior as shown in Figure 1.4a.

The explanation of this finding has been given by Hodgkin and his colleagues with the onset of activity in the nerve at any one point, there occurs a large (500 x) transient increase in the permeability of the nerve membrane to sodium, so that the relative permeability of the fibre to potassium becomes temporarily small [24,6]. As a result the membrane potential transiently approaches the equilibrium potential for sodium which would be

$$E_{Na} = 58 \log \frac{[Na^+]_o}{[Na^+]_i}$$

$$= 58 \log \frac{10}{1} = + 58 \text{ mV}$$

(outside negative with respect to inside).

nce the electrode in the cell interior records a change of
tential from - 70 mV to, say, + 40 mV, and this accounts for
e upstroke of the spike which is about 110 mV in height
ig. 1.4b].

The rise in sodium permeability is, however, extremely
ort-lived and it is quickly followd by a rise in potassium
rmeability so that within 0.3 m sec. of threshold excitation
leaves the fibre faster than Na^+ enters. This restores the
sting membrane potential at the site of excitation and the
ore is once more responsive to further stimulation [12].

Threshold electrical stimulation of a nerve initiates a
pagated nerve impulse. The conduction of the impulse is
ociated with the passage of an action potential along the
n. The propagation of the impulse is effected by electrical
rents which flow between the active area of the nerve and the
ctive regions ahead of the nerve impulse. Thus the passage
the nerve impulse is accomplished by the reversed potential
the stimulated region causing ion movement, as shown by the
ows in Fig. 1.5, which inturn depolarizes the region to the
ht [6,8].

When a weak current is briefly applied to the nerve
assive redistribution of ions across the membrane causes a
nge of potential. Under the cathode the membrane potential
reduced whereas at the anode it is increased. There is an
ward flow of current at the cathode and an inward flow at
anode. These electronic potentials can be observed most
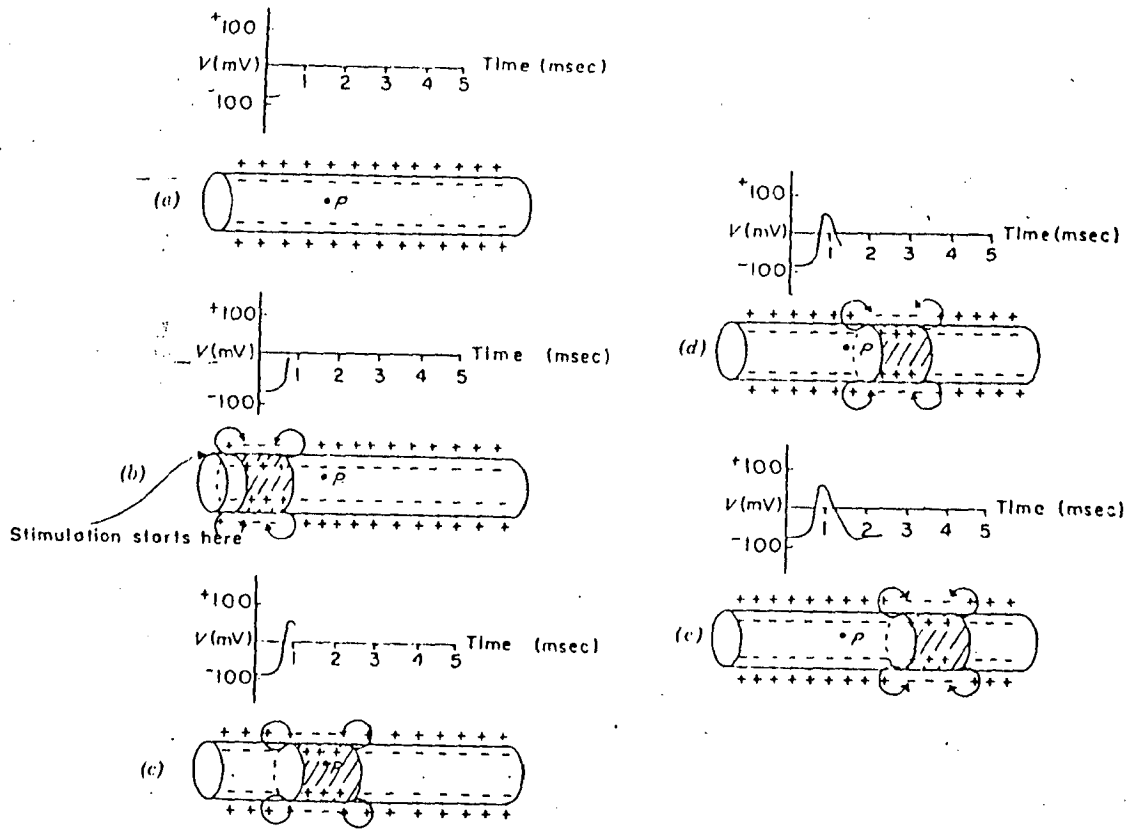
FIG. 1·5 The transmission of a nerve impulse along an axon
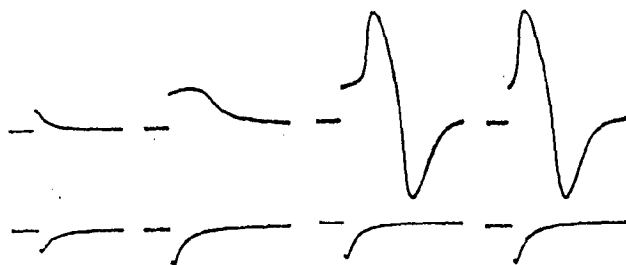
FIG. 1·6 Outward flow of current at the cathode (upper line) causes a local electrical response

clearly when the current is too weak to excite the propagation of an action potential as shown in Fig. 1.6. As the current strength of the stimulus is increased the repolarization of the membrane under the cathode does not occur as simply as before. There develops a local response due to processes inherent in the nerve itself which can best be seen by comparing the cathodal electrotonic potential with the anodic electrotonic potential [Fig. 1.6]. This local response becomes increasingly more obvious as the stimulus is strengthened until an action potential develops from it [Fig. 1.6]; the current strength required for this to occur is defined as threshold. Once the spstroke of the spike is initiated, the membrane at that point becomes freely permeable to sodium where as at sites immediately ahead in the axon the membrane is potassium permeable. Current therefore flows in the nerve impulse in the axon [Fig. 1.4a] between points A and B and returns in the opposite direction in the external fluid. This current reduces the membrane potential just ahead of the active region by drawing charge out of the membrane capacity. When the potential difference at 'B' has been reduced by about 20 mV the permeability of B to sodium rises rapidly and the interior of the axon becomes positive at this point, a spike potential being initiated. The sequence is repeated along the length of the nerve [5,6]. The propagation of the nerve impulse within the unmyelinated axon is thus by excitation of successive parts of the axon by the axon currents. The spike potential behaves like a travelling cathode [8].

An axon can transmit in either direction. However, the synapse that connects it to another neuron only permits the action potential to move along the axon away from it's own cell body [9].

Examination of the axons of various neurons indicates that there are two different types of nerve fibres. The membranes of some axons are covered with a fatty insulating layer called myelin that has small uninsulated gaps called nodes of Ranvier every few millimeters, as shown in Fig. 1.7a ; these nerves are referred to as myelinated nerves. The axons of other nerves have no myelin sleeve (sheath), and these nerves are called unmyelinated nerves. This is a somewhat artificial classification; most human nerves have both types of fibres. Much of the early research on the electrical behaviour of nerves was done on the unmyelinated giant nerve fiber of the squid [6]. Myelinated nerves, the most common type in humans, conduct action potentials much faster than unmyelinated nerves.

Unmyelinated fibres : It resembles a tube that is filled with a weak solution mostly of potassium ions (K^+) and relatively large organic negative ions as shown in Fig. 1.7b. The diameter of the fibers ranges between 0.3 and 1.3 μmeter. The conduction speed for typical fibers is 1.73 x 10^6 diameters per second, indicating speeds between 0.5 and 2.3 meters/sec.,[4].

Myelinated fibers : It's conduction speed, upto 120 meters/sec., is considerably greater than that of the unmyelinated axon [11]. On the other hand the relatively thick layer of myelin presents

(a)

Nodes of Ranvier

(b)
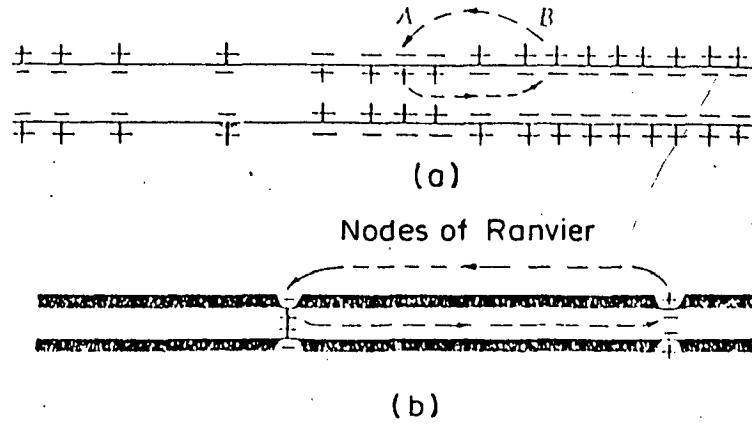
FIG.1·7 Diagrams illustrating local circuit theory

(a) Unmyelinated nerve fibre
(b) Myelinated nerve fibre

[Hodgkin,A.L.(1958) Proc.roy. Soc. B.148,1.]
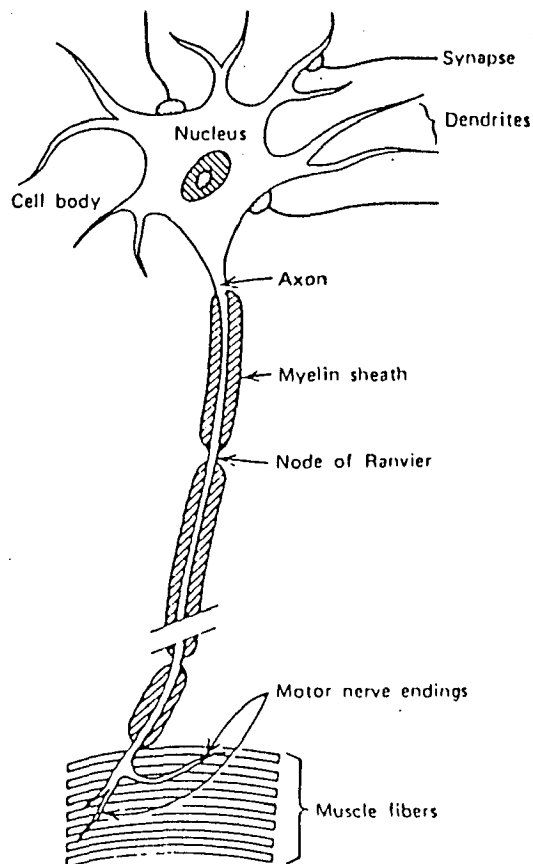
FIG.1·8 Schematic of a motor neuron

a space problem. Only one-third of the fibers in mammalian nerve trunks, those involved with rapid muscular response are myelinated Fig. 1.8 illustrates a motor neuron also shown in is that feeds muscle fibers. The myelin sheath is periodically interrupted by the nodes of Ranvier, in which the cross section is substantially that of an unmyelinated fiber. It is at the modes that the action potential is regenerated in the usual way, by an inward diffusion of sodium ions.

Myelinated axons conduct differently than the unmyelinated axon. The myelin sleeve is a very good insulator, and the myelinated segment of an axon has very low electrical capacitance. The action potential decreases in amplitude as it travels through the myelinated segment just as an electrical signal is attenuated when it passes through a length of cable. The reduced signal then acts like a stimulus at the next node of Ranvier (gap) to restore the action potential to it's original size and shape. Since between one node and the next the fiber behaves like a passive RC cable; that is, if a 100 mV spike originates at a particular node it will appear at the next node with increased width and reduced heigh [9,12]. The height is normally sufficient to overcome easily the minimum threshold requirement of 20 mV peak , so that regeneration takes place. This process repeats along the axon; the action potential seems to jump from one node to the next, that is, it travels by saltatory conduction, as shown in Fig. 1.9. In the nerve fiber the energy for regeneration is supplied by metabolic processes.
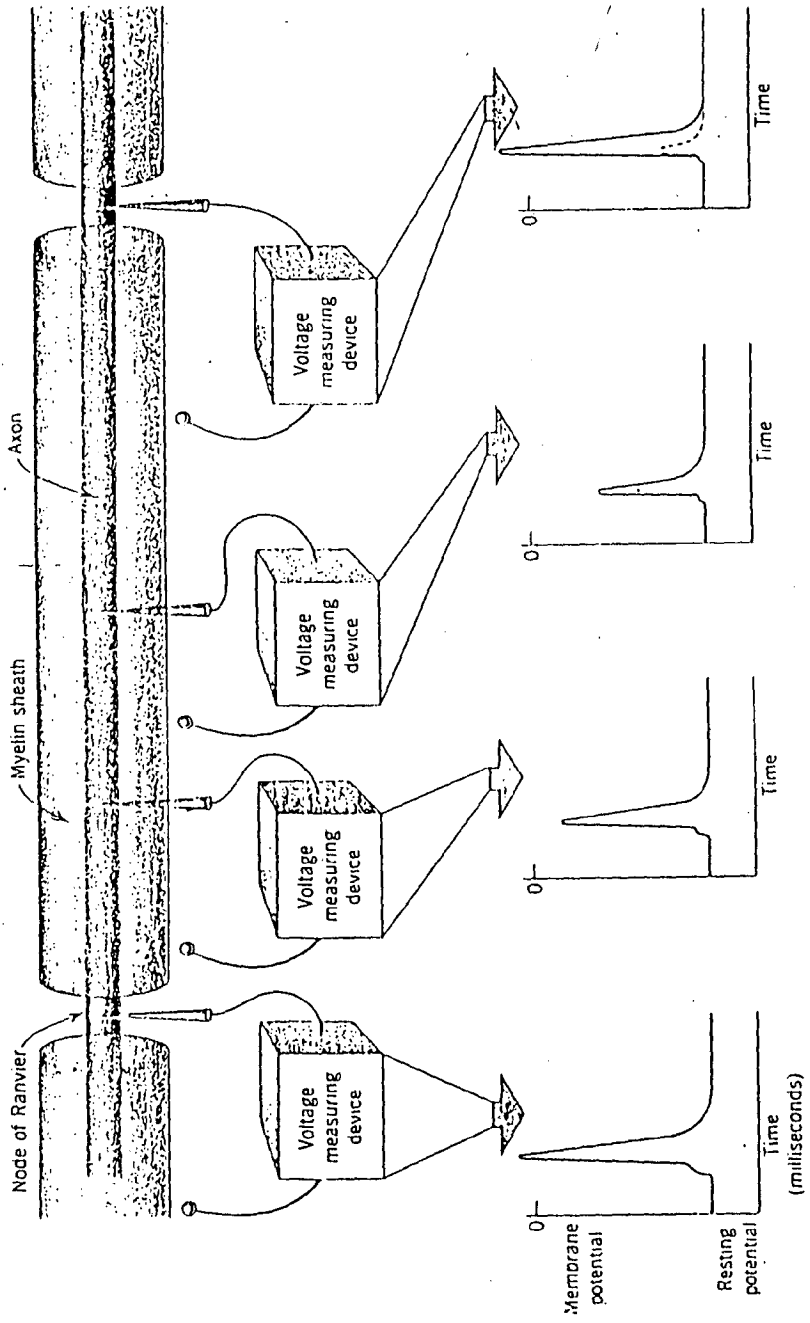
FIG. I·9 Conduction of an action potential along a myelinated axon

Whether the depolarization from the action potential is above threshold or not by the time it has spread passively through the internode region depends of course on how far the nodes are apart. Usually they are close enough together so that an action potential can spread two or three times the average internode distance and still be above threshold [7]. Thus the action potential moves along the axon by passive spread in the myelinated regions and by the occurrence of action potentials at the nodes [Fig. 1.9].

The mechanism by which an action potential is conducted along a nonmyelinated axon is basically the same as that for the myelinated axon, except that it sweeps continuously along instead of jumping from node to node.

Two primary factors affect the speed of propagation of the action potential : the resistance within the core of the membrane and the capacitance (or the charge stored) across the membrane. A decrease in either will increase the propagation velocity. The internal resistance of an axon decreases as the diameter increases, so an axon with a large diameter will have a higher velocity of propagation than an axon with a small diameter.

The greater the stored charge on a membrane, the longer it takes to depolarize it, and thus the slower the propagation speed. Because of the low capacitance, the charge stored in a myelinated section of a nerve fiber is very small compared to that on an unmyelinated fiber of the same diameter and length. Hence the

conduction speed in the myelinated fiber is many times faster. The unmyelinated squid axons ($\sim$1 mm in diameter) have propagation velocities of 20 to 50 meters/sec., whereas the myelinated fibers in man ($\sim$10 μm in diameter) have propagation velocities of around 100 to 120 meters/sec. This difference in conduction speed explains why the signal appears to jump from node to node in myelinated nerves.

The advantage of myelinated nerves, as found in man, is that they produce high propagation velocities in axons of small diameter. As large number of nerve fibers can thus be packed into a small bundle to provide for many signal channels. For example, 10,000 myelinated fibres of 10 μm in diameter can be carried in a bundle with a cross-sectional area of 1 to 2 mm^2, whereas 10,000 unmyelinated fibers with the same conduction speed would require a bundle with a cross-sectional area of approximately 100 cm^2, or about 10,000 times larger.

1.4.3 Threshold Depolarization :

Both the sodium conductance and the potassium conductance show graded responses to the degree of depolarization induced as shown in Fig. 1.10. Yet it is well known that in natural circumstances a depolarization of some -15 mV is required to produce an action potential. At such a degree of depolarization the sodium conductance rises sufficiently to allow the inward current of sodium ions to continue to depolarize the membrane despite the mounting outward potassium current. This increasing depolarization serves to heighten the sodium conductance and the
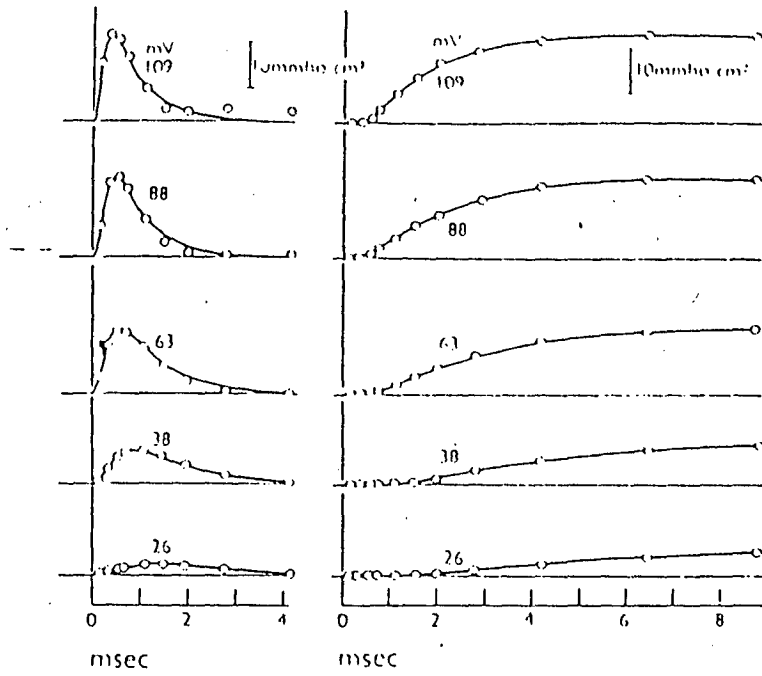
FIG. I·IO Time course of sodium (left) and potassium (right) conductances for different displacements of membrane potential

[Hodgkin, A.L. and Huxley, A.F. (1952)]
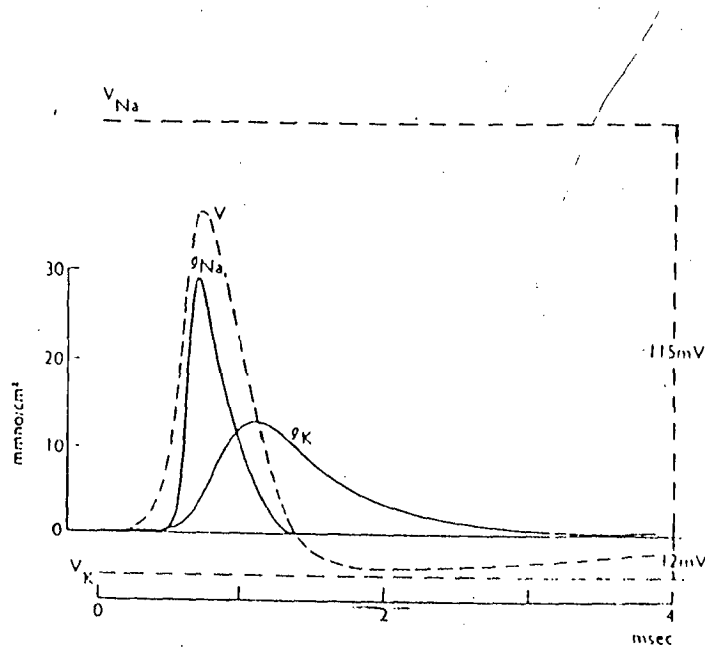
FIG. I·II The computed conductances for Sodium (g$_{Na}$), and potassium (g$_K$) are shown in relation to the action potential (V)

[Hodgkin and Huxley, 1952]

response thereupon becomes regenerative. If the stimulus causes a smaller depolarization than, say, 15 mV the feeble increase in g_{Na} is insufficient to cause an inward sodium current adequate to overcome the outward potassium current. When the depolarization is sufficient the early sodium current is stronger than that of potassium and the action potential develops. The spontaneous decrease of sodium conductance together with the continued rise of potassium conductance then produce the recovery of the membrane potential to it's resting state. Figure 1.11 shows the calculated variations of g_{Na} and g_K during the action potential.

As the impulse advances along the nerve fiber the potential difference across the membrane immediately infront of the active region is altered by electric currents flowing in a local circuit through the axoplasm and the surrounding fluid medium [Fig. 1.7]. This increases g_{Na} and sodium ions which enter render the inside of the axon positive and provide the current needed to excite the next segment. At the crest of the impulse the slower changes which result from depolarization take effect; g_{Na} falls and g_K rises so that K^+ leaves the fiber at a greater rate than that which Na^+ enter. As a consequence the potential swings towards the equilibrium potential of the potassium ion.

The immediate effect of the passage of a series of impulses is that a nerve fiber gains a tiny amount of sodium and loses a similar quantity of potassium. Metabollic energy is used to pump out the sodium ions and to reabsorb the potassium ions.

1.4.4 Saltatory Conduction :

When the velocity of propagation of the nerve impulse
in an unmyelinated axon is compared with that in a myelinated
axon of the same diameter it is found that the impulse travels
at a much greater rate in the myelinated fiber. This suggests
that the mechanism of propagation may be different and has led to
the hypothesis of saltatory conduction. Saltatory means leaping
(saltare = to leap) and the term is used to describe a process
in which the active process leaps from node to node of Ranvier
[Fig. 1.9]. On this view the active generation of current (which
is due to the entry of sodium) is confined to the nodes but
depolarizes the whole internodal length of fiber by local circuit
action as shown in Fig. 1.7. The myelin sheath acts as an insu-
lator which increases the donduction velocity by thus making the
local circuits act at a considerable distance ahead of the region
activated.

1.4.5 Changes in Nerve During and After Activity :

Changes in excitability and conductivity occur after the
appearance of the nervous impulse, and these changes run parallel
to one another.

Absolute refractory period : For the duration of the spike
potential the fiber is absolutely refractory. This duration which
is of about 1 m sec., is known as absolute   refractory period.
No stimulus, no matter how strong, can initiate a fresh impulse
in this region ; nor can an impulse generated elsewhere pass
through this area Neither excitability nor conductivity, therefore,

is present [5].

Relative refractory period : The next few milliseconds represent the period of partial refractoriness. This period is also known as relative refractory period. At first a very strong current can excite the fiber, which responds with a subnormal spike. The strength of the minimal exciting stimulus progressively falls until excitability returns to normal [11].

These stages of refractoriness are due to the inactivation of the sodium carrier mechanism caused by the intense depolarization of the membrane during the propagated impulse; coupled with this is the high level of potassium conductance that ensues upon the action potential. Both these changes raise the threshold of the axon to further excitation, i.e., they increase the level of depolarization that is required for the inward sodium current to exceed the outward potassium current.

The fibers of largest diameter recover to 90 percent of the normal in one millisecond; this means that they could conduct 1000 impulses/sec of nearly full size, at least for short periods. Motor fibres rarely have to conduct naturally at rates exceeding 100 - 150 impulses/sec.; sensory fibres under extreme experimental conditions may have to conduct at 300 - 400 impulses/sec. Normally then these fibres can readily cope with the lower frequencies with which they have to deal [6,9].

Fibres of smaller diameter recover more gradually and consequently the upper limit of impulse frequency which they can transmit is lower than in the case of large fibres.

1.4.6 <u>ALL-OR-NONE Relationship Between Stimulus and Response</u> :

The magnitude of the spike potential (impulse) set up in any single nerve fiber is independent of the strength of the exciting stimulus, provided the latter is adequate. This property of the single nerve fiber is termed the all-or-none relationship. It should be emphasized that this relationship applies only to the unit of the tissue. Stimuli too weak to produce a spike do, however, set up a local electrotonus; as already explained. The magnitude of the electrotonic potential progressively increases with the strength of the stimulus until a spike is generated. The all-or-none relationship applies only to spike production [8].

The above account deals, as stated, with the response of a single nerve fiber. If a nerve trunk is stimulated, then as the exciting stimulus is progressively increased above threshold with which progressively larger number of fibers respond till saturation [6].

1.4.7 <u>Time Factor In Excitation</u> :

Any agent that sharply increases the sodium permeability of a membrane stimulates excitable tissue. Nerve can be stimulated by electric current, mechanical action (pinching, striking, or cutting), sudden chilling or heating, or by various acids, alkalis, and concentrated salt solutions, etc.

Among all these stimuli electric current has a special place, since (a) it can easily and accurately be dosed in strength, duration, and steepness of increase, and (b) it does

not damage living tissue, while it's action is quickly and completely reversible when it is strong enough to cause excitation [4]. Study of the action of electrical stimulation on excitable tissue is of great interest to physiology because excitation is transmitted through the nerves by local currents arising between the excited and resting portions of tissue [Fig. 1.7].

In considering the effectiveness of a stimulus, attention must be paid not only to the strength of the current, but also to the time during which it is allowed to flow through the tissue. A strong current produces a response after a very short time of flow ; as the strength of the current is reduced a longer duration of flow is required to stimulate ; if the current falls below a minimum value it fails to stimulate no matter how long the duration of flow [Fig. 1.12]. The relationship between the current strength and the duration of current flow necessary to stimulate is shown in a strength-duration curve of Fig. 1.12 [2].

1.4.8 Chronaxie and Rheobase :

The weakest current strength which can excite a tissue if allowed to flow through it for an adequate time is called the rheobase. A still weaker current fails to stimulate no matter how long the duration of current flow. The tissue is then tested with a current strength equal to twice the rheobase. The duration of the current flow which stimulates the tissue under these conditions is called the chronaxie [Fig. 1.12]
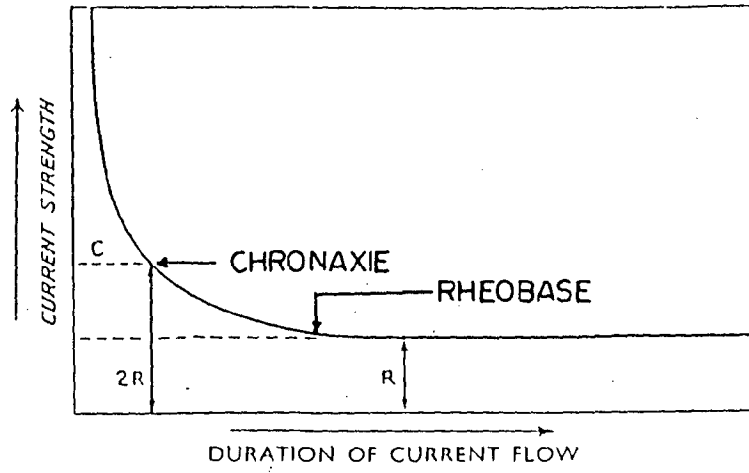
FIG. 1·12 Strength-duration curve. Rheobase and chronaxie
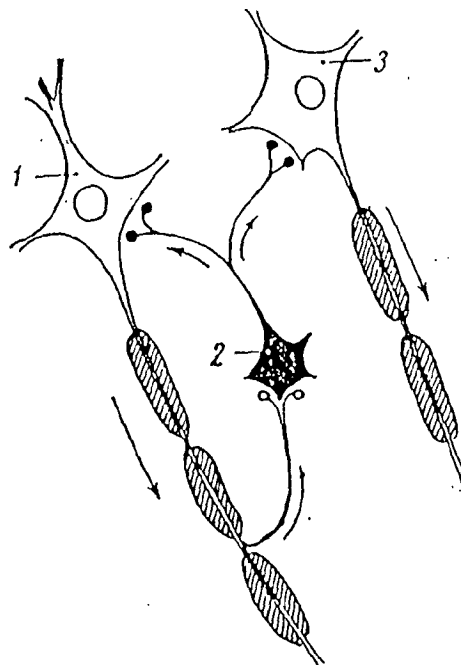
FIG. 1·13 Schematic view of the connections between
motor neurons and Renshaw cells

Chronaxic values are a useful index of the relative excitability of tissues. The chronaxie of nerves fibres is considerably shorter than that of skeletal muscle [11].

1.4.9 Accomodation :

If a nerve is subject to the passage of a constant subthreshold current, the site of the nerve under the cathode shows an increase of excitability, whereas that under the anode shows a decrease of excitability. This effect is called accomodation. Accomodation is due to partial inactivation of the sodium carrier mechanism of the nerve fiber, by a prolonged depolarization which is stself of insufficient intensity to excite the sodium carrier mechanism and therefore to set off an action potential [6].

Similarly a current which rises suddenly to it's full value is more effective and excites at a lower threshold value than if it rises slowly. The current must have a minimal rate of application in order to excite. If the current rises more slowly than this it is ineffective [11].

To determine the accomodation the nerve is stimulated with currents which increase in strength and different rates ; the threshold strength is noted in each case. If accomodation is rapid then the threshold strength with a given rate of current rise is high; if accomodation is slow then the same rate of current rise causes excitation at a low strength of current. A similar feature of nerve endings is called adaptation. The fibres of sensory nerves have far less powers of accomodation than

those of motor nerves; fine pain fibers show almost no accomodation at all [1,2].

1.4.10 The Sodium-Potassium Pump :

Efforts to elucidate the relationship between metabolism and the passage of ions through the membrane led to discovery of the so called sodium-potassium pump.

It's functioning is linked with metabolic energy expenditure. Indeed, to remove sodium ions from the protoplasm into the external solution where their concentration considerably exceeds that within the cell, requires a certain amount of work. At rest it need not be great since the sodium permeability of the resting membrane is very low, but during excitation the intensified passage of sodium ions into the protoplasm activities the pump, which ensures the restoration of the disturbed concentration gradients. It should be emphasized however, that this restorative process proceeds very slowly, over a period of many minutes and even hours [4,7].

1.4.11 Irradiation of Excitation :

Impulses arriving at the central nervous system induce excitation not only in the neurons of a given reflex centre but also in those of other centres. This spread of excitation through the central nervous system is known as irradiation.

1.4.12 Renshaw-Cell Inhibition :

An important role is played in the limitation of irradiation of excitation by the nerve cells discovered by Renshaw in the

spinal cord. He found that before leaving the spinal cord the axons of motor neurons often form one or more collaterals, which terminate in Renshaw cells the axons of which often form inhibitory synapses with the motor neurons of a given segment of the spinal cord as _shown in Fig. 1.13. For that reason excitation arising in a motor neuron irradiates by the direct route to it's peripheral skeletal muscle, but activates that inhibitory cell along collateral pathway which supresses the excitation of the motor neuron. The stronger the excitation of a motor neuron and, consequently, the higher the frequency of the impulses issuing from it to the periphery, the stronger is the excitation in the Renshaw cell, which inhibits it's activity. Thus there is a mechanism automatically protecting nerve cells against excessive excitation [7].

The inhibition arising through Renshaw cells is called recurrent inhibition. It plays an important role in the activity of all parts of the central nervous system [11].

1.5 DENDRITES :

The dendrite has certain properties which specialize it for receiving the information transmitted along the axon. In fact, at the dendrite, nerve impulse frequency is translated back into a depolarization similar to the one which originally generated the axonal nerve impulses.

The nerve impulses arrive at many synapses, and if at such a synapse, electrodes are inserted into the axon near it's synaptic termination on a dendrite and into the postsynaptic

region of the dendrite itself, in order that membrane potential fluctuations in these regions may be measured, recording of activity near the axon terminal [Fig. 1.14a] would typically reveal nerve impulses arriving at a frequency which varied over time [Fig. 1.14b]. Simultaneous records from the postsynaptic electrode would, in the variety of synapses, indicate a somewhat jagged variation in the dendrite membrane potential which reflects, at least approximately, the frequency of presynaptic nerve impulses arrivals [Fig. 1.14c]. In other words, there would be a dendritic depolarization whose magnitude is approximately proportional at each instant to the frequency at which nerve impulses are arriving. Thus the frequency of axonal impulses is, at this type of synapse, converted into a maintained dendritic depolarization [5].

After a nerve impulse arrives at an axon terminal, there is a brief delay of about a half-millisecond to one-millisecond, followed by a characteristic fluctuation of the dendritic membrane potential. This fluctuation is known as the postsynaptic potential or PSP [Fig. 1.15]. Tye typical PSP has a rapid rise to a peak, followed by a much longer (often approximately) exponential return to the resting potential. Particularly striking are two differences between PSPs and action potentials. PSPs are much longer than an action potential, tens or in some cases hundreds of times longer, and also are much smaller in amplitude, again by a factor often as large as several hundred [3,9]. The arriving nerve impulse causes the release of a small quantity of a chemical, generally known as a transmitter substance, which
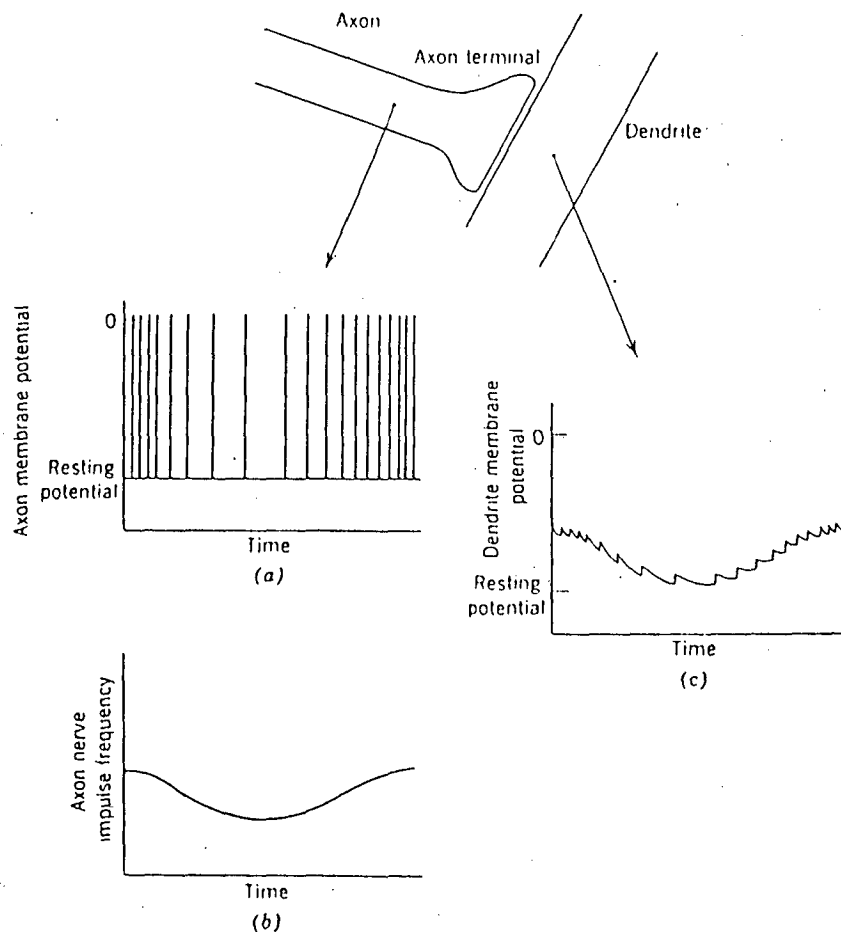
Fig. 1·14 Translation of axonal impulse frequency into a depolarization at a dendrite.

Axon terminal — Dendrite

Axon terminal membrane potential

0

Resting potential

Time (milliseconds)

5   10   15   20   25

(a)

Dendrite membrane potential

0

Resting potential

5   10   15   20   25

Time (milliseconds)

(b)

Synaptic delay
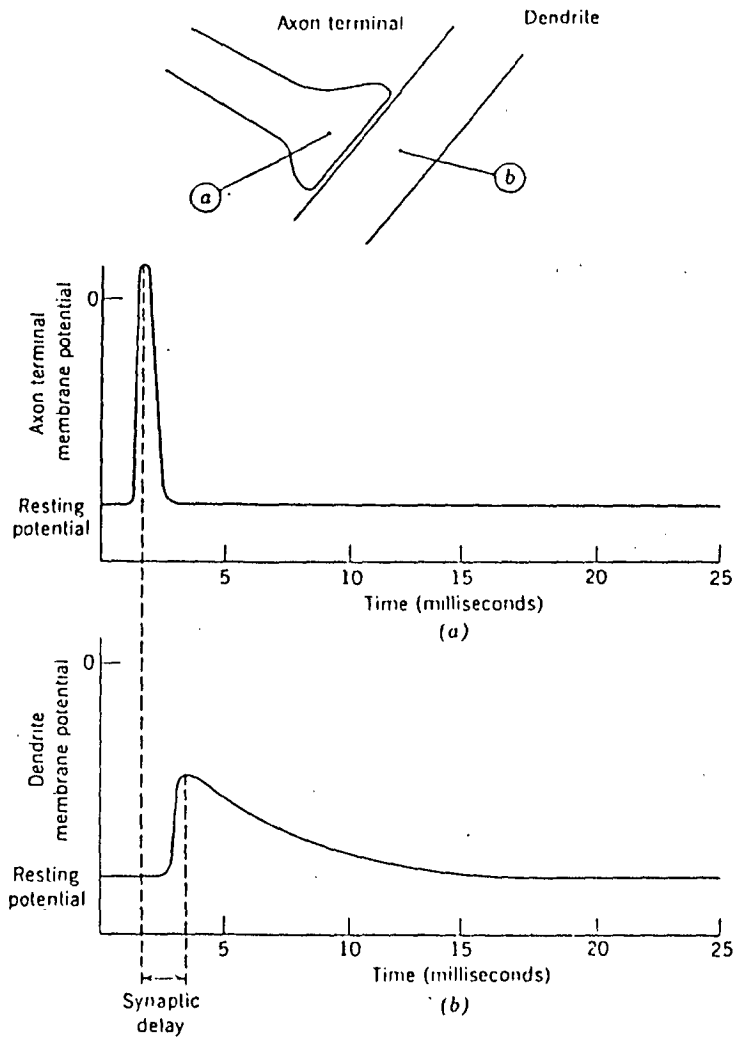
FIG. 1·15 Transmission of information at a synapse.

Dendrite membrane potential

0

Resting potential

Time

FIG. 1·16 Temporal summation of PSPs. Arrows indicate arrival of nerve impulses at the axon terminal.

diffuses across the synaptic cleft and results in the dendritic electrical response. It should be emphasized that this behaviour is quite different from that seen in the axon, where application of transmitter does not produce a PSP - like response. The dendritic membrane is thus said to be chemically excitable to distinguish this important property from the usual electrical excitability of the axonal membrane [1,3].

Axons and dendrites share a number of electrical properties. The one important is, the dendrite like all parts of the nerve cell including the axon, has a resting potential of approximately -60 millivolts; this resting potential is thought to be constant over the length of the dendrite and indeed over the entire neuron.

Two important properties of dendrites follow from the fact that dendritic depolarization depends directly upon local transmitter concentration. The first of these may be termed graded responsivenes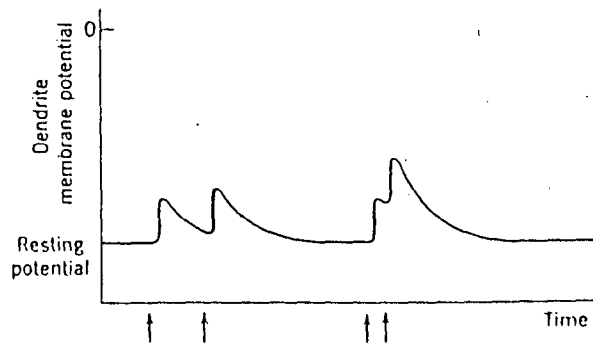s, and the second, temporal summation. Graded responsiveness refers to the fact that the size of a PSP is proportional to the amount of transmitter released and is to be contrasted with the threshold and all-or-none behaviour characteristic of the axon [4].

The existence of graded responsiveness implies that the effects of two quantities of transmitter applied simultaneously become added together; from this, it can be inferred that the effects of two quantities of transmitter applied at different times will also be added together. More specifically, that if

a nerve impulse arrived at a synapse before the PSP caused by a preceding impulse had completely disappeared, the PSP from the second impulse would simply add to what remained of the first PSP. The same fact may be formulated in a slightly different manner by saying that the dendrite in contrast to the axons, shows no refractory period. This is illustrated in Fig.1.16 where two PSPs occuring in rapid succession are seen to sum. This importent property, the fact that a new PSP simply adds to what remains of all preceding PSPs is referred to as temporal summation [5,7].

The distinctive property of the axon is it's active response to above-threshold depolarizations, the action potential, where as dendrites do not respond to depolarization, as do axons, by producing action potentials, but rather show only passive responses to both depolarizing and hyperpolarizing stimuli of all magnitudes. Thus, for large as well as small depolarizations, the response of a dendrite is the mirror images of the response to hyperpolarizing stimuli [12]. This is illustrated in Fig. 1.17 where the responses of a dendrite and axon to various stimuli are compared.

To this point, PSPs have been discussed as depolarizing the cell. Neurons, however, characteristically display a second type of PSP which is hyperpolarizing rather than deppolarizing. The hyperpolarizing PSP has a shape much like that of the depolarizing PSP, except that it is inverted ; that is, it consists of a rapid hyperpolarization followed by a relatively

prolonged return to the resting potential as shown in Fig. 1.18. Since depolarization of the neuron results in the production of nerve impulses, the depolarizing PSP is termed an excitatory postsynaptic potential (EPSP). The hyperpolarizing PSP, on the other hand, is known as an inhibitory postsynaptic potential (IPSP) because it opposes the action of EPSPs and tends to prevent the generation of action potentials.

There is, as it happens, only a single type of action potential whether an action potential gives rise to an EPSP depends entirely upon the properties of the synapse; that is, some synapses are specialized to produce EPSPs and others, IPSPs. Although the evidence is not entirely clear as yet, it appears that a given axon liberates at all of it's synaptic terminals only one particular type of transmitter substance, and that whether this transmitter produces an EPSP or an IPSP depends upon the characteristics of the postsynaptic membrane. As yet, however, the chemistry of their action is very poorly understood [3,5]. However, that a synapse will be of one or the other variety and cannot be inhibitory at some times and excitatory at others. Except for the fact that one is depolarizing and the other is hyperpolarizing, EPSPs and IPSPs do indeed share the same properties. Thus IPSPs show temporal summation, and, if they occur at a constant rate, IPSPs also can sum to give an average hyperpolarization proportional to the frequency of nerve impulses causing them, where as EPSPs can transform nerve impulse frequency into a maintained depolarization, IPSPs can convert nerve impulse frequency into a maintained hyperpolarization [8,12].

a nerve impulse arrived at a synapse before the PSP caused by a preceding impulse had completely disappeared, the PSP from the second impulse would simply add to what remained of the first PSP. The same fact may be formulated in a slightly different manner by saying that the dendrite in contrast to the axons, shows no refractory period. This is illustrated in Fig.1.16 where two PSPs occuring in rapid succession are seen to sum. This importent property, the fact that a new PSP simply adds to what remains of all preceding PSPs is referred to as temporal summation [5,7].

The distinctive property of the axon is it's active response to above-threshold depolarizations, the action potential, where as dendrites do not respond to depolarization, as do axons, by producing action potentials, but rather show only passive responses to both depolarizing and hyperpolarizing stimuli of all magnitudes. Thus, for large as well as small depolarizations, the response of a dendrite is the mirror images of the response to hyperpolarizing stimuli [12]. This is illustrated in Fig. 1.17 where the responses of a dendrite and axon to various stimuli are compared.

To this point, PSPs have been discussed as depolarizing the cell. Neurons, however, characteristically display a second type of PSP which is hyperpolarizing rather than deppolarizing. The hyperpolarizing PSP has a shape much like that of the depolarizing PSP, except that it is inverted ; that is, it consists of a rapid hyperpolarization followed by a relatively
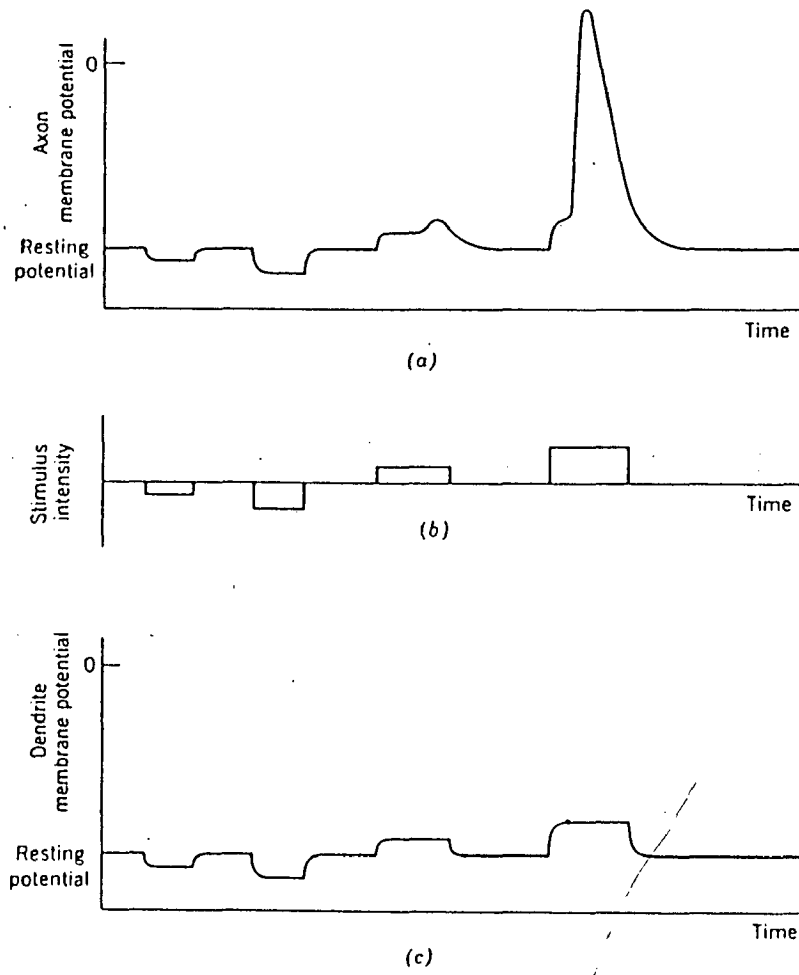
FIG. 1·17 Comparison of axon and dendrite responses to hyper-and
depolarizations.

prolonged return to the resting potential as shown in Fig. 1.18. Since depolarization of the neuron results in the production of nerve impulses, the depolarizing PSP is termed an excitatory postsynaptic potential (EPSP). The hyperpolarizing PSP, on the other hand, is known as an inhibitory postsynaptic potential (IPSP) because it opposes the action of EPSPs and tends to prevent the generation of action potentials.

There is, as it happens, only a single type of action potential whether an action potential gives rise to an EPSP depends entirely upon the properties of the synapse; that is, some synapses are specialized to produce EPSPs and others, IPSPs. Although the evidence is not entirely clear as yet, it appears that a given axon liberates at all of it's synaptic terminals only one particular type of transmitter substance, and that whether this transmitter produces an EPSP or an IPSP depends upon the characteristics of the postsynaptic membrane. As yet, however, the chemistry of their action is very poorly understood [3,5]. However, that a synapse will be of one or the other variety and cannot be inhibitory at some times and excitatory at others. Except for the fact that one is depolarizing and the other is hyperpolarizing, EPSPs and IPSPs do indeed share the same properties. Thus IPSPs show temporal summation, and, if they occur at a constant rate, IPSPs also can sum to give an average hyperpolarization proportional to the frequency of nerve impulses causing them, where as EPSPs can transform nerve impulse frequency into a maintained depolarization, IPSPs can convert nerve impulse frequency into a maintained hyperpolarization [8,12].
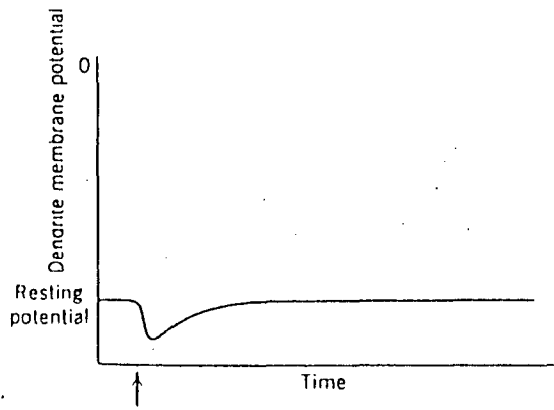
FIG. 1·18 An inhibitory post-synaptic potential.

Thus, the properties of axon can result in the trans-
formation of depolarization into impulse frequency, while
dendritic properties can serve to decode impulse frequency, into
depolarization again to receive the information from the axons;
overall, a depolarization has been moved (perhaps with some
distortion) from the axon of one nerve cell to the dendrite of
another [5,7].

1.6 SYNAPTIC JUNCTIONS :

Information partinent to the synaptic junction is given
by Eccles [13]. The specific transmitter substance of a synapse
is not known. Acetylcholine is identified with certainty. It is
not known about the mechanism by which the transmitter substance
is injected into the synaptic gap. How this leads to discharge
on the other side of the gap is not clear [12].

Excitatory and inhibitory synapses are alike. The excitat-
ory postsynaptic potential (EPSP) is a mirror image of the
inhibitory postsynaptic potential (IPSP). The neuron Soma is
contained within a thin wall that is akin to that of an unmyeli-
nated fiber and it behaves in a similar fashion [5]. With no
input signals, the inside of the neuron is at -70 mV with respect
to the interstitial fluid. Excitatory chemical transmitters
make this voltage less negative and inhibitory transmitters make
this voltage more negative. When the algebraic sum of chemically
induced changes brings the neuron to a threshold level of, say
-20 mV, it fires or discharges [12,13].

Because excitation decreases the magnitude of the transmembrane potential, it is also known as depolarization; inhibition, which increases the magnitude, is also known as hyperpolarization.

Eceles research indicates that all of the collateral branches of a neuron must either be excitatory or inhibitory, depending on the neuron. Thus, in Fig. 1.3, the incoming synaptic junctions babeled(+)and(-)will be coming from different neurons. The neural junction, labeled (0), can not normally occur. The three outgoing collateral branches will all be (+) or all (-) [2,12].

Continued research seems to uncover more questions than answers. It is possible that the sign of a junction is determined at the postsynaptic membrane and not by the presynaptic vesicles, as Wilson [13] has summed up the situation.

A great deal remains to be learned about the excitatory and inhibitory processes that regulate nervous activity. It is not even universally accepted that cells can be classified as either excitatory or inhibitory; it may yet develop that different branches of one fiber, liberating the same transmitter can inhibit one cell and excite another. The chemical structure of most transmitters remains a mystery. The precise events leading to changes in membrane permeability need to be outlined in detail [1,8]. And there are other synapses - apparently less common in the vertebrate central nervous system - at which one cell excites or inhibits another by a purely electrical inter-action [6].

Certainly a very striking feature of the neuron is the large proportion of it's membrane area receiving synaptic contacts from other nerve cells. To the neurophysiologist this anatomical fact means that a neuron may receive information simultaneously from a large number of other neurons. At the same time, the nerve cell body characteristically gives rise to only a single axon and thus to a single channel through which information flows out of the neuron. This axon typically branches, of course, but the same information flows over all the branches. A neuron, then, receives information from a number of sources and must integrate this information to determine what emerges from the single output. We have seen, for example, that the nerve impulse frequencies at the various excitatory and inhibitory synapses of a neuron can be converted into depolarizations or hyperpolarizations and also that the axon can reconvert depolarization into impulse frequency for transmission to still other neurons [2].

A preliminary understanding of the integration process depends upon knowing only one additional property of neurons : EPSPs and IPSPs arriving over different synapses sum, to a first approximation, simply algebraically. This property known as spatial summation. It is not surprising in view of the existence of temporal summation; since PSPs from a single synapse add together it is entirely reasonable to expect the same behaviour of PSPs from different synapses. Thus various inputs to a neuron combine by summation to determine the single

output. This is the central point of the basis for computation in the nervous system [4,5].

1.7 SOMA AND AXON HILLOCK :

A sharp distinction has been drawn between the properties of dendrites and axeons by stating that dendrites are electrically inexcitable and donot give rise to action potentials. If the dendrites are inexcitable while the axons give rise to nerve impulses, there must be some region of the cell closest to the dendrites which is electrically excitable. This region is believed to be at the axon hillock, the junction between Soma and axon. Thus a depolarization arising in a dendrite spreads passively down the dendrite, through the Soma and finally to the axon hillock where nerve impulses are generated. The axon hillock, then, is the point in a neuron where all nerve impulses arise. That this fact is important to the operation of the nervous system.

The portreyal of a neuron as an integrative (summing) device for input signals is probably oversimplified. Measurements show that each excitatory (or inhibitory) input is equivalent to a positive (or negative) pulse whose trailing edge exponentially decays with a time constent of 4 msecs. Physically distant dendrites cannot possibly be in instant communication with each other, so local integration within each dendrite must also be important [8,12].

1.8 SELECTION OF PROBLEM :

The neuron or nerve cell is the basic structural and functional unit of the human nervous system. The neurons play an important role in the functioning of the nervous system to which they conform. There are enumerable control mechanisms which are effected in some way or the other by nervous activity. The imbalance or failure of the neuronal mechanisms causes diseases, - some of which are diagnosed and some others not as yet [1,12]. Hence it becomes highly essential, to analyze and understand the functioning of the neurons and the nervous tissue under a varieties of conditions. But it is very difficult rather impossible to carry out such experiments on the neurons in-vivo. It is still difficult to extricate the nerve cells in intact condition for investigation purposes. Under such constrained situations modelling serves the purpose to a great deal. The models are similar in functions but different in structure from the original biological systems.

The neuroelectric model to be developed and analyzed here is expected to permit the investigations for any desired neuron geometries of practical interest. The model will offer a convenient means for understanding the functional details of the neurons under various conditions which the living neuron can not permit. Existing models will be used in this model development process. The important properties like accomodation, adaptation, subthreshold phenomenon, absolute and relative refractory periods, Renshaw cell feedback will be studied.

Active axon and synaptic junction potentials will be simulated
accurately and economically, which have not been considered in
the earlier models. The simulation and understanding of the
synaptic junction potentials interaction is important because
the communication between the neurons and between different
parts of the nervous system takes place through the synaptic
junctions. The model will permit to observe the responses of
the whole or part of the system as the experimental conditions
are manipulated, and thus will provide an effective kind of
interaction with the user.

Secondly, the electrical stimulation of peripheral
nerves is in wide spread use in clinical applications during
the last few years [63]. Such applications include the stimul-
ation of the phrenic nerve for patients with litle or no res-
piratory function [52], and stimulation of the peroneal nerve
of stroke patients who have suffered paralysis in muscles of
the Leg [53]. Also, experimental work is underway to develop
neuroelectric prostheses for the deaf and blind [63]. Many
patients are being treated for chronic pain by external
electrical stimulation using surface electrodes [43].

With these increasing clinical efforts, it becomes
imperative that a model for nerve stimulation be available to
provide an analytical foundation for these applications.

A review of the literature for the last ten years has
indicated that, the effect of the stimulation, neuron geomet-
ries and the excitation electrode distances on the behaviour
of the neuron have not been considered in the analysis. Consi-
deration of these parameters is important because the neurons
vary in geometries in different parts of the human nervous

system. Also, that the neurons are subject to various types and levels of physiological stimulations depending on their location in the nervous system [5,12]. All these parameters will be considered in the analytical work to be presented here. The software developed here will facilitate to select a wide variety of stimulus parameters, including different waveshapes, neuron geometries to study their effects on the responses of the actual neurons. Three neuron geometries, five types of excitation functions,— constant, triangular, ramp, pulse, and sinusoidal, and a range of electrode distances (0.05 cm to 0.45 cm.), and excitation magnitudes (0.05 mA to 0.25 mA) will be considered. A large number of membrane potential and current waveforms will be obtained. Thus the model is expected to provide a versatile tool for guiding and interpreting experiments, and for studying variables that may not be easily implemented in the laboratory.

1.9 ORGANISATION OF THE DISSERTATION :

The entire thesis work is divided into two parts — the hardware and the software simulations. In Chapter — I, introduction, structural and functional details of neuronal systems and selection of the problem are provided. Chapter — II gives a review of the existing models and Chapter — III the new electronic model. Chapter — IV provides the programs and the analytical framework of the neuroelectric model. Finally in Chapter — V the conclusions and the scope for future work are discussed at length.

It is hoped that this thesis work will provide a background for both hardware and software simulations of the neuronal network.

****

CHAPTER - II

EXISTING NEURAL MODELS

2.1 INTRODUCTION :

Representation of the biological neurons by the electronic equivalent circuits has grown over the last three decades. Neural models serve as an excellent aid to the Neurophysiologists and Bioengineers to study the neuron behaviour under a variety of conditions as compared to actual neurons. In the electronic neural models, since the various signal processing parts of the actual neuron are represented by the individual blocks of similar signal processing capabilities, it is possible to vary the parameters at each block independently, and study the effect on the behaviour of the whole neuron.

A number of electronic circuits have been developed in the past ranging from the ones, simulating just the membrane ionic currents to the most complex ones, incorporating most of the important features of the actual neurons [64,23,25,27].

The following electronic models have been reviewed in the present work.

2.2 Hodgkin-Huxley Model [24].

2.3 A simple electronic analog of the squid axon membrane : The NEUROFET by Guy Roy [26].

2.4 Saxena Models [23,25]

    (i) An electronic Model of Neuron.

    (ii) Electronic model of neuron processes including feedback through Renshaw cell.

2.5 Chitore Model [27]: An electronic representation of Neural transmission process.

2.6 Dendritic compartmental model of neuron [35].

2.7 French and Stein Model [40].

2.8 A comparison of dynamic and steady-state model by D.A. Teicher [29].

2.9 An active pulse transmission line simulating nerve axon by Nagumo [50].

2.10 Sensory effects of transient electrical stimulation-Evaluation with a neuroelectric model by J.Patrick Reilly [63].

2.11 An electronic model for neural transmission of informations-by J.K.Chowdhury et al. [36].

2.12 LEWIS MODELS.

(i) The locus concept and it's application to neural analogs [64].

(ii) Using electronic circuits to model simple neuroelectric interactions [49].

2.2 HODGKIN-HUXLEY MODEL [24] :

Kodgkin and Huxley proposed a mathematical model for squid nerve to meet the experimental results of voltage. According to this model, the membrane current could be separated into ionic currents with conductance parameters. Both parameters are functions of time and voltage. The model is shown in Fig. 2.1.
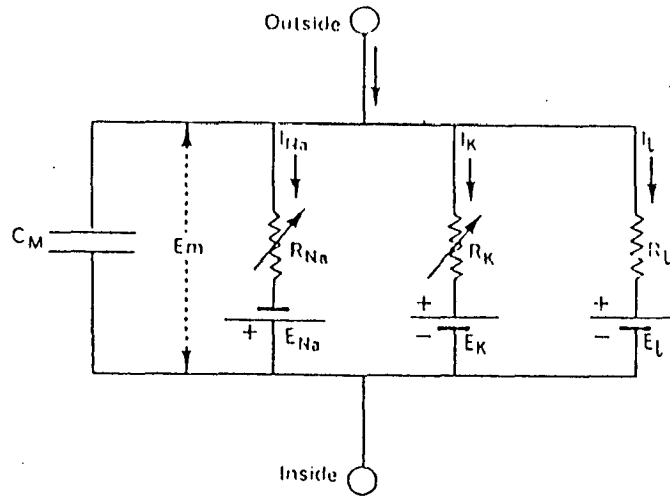
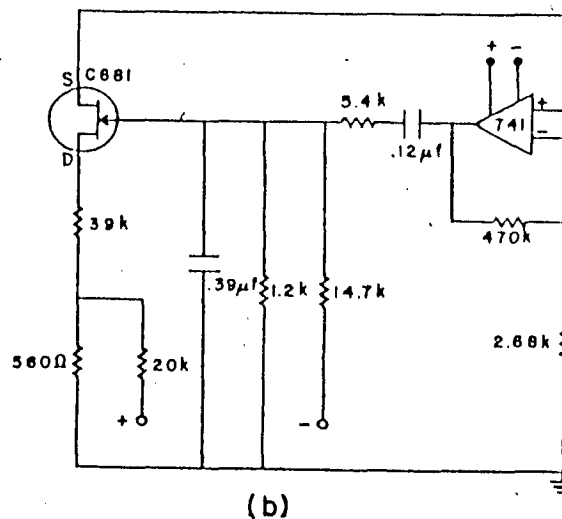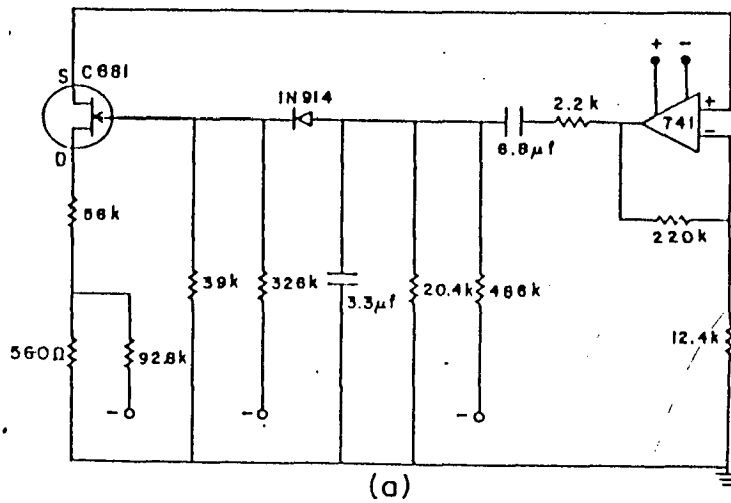FIG. 2·1 Hodgkin- Huxley Model

(a)

(b)

FIG. 2·2 GUY ROY MODELS

Circuits simulating (a) the potassium, and (b) the sodium currents in the squid axon membrane.

This model of Hodgkin and Huxley has provided a satisfactory explanation of the phenomenon responsible for the production of an action potential, when a nerve cell is excited.

They represented the membrane by an equivalent electric circuit. Current can be carried through the membrane either by charging the membrane capacity or by the movement of ions through the resistances in parallel with the capacity. The ionic current is divided into components carried by sodium and potassium ions (I_{Na} and I_K) and a small leakage current, made up by chloride and other ions. Each component of the ionic current is determined by a driving force which may conveniently be measured as an electric potential difference and a permeability coefficient which has the dimensions of a conductance.

Total membrane current I, consists of capacitive and ion current and is given by,

$$I = C_m \frac{dv}{dt} + I_i$$

where I_i = ionic current,

   V = displacement of membrane potential from it's resting value

   t = time

Ionic current is given as :

$$I_i = I_{Na} + I_K + I_L$$

where I_{Na} = Sodium ionic current.

I_K = Potassium ionic current.

I_L = Leakage current.

The values of individual ionic currents are given as :

$$I_{Na} = g_{Na}(E - E_{Na})$$

$$I_K = g_K(E - E_K)$$

$$I_L = g_L(E - E_L)$$

Here g_{Na} and g_K are the conductances of sodium and potassium and dependent on membrane voltage and time, g_L is the leakage conductance and independent of voltage and time. These three ionic current components are in parallel. C_M is the membrane capacitance, E_K, E_{Na} and E_L are the constant voltages, C_M is also constant. The membrane potential E affects the permeability factors g_{Na} and g_K. Here,

E_{Na} = equilibrium potential for sodium

E_K = equilibrium potential for potassium

E_L = equilibrium potential for leakage ions

E = the potential at which leakage current due to chloride and other ions is zero.

The membrane conductances are shown as parallel resistors in which $R_{Na} = 1/g_{Na}$, $R_K = 1/g_K$ and $R_L = 1/g_L$ and the diffusion tendency for each ion is shown as a battery of voltage equal to the equilibrium potential of that ion.

At rest R_{Na} is high compared with R_K and R_L, and it's battery E_{Na} would have litle effect on the net potential developed. Hence the resting membrane is negative inside with respect to outside. Once activation of the membrane occurs R_{Na} becomes low and the sodium battery secures a positivity of the inside compartment.

The point which emerges is that, changes in permeability appear to depend on membrane potential and not on membrane current. At fixed depolarization of sodium current follows a time course whose form is independent of current through membrane. If Na concentration is such that $E_{Na} < E$, the Na current is onward. If $E_{Na} > E$, the current changes in sign but follows some time course.

2.3 A SIMPLE ELECTRONIC ANALOG OF THE SQUID AXON MEMBRANE : THE NEUROFET BY GUY ROY [26] :

Guy Roy proposed a simple electronic circuit as an analog of the excitable membrane. It is based on the Hodgkin-Huxley model [24] and their squid axon voltage clamp data. The simulated potassium and sodium conductances are reproduced satisfactorily and the electronic action potentials are very similar to the experimentally recorded ones. The models are shown in Fig. 2.2.

Since this analog contains only a few electronic elements, it is small and inexpensive to build. It would be very useful as a means of simulating a wide variety of membrane conductances

and different types of action potentials. Also the simplicity of the circuit makes it an ideal unit to build complex neuron net works.

Here a FET is used as a variable resistor when it is operated at a low drain-source voltage (V_{ds}). The drain-source conductance g_{ds} can be varied by the gate potential V_g. When g_{ds} is measured as a function of V_g, it is found that the FET characteristic is very similar to that of the axon, membrane conductances.

To simulate the voltage and time dependence of the sodium and potassium conductances as given by Hodgkin and Huxley [24], the following equivalences are introduced : the transconductance g_{ds} represents either g_{Na} or g_K. One FET is used for g_K and one for g_{Na}. The voltage across the axon membrane is represented by the drain-source voltage V_{ds} and the membrane current is represented by the drain-source current, I_{ds}. It is necessary at first to establish a negative bias on the gate of each FET to bring g_{ds} to a low value corresponding to that of g_K and g_{Na} in their resting state.

The basic circuits used to simulate, both potassium and sodium conductances are shown in Fig. 2.2. Additional elements are necessary to simulate each conductance more accurately. To reproduce the transient changes of the potassium conductance, it is necessary to have a delayed rise. This effect was produced with a diode connected as shown in Fig. 2.2a. The negative biases are adjusted. So that the diode is not conducting when

V_{ds} is zero. When a source voltage V_{ds} is applied the voltage on the capacitor (3.3 µp) becomes less negative. This makes the diode conducting and brings a delayed rise in the gate voltage. The delay can be adjusted at will by varying the two negative biases on the diode. A coupling capacitor (6.8 µp) was added to cut the d.c. biases from the source terminal of the FET. It has the effect of bringing the conductance back to it's initial value when a step voltage V_{ds} is maintained too long. This can be called a slow inactivation of the potassium conductance.

To reproduce the sodium conductance, a similar circuit was used [Fig. 2.2b], but the diode has been removed because the initial delay is negligible on the experimental curves for the sodium conductances [24]. The time constant for the rise of g_{ds} is made more rapid and the coupling capacitor (0.12 µF) is much smaller in order to provide a faster inactivation for the sodium conductance, all in accordance with the experimental data.

The authors made the measurements with these circuits to determine the steady state amplitudes of the conductances when the source voltage V_{ds} is varied. The results correspond quite closely to the data of Hodgkin and Huxley. Also the author measured the transient changes after a series of voltage steps were applied; the author found that, the results were in good agreement with the data.

2.4 SAXENA MODELS [23,25] :

(i) An Electronic Model of Neuron [23] :

Saxena et al. proposed an electronic model of the neuron, that incorporated most of the important features of the actual neuron [Fig. 2.3a]. This model has electronic analogous blocks for cell body axon hillock and axon of the nerve cell. The cell body is represented by an integrator, the axon-hillock by a monostable multivibrator, and the axon by a passive RC networks. The model also incorporates the absolute refractory period, relative refractory period, and accomodation and adaptation phenomenon of the actual neuron. With the help of this model it is possible to study the effect of variation of different parameters on individual blocks and on the whole neuron. This model is a very good aid for the bioengineers and neurophysiologists to study the various important functional characteristics of the actual neuron.

(ii) Electronic Model of Neuron Processes Including Feedback Through Renshaw-Cell [25] :

Saxena proposed a compact, reliable and inexpensive model to simulate the various important functional details of the actual neuron as mentioned above in (i). The most important feature of this model is that, it includes the model for local inhibitory feedback through the Renshaw cell as shown in Fig2.3 b. The Renshaw cell feedback loop is connected at one point on the axon. Since the output action potential pulses are distorted
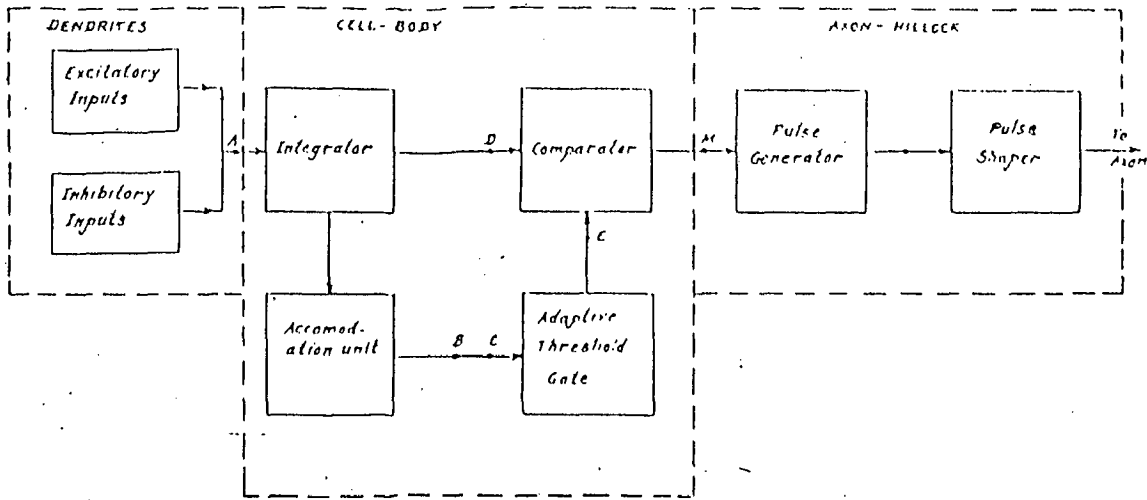
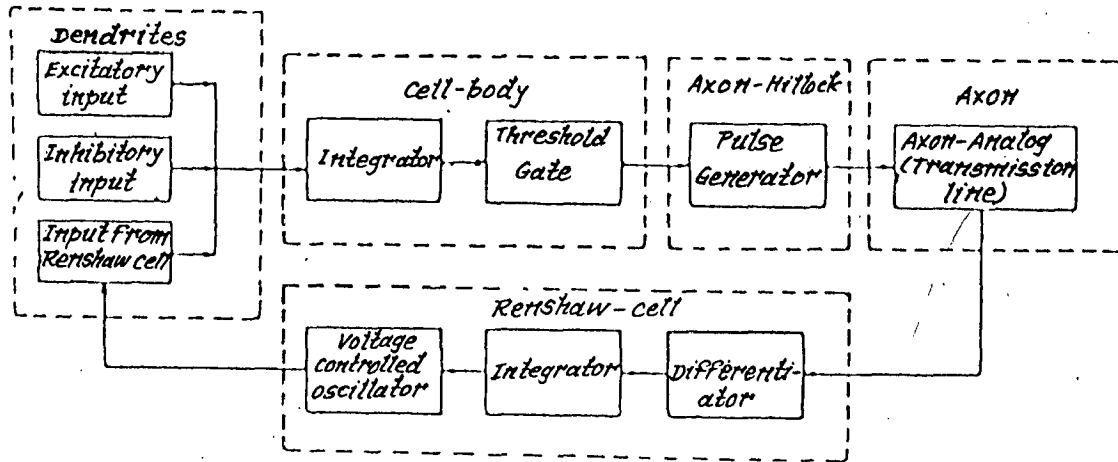FIG. 2·3(a) Block diagram of neuron model By Saxena [1977]

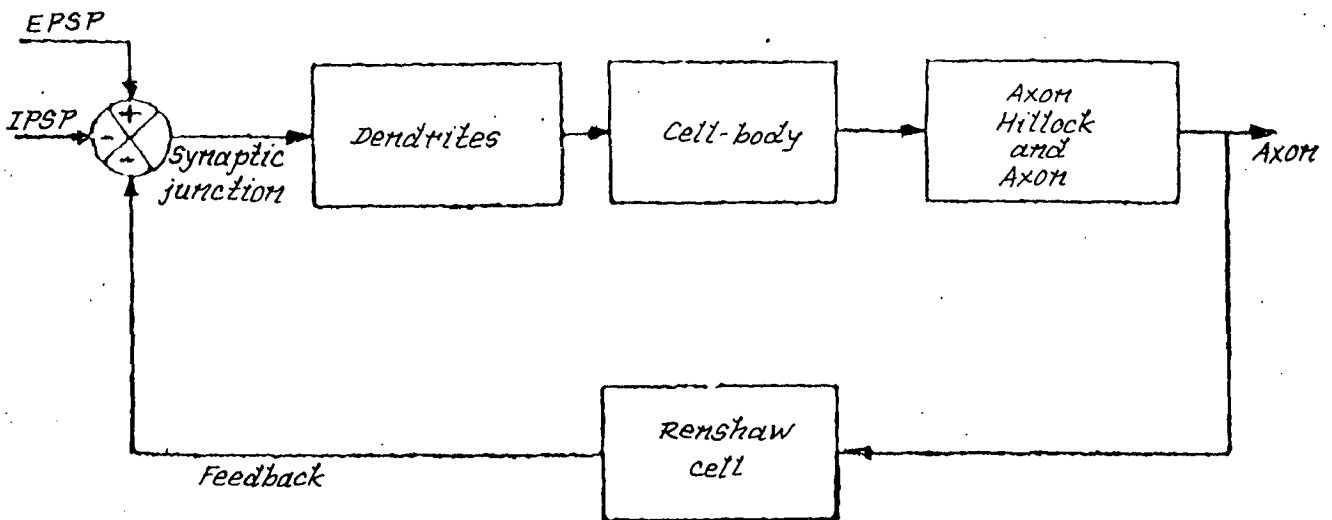FIG. 2·3(b) Saxena Model including Renshaw cell feedback [1979]

FIG. 2·4 Block diagram of neuron model By Chitore [1987]

while being transmitted through the axon analog the distorted pulses are passed through a differentiator, and then through an integrator. The output of the integrator is given, to a voltage controlled oscillator, whose output pulse frequency, is controlled by the signal coming from the integrator. The output from the VCO is connected as inhibitory input to the integrator, i.e., cell body of the neural analog. This model helps to study the effect of the inhibitory input from the Renshaw cell on the responses of the whole nerve cell.

2.5 CHITORE MODEL [27] : An Electronic Representation of Neural Transmission Process :

In this model presented by Chitore et al., the neuron and it's feedback loop is divided into, dendrites, cell body, axon hillock, axon, and Renshaw cell [Fig. 2.4]. The cell body representation consists of an integrator, threshold gate and temperature dependent threshold level. As the temperature changes the value of the threshold changes, which is similar to changes in resting potential of the actual neuron with temperature. The resting potential at $19^{\circ}C$ is taken to be -80 mV. As the temperatures changes to $40^{\circ}C$, the value of resting membrane potential changes from -80 mV to -72 mV. If the resting potential decreases to a value of -60 mV, the action potential is generated, even when there is no input at that instant. To get this value of resting potential, a resistance of $10 \, \Omega$ and a thermosensor of $107 \, \Omega$ were used in the threshold gate circuit. This model helps to study the effect of variation of temperature on the responses of the actual neuron.

2.6 DENDRITIC COMPARTMENTAL MODEL OF NEURON BY POTTALA ET AL[34]:

In this model the authors have simulated the activities of an actual neuron treating that the dendrite is made up of several compartments. In this model there are four dendritic compartments and the fifth compartment corresponds to the Soma and the axon hillock.

The model is shown in Fig. 2.5. Here the dendritic compartments are given the inputs from the excitatory and inhibitory conductance generators. The simulated membrane voltage from the Soma and axon hillock compartment is given to an amplifier and comparator. The output action potential generated from the one shot is again used to generate the depolarizing and hyperpolarizing conductances which are in turn fed-back to the Soma and axon hillock compartment.

Thus this model is helpful to understand the manner in which the action potential and the de- and hyperpolarizing conductances are interdependent. This model can be used to study the spatial-temporal interactions among postsynaptic potentials and between postsynaptic potentials and action potentials. Using this model it is possible to show that a distally applied excitatory conductance change may have either an excitatory or an inhibitory effect on the model's firing, depending on it's timing relative to proximally applied inputs.

This model can be used to simulate the basic physiological phenomenon of the actual biological neuron.
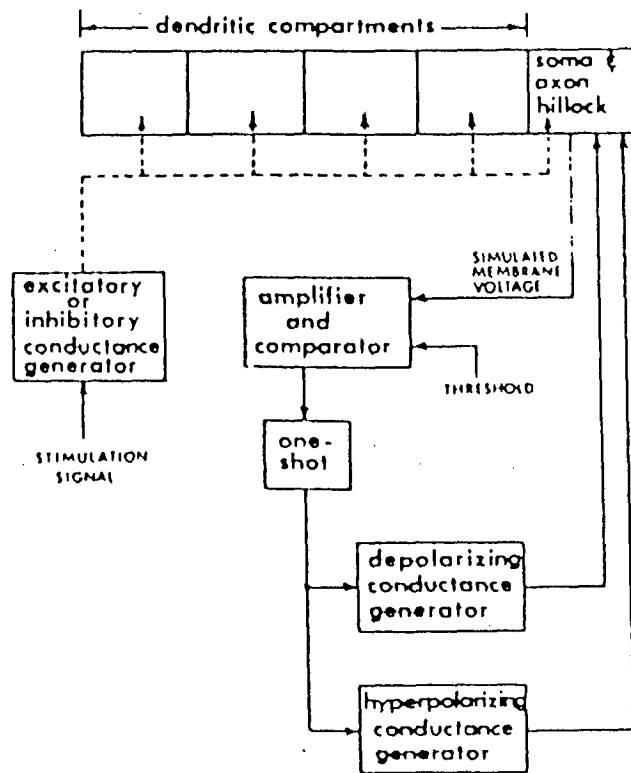
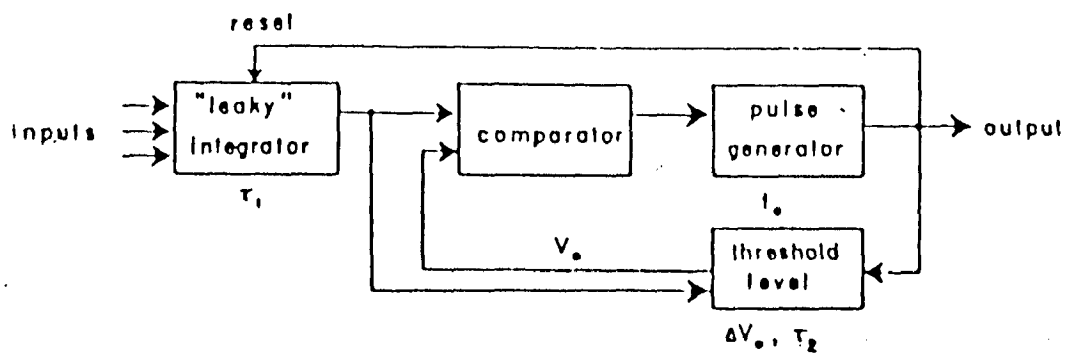FIG. 2·5 Block diagram of the neuron Model By Pottala

FIG. 2·6 Block diagram of the neural ahalog. By French and Stein

2.7 FRENCH AND STEIN MODEL [40] :

In this electronic analog of the neuron, the authors have incorporated, the dendritic, cell-body, threshold, and axon-hillock equivalences corresponding to the integrator, threshold gate, and pulse generator in the electronic circuit : [Fig. 2.6]. This model also incorporates the accomodation and adaptation phenomenon of the actual neuron by an inverting amplifier and adaptive threshold gate. It also incorporates the absolute refractory period and relative refractory period. It is possible to change both the refractoriness at will. With this it is possible to study the interaction between the excitatory and inhibitory inputs, the effect of the subthreshold inputs on the threshold of the analog for the next coming input signals.

Since this circuit is simple, and inexpensive components are used to construct the model, it serves as a good aid for simulating the activity of both single neurons and small neural systems.

2.8 A COMPARISON OF DYNAMIC AND STEADY STATE MODELS BY DAVID A.TELCHER AND DONALD R.McNEAL [29] :

The dynamic and steady state models are shown in Fig. 2.7. The model shown in Fig. 2.7a represents the dynamic model and the model shown in Fig. 2.7b represents the steady state model. The basic difference between the steady state model and the dynamic model is that, in the dynamic model the membrane conductance G_m at the node of excitation is allowed to vary in accordance with the generally accepted properties
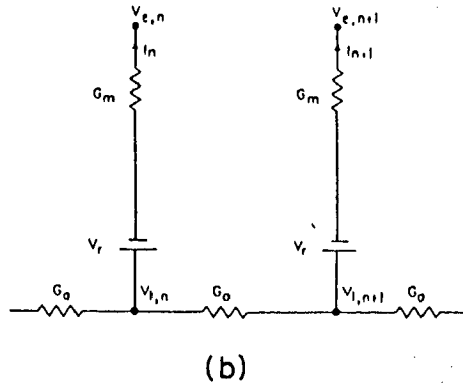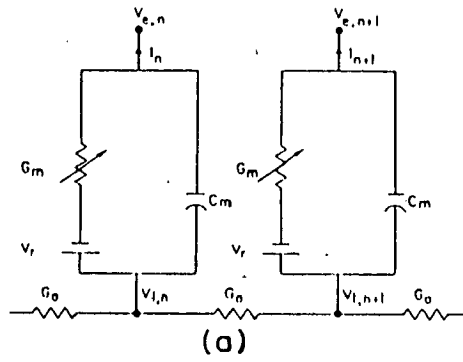
(a)

(b)

FIG. 2·7 Electrical network representations of a myelinated nerve
fiber (a) Dynamic Model By Mcneal (b) Steady-State Model By Bean
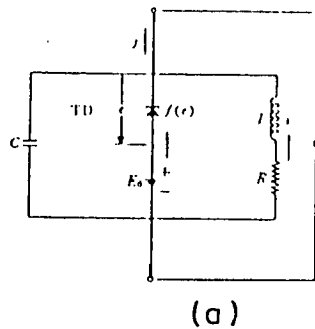
(compared By D.A. Teicher)

(a)

FIG. 2·8 An electronic simulator of the BVP model. By Nagumo
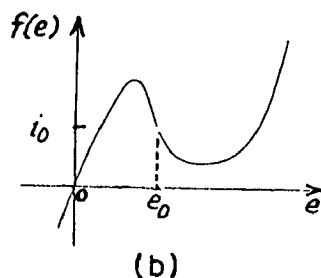

(b)

FIG. 2·8 The voltage-current characteristic of the tunnel diode.

as expressed by Frankenheansser and Huxley [56], where as in the steady state model the nodal membrane conductance G_m is assumed to be constant. The other difference is that, the nodal membrane capacitance C_m not taken in to consideration in the steady-state model, but in the dynamic model it is present. In both the models it is assumed that the fibers are myelinated and the myelin sheath to be a perfect insulator.

The important assumptions that are made in these models are that, (i) the nerve fiber is infinitely long (ii) the modes of Ranvier are spaced at regular intervals (iii) the medium external to the fiber is homogeneous and purely resistive. The constants used in these models are consistent and are equal to those used by McNeal [42].

For the purpose of analysis and comparison of the threshold values the authors have used the pulse durations of 10, 100 and 1000 µs, in both the models. The threshold values were calculated for these pulse durations for a fiber diameter of 20 µ and an internodal spacing of 2 mm. The electrode was positioned at various distances above the nerve fiber and at distances along the fiber axis of 0, 0.5 and 1.0 mm from the node. In this it is necessary to compute the thresholds from 0 mm to 1.0 mm along the axis of the fiber and at the remaining locations the same can be determined from the symmetry.

It has been found that the threshold values obtained for long pulse durations are closely agreeable, because the

solution of the steady state model is equivalent to the steady state solution of the dynamic model with the membrane conductance held constant. But the difference increases with the decreasing pulse durations. For most clinical applications 100 μs to 200 μs pulse durations are used. For this range, the comparison between the solutions is close enough, so that the steady-state model can be used for investigating the various configurations of the electrodes.

2.9 AN ACTIVE PULSE TRANSMISSION LINE SIMULATING NERVE AXON BY NAGUMO [50] :

In this model Nagumo et al., proposed an electronic model to simulate the active pulse transmission characteristics of the nerve cell axon. The electronic model presented here is based on the BVP (Bonhoeffer-Van der Pol) model and is shown in Fig. 2.8a. The voltage current characteristics of the tunnel diode are shown in Fig. 2.8b. This circuit used in their experiments comprised of $L = 4$ mh, $R = 70\Omega$, $E_o = 100$ mV, and $C = 0.01$ μF.

The authors used nine such circuits [Fig. 2.8a] in cascade, with a coupling resistance $r = 500\Omega$ as shown in [Fig. 2.8c]. The expected results were obtained. It was found that, the shaping action in respect of the signal height was completed at the first stage. The shaping action is respect to the signal width was very weak in comparison with that of the signal height.

The active line shows the following characteristics in the transmission of signals.

1. The circuit has a specific threshold value with regards to the height of the signal, and as a result of this the signals below the threshold value or noice are effectively eliminated during the course of transmission along the line.

2. This active transmission line model is capable of shaping the signal waveforms passing through it. In the sense that, this line has a specific pulse-like waveform peculiar to it; there by smaller signals are amplified, larger ones are attenuated, narrower ones are widened and those signals which are wider are shrunk during transmission through the line all approaching the waveform that is specific of the line.

3. The model of the line presented here is symmetrical. The signal transmission through the line is bidirectional. Hence if the signals are initiated from both the ends simultaneously, mutual annihilation of the pulses occurs at the centre. Bidirectional propogation will take place if the pulses are initiated at the centre of the line.

This line has a threshold and the pulse shaping ability. Hence this line can be used as a highly reliable pulse

transmission line. It also serves as a very good means for various kinds of information-processing systems. The line behaves similar to the living axon, but the representation is gross.

2.10 SENSORY EFFECTS OF TRANSIENT ELECTRICAL STIMULATION-EVALUATION WITH A NEUROELECTRIC MODEL, BY J.PATRICK REILLY [63] :

Reilly et al.,presented a neuroelectric model for the study and analysis of a myelinated nerve axon for the initiation and propogation of action potentials under a variety of extracellular electrical stimuli.

The model used in this work is basically that of McNeal [42]. The McNeal model uses a linear electrical circuit to represent each of several nodes of Ranvier, except for one excitation node at which the non-linear equations of Frankenheusser and Huxley are employed. But in this model the modifications are done to include the 'Frankenheusser - Huxley conductances at each of several adjacent nodes.

The equivalent circuit of the model is shown in Fig. 2.9. In this model the individual nodes of Ranvier are represented by the circuit elements comprising the transmembrane capacitance C_m, and resistance R_m, and voltage source E_r both in parallel with the transmembrane capacitance C_m. The voltage source represents the resting potential, which is negative with respect to outside. It is approximately of the order of 70 mV. The
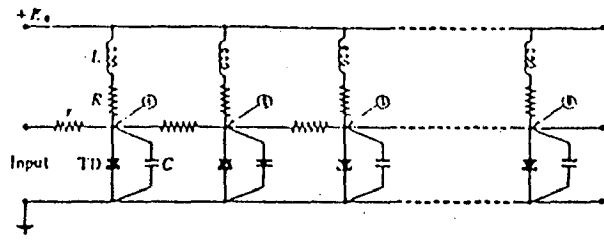
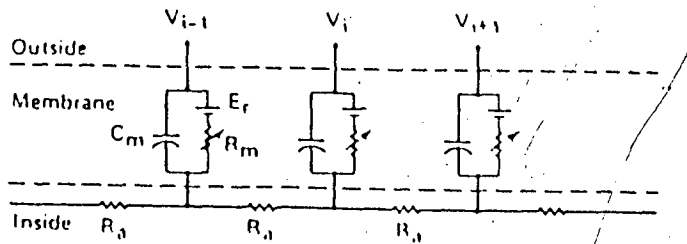FIG.2·8(c) Nine stages as in FIG.2·8(a) Cascaded

FIG. 2·9 Equivalent circuit model for excitable
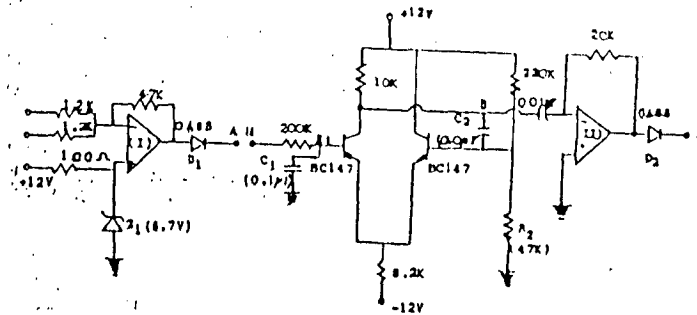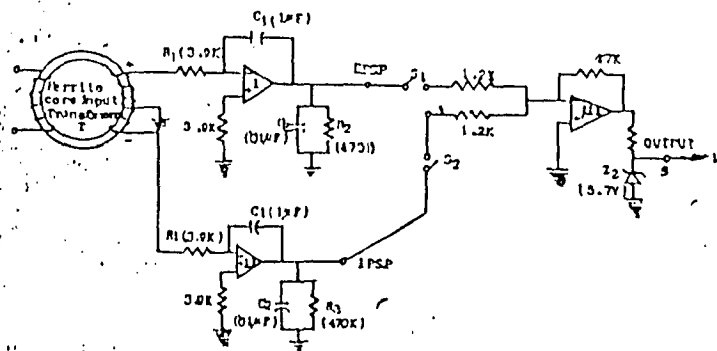membranes   By J.P. Reilly.

FIG.(a)

FIG.2·10 Models for (a) neural transmission and (b) Synaptic
transmission   By J.K.chowdhury et al.

nodal admittances are interconnected by the resistances R_a through the conductive intracellular axoplasm.

Here the myelin sheath is assumed to be a perfect insulator, and hence the nodes toward outside of the fiber are open. The voltages, V_{i-1}, V_i, V_{i+1}, external to the fiber, shown at the nodal locations are due to the stimulating current from the electrode. The voltage distributions used in this work assume isotropic current propogation from a point electrode, placed in a uniform medium.

The voltage at a radial distance r from the electrode is given by,

$$V(r) = \rho I / 4\pi r$$

where V   = the voltage relative to the electrode

      I   = the electrode current,

      ρ = resistivity of the medium.

In this model the authors have assumed a 20 μm fiber, and an internodal spacing of 2 mm. In the range of the neural fiber sizes, the fiber of 20 μm diameter represents the axon of a large myelinated neuron. It is assumed that the electrode is placed 2 mm away from the axon and is centred above it's central node.

The results of this model are compared with the data from human sensory experiments and from animal electrophysiological experiments and are found to be in good agreement.

2.11 AN ELECTRONIC MODEL FOR NEURAL TRANSMISSION OF INFORMATIONS BY J.K.CHOWDHURY et. al. [36] :

In this model the authors have incorporated the important functional details of the actual neuron, such as the threshold phenomenon and the all-or-none law, and the refractory period [Fig. 2.10 a].They also carried out the studies of constant d.c. signal input to the model. They found that for a constant d.c. stimulus above threshold, a repetitive discharge occurs within a neuron. This is because once the neuron discharges, it will not respond for some time, i.e., for the absolute refractory period and will there after respond to increased level of input signal, i.e. during the relative refractory period. But when there is, a maintained d.c. signal, every time , the threshold of the neuron returns to normal, if the maintained d.c. signal is above the threshold, the neuron with continue to discharge at every such time. They also found that the output frequency increases with the increase in the input d.c. signal. The frequency of discharge by a constant d.c. stimulus, depends mainly on two factors :

(i) duration of stimulation, to excite a neuron, and

(ii) the refractory period.

The authors also presented the circuit for the generation of excitatory and inhibitory postsynaptic potentials. [Fig. 2.10b]. The mechanism of synaptic transmission can be simulated by the cascade connection of Fig. 2.10b with the circuit of Fig. 2.10a.

In Fig. 2.10b two identical circuits have been used for the generation of excitatory postsynaptic potential (EPSP) and inhibitory postsynaptic potential (IPSP), which are infact mirror images of each other. The values of R_1 and C_1 in Fig. 2.10b have been chosen to simulate the rise time of EPSP and IPSP, which is of the order of 2ms. Similarly R_2 and C_2 have been chosen to conform to the decay time of the above potentials, which is of the order of 5 ms.

Here it is possible to obtain the excitatory and inhibitory inputs separately or simultaneously, at will, by applying a pulse voltage to the ferrite core input transformer T. This transformer has 3000 turns in both the primary and secondary, windings, and has a centre tap on the secondary winding.

In this model the EPSP and IPSP can be connected to the amplifier-III separately or simultaneously. The output of the op.amp. III is clamped to 5.7 V by the zener diode Z_2. For the purpose of simulating EPSP and IPSP, the amplitude of the pulse to the input transformer T should be such as to develop a voltage greater than 5.7 V at the output terminal S of the op. amp. III.

In these electronic models of Fig. 2.10a and Fig. 2.10b the authors could achieve the voltage scale of the order of 100 times of the actual potential occuring in mammalian nerve cells, and could achieve the time scale of the same order as the actual nerve cells.

2.12 LEWIS MODELS [64,49] :

(i) The Locus Concept and it's Application to Neural Analogs [64]:

The membranes of cell body or Soma, dendrites and axon are different in their properties. These are funtionally divided into different loci. But the responses of all these sections of a neuron integrate into one spike generator, and hence are lumped together into the one locus.

The input to the synapse are, a spike or a series of spikes originating from the presynaptic neuron. The presynaptic impulses are short (about 1 mS). In response to these the post synaptic membrane produces, postsynaptic potentials which show brief rise and decay very slowly (about 40 mS). These slowly decaying postsynaptic potentials are called ballistic potentials due to their analogy to the ballistic pendulum.

These pre-and post-synaptic potentials are shown in Fig. 2.11a. The simple RC-ballistic network is shown in Fig. 2.11b. For simulating this ballistic response, the author assumes the three independent parameters, the rise of the PSP, (Post Synaptic Potential), it's maximum amplitude and the decay or fall time of the post synaptic potential. The functional power of a neuron lies in it's ability to respond and integrate a single spike or a series of spikes coming from one or several adjacent neurons. The single neuron is capable of responding differently for different spike inputs, of different frequencies. It can also differentiate, the various types of incoming pulse patterns.
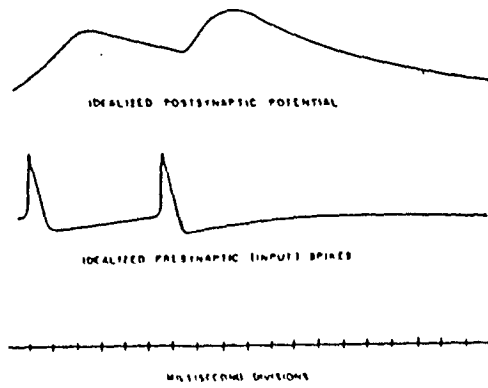
IDEALIZED POSTSYNAPTIC POTENTIAL

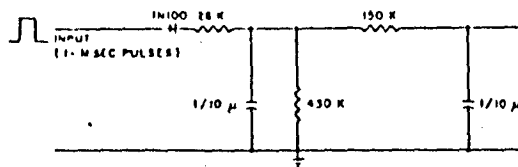IDEALIZED PRESYNAPTIC (INPUT) SPIKES

MILLISECOND DIVISIONS

FIG. 2·II (a) Postsynaptic ballistic potentials.

INPUT
(I - M SEC PULSES)
IN100 18 K
150 K
1/10 μ
430 K
1/10 μ

FIG. 2·II (b) Simple RC ballistic network

IDEALIZED POSTSYNAPTIC POTENTIAL

IDEALIZED PRESYNAPTIC SPIKES

FIG. 2·II(c) Facilitation

IDEALIZED POSTSYNAPTIC POTENTIAL

IDEALIZED PRESYNAPTIC SPIKES
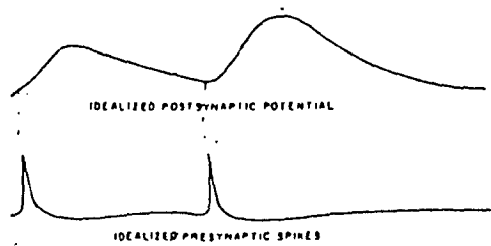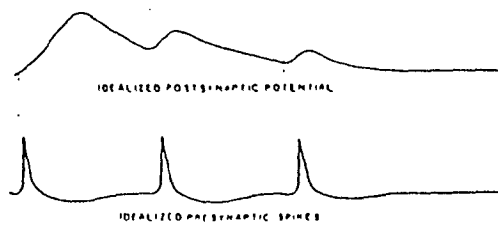
FIG. 2·II (d) Antifacilitation

In order to incorporate the above capabilities, there are two important mechanisms in the neuron. They are facilitation and antifacilitation. The consecutive presynaptic Spikes will generate a cumulative effect on the ballistic postsynaptic potentials.

Now suppose that, a synapse is at rest. Suddenly if a spike impinges on the resting synapse, a ballistic potential results from this spike. The amplitude of this ballistic potential is called as basic amplitude. Apart from generating a basic amplitude, the presynaptic spike also leaves some effect on the synapse so as to alter the amplitudes of the subsequent ballistic potentials. There are two possibilities in such a synaptic condition. In one, the first impulse conditions the synapse in such a way, as to enhance or facilitate subsequent responses, as show in Fig. 2.11c.

Thus, in the facilitating synapses, the amplitude of the ballistic potential due to any presynaptic spike is greater than or equal to the basic amplitude for that synapse. In the other, the first spike conditions the synapse in such a way as to reduce or contifacilitate the responses to the subsequent spikes; that is, in the antifacilitating synapse the amplitude of the ballistic potential is always less than or equal to the basic amplitude [Fig. 2.11d]. The corresponding circuits for facilitation and antifacilitation are shown in Fig. 2.11e and Fig. 2.11f, respectively. Some times it is possible that a facilitating synapse functions as antifacilitating and vice-versa. It is shown in Fig. 2.11g. Here a

second spike occurs quite close to the first one and is
facilitated, where as the third spike occurs relatively later
and is antifacilitated. But the amplitude of the PSP is greater
than that of the basic amplitude.

(ii) Using Electronic Circuits to Model Simple Neuroelectric
     Interactions [49] :

The Lewis model in this work is a combined represent-
ation of the findings of Eccles,and Hodgkin and Huxley. It is
shown in Fig. 2.11h. It is a circuit representation of a patch
of electrically excitable membrane contiguous with a patch
of subsynaptic membrane. The horizontal conductor on the top
of the circuit represents the conductive medium inside the
nerve cell; the bottom conductor represents the conductive
medium outside the cell. The four elements on the right of
the dashed line are the four shunt admittances across and
electrically excitable membrane according to the Hodgkin-Huxley
description. The three elements on the left are the three shunt
conductances across synaptic membrane according to the des-
criptions of Eccles.

Lewis further designed the electronic circuits to
simulate faithfully the seven elements of the combined system
shown in Fig. 2.11h. The capacitance C_M and leakage conductance
G_L of course were very easy to simulate. Simulation of the
potassium and sodium conductances, on the other hand, required
elaborate nonlinear, active filters to transform the simul-
ated membrane potential into the time-and voltage-dependent
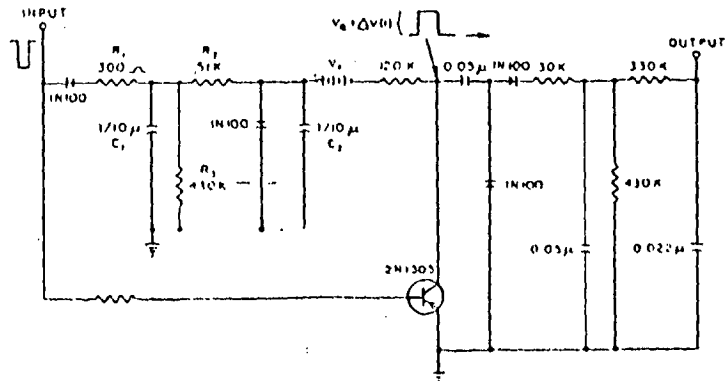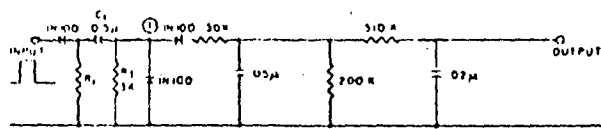
FIG. 2·II (e) Facilitating network
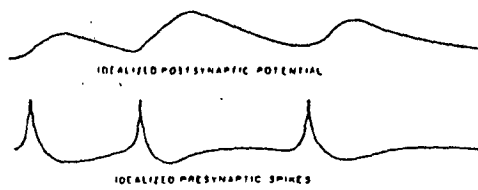

FIG.2·II(f) Antifacilitating network

FIG. 2·II (g) False antifacilitation

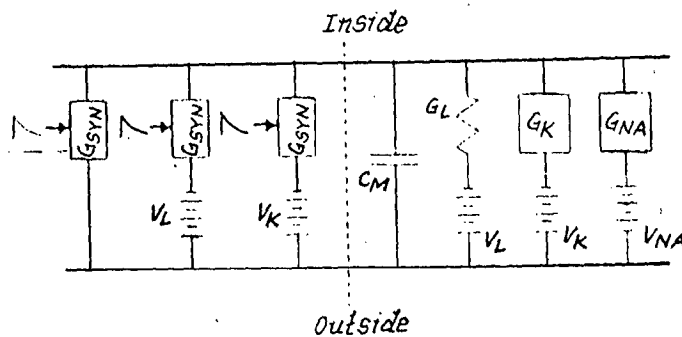FIG.2·II(h) A circuit representation of a patch of electrically
excitable membrane   By Lewis

FIG. 2·II (b,e,f,h) Lewis Models

conductance functions, specified by Hodgkin and Huxley. The
decaying exponential synaptic conductance functions were
simulated by simple RC filters, since the current through a
conductance is proportional to the product of the conductance
itself and the voltage across it, the simulated conductance
functions were transformed into equivalent conductances by
means of electronic multipliers. The complete electronic
model basically was a two-terminal network, with one terminal
representing the conducting medium inside the nerve cell and
the other terminal representing the conducting medium outside
the cell. Between the terminals were seven circuits connected
in parallel. The model was a point model in that it represented
a patch of membrane over which there was no variation of potential.
It may be considered to represent a patch of subsynaptic membrane
with a contiguous patch of spike-generating membrane, or it may
be considered to represent either a mosaic or a homogeneous
mixture of the two. Since the circuit elements are parallel these
configurations electrically are equivalent. With the parameters
of the elements on the right side of Fig. 2.11h, set to the values
specified by Hodgkin and Huxley, the synaptic responses of the
electronic model were examined. Each synaptic conductance had
two parameters : the magnitude of the conductance increment
per presynaptic spike, and the time constant of the conductance
decline. These parameters in conjunction with the three synaptic
conductances proved to be completely sufficient to account for
all of the synaptic degrees of freedom.

The author used these circuits to simulate single neurons and small neural nets. So such blocks were used to simulate a finite length of axon, and two such circuits were connected to simulate the interactions of single neurons and pair of neurons. These circuits required large number of components and were expensive to construct.

2.13 LIMITATIONS OF THE ABOVE MODELS :

From a study of the above models, the following observations have been made.

Hodgkin and Huxley [24] applied voltage steps across isolated patches of squid-axon membrane, and observed the time course of the current in each case. They resolved the current into a capacitive component and three ionic components (potassium-ion current, sodium-ion current, and leakage current due to all other ions). Defining the driving force for each of the three ionic currents as the difference between the actual voltage across the membrane, and the voltage at which that particular current reversed. Hodgkin and Huxley described their results in terms of the equivalent circuit [Fig. 2.1]. Their experiments indicated that the equilibrium potentials V_K, V_{Na} and V_L, the capacitance C_M, and the leakage conductance G_L were constant but that the equivalent potassium conductance G_K and the sodium conductance G_{Na}, were functions of membrane potential and time. From their data, they were able to formulate explicit descriptions of G_K and G_{Na} which were valid

within the constraints of their experiments, that is valid for stepwise changes of membrane potential. Also, their experiments did not cover the variations of V_{Na}, V_K and V_L with time. They predicted virtually every aspect of the squid axon spike in minute detail, but this would lead to complex circuit in simulation of entire nerve cells.

In the models by Guy Roy [26], Potdala et al. [35], and Lewis [49], [69], the inner details of the membrane currents are simulated, at different parts of the neuron. The neuron, as far as the information processing is concerned, is not simply one of many uniform elements in a large nervous system, but rather, a complex system in itself - a system of loci. In their concept each locus is viewed as a basic information processing unit, and the spatial distribution of the loci within a single neuron would determine it's over-all characteristics. To examine these detailed physiological characteristics, with electronic models, then, it is necessary to simulate each type of locus individually and connect the resulting networks together in various configurations to simulate entire neurons. With these networks for simulation of ionic current fluxes across the membrane would lead to complex and costly set up. Moreover, a very large number of this type of simple systems may have to be explored before we can evaluate the information processing capabilities of more complex real neurons. Hence these are not suited for simulation of couplete neurons and the neural nets.

In the model by J.P.Reilly [63], the different geometries of neurons and different excitation functions to which the neurons are expected to be exposed physiologically [2,4] are not considered. In the present analytical part of the work these aspects are taken into consideration.

In the S.C.Saxena models [23, 25] and in the model by Chitore [27] most of the important characteristics are incorporated. But the axon is simulated by a passive RC network. In the present model the passive axon network is replaced by an active patch membrane model to make it more close to the axon of the real neuron.

In the model by Nagumo [50], the active transmission line has it's own characteristics waveform. With this it becomes difficult to simulate a wide variety of output action potentials. In the present model this difficulty is overcome since the active axon has no such characteristic waveform of it's own, but it is governed by the input excitation pulse.

In the model by Teicher [29], there is nothing specific to be said. It is only a comparison work. A point, is taken from this work, to supplement, the analytical part of the work here, that, the neuroelectric model of myelinated nerve can serve as both steady state and dynamic model for analysis upto 200 μS.

In the model by Freinch and Stein [40], the accomodation is provided for both EPSP's and IPSPs. But in the actual

neurons accomodation comes into play only for EPSPs [5,12]. In the present model the accomodation is provided only for the EPSPs as in the real neurons.

In the model by J.K.Chowdhury et al. [63], the synaptic potentials are simulated without using an axon analog. But in the present model, the active membrane patch circuits of the active axon, are used along with synaptic junction circuits to simulate the Excitatory- and Inhibitory post synaptic potentials to make it more close to the real neuron.

All the above models are valuable, because they provide a translation of the neuronal physiological concepts into a more definite and logical language, but still they lack in representation of some important characteristics of neuron. Effort has been made in this dissertation to include some more features compared to existing models of neuron.

**

CHAPTER - III

ELECTONIC MODEL OF NEURON

3.1 INTRODUCTION :

A number of circuits have been designed to simulate the characteristics of nerve cells [23] - [27]. The complexity of the circuits increases with the increase in the number of variables in order to describe accurately the time course of the ionic currents that flow across nerve membranes [49]. Although such a complete description may be valuable, it can also be of disadvantage in some applications for the following reasons.

1. A quntitative description of the ionic currents is available only for a limited number of neurons, so there is likely to be a large number of undetermined and often undeterminable parameters for all other cells.

2. A complete description would involve not only parameters to model the ionic currents of a unit membrane, but also parameters to describe the spread of this voltage along the often geometrically complex processes of a nerve cell [35].

3. Many of the complexities may sometimes be ignored if one is primarily interested in the function of a nerve cell in transferring information from one part of the nervous system to another rather than in the mechanisms underlying this function.

The electronic models of the neuron can widely be classified into two groups. The first one representing those electronic neuron models in which only the inputs and outputs of the neuron as a whole are incorporated and the second one includes such of those electronic neuron models in which only a part of the neuron is simulated e.g. a model simulating the patch of excitable membrane, of the neuron.

The examples of the first group of the neuron models are those developed by Guy Roy [26], French and Stein [40], S.C.Saxena [23], [25], D.S.Chitore [27], Hallgren [46], Thexton [41]. The main feature of these models is that the input terminals are separated from output action potential generating part, by the intermediate processing blocks of the neuron analog. In these models provisions are often made for accomodation, subthreshold behaviour, generation of the action potential and the refractory periods. In all the models mentioned above the whole neurons are modelled rather than any specified part of the neuron. As a result of this, it becomes very difficult or almost impossible to observe in these models, the changes and interactions occuring as a result of say generation and propogation of action potentials, the interactions taking place at the synaptic junctions, and electronic spread of subthreshold potentials within the neuron cell etc.

In the past a number of circuits have been developed [35,46,64] to simulate the patch of active and/or passive

membrane of the neuron, in order to improve the observability
of the various parameters mentioned in the above paragraph,
which are confined to only parts of the neuron. These localized
changes, however, contribute to the functional features of
neuron as a whole. One branch of such modelling centres around
the development of neuristors [38,47,48]. The neuristors are
the ladder networks which generally have uniform character-
istics. It is an exception to the specialized synaptic conn-
ections. In the development and analysis of neuristors the
emphasis has been given to analysis of propogation of pulsat-
ile signals, that is, action potentials. In the neuristors the
analysis of the subthreshold events can not be carried out.
The models by Crane [38], Cote [47] [48], Mattson [51], and
Nagumo et al.,[50] are of this type.

These models incorporate the details at the ionic
current levels. Here it is possible to observe and identify
the changes in transmembrane potential due to the ionic currents,
and further the generation of action potential and passive
responses to the subthreshold stimuli can be observed. But the
models incorporating these details are highly complex ones.
The model developed by Lewis [49] belongs to this class of
models. In this model individual circuits have been used to
represent the voltage and time dependent variations in the
transmembrane ionic currents. The models given by Guy Roy [26]
and Pottala et al.,[35] are of similar type. As these two
models incorporate less details compared to the model of
Lewis [49], they are comparitively less complex too.

In the present model the interest is in developing
a neural analog which should give an accurate functional rep-
resentation of nervous activity with few undetermined para-
meters. The important features to be included in this model
are as follows :

1. The use of integrated circuits may facilitate the
    construction of a reliable, compact, and reasonably
    inexpensive device.

2. Operational amplifiers will be used extensively
    so that the signals at each stage bear a simple
    mathematical relationship to those at earlier
    stages, permitting comparisons with actual neuronal
    data.

3. Circuitry will be chosen to include   important
    neural properties, like adaptation, accomodation
    and Renshaw cell feedback processes in the model.

3.2   BLOCK DIAGRAM OF THE NEURAL ANALOG :

Fig. 3.1(a) shows the block diagram of the neural analog.
The integrator sums the inputs from number of sources over a
period determined by it's time constent. This time constant
represents the membrane time constant. This is often effect-
ively slowed by passive spread of signals from the dendrites
or by a transmitter whose action decays with a time constant
long compared to the membrane time constant. The length of
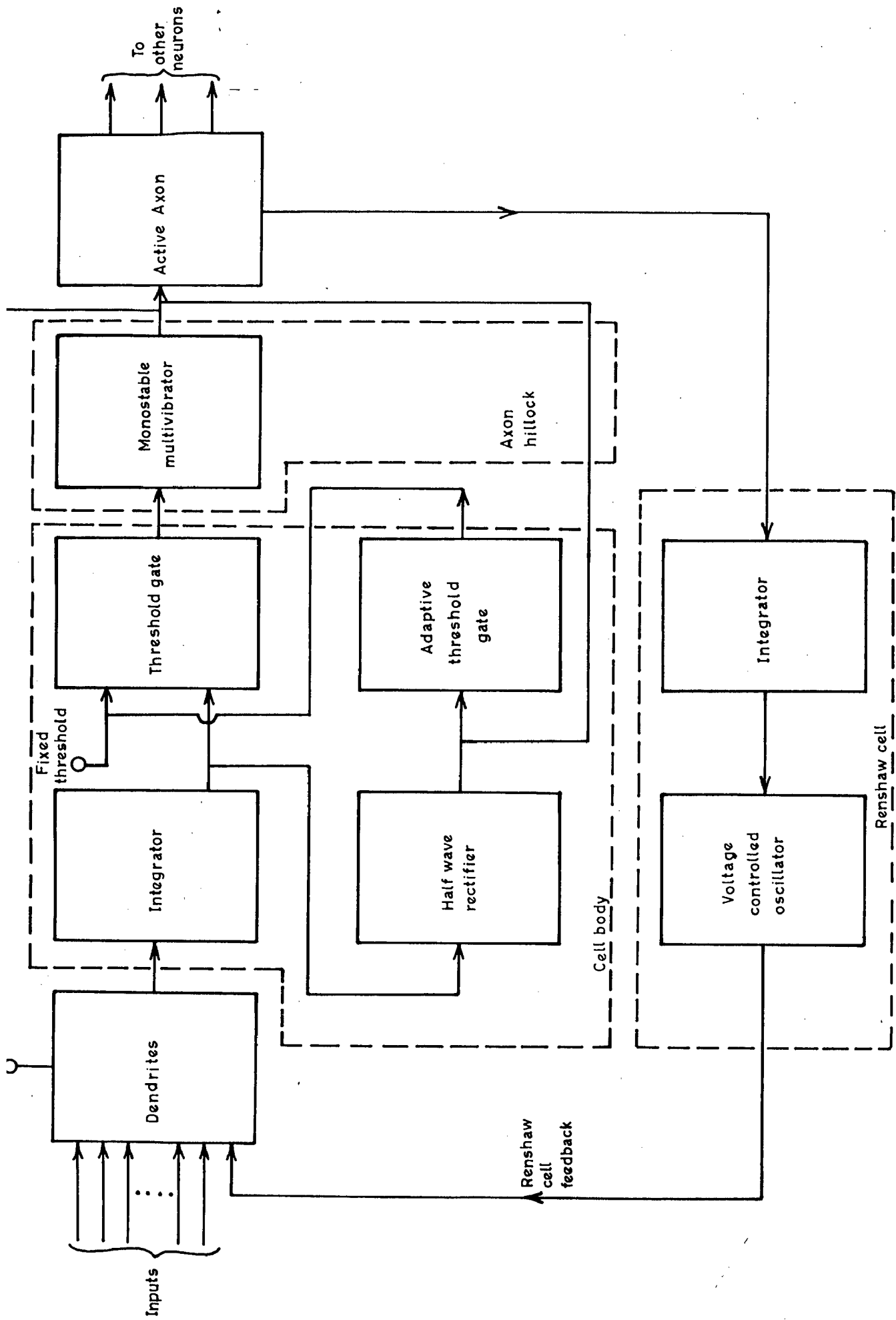the dendrite, i.e. the distance between the synaptic junctions

Fig. 3.1(a): Block diagram of the neural analog.

and the cell body is represented by a resistance. The integrated voltage is continually compared to a threshold voltage, and when this exceeded a pulse is generated at the output. Subthreshold voltages are fed forward to increase the threshold level with another time constant so that the analog model incorporates accomodation to slowly rising inputs.

The cell body is represented by an integrator, half-wave rectifier, adaptive threshold gate and a comparator. The axon hillods is modelled by a pulse generator. The axon is given the transmission line analogy. Renshaw cell consists of a differentiator, integrator, a voltage controlled oscillator (VCO) and active patch membrane circuit simulates the active axon.

3.2.1 Circuit Details Of The Neural Analog :

The integrator sums up the inputs from number of sources. The gain of each input can be varied by switching the value of it's input resistor. The detailed circuit is shown in Fig. 3.1(b). There is also a continuously variable bias input which in the absence of other inputs produces a steady frequency of output pulses. The presence of the resistor and capacitor in parallel in the feedback path provides the time constant of the integrator, which is variable over a wide range. A time constant of 1 ms is used in this model. This time constant represents the cell membrane time constant. Depending on it's base voltage, the switching transistor T1 has a resistance either very high or very low compared to the feedback
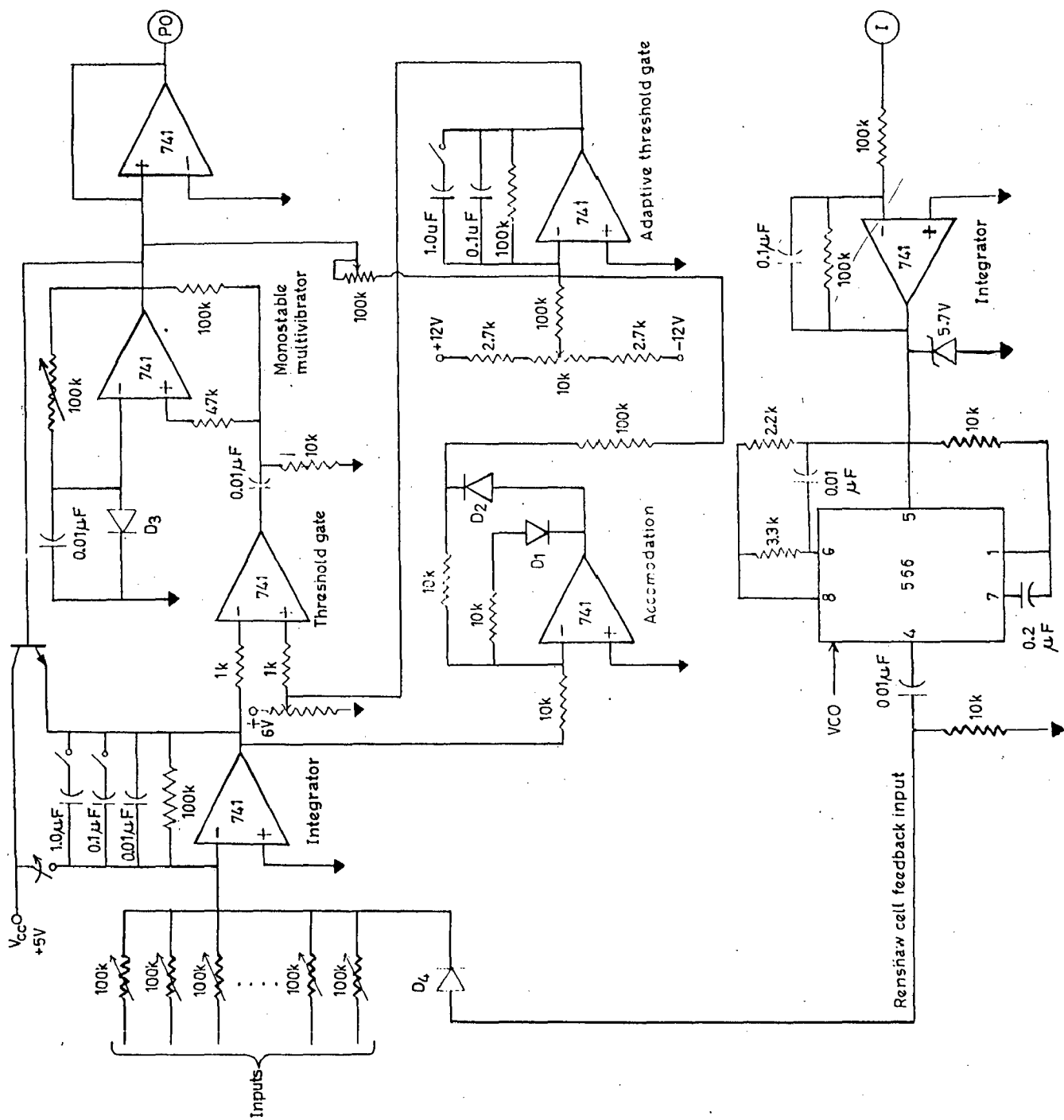
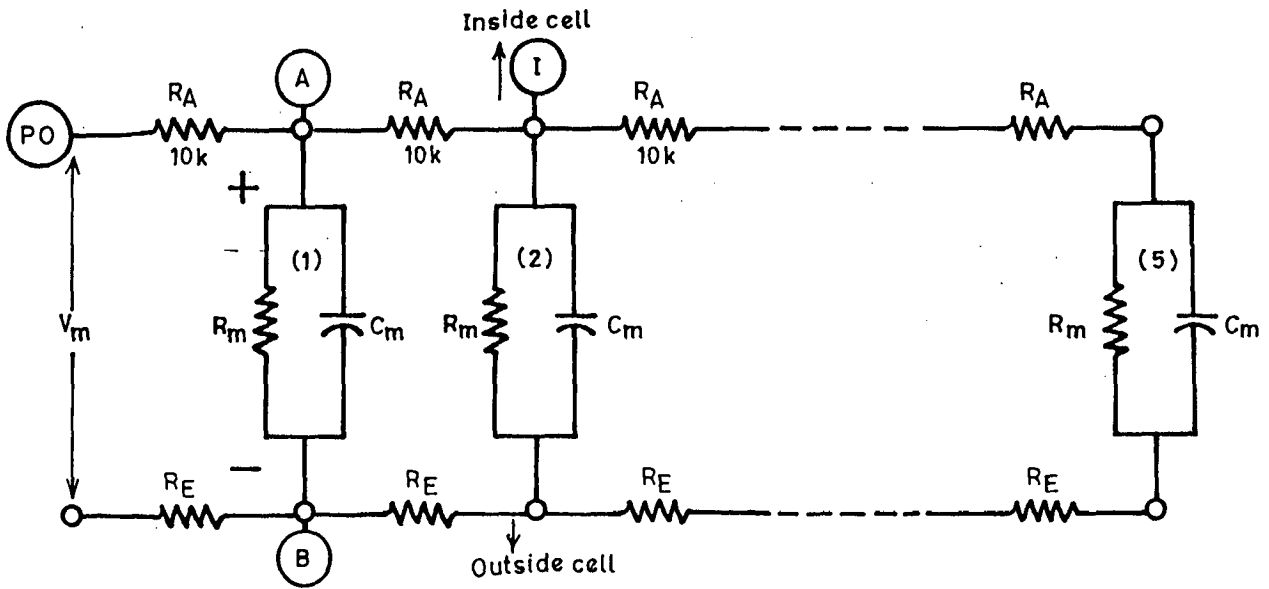Fig. 3.1(b): Detailed circuitry of the neural analog (contd. on next page).

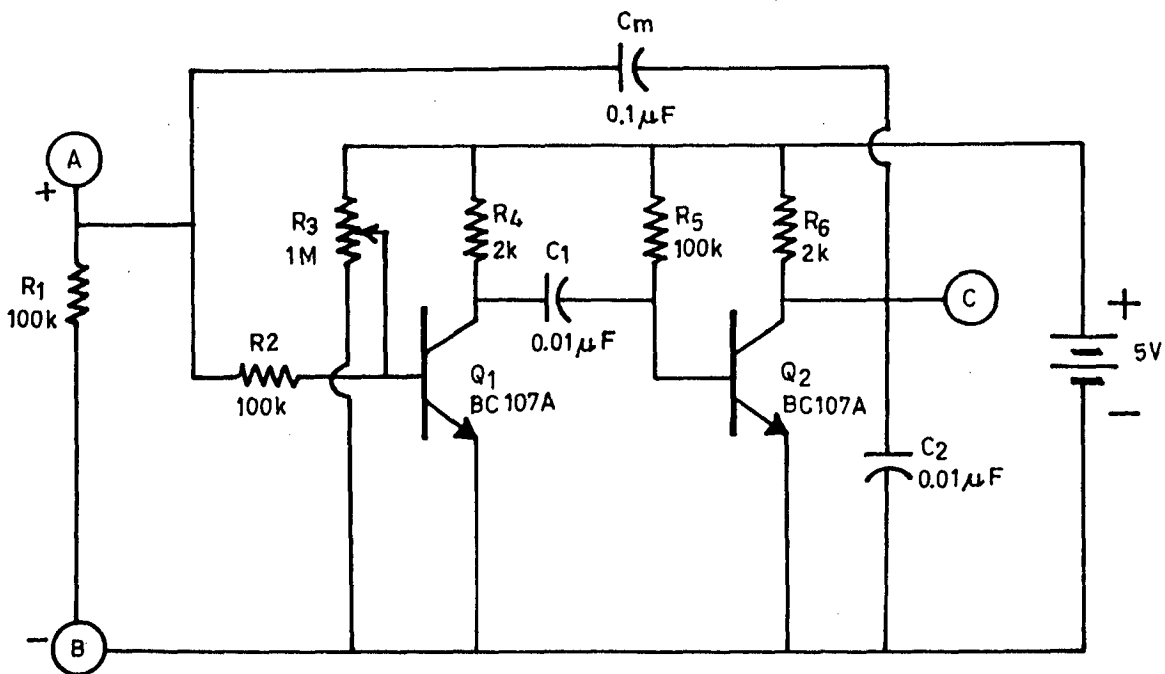Fig.3.1 (b) : (continued) Ladder network representation of the active Axon.

Fig.3.1 (b) : (continued) Active membrane patch circuit;
[A block of the active Axon (above)]
Terminal Ⓒ relates to Fig.3.3 (a).

resistor. When the transistor is on (low-resistance) the integrator is reset and held at ground. The comparator is a high-gain openloop amplifier which switches from logi level 1 to a logi level 0, when the output of the integrator exceeds the threshold level. This produces an output pulse in the monostable circuit, with a time duration determined by it's time constant. This pulse is used to reset the integrator, after having it's level changed by T2 so that it switches T1 hard on or off. The pulse is also used in another integrator to increment the threshold voltage. This will make it more difficult for another pulse to be discharged unless the interval between the pulses is long compared to the time constant of the adaptive threshold gate. A typical value of 10 ms is taken in this model. The capacitance of 1 microfarad and 10 microfarad can be connected in place of 0.1 microfarad for getting the values of relative refractory period as 100 ms and 1 second respectively. When the rate is large, the effects of successive pulses will be sumed up to produce a progressive decline in pulse frequency corresponding to neural adaptation. This adaptation simulates the effects of action potentials on subsequent activity and is essentially a form of negative feedback.

Subthreshold activity can also depress excitability through an additional pathway fed forward from the output of the integrator to increase threshold. The gain of this pathway is also adjustable.

In the neural analog the excitatory (EPSP's) and inhibitory (IPSP's) inputs are summed in the integrator. The integrated value is then compared with a reference threshold voltage and, if this is exceeded, the neural model fires, i.e., it generates an output pulse and resets the integrator to zero. The integrator voltage is, however, also fed through a half-wave rectifier and summed with the positive reference threshold voltage at yet another stage which inverts that sum. The total (now negative in sign) is then presented to the comparator so that if the original excitatory inputs do not produce an integrator output voltage of more than reference threshold sufficiently rapidly, a temporary rise of threshold at the comparator is obtained. This model exhibits accomodation effect of a neuron when subjected to subthreshold excitation. On the other hand, inhibitory inputs to the neural model displace the integrator voltage away from threshold which depresses or prevents firing. The output of the half-wave rectifier subserving the accomodation is zero for positive inputs. This means that only excitatory (positive) inputs to the neural model (negative output from the integrator) operate through the accomodation unit and change threshold that means the threshold adapts to the changes as in actual neurons [7]. Inhibitory inputs render the neural model less excitable, Since, the difference between integrator output voltage and overall threshold voltage is increased [41].

Each output pulse resets the integrator and holds it at it's initial value until the end of the pulse. The pulse

duration therefore determines the absolute refractory period of the analog i.e. the period during which a second pulse can not be generated. An absolute refractory period of 0.5 ms is used in the present model ($T = 0.7\ R_1C_1$) [14]. Each pulse also increases the threshold by a small amount ΔV and effect decays with the time constant of the adaptive threshold gate, which is 10 ms in this model. If this time constant is short compared to the normal intervals between pulses, it determines the relative refractory period in which a second pulse is less readily elicited. However, if this time constant is long (as in this model) compared to the intervals between pulses, these increments in threshold accumulate and produce a progressive slowing of the discharge. This time constant determines the time course of adaptation.

The output voltage of the integrator is given to the comparator for it's comparison against the threshold level. When the integrator output voltage exceeds the reference level (threshold) the threshold gate changes it's state and the monostable circuit generates an output pulse. If the integrator output voltage is less than the threshold, the comparator gives no response. This incorporates the all-or-none relationship of the neuron [5].

There is a threshold level for an input to cause excitation, and as the input voltage is increased beyond this point, the frequency increases toward a limiting value determined by the absolute refractory period.

The output pulse generated by the monostable circuit travels down on the resistance capacitance analog of axon. As the length of axon increases the number of resistance capacitance groups also increases. It is assumed as a long transmission line which is uniformly distributed over the entire length. No processing takes place in the axon analog. It only shows the elapse of transit of the signal in the axon.

The shape of the output pulses is distorted due to the transmission of pulses along the entire length of the passive axon, analog. To overcome this, the axon is connected to a differentiator and then to an integrator. The output of the integrator is given to the voltage controlled oscillator. In this neural analog IC-566 is used as a voltage controlled oscillator. The voltage controlled oscillator with the connections made as shown in the Fig.3.1(b) will generate, an output frequency given by,

$$f_o = \frac{2(V^+ - V_c)}{R_1 C_1 V^+}$$

where V_c is the control voltage and R_1 is in the range of $2K\,\Omega$ to $20\,K\,\Omega$, and V^+ is the supply voltage.

The output of the VCO is connected as an inhibitory input to the dendrites. It decreases the sum of the overall inputs. The increase in the output frequency of VCO decreases the excitation input to neuron.

3.3 ACTIVE AXON ANALOG :

The active axon model which will be presented in this work is developed to study the propogation of action potential along the axon, effect of subthreshold graded potentials and interactions taking place at the synaptic junctions. This basic active patch membrane model which is capable of replicating the above characteristics, can be used in cascade to model neural network to simulate the behaviour of the whole neurons. In this model it is possible to vary the threshold at different locations as in the actual neuron and study it's effects.

With the circuit presented here, it is possible to construct a large number of models, to combine them to study the behaviour of the whole neurons at a low cost.

3.3.1 Model For The Excitable Patch Of Membrane :

The biological neurons are generally, represented in the form of ladder networks as shown in Fig. 3.2(a) [8,33,29]. In this type of ladder networks representation, the whole neuron is divided into a number of blocks. The protoplasmic resistance is represented by the resistance R_A. R_E represents the extracellular resistance. The transmembrane resistance is represented by R_m and the transmembrane capacitance is represented by C_m. The circuit shown in Fig. 3.2(b) models the active membrane patch.
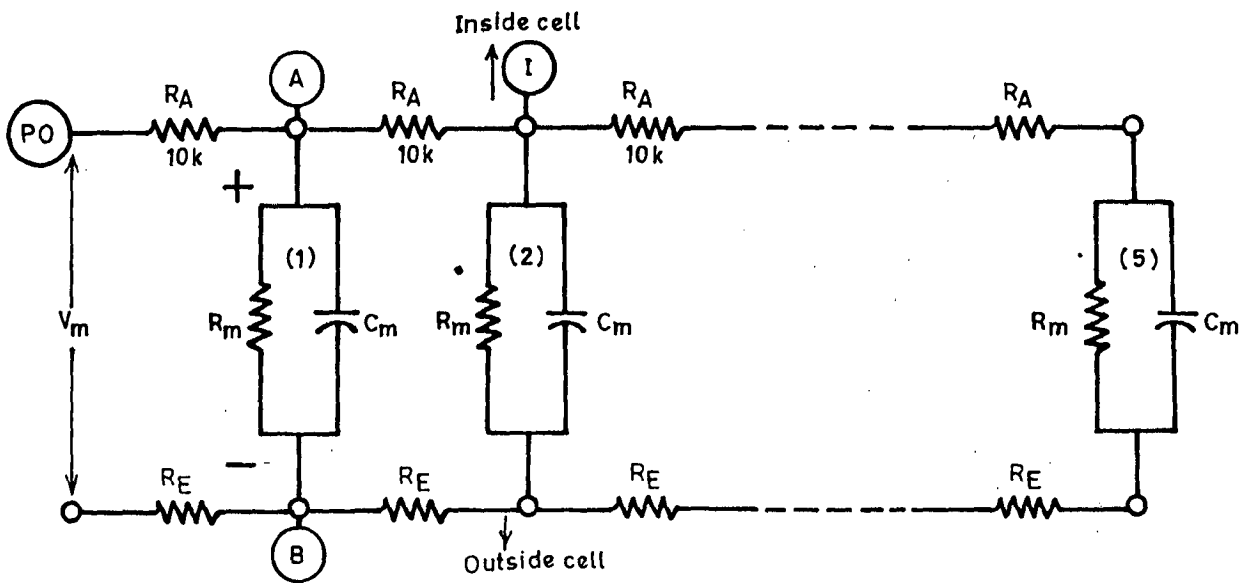
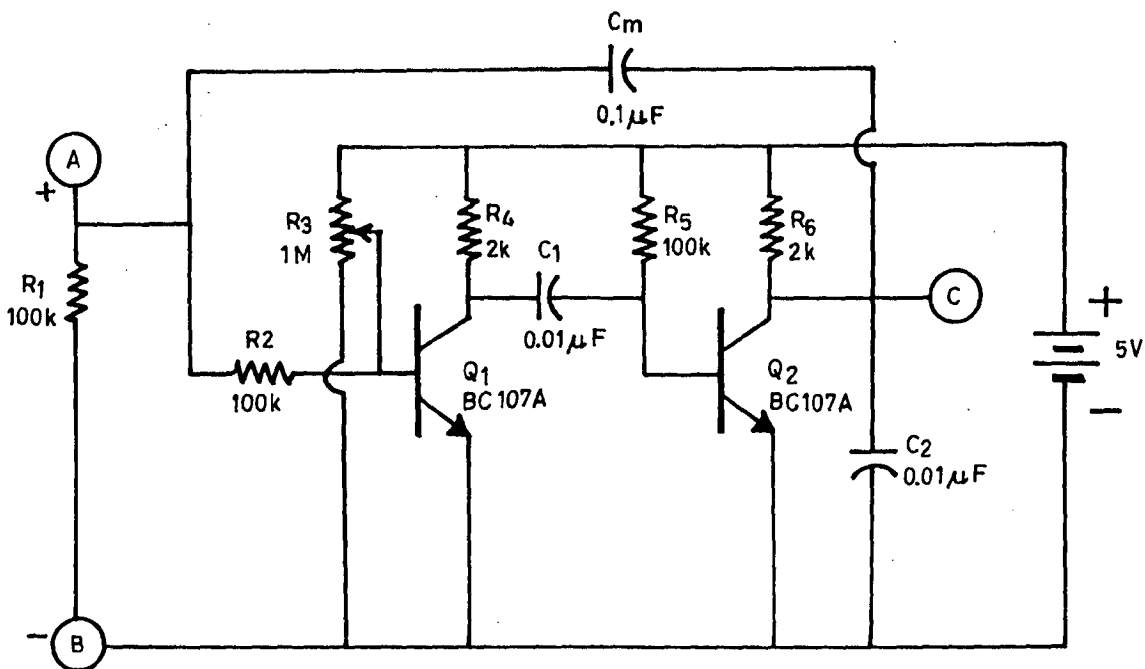Fig.3.2(a): Ladder network representation of the active axon.

Fig.3.2(b): Active membrane patch circuit.
Terminal Ⓒ relates to Fig.3.3(a).

This active circuit used to represent the transmembrane resistance R_m and the transmembrane capacitance C_m is derived from the collector coupled astable multivibrator configuration. Here a large resistance (R_2) is used in the base of the transistor Q1. This circuit can operate as both an active circuit to represent the active features of the active membrane patch and axon, and as passive circuit to represent passive features of any communication cable having the equivalent parameters. This active and/or passive operation of the circuit can be achieved by varying the setting of the 1MΩ potentiometer connected between the base-emitter terminals of the transistor Q1. The passive operation of the circuit is used to study the passive propogation of response for the subthreshold graded stimuli.

3.3.2 Functional Details Of The Circuit :

The axoplasmic and extracellular resistances are established by fixed resistances of appropriate values. In the model presented here R_A (= 10 KΩ) is used, to represent the axoplasmic resistance [9] [39]. The resistance offered by the extracellular medium is extremely low (almost zero) hence resistance R_E is assumed to be zero in this case [9] [29]. Initially the 1MΩ potentiometer (R_3) in Fig. 3.2(b) is set in such a way that it biases the transistor Q1 into cut off when there is no signal input at the terminal A, the node of the axon. When the transistor Q1 is in the off state, the

resistance R_3 biases the transistor Q2 in saturation, because of the high output at the transistor Q1.

When the resistance included by the $1M\Omega$ potentiometer (R_3) between the base-emitter terminals of transistor Q1 is zero, any amount of signal input i.e., action potentials which is nothing but the transmembrane potential V_m, will not make the transistor Q1 to conduct. This is equivalent to setting the threshold voltage for the patch to a very high value. Under these conditions when the transistor Q1 is in off state and the transistor Q2 is in the saturation state, the impedence seen looking into the terminals A – B is then a capacitance C_m. This is in series with the saturation resistance of the tranisistor Q2, which is negligibly small. This C_m is now in parallel with the equivalent resistance which can be given by the following relation [20]. It is represented by R_m as in Fig. 3.2(a).

Therefore,

$$R_m = (R_1)(R_2 + \frac{R_{3a} R_{3b}}{R_{3a} + R_{3b}}) / (R_1 + R_2 + \frac{R_{3a} R_{3b}}{R_{3a} + R_{3b}})$$

where $R_{3a} + R_{3b} = R_3$

As long as we set $R_{3b} = 0$ the transistor Q1 is always in cut – off since V_{BE1} is always set to zero. So, until the transistor Q1 is in cut – off and transistor Q2 is in saturation, the active circuit in Fig. 3.2(b) is represented by the passive components C_m and R_m in parallel and behaves

similar to a passive RC - cable of equivalent values. When a small value of R_{3b} is introduced between the base-emitter terminals of the transistor Q_1 to set a small voltage V_{BE1} at the transistor Q_1, and if this is still insufficient i.e., less than 0.7 V in this case, then the circuit can be represented by the same passive components R_m and C_m in parallel. But now with the introduction of R_{3b} at Q_1, the transistor Q_1 can start conducting when there is some input signal, i.e., when there is an increase in the transmembrane potential V_m, causing the V_{BE1} to increase to a value sufficient for driving the transistor Q_1 in to conduction. The value by which the transmembrane potential V_m i.e., the value by which the excitatory input at the terminal 'A' has to increase is here referred to as the threshold of the patch membrane. Hence by varying R_{3b} it is possible to vary the magnitude of the input signal required to make Q_1 conducting. In other words the threshold at the various patches can be independently varied, since each patch is represented by a individual block. This feature can be used to simulate the non-uniform distribution of the excitability within the neuron.

When the transmembrane potential V_m is sufficiently high to cause the transistor Q_1 to start conducting then the output of the transistor V_{CE1} becomes low. This low output from the transistor Q_1 will make the transistor Q_2 to go to off state. As a result of this the output V_{CE2} of the transistor Q_2 becomes high. This change in voltage is communicated

to the point 'A' via the capacitor C_M. This will further increase the transmembrane potential V_m at the point 'A'. This condition of Q_1 into conducting state and Q_2 into the off state will continue until the time R_5C_1 becomes discharged. Once R_5C_1 is discharged, the transistor Q_2 is again set into saturation. This change over in the states of the transistor Q_1 from cut off to conducting and again to cut off state and that of transistor Q_2 from saturation to cut off and again back to saturation is an astable oscillation, which gives rise to an output of pulsatile nature. It is possible to control the width of pulsatile output by varying the R_5C_1 product. Also the repetition rate of the output pulses can be controlled by varying the R_mC_m product. Hence in this circuit by appropriately setting the various parameters like R_5C_1, R_mC_m, and R_3,R_{3a},R_{3b}, the pulsatile output from this circuit can be made to match the action potential output from the biological neurons.

In the present work 5-blocks of individual patch membrane circuits Fig. 3.2(b) are connected together as shown in Fig. 3.2(a). Here R_A = 10 KΩ is selected and R_E is set to zero. By including a small value of R_{3b} at all the patch membrane blocks a small value of V_{BE1} can be set, but not sufficient to make the transistor Q_1 to conduct when there a signal input at the terminal 'A' the circuit functions as explained in the earlier paragraphs and gives the active responses, thereby generating a pulsatile out put, which is equivalent

to the action potential in the actual neurons. This action
potential will propogate down the axon analog without any
attenuation, since the circuit is operating in the active
mode. This active operation of the patch membrane circuits
results in the action potential of the same magnitude to be avai-
lable at all the 'A' points on the length of the axon. This is
similar to the action potential of the same magnitude observed at
different nodes of Ranvier over the entire length of the axon.

When the circuit is made passive by setting R_{3b} to zero,
it's responses are similar to that of a passive RC - cable
having the equivalent RC parameters. As a result the pulse
i.e., the action potential, applied at one node will appear
at the next node (point A), with increased width and reduced
height. This response is similar to the response of the axon
as passive RC communication cable.

3.3.3 Circuit To Simulate The Synaptic Junctions :

In the actual biological neurons the communication
from one neuron to the other takes place through the special-
ized junctions known as synaptic junctions. The axon makes
synapse with the dendrites and cell body of the other neurons
which are known as axo-dendritic and axo-somatic synapses. In
a rare event the axon makes synapse with the axon itself
known as axo-axotic synapses. The synaptic junctions are
unidirectional in conduction. The synaptic potentials -
excitatory or inhibitory flow from the terminal arborization
of the axon of one neuron to the dendrides and cell body of

the other neuron but not in opposite direction. Also the
action potential originating from a axon billock travels away
from the cell body of that neuron [9]. Depending on the type
of the synaptic junction - excitatory or inhibitory the same
action potential results in to an excitatory or inhibitory
presynaptic potentials. These in turn are converted into small
excitatory postsynaptic potential (EPSP) or inhibitory post-
synaptic potential (IPSP), by the appropriate transmitter
substance released by the synaptic vesicles. These are briefly
rising and slowly decaying potentials, whose sum if exceeds
the threshold of the next neuron, another action potential
results [5] [6] [45].

The transistor circuit shown in Fig. 3.3(a) simulates
the similar features of the synaptic junctions. The membrane
patch model circuits shown in Fig. 3.2(b) are used as pre-
synaptic and postsynaptic membrane patches. In the present
work one block [Fig. 3.2(b)] is used as a presynaptic cell
and another block is used as a postsynaptic cell. The points
B and C correspond to those same points in Fig. 3.2(b), which
is used as a presynaptic cell. The same V_{cc} is connected in
this circuit also as in the circuit shown in Fig. 3.2(b).
The extracellular point B of both the presynaptic and post-
synaptic circuit are connected. When point C of the synaptic
circuit [Fig. 3.3(a)] is connected to the same point on the
presynaptic circuit [Fig. 3.2(b)], then EPSP and IPSP outputs
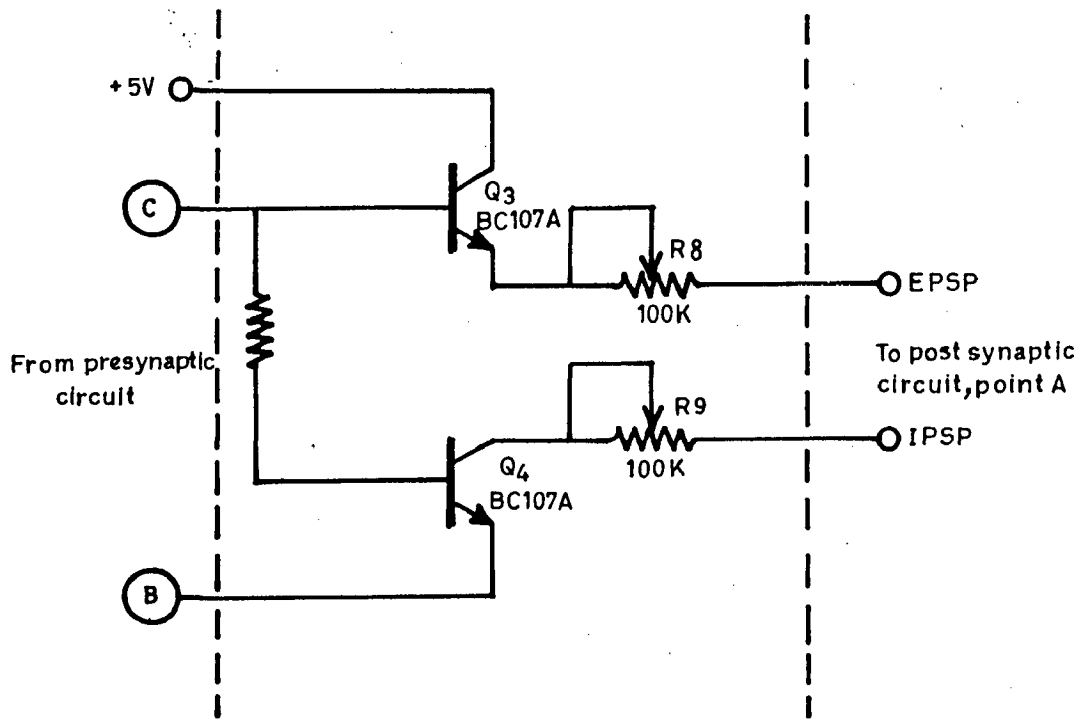are generated at the corresponding output terminals of the

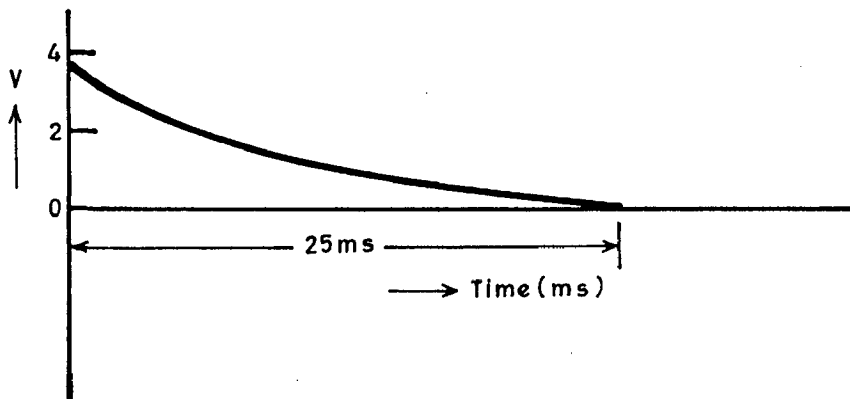Fig.3.3(a): Excitatory and inhibitory synaptic terminal circuit.
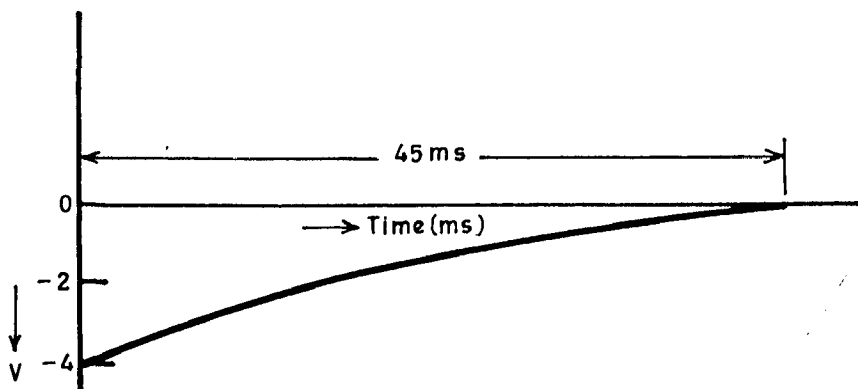

Fig.3.3(b): Typical EPSP.

Fig.3.3(c): Typical IPSP.

synaptic circuit. The typical EPSP and IPSP outputs observed
in the present circuit are shown in Figs. 3.3(b) and Fig.
3.3(c) respectively. The EPSP or IPSP output terminal of the
synaptic circuit is connected to the input terminal A of the
postsynaptic circuit. Accordingly an EPSP and/or an IPSP is
generated at the output point C of the postsynaptic circuit.
An EPSP means a depolarizing stimulus applied to the next
neuron and an IPSP means a hyperpoolarizing stimuli applied
to the next neuron. The size of the EPSP can be controlled by
varying R_8 and that of IPSP can be controlled by varying R_9.

3.4 TESTING OF THE NEURAL ANALOG :

The electronic circuit shown in the Fig. 3.1(b) was
fabricated and tested for the electrical characteristics of
the actual neuron as discussed below.

1. There is a threshold level for an input to cause
    excitation, below which no action potential is
    generated. All the threshold and above threshold
    inputs, excite the neural analog and an output
    _ action-potential is observed.

2. The integrated output voltage is compared contin-
    ually, with the reference threshold, voltage and
    if this is exceeded, the neural model fires, i.e.
    if generates an output pulse and resets the inte-
    grator to zero. The integrator output is, however,
    also fed through a half-wave rectifier, and is
    summed with a positive reference threshold voltage

at yet another stage. The total is presented to the comparator, so that if the original excitatory inputs do not produce an integrator output voltage of more than reference threshold sufficiently rapidly, a temporary rise of threshold at the comparator is obtained. This models the accomodation effect of the neuron when subjected to excitation insufficient to cause firing. The output waveforms at the halfwave rectifier and the integrator are shown in Fig. 3.4(a) and in Fig. 3.4(b). The effect of accomodation on the amplitude and frequency of output action potential is shown in Fig. 3.4(c)

3. Each output pulse resets the integrator and holds it at it's initial value until the end of the pulse. The pulse duration therefore determines the absolute-refractory-period of the analog, ie., the period during which a second pulse can not be generated. In the present model an absolute refractory period of 0.5 ms is obtained.

4. Each pulse is also used to increase the threshold by a small amount ΔV_o and the effect decays with the time constant determined by the time constant of the adaptive threshold gate. If this time constant is short compared to the normal intervals between pulses, it determines a relative-refractory -period, in which a second pulse is less readily
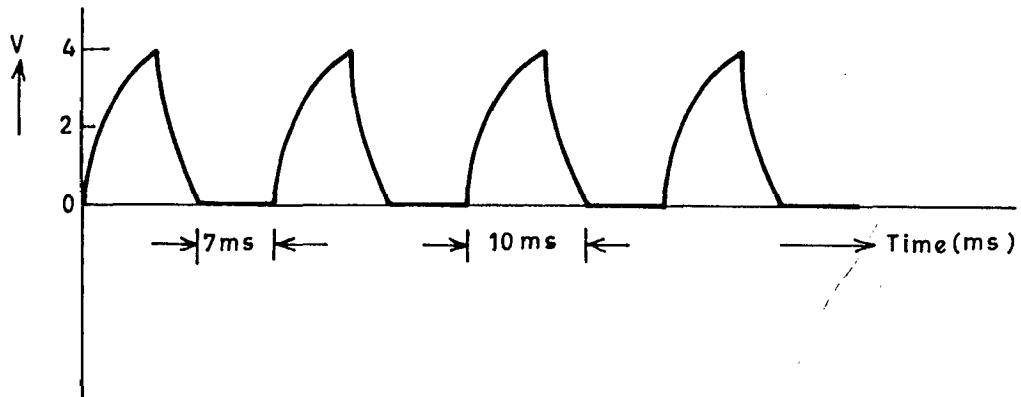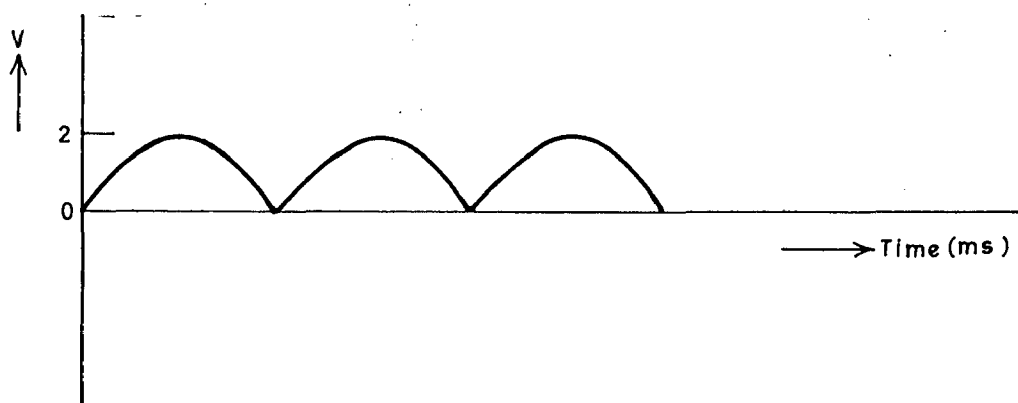
Fig.3.4(a): Output of the half-wave rectifier.

Fig.3.4(b): Output of the integrator (of accomodation path)
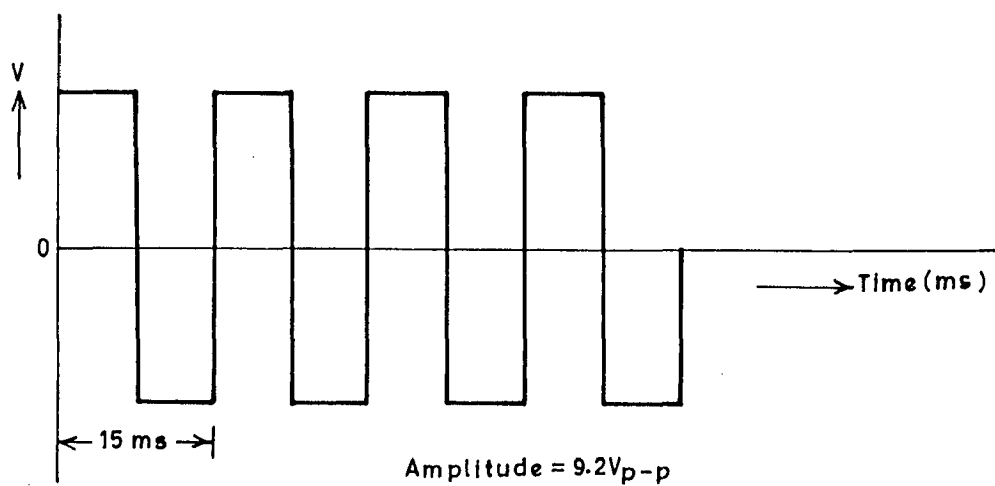

Amplitude = 9.2V_{p-p}

Fig.3.4(c): Output pulse with accomodation connected.

elicited. In the model presented here a relative refractory period of 10 ms is simulated.

5. The output pulse is also used in the adaptive threshold gate to increment the threshold voltage. This will make it more difficult for another pulse to be discharged unless the interval between pulses is long compared to the time constant of the adaptive threshold gate. When the rate is large, the effects of successive pulses will sum and produce a progressive decline in pulse frequency corresponding to neural adaptation. This effect is shown Fig. 3.4(d).

6. The output from the voltage controlled oscillator, fed back as inhibitory input to the integrator. This decreases the overall sum of the inputs and prevents the over excitation of the neural analog. This models the inhibitory feedbacks phenomenon from the Renshaw cell in the actual neuron. The effect of Renshaw cell inhibitory feedback on the amplitude and frequency of output action potential is shown in Fig. 3.4(e). The output pulses from the VCO are shown in Fig. 3.4(f).

7. The output of the integrator is given to the threshold gate for it's comparison against the reference level.When the integrator output exceeds reference level i.e., the threshold, the comparator
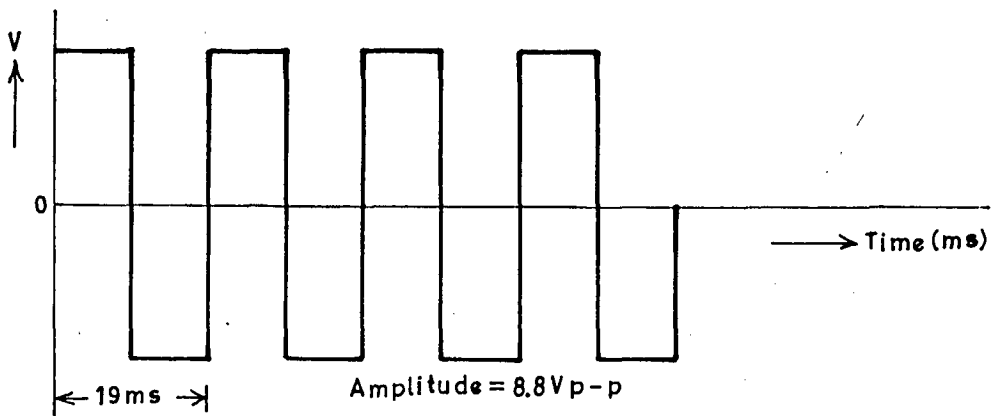
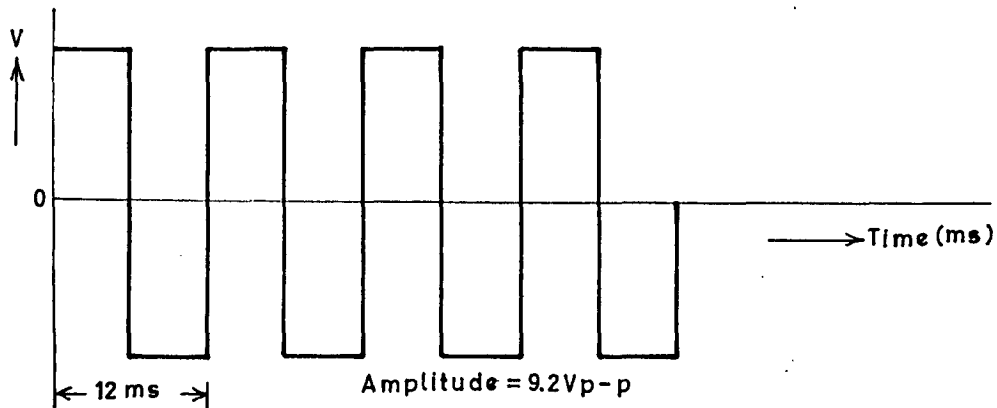Fig.3.4(d):Output pulse with the adaptation
feedback connected.

Fig.3.4(e):Output pulse with Renshaw cell
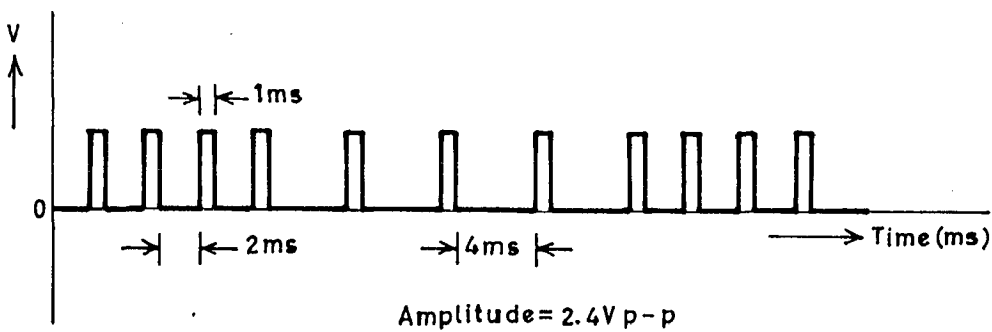feedback input connected.

Fig.3.4(f):Output of the VCO.

changes it's state, and causes the generation of
an output action potential from the monostable
multivibrator. If the integrator output is less
than the reference level, the threshold gate
gives no response, so that there is no output
action potential generated from the monostable
multivibrator. Thus the model incorporates the
all-or-none relationship of the actual neuron. In
the present model a threshold of 250 mV is used at
the threshold gate.

8. The frequency response of neural analog was tested,
    as shown in TABLE - I. As the frequency of the
    signal at the input of the neural analog is
    increased gradually the output pulses are observed
    for the period satisfying the absolute refractory
    period of the analog. The output pulses are obser-
    ved up to 2000 Hzs of the input signal frequency
    which corresponds to an absolute refractory period
    of 0.5 ms. The absolute refractory period can be
    varied by varying the resistance and capacitance in
    the feedback path of the op-amp., in the monostable
    multivibrator. As the absolute refractory period
    is increased the frequency response of the neural
    analog is reduced as in the actual biological
    neuron.

TABLE - I

Input signal frequency (Hz)	Output action potential
50	Present
100	Present
150	Present
200	Present
250	Present
300	Present
350	Present
400	Present
450	Present
500	Present
⋮	⋮
1000	Present
1050	Present
⋮	⋮
1950	Present
2000	Present
2050	Absent
2100	Absent

9. The active axon analog model was tested by giving a square wave input of $4V_{p-p}$ and frequency 15 Hzs, at point 'A' of stage - 1 analogous to an action potential resulting from a neuron model. Since this input is above threshold, the membrane patch model responds actively and the squar wave (analogous to the action potential) is transmitted without attenuation to the successive patch models from the each preceding block. The waveform observed at point 'A' from stage - 2 to stage - 5 is shown in Fig. 3.4(g). It is exactly similar to the input at point 'A' of stage - 1, both in frequency and amplitude.

10. The output waveform at point 'C' for stages 1 to 4 was observed. It is shown in Fig. 3.4(h). This is connected to point 'C' on the synaptic junction circuit for producing the excitatory postsynaptic potential (EPSP) and the inhibitory postsynaptic potential (IPSP). The EPSPs and IPSPs observed at the synaptic terminals are shown in Fig. 3.3(b) and Fig. 3.3(c) respectively. These resemble to the excitatory and inhibitory PSPs produced in the actual neurons.

11. The EPSP or IPSP output terminal of the synaptic circuit is connected to the input terminal 'A' of the postsynaptic circuit. Accordingly an EPSP or
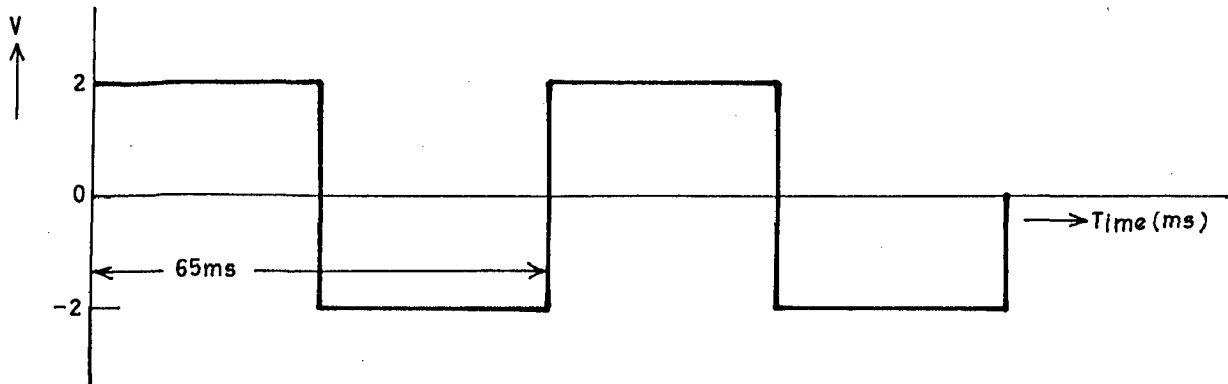
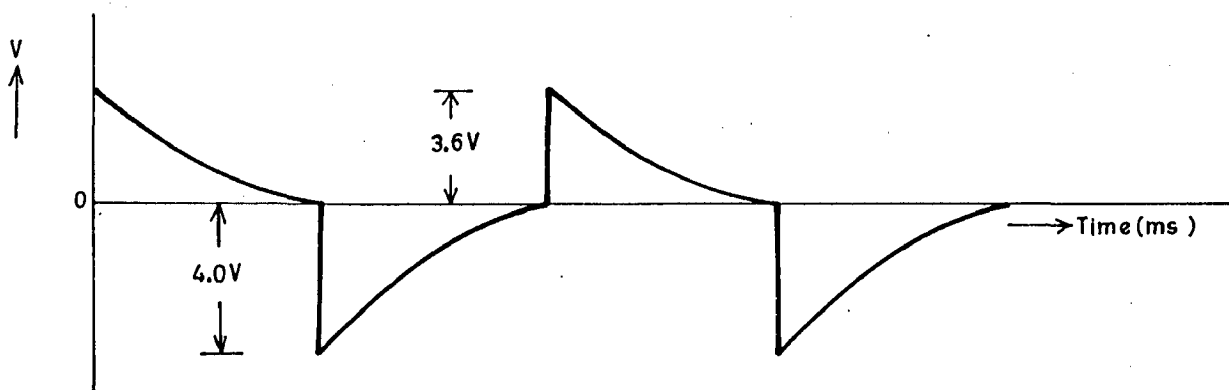Fig.3.4(g): Signal at point A for stages 2 to 5.

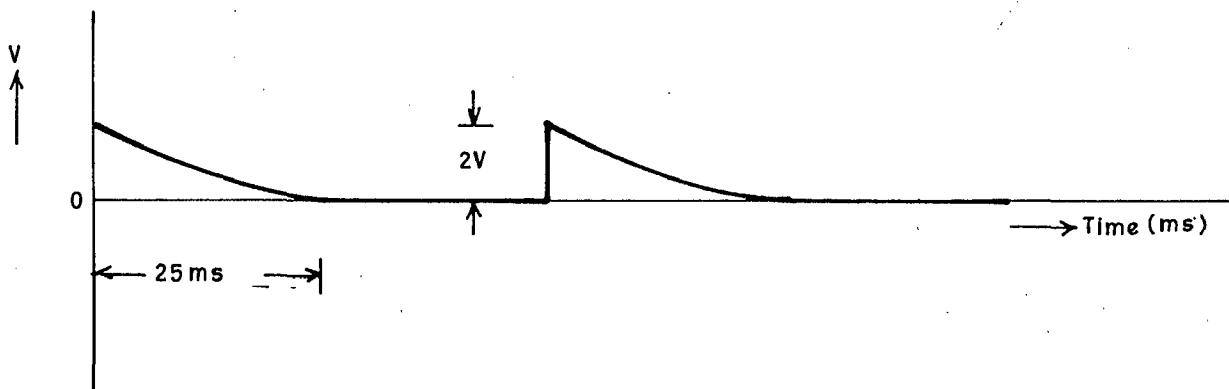Fig.3.4(h): Signal at point C for stages 1 to 4.

Fig.3.4(i): Signal at point C of stage 5 for EPSP input at it's point A.
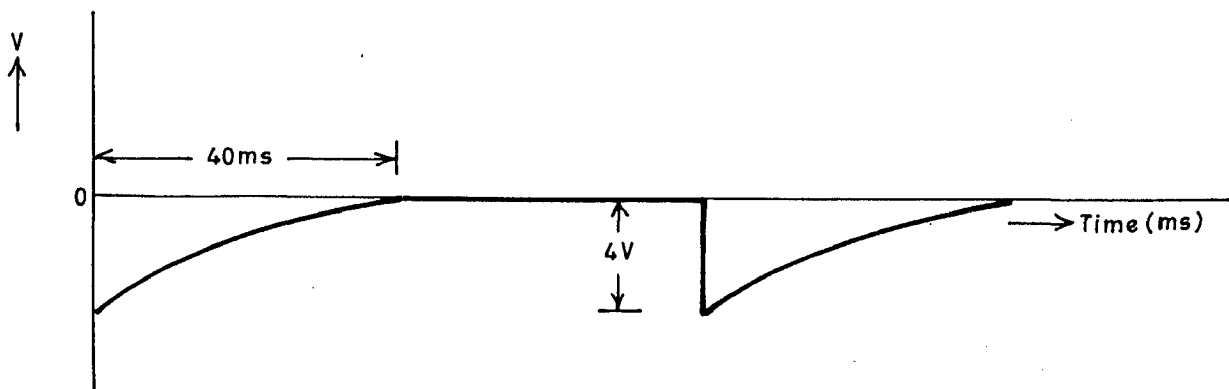

Fig.3.4(j): Signal at point C of stage 5 for IPSP input at it's point A.

IPSP is generated at the output point'C'of the postsynaptic circuit. An EPSP means a depolarizing stimulus applied to the next neuron and an IPSP means a hyperpolarizing stimulus applied to the next neuron. The size of the EPSP can be controlled by varying R_8 and the size of the IPSP can be controlled by varying R_9. The EPSPs and IPSPs observed at the output terminal'C'of the post-synaptic circuit are shown in Fig. 3.4(i) and Fig. 3.4(j) respectively. They are similar to the input excitatory and inhibitory - PSPs as in the living neuron.

12. The waveforms at the different stages of the neural analog model are shown in Figs. 3.4(k) to 3.4(q) at the end of this chapter. Fig. 3.4(k) represents the input to the integrator. Fig. 3.4(l) gives the output of the integrator. The output of the threshold gate is given in Fig. 3.4(m). The input to the Monostable Multivibrator is given in Fig. 3.4(n). The output pulses from the Mono-stable Multivibrator without accomodation and adaptation is shown in Fig. 3.4(o). The output spikes at the differentiator output after the VCO are shown in Fig. 3.4(p) and the inhibitory input signal from the Renshaw cell is shown in Fig. 3.4(q).
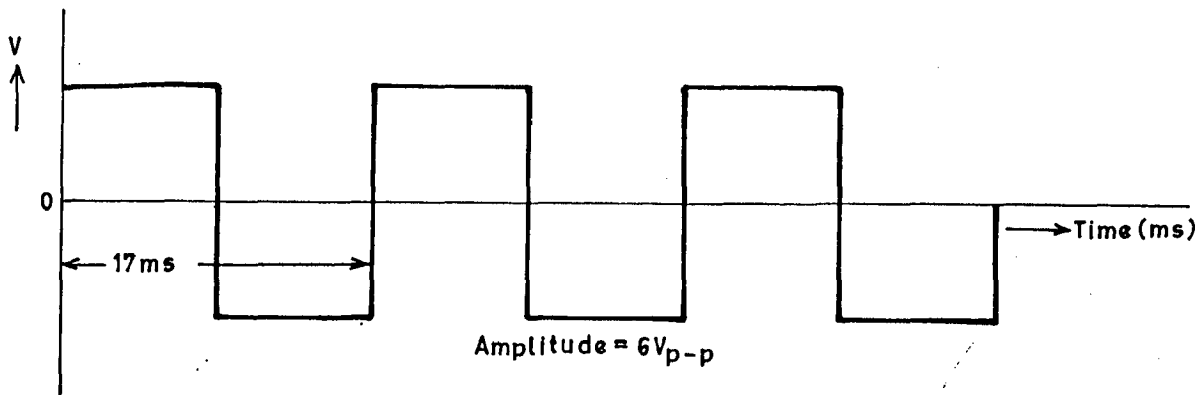
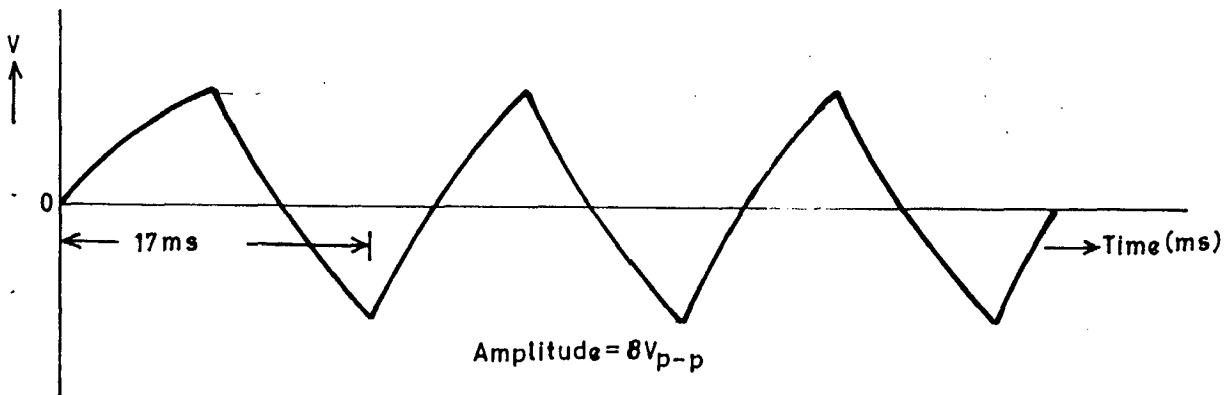Fig.3.4(k): Input to the integrator stage.
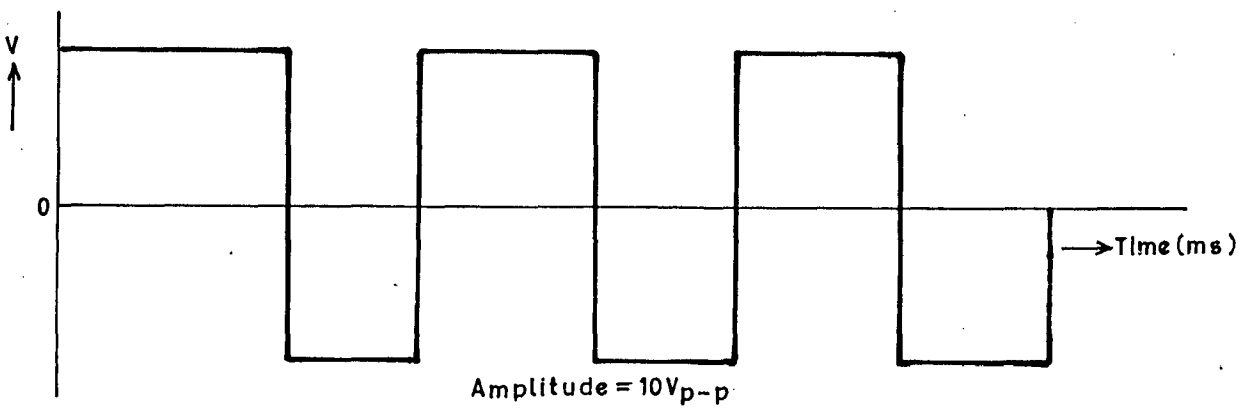

Fig.3.4(l): Output of the integrator.

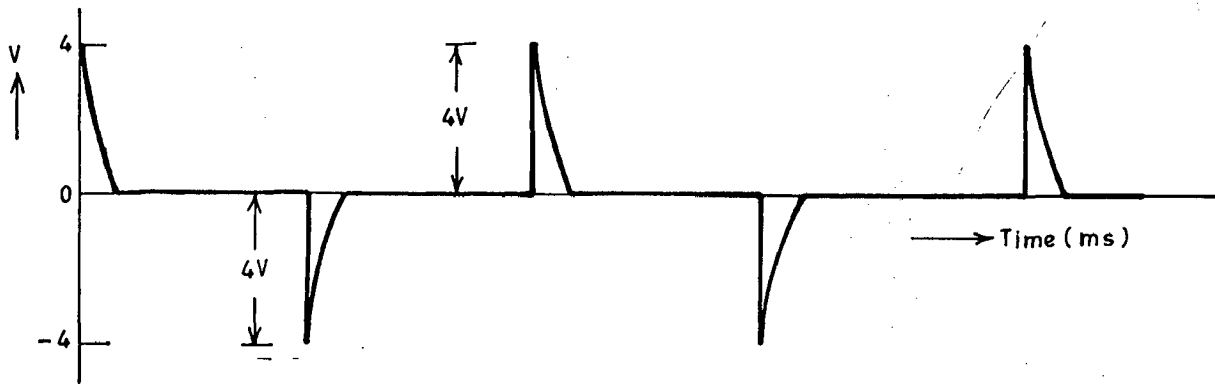Fig.3.4(m): Output of the threshold gate.

Fig.3.4(n): Output of the differentiator just before the monostable multivibrator.
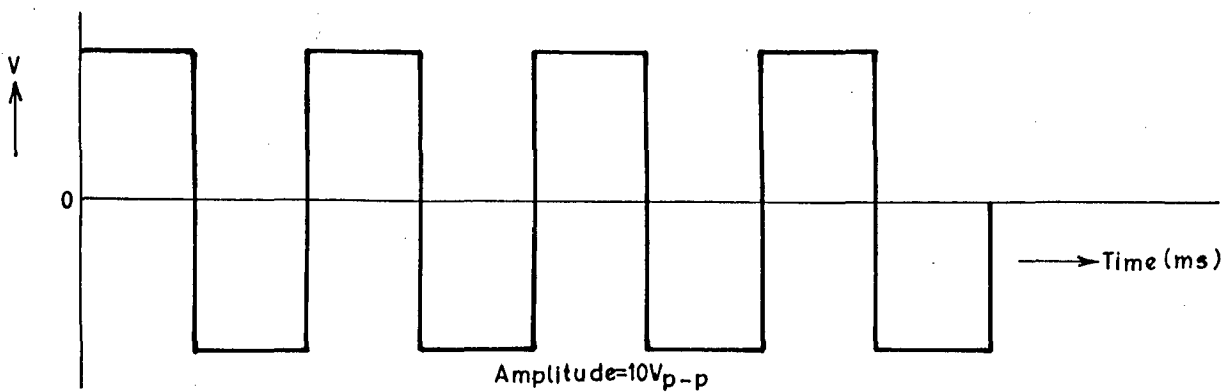

Amplitude=10V_{p-p}

Fig.3.4(o): Output pulse from the monostable multivibrator without accomodation and adaptation.
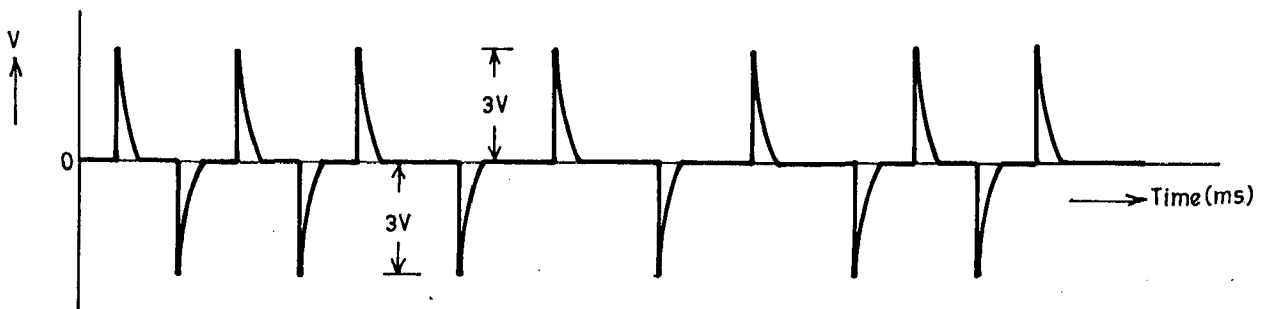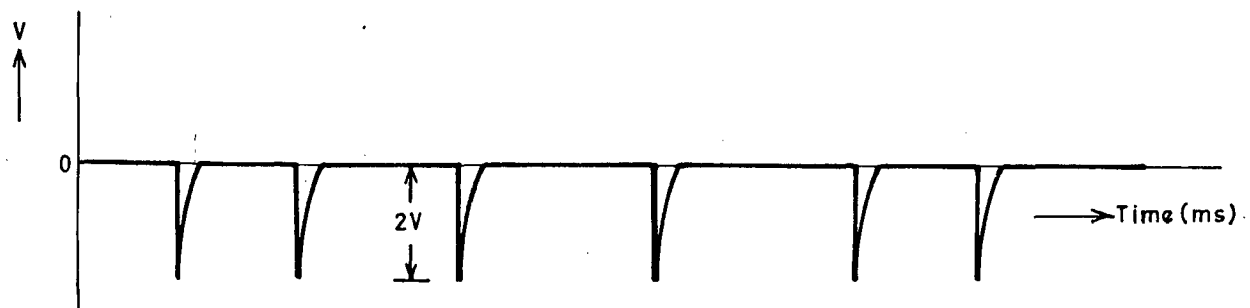

Fig.3.4 (P): Output at the differentiator after VCO.

Fig.3.4(q): Input to the integrator from the Renshaw cell feedback.

3.5 DISCUSSION :

The neural analog presented here incorporates most of the important features of the actual biological neurons. One important advantage of this neural analog is that, the out puts at the various stages of the analog can be processed in an identical fashion to that of the actual neural data for the direct comparison of the two. This model is very flexible in it's principle of operation and studies can be carried out on the electrical characteristics of the different kinds of nerve cells by the simple process of changing the required parameters of the circuit.

Since the low cost integrated chips are used in the present model, it serves as a valuable aid to study the single nerve cells as well as the neural nets incorporating few neurons.

The model can be updated in the future as more neural data become available.

Since it is possible to control the amplitudes of the EPSPs and IPSPs and also their rates of occurrence this circuit will serve as a very good aid to study the interactions of EPSPs and IPSPs of various amplitudes and frequency. Since it is possible to set different thresholds by varying the setting of R_{3b} at the different membrane patch models, by using more than one postsynaptic membrane patch models in the ladder network, [Fig. 3.2(a)], this circuit serves as a

good means to study the effects of the synaptic inputs at several areas of the postsynaptic membrance having non-uniform distribution of excitability. It is seen that the action potential and the synaptic potentials are transmitted without any distortion as in the living axon.

**

CHAPTER - IV

ANALYSIS OF A MYELINATED NERVE MODEL FOR
EXTERNAL STIMULATION

4.1 INTRODUCTION :

Electrical stimulation of nerves is gaining import-
ance because of it's increasing clinical applications, such
as treatment for chronic pain and other neural abnormalities,
using superficial and implented electrodes. The scientists
like BeMent and Ranck [58] gave the relationship between the
threshold of a myelinated nerve and the distance of the
electrode from a node. AbLug et al. [60] derived a solution,
for the electrode close to the node and an iterative solution
for the arbitrary locations of the electrode. FitzHugh and
Pickard [54,55] analyzed the propogation of action potential
along a myelinated nerve. They modeled the myelin skeath as
a distributed leaky capacitance and assumed that the membrane
obeying the equations of Hodgkin and Huxley [24]. Goldman
and Albus modeled the nodal membrane using a similar model
and empirical equations were derived by Frankenheuser and
Huxley [56]. In each of these analysis, excitation was assumed
to be initiated by a stimulus current applied at one of the
nodes. This assumption is valid in cases where the stimulus
is applied using microelectrodes. If the surface electrodes
are used for applying stimulus, then this assumption does not
hold good.

Lussier and Rushton [57] obtained analytical solution for excitation of myelinated nerve fibers, for threshold. In their analysis they assumed the electrode to be in direct contact with the nerve.

In all the papers referred in the above paragraphs the analysis was carried out for steady-state conditions, in which case the threshold is determined only for a pulse of infinite duration. Threshold for the finite duration pulses, has to be determined with reference to an experimentally determined strength-duration curve.

Therefore it is essential that a neuron model and it's analysis for the external stimulation be carried out in detail to provide the necessary foundation in different applications. Such work may find its use in development of neuroelectric prostheses aids for the deaf and blind [42].

The purpose of this work is to present and analyze the model for the electrical properties of a myelinated nerve fiber that allows the computation of strength-duration curves for the different geometries of the neurons and time-varying transverse membrane current and membrane potential at each of the nodes of Ranver are determined from the model.

The emphasis in this work is on a detailed presentation and discussion of the model as well as a thorough examination of the transient response for the special case of various levels of constant depolarizing stimulations (external excitations) for electrode located directly over one of the

nodes. The effect of variation of the electrode distance is also studied. Sub-threshold and threshold responses are presented for pulse,ramp, sinusoidal and triangular types of excitations, for the typical dimensions of the neurons with the electrode located directly over, 1 mm away from one of the nodes.
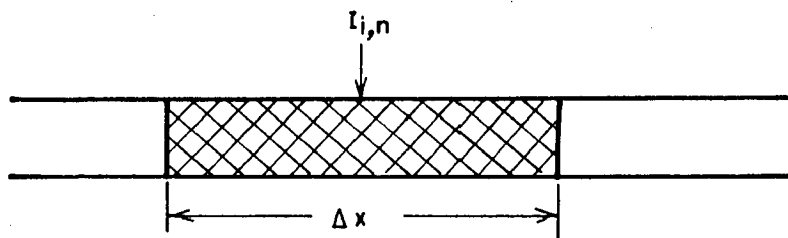
4.2 MODEL FOR MYELINATED NERVE FIBER :

The membrane of the myelinated nerve fiber is approximated by an equivalent electrical network consisting of voltage source, capacity, and resistance as shown in Fig. 4.1(a). In case of unmyelinated fibers, the computation uses segments labelled n = 1,2,... of length Δx within which all points of the membrane have the same properties [Fig. 4.1(b)]. In myelinated fibers active parts exist only at the nodes of Ranvier of width 1 which are spaced by L along the membrane as shown in Fig. 4.1(c). The ionic current I_i passing through the nth active part of the membrane with capacity C_m is denoted by $I_{i,n}$. $I_{i,n}$ is a function of the voltage between the inside potential $V_{i,n}$ and the outside potential $V_{e,n}$. The current running in the axon is driven through the axon conductance G_a by the inside potentials at the locations n-1, n and n +1.

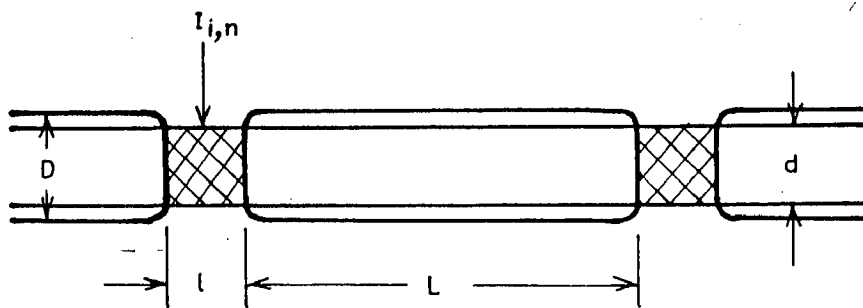The symbols and values used for different variables and constants in this analysis are given in Table- I.
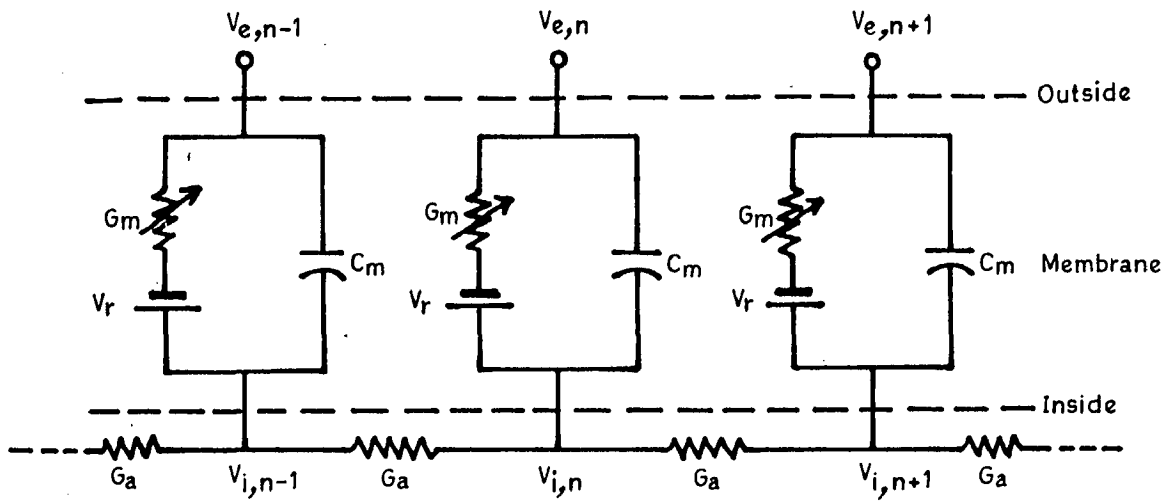
Fig.4.1:(a) Electrical network representation of a myelinated
nerve fiber, (b) Unmyelinated nerve fiber and
(c) Myelinated nerve fiber.

TABLE - I

_VARIABLES AND CONSTANTS

Variables	
V_n	membrane potential at node n minus the resting potential (millivolts)
I_n	membrane current at node n (Pa)
$V_{e,n}$	external potential at node n
$V_{i,n}$	internal potential at node n
G_a	axial internodal conductance
G_m	nodal membrane conductance
C_m	nodal capacitance
D	fiber diameter (external myelin diameter)
d	axon diameter (internal myelin diameter)
L	internode length
$I_{i,n}$	total ionic current at node n
i_{Na}	sodium current density
i_K	potassium current density
i_p	non-specific delayed current density
i_L	leak current density
I	stimulus current

T		stimulus duration
t		time (microseconds).

Constants

ρ_i	110 Ω cm	axoplasm resistivity (stampfli)
ρ_e	300 Ω cm	resistivity of external medium (Abzug et al.)
c_m	12 μF/cm^2	membrane capacitance/unit area (Frankenhaenser and Huxley)
g_m	30.4 m mho/ cm^2	membrane conductance/unit area (Frankenhaeuser and Huxley)
1	2.5 μm	nodal gap width (Frankenhaeuser)
L/D	100	ratio of internodal space to fiber diameter (Hursh and Dodge and Frankenhaeuser)
d/D	0.7	ratio of axon and fiber diameters (Goldman and Albus)
V_r	−70 mV	resting potential (Frankenhaenser and Huxley).

4.2.1 Assumptions :

1. The assumptions generally follow those of Fitz Hugh [54], except that it is assumed here that the myelin sheath is a perfect insulator. The validity and effect of this assumption is considered later in the Discussion Section.

2. Following Fitz Hugh [54], it is assumed that the fiber is infinitely long with nodes that are regularly spaced.

3. Both internodal distance and axon diameter are assumed to be proportional to fiber diameter.

4. This model assumes that the electrical potential outside the fiber is determined only by the stimulus current, tissue outside the nerve fiber and is not distorted by the presence of the fiber. This is reasonable since the dimensions of a single nerve fiber are small and also our interest is limited to the period of time prior to excitation (i.e. before internally generated currents become significant).

5. The small dimensions of the fiber also allow the simplification that the external surface of the membrane at any one node is at an equipotential. This implies that variations in the membrane current density over the nodal surface can be neglected. These assumptions are considered further in the Discussion Section.

6.   It is assumed that the potential on the inner
     surface of node n will vary, but the variation will
     be small in comparison with the difference in internal
     potential between adjacent nodes.

7.   It is also assumed that the axial currents flowing
     into node n and the total membrane current at node n
     will be approximately equal to $G_a(\dot{V}_{i,n-1}-2V_{i,n}+V_{i,n+1})$
     neglecting the effect of current leaking through the
     myelin sheath.

8.   It is assumed that for subthreshold stimuli the
     membrane conductance is constant at all nodes, and
     near threshold the membrane conductance is constant
     all nodes prior to the initiation of the action
     potential except at the excitation node where the
     membrane is modeled by the Frankenhaeuser-Huxley
     equations [56].

9.   In this analysis, it is assumed that the medium
     external to the nerve fiber is infinite and isotropic.
     calculation of the potential, throughout the medium,
     of course, becomes more complex as more realistic
     models for the external environment are formulated.

10. An axon changes the extracellular potential also by
     it's own activity, but only below 1 mV, whereas the
     intracellular contribution of voltage is high. As
     the threshold for extracellular stimulation is about
     30 mV, the influence of the inherent potentials of
     the axon to the extra-cellular potential is not

essential, and is not considered here.

11.   For nodes more than 11, since the set of differential
equations is large enough, it is assumed that the
membrane potential at the boundary nodes and at all
other nodes outside the selected set is negligibly
small, (almost equal to zero) and is not taken in to
consideration [29,43,63].

4.2.2   Mathematical Formulations :

The axial internodal conductance G_a can be calculated
from the following relations

$$G_a = (\frac{1}{\text{internodal resistance}}) \text{ mhos}$$

i.e.,

$$G_a = \frac{\pi d^2}{4 \varrho_i L} \text{ mhos} \qquad \qquad \text{....(1)}$$

The modal membrane impedence is represented by a
nodal capacitance C_m and nodal membrane conductance G_m in
parallel. It is expressed as

Nodal membrane G_m =   membrane conductance per unit area x
conductance   nodal area

$$G_m = g_m \pi d l \text{ mhos} \qquad \qquad \text{...(2)}$$

and membrane C_m =   membrane capacitance per unit area
capacitance   x nodal area

$$C_m = C_m \pi d l \text{ Farads} \qquad \qquad \text{...(3)}$$

All the three of these components, G_a, G_m and C_m are proportional to fiber diameter. For a given diameter of the fiber, G_a and C_m are constants, but G_m is in general, a complex function of the membrane potential.

The membrane current at node n is equal to the sum of the incoming axial currents and to the sum of the capacitive and ionic currents through the membrane. Hence at node n of the nerve fiber of Fig. 4.1(a), the following equation have been obtained [43,63] for the currents.

$$\frac{C_m \, d(V_{i,n} - V_{e,n})}{dt} + G_m(V_{i,n} - V_{e,n} + V_r)$$

$$+ G_a(V_{i,n} - V_{i,\,n-1}) + G_a(V_{i,n} - V_{i,\,n+1}) = 0$$

$$...(4)$$

V_n = the membrane potential at node n minus the resting potential

$$(V_{i,n} - V_{e,n} + V_r) - V_r$$

$$V_n = V_{i,n} - V_{e,n} \qquad ...(5)$$

also

$$V_{i,n} = V_n + V_{e,n} \qquad ...(6)$$

Substituting values of V_n and $V_{i,n}$ in equation (4), we get

$$C_m \, \frac{d \, V_n}{dt} + G_m V_n + G_a (V_{i,n} - V_{i,n-1} + V_{i,n} - V_{i,n+1}) = 0$$

$$C_m \, \frac{d \, V_n}{dt} + G_m V_n = G_a (V_{i,n-1} - 2V_{i,n} + V_{i,n+1})$$

For the subthreshold stimuli, it can be assumed that the membrane conductance G_m is constant. The ionic current $I_{i,n}$ at node n is then given by $G_m V_n$

i.e., $\quad I_{i,n} = G_m V_n$ ...(7)

Substituting this into the above expression, it can be shown that the myelinated nerve fiber is described by the following infinite set of linear, first-order differential equations.

$$C_m \frac{d V_n}{dt} + I_{i,n} = G_a (V_{i,n-1} - 2V_{i,n} + V_{i,n+1}) \quad ...(8)$$

$$\frac{d V_n}{dt} = \frac{1}{C_m} [G_a (V_{i,n-1} - 2V_{i,n} + V_{i,n+1}) - I_{i,n}]$$

Substituting from equation (6), above,

$$\frac{d V_n}{dt} = \frac{1}{C_m} [G_a (V_{n-1} - 2V_n + V_{n+1} + V_{e,n-1} - 2V_{e,n} + V_{e,n+1}) - I_{i,n}]$$

...(9)

for $\quad n = \ldots -2,-1,0,1,2 \ldots$

The initial conditions are

$$V_n(0) = 0 \text{ for all } n \qquad ...(10)$$

The solution to (9) and (10) can be obtained by selecting a finite set of differential equations that enclose the nodes of interest and then integrating the finite set to obtain the membrane potentials. Since the set of differential equations is large enough, it can safely be assumed that the

membrane potential at the boundary nodes and at all nodes outside the selected set is not taken into consideration, as they are negligibly small [43,63]. In the present analysis the solution for 11 nodes is obtained. From equation (7) it is seen that the ionic current $I_{i,n}$ is a function V_n and t. Equation (9) shows the influence of the external potentials $V_{e,n}$, which are generated by the stimulating external electrodes positioned at some distance from the axon, on the inner distribution V_n. $V_{e,n}$ is determined by the electrode positions and the conductivity of the outside medium.

The node at which excitation will initially occur can be predicted from the subthreshold response. Excitation will occur at the node at which the membrane potential is maximum during the time of stimulus application. This node will be referred to as the excitation node. As the stimulus is increased to threshold or suprathreshold values, the membrane conductance at the excitation node changes markedly during the stimulus as the membrane becomes more permeable to sodium ions. It can be assumed that the membrane conductance at all other nodes is const nt, since the membrane potential at these nodes will be subthreshold prior to the initiation of an action potential at the excitation node. This is a satisfactory assumption, since our interest, in the present analysis, is confined to (1) determining whether an action potential is initiated and (2) calculating the transient response for subthreshold stimuli and for suprathreshold

stimuli up to the time an action potential is initiated. It is possible that in certain cases (e.g., electrode located exactly between two nodes) the maximum depolarization is the same or nearly the same at two or more nodes. The following equations are written for the case where only one node is significantly depolarized.

For stimuli sufficient for excitation the ionic current at the excitation node (assumed to be node 0) is given by

$$I_{i,0} = \pi dl \ (i_{Na} + i_K + i_p + i_L).$$

where the terms on the right are the individual components of ionic currents expressed as current densities. The complete set of equations describing the time course of the membrane potential at all nodes prior to excitation is given by

$$\frac{d \ V_n}{dt} = \frac{1}{C_m} \ [G_a(V_{n-1} - 2V_n + V_{n+1} + V_{e,n-1} - 2V_{e,n} + V_{e,n+1})$$
$$-G_m \ V_n] \qquad \ldots(11)$$

for $n \neq 0$

$$\frac{d \ V_0}{dt} = \frac{1}{C_m} \ [G_a(V_{-1} - 2V_0 + V_1 + V_{e,-1} - 2V_{e,o} + V_{e,1})$$
$$- \pi dl(i_{Na} + i_K + i_p + i_L)] \qquad \ldots(12)$$

$$V_n(0) = 0 \text{ for all n} \qquad \ldots(13)$$

Equations (11) and (12) can be solved by integrating a finite set of equations.

Calculation of the external potential at each node is as follows. In an isotropic medium, the electrical potential

at a distance r from the electrode is [Fig. 4.2] calculated from the following relation

$$V_e = IR$$

$$\therefore V_e = \frac{\rho_e I}{4\pi r} \qquad \ldots(14)$$

Current flowing toward the electrode is considered to be positive. Once the location of electrode is fixed with respect to the nerve the external potential is calculated at each node using equation (14). It shows that the external potential is time-invariant. The external potential at nodes n and -n is equal for all $n \neq 0$, because of the assumed symmetry of the location of the electrodes which implies that the membrane potential and current at nodes n and -n will be identical.

4.3 DEVELOPED SOFTWARE :

In this section the programs used for carrying out the computational work have been presented. Two programs are developed. In one program various geometries of the neuron, different electrode distances and excitation currents have been considered. In the other program, the various types of excitation functions are considered. The programs have been made interactive. This helps one to select desired starting value, increment step and final value for different parameters. So it is possible to consider wide variety of combinations of electrode distances, stimulus parameters, and neuron geometries of practical interest; including, waveshapes of excitation current.
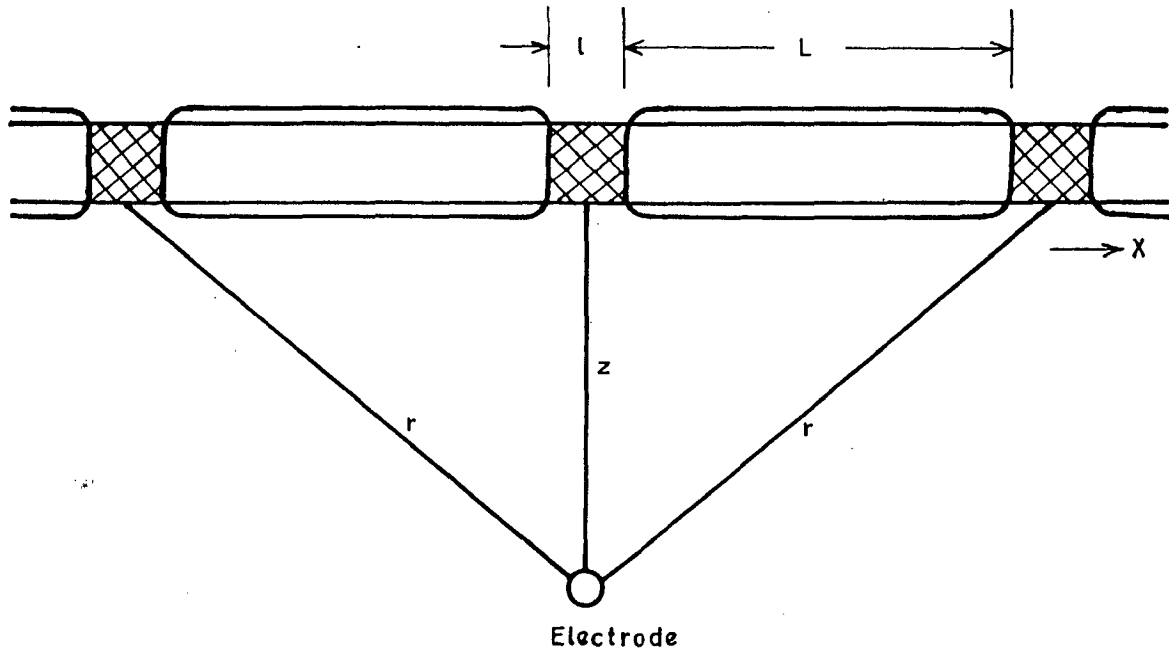
Fig.4.2: The electrode at distance z produces symmetric
effects at the positions X and −X.

In the present work four types of excitation wave shapes have been considered, namely, triangular, ramp, pulse and sinusoidal type.

The programs are written in Fortran IV and run on DEC 2050 system. For computational purposes here, eleven nodes, including one under the electrode are taken into consideration. The system of differential equations representing transmembrane currents are solved using fourth-order Runge-kutta method. The initial condition of $V_n(0) = 0$ for all n is used [42]. The time steps of 1 μs are taken for computational work. The details of Runge-kutta method are given in appendix - A. The results obtained with the sinusoidal type of excitation function match well with the results obtained by other researchers [63].

4.3.1 Flow Chart :

The flow chart is shown in Fig. 4.3. After accepting the data and calculating the required parameters, GA, GCM, CCM the radial distances between the electrode and the nodes are calculated and stored in one dimensional array R.

External potential at the different nodes is calculated, after obtaining the electrode radial distance.

In the case of the program-2, the external voltage is a function of time, and is calculated accordingly as the selection of the excitation function by the user.
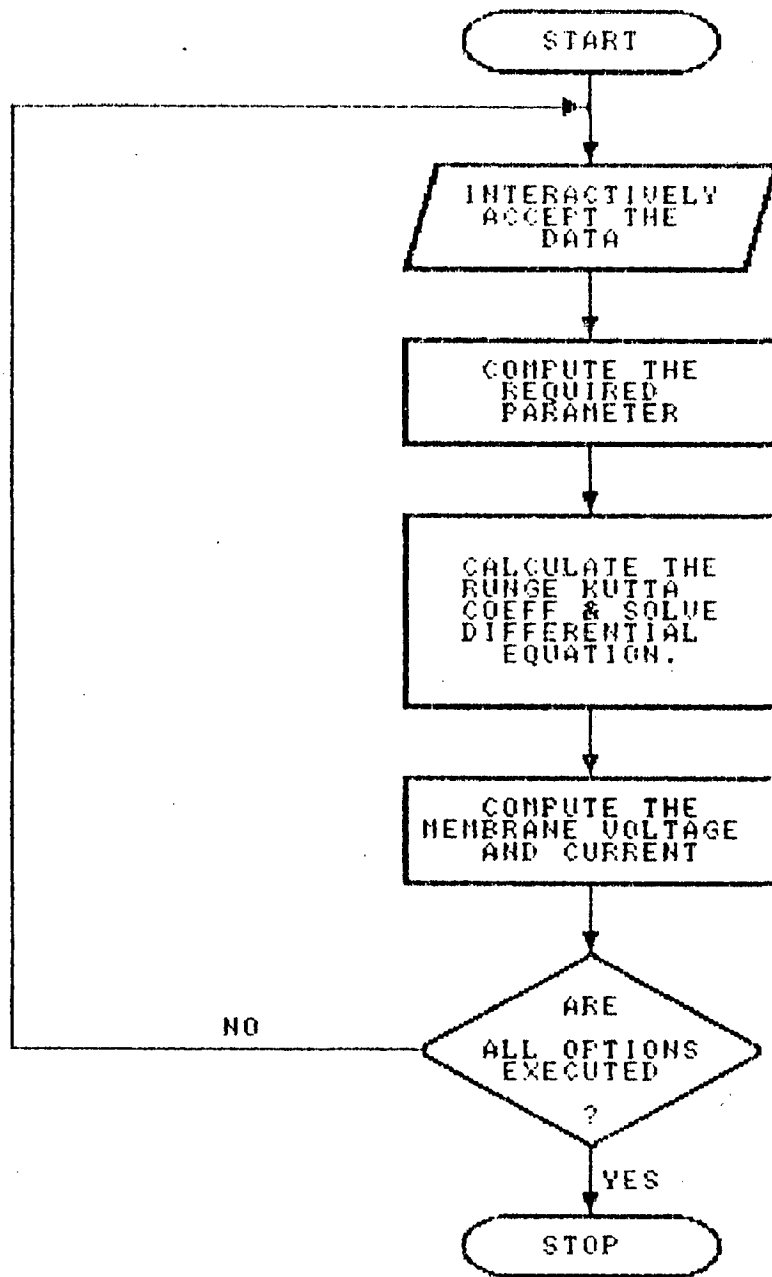
FIG.4.3 FLOW CHART FOR THE ANALYSIS OF MYELINATED
NERVE MODEL.

Next the Runge-Kutta coefficients are calculated. There is one basic function of differential equation representing the transmembrane current, which results in a set of equations at different modes. For calculating the membrane voltage and membrane current at any nodes, three nodes are taken into consideration- the node under the electrode, and one adjacent node on each side.

In these equations $V(I,J)$ represents the membrane potential at node I, and at time J.

In the program, $V(I,1) = 0.0$ (the initial condition) is the membrane potential at node I and time J = 1 corresponds to time t = 0.
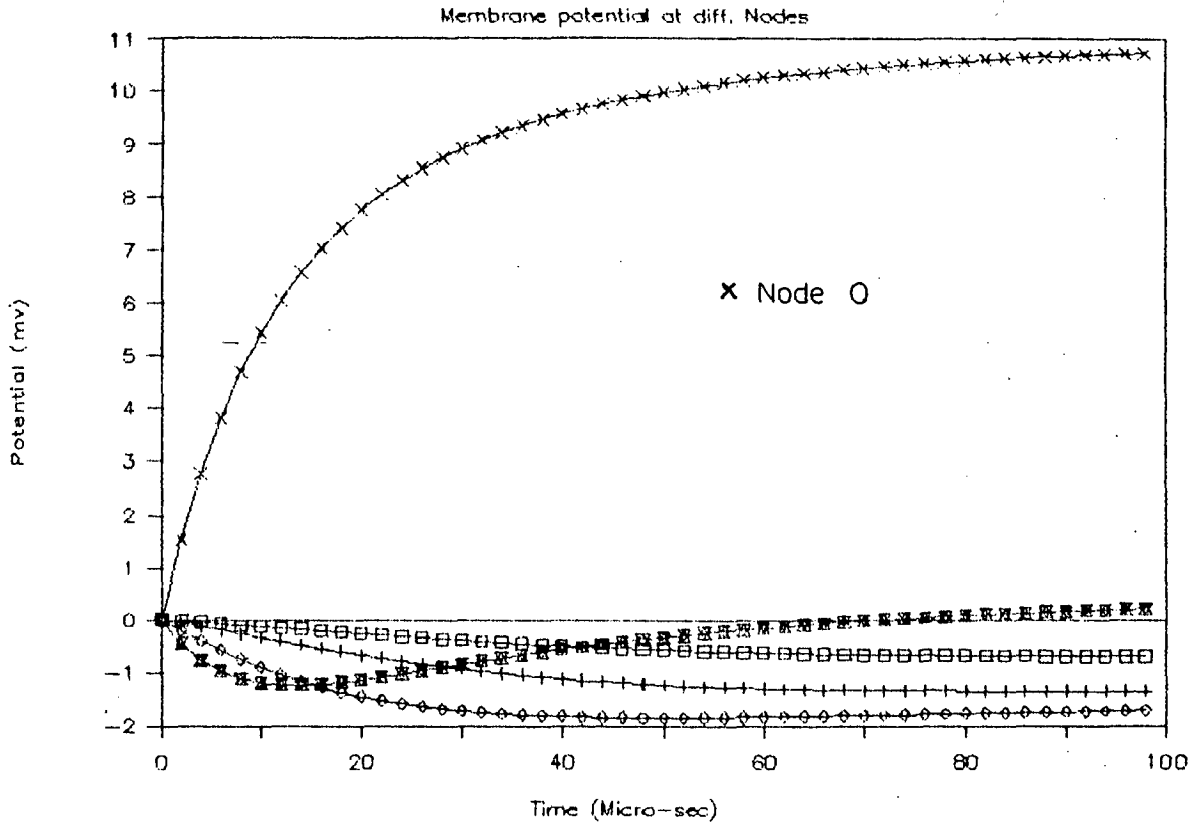
I case of the program - 2, the function EC is used to calculate the current amplitudes of the chosen excitation waveform.

Using the Runge-Kutta coefficients the membrane potentials at different nodes are calculated, which are used to compute the membrane currents at the corresponding nodes. Here we have considered eleven nodes - one under the electrode, and five nodes on each side of it.
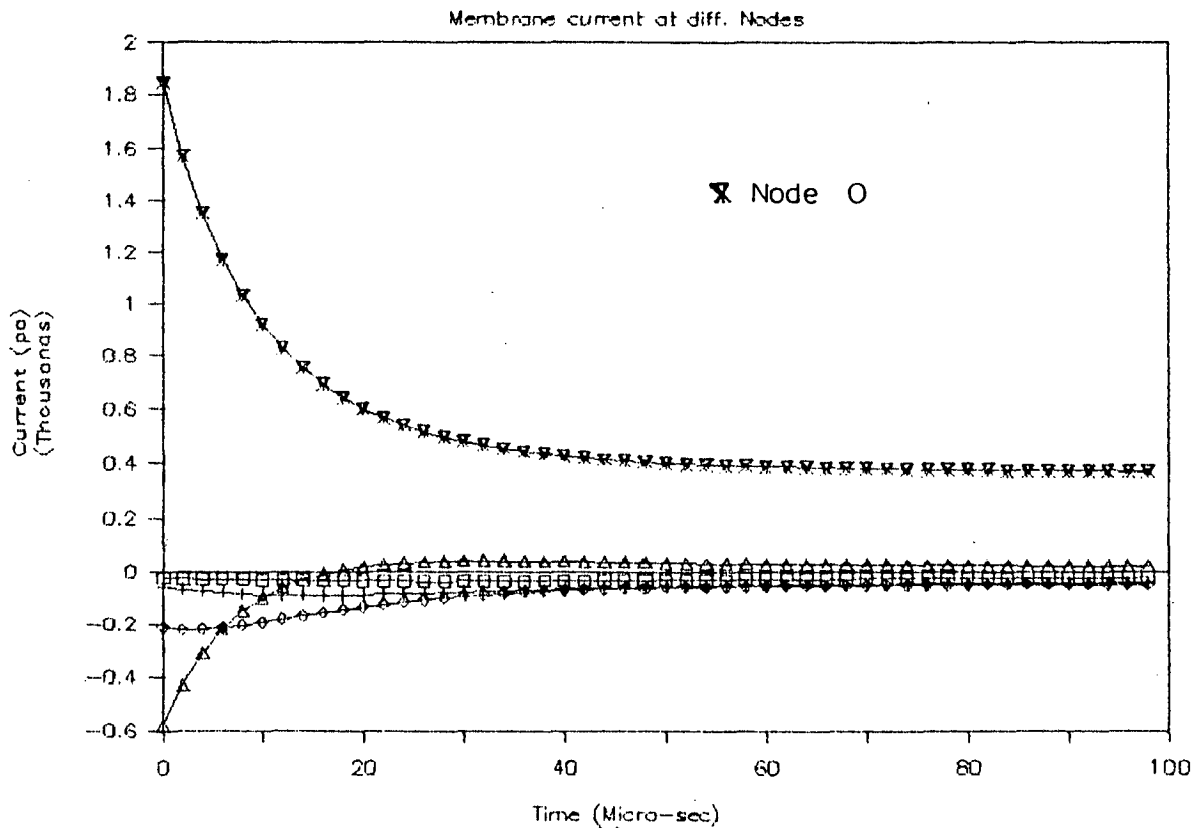
For better accuracy the membrane voltages and currents are calculated in the time steps of 1 μs.

A hard copy of the membrane voltages and currents is generated in the time steps of 10 μs for comparison purposes.

FIG.4.4 (a) Membrane potential at different nodes
         (b) Membrane current at different nodes
For, L=0.2Cm, d=0.14E-2Cm, l=0.25E-3Cm, I=0.1E-3A, EDist=0.1Cm
✗, ✗ Node 0; △ Nodes -1,1; ◇ Nodes -2,2; ✦ Nodes -3,3; ◻ Nodes -4,4

Next the Runge-Kutta coefficients are calculated. There is one basic function of differential equation representing the transmembrane current, which results in a set of equations at different modes. For calculating the membrane voltage and membrane current at any nodes, three nodes are taken into consideration- the node under the electrode, and one adjacent node on each side.

In these equations V(I,J) represents the membrane potential at node I, and at time J.

In the program, V(I,1) = 0.0 (the initial condition) is the membrane potential at node I and time J = 1 corresponds to time t = 0.

I case of the program - 2, the function EC is used to calculate the current amplitudes of the chosen excitation waveform.

Using the Runge-Kutta coefficients the membrane potentials at different nodes are calculated, which are used to compute the membrane currents at the corresponding nodes. Here we have considered eleven nodes - one under the electrode, and five nodes on each side of it.

For better accuracy the membrane voltages and currents are calculated in the time steps of 1 μs.

A hard copy of the membrane voltages and currents is generated in the time steps of 10 μs for comparison purposes.

The file names for the membrane voltages and currents can be chosen by the user.

All the programs are given in Appendix - B and Appendix - C.

## 4.4 RESULTS OF ANALYSIS OF VOLTAGE AND CURRENT RESPONSES :

4.4.1 Effects Of Variation Of The Electrode Distance :

The variations of the membrane potentials and membrane currents at different nodes for subthreshold excitations are obtained and analyzed. Here a fiber diameter of 20 μm is taken into consideration [9] and an excitation current of 0.1 mA of infinite duration is applied. The computations of membrane potential and membrane current at various nodes are done using equations (9) and (10), and are shown in Fig. 4.4(a) and Fig. 4.4(b) respectively. The neuron parameters used for this computation are : Internode length = 0.2 cm, axon diameter = 0.14E-2 cm., nodal gap width = 0.25E-3 cm., and a stimulus current of 0.1E-3A is used.

As seen from Fig. 4.4(a), initially only node 0 i.e. the node under the electrode is depolarized and all the other nodes are hyperpolarized. But nodes - 1 and 1 initially being hyperpolarized reverse sign after 70 μs and remain depolarized from that time on. Nodes -4 and 4 are less hyperpolarized, nodes -2 and 2 are more hyperpolarized and nodes -3 and 3 are moderately hyperpolarized. The depolarization attained
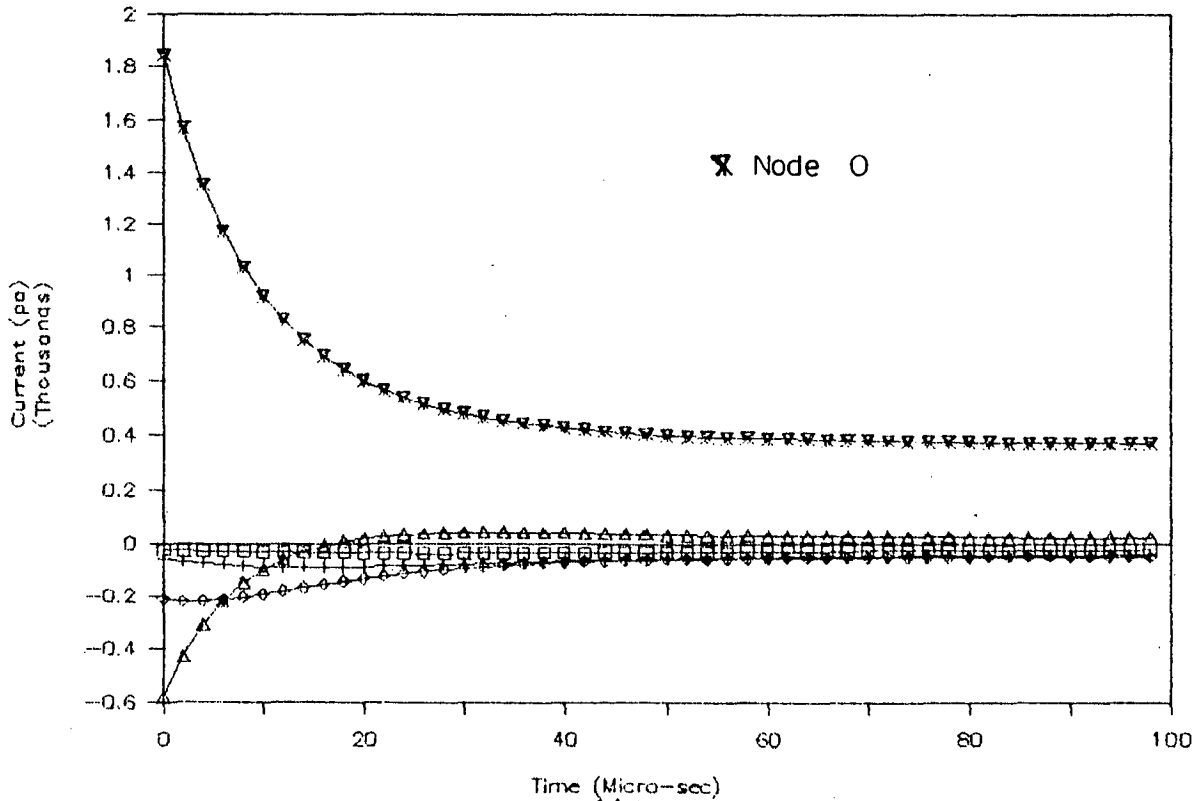
Analysis of Myelinated Nerve

Membrane potential at diff. Nodes

× Node 0

(a)
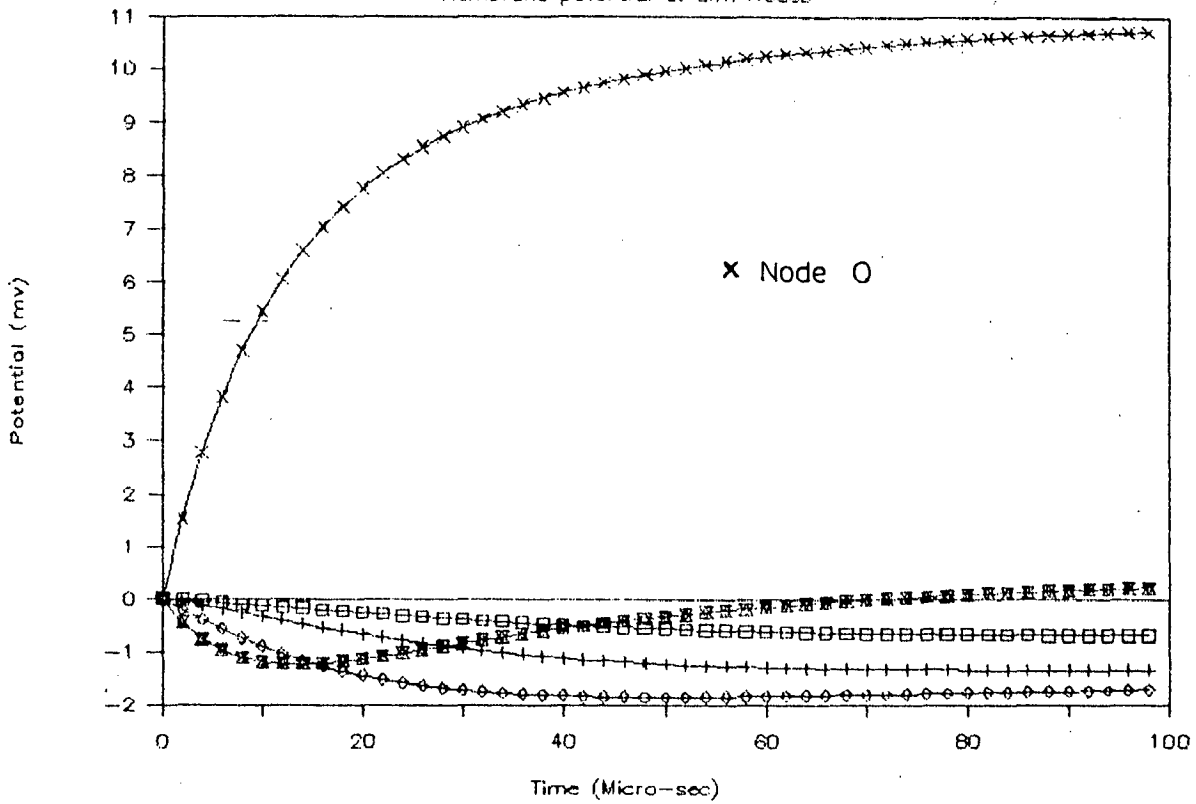
Membrane current at diff. Nodes

𝕏 Node 0

(b)

FIG.4.4   (a) Membrane potential at different nodes
(b) Membrane current at different nodes
For, L=0.2Cm, d=0.14E-2Cm, l=0.25E-3Cm, I=0.1E-3A, EDist=0.1Cm
×, 𝕏 Node 0; △ Nodes -1,1; ◇ Nodes -2,2; + Nodes -3,3; □ Nodes -4,4

by the nodes -1 and 1 is less than 0.5 mV. Fig. 4.4(b) shows the time response of the membrane currents at these same nodes. Membrane current from inside to outside is taken to be positive [42]. Even though the excitation current is constant at 0.1 mA, the membrane current at node 0 decreases very rapidly. From Fig. 4.4(b) it is seen that, at 20 µs the membrane current at node 0 has fallen to approximately one-third of the initial value. It further continues to fall till it reaches the steady state value which is about one-fifth of the initial value. The membrane current at nodes -1 and 1 is initially negative but becomes positive at 20 µs, and remains positive from that time on. This reversal of the membrane current at nodes -1 and 1 accounts for the eventual reversal of the membrane potential at the same nodes [Fig. 4.4(a)]. The membrane currents at all the other nodes is negative.

Under these conditions of excitation current, electrode distance, and neuron dimensions only node 0 is excited, and nodes -1 and 1 are mildly depolarized. Hence if it is desired to excite only node 0 and keep the other nodes hyperpolarized then this electrodes distance and excitation current can be used effectively.

The dimensions of neurons as whole and the dimensions of the various parts of the neuron itself vary to a great extent [6,9]. The effects of the electrode distance and stimulus current on membrane potential and current of

dimensionally different neurons is considered in the follow-
ing analysis.

In Fig. 4.5(a), Fig. 4.6(a), Fig. 4.7(a) and Fig. 4.8(a)
the change in membrane potential at the node below the elect-
rode and at the four adjacent nodes is shown corresponding
to the electrode distance of 0.05, 0.15, 0.25 and 0.35 cm
respectively.

For the electrode distance of 0.05 cm from the nerve
fiber, [Fig. 4.5(a)] only node 0 is depolarized. All other
nodes are hyperpolarized with the nodes 1 and -1 undergoing
a transient change in hyperpolarization up to 20 µs and there
after the hyper-polorization gradually decreases. The nodes
4 and -4 are under constant hyperpolarization and is lowest
compared to all other hyperpolarized nodes.

As a result the excitation occurs and the action pot-
ential is initiated only from node 0 as all the other nodes
are hyperpolarized.

The change in membrane potential for the electrode
distance of 0.15 cm is shown in·Fig. 4.6(a) and that for the
dectrode distances of 0.25 and 0.35 cm are shown in Fig. 4.7(a),
and Fig. 4.8(a). In all these cases both the node 0 and nodes
1 and -1 are depolarized and all the other nodes are hyper-
polarized with one marked difference that nodes 1 and -1
reverse sign after 20 µs and remain depolarized from that
time on, in Fig. 4.6(a). As expected the level of depolari-
zation and hyperpolarization reached by the respective nodes
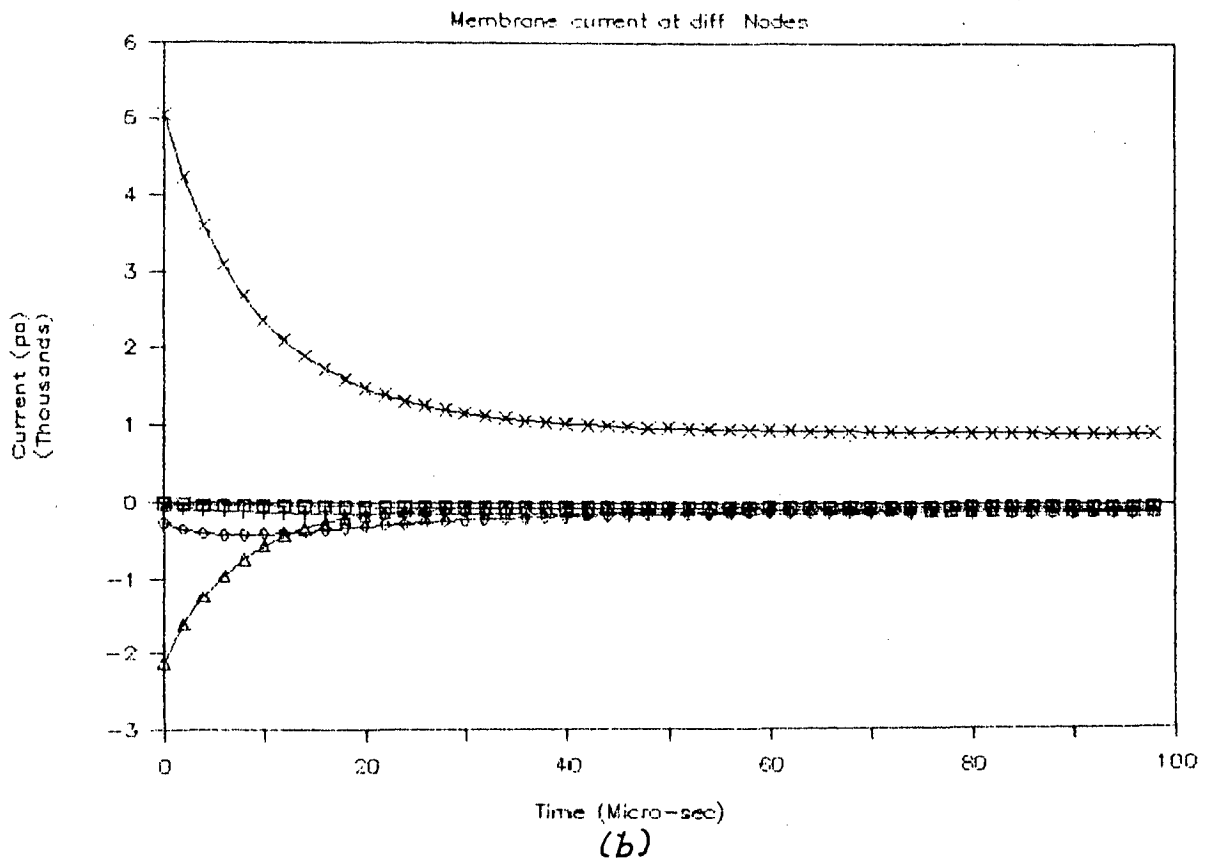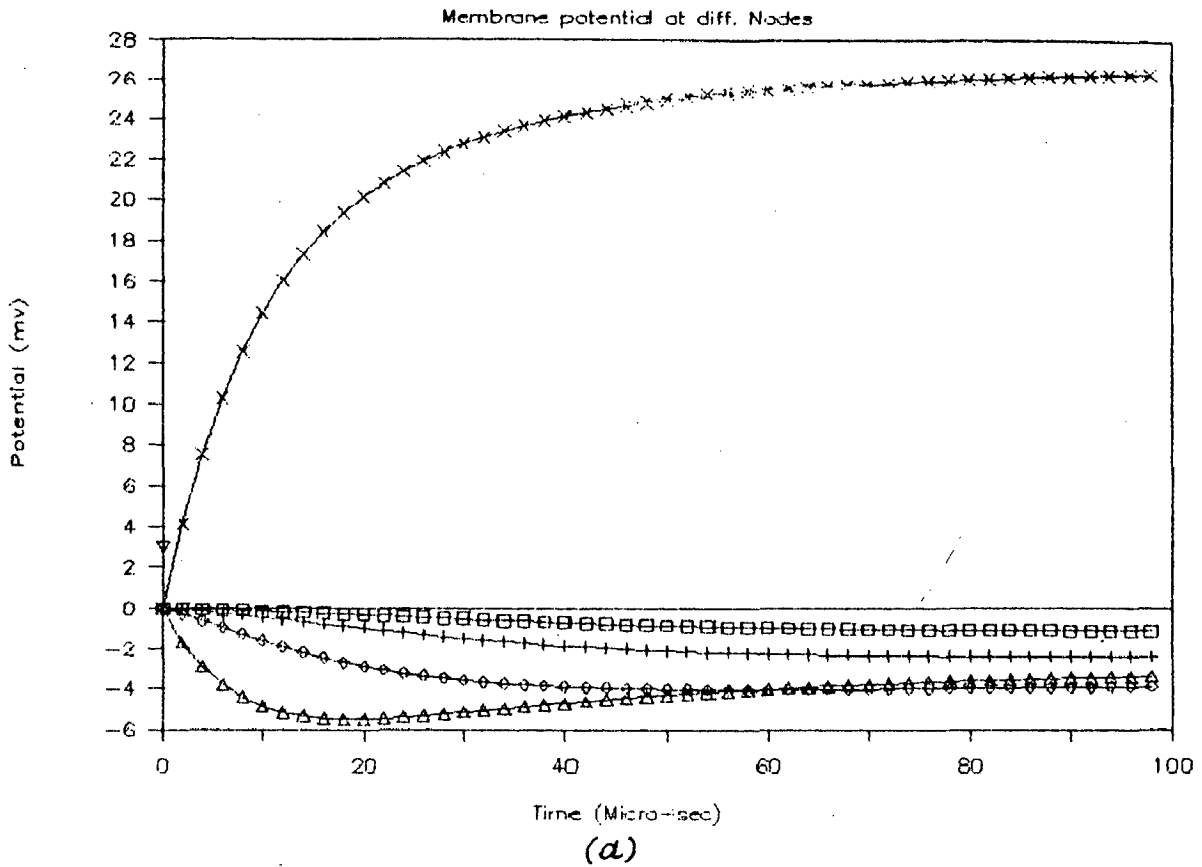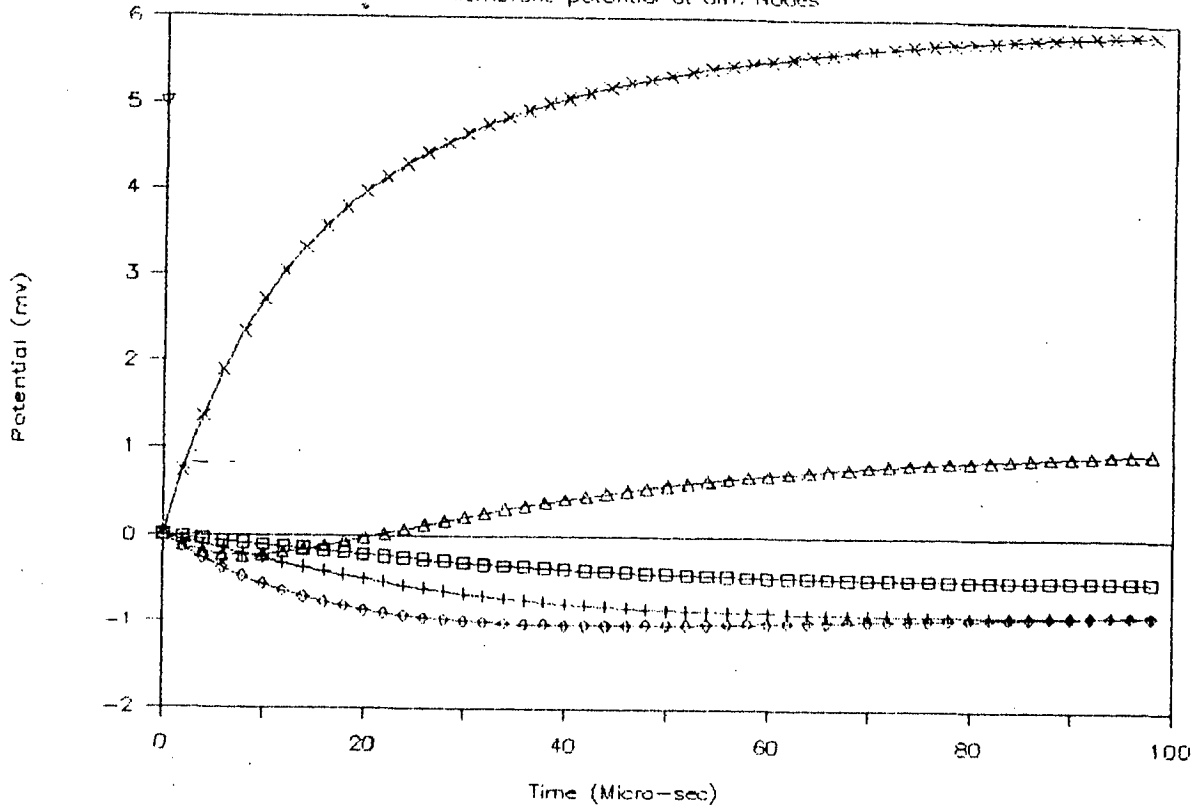
Analysis of Myelinated Nerve

Membrane potential at diff. Nodes

(a)

Membrane current at diff. Nodes

(b)

FIG.4.5   (a) Membrane potential at different nodes
(b) Membrane current at different nodes
For, L=0.2Cm, d=0.14E-2Cm, l=0.25E-3Cm, I=0.1E-3A, EDist=0.05Cm
X Node 0; △ Nodes -1,1; ◇ Nodes -2,2; + Nodes -3,3; ❑ Nodes -4,4

Analysis of Myelinated Nerve

Membrane potential at diff. Nodes

(a)

Membrane current at diff. Nodes

(b)

FIG.4.6 (a) Membrane potential at different nodes
(b) Membrane current at different nodes
For,L=0.2Cm,d=0.14E-2Cm,l=0.25E-3Cm,I=0.1E-3A,EDist=0.15Cm
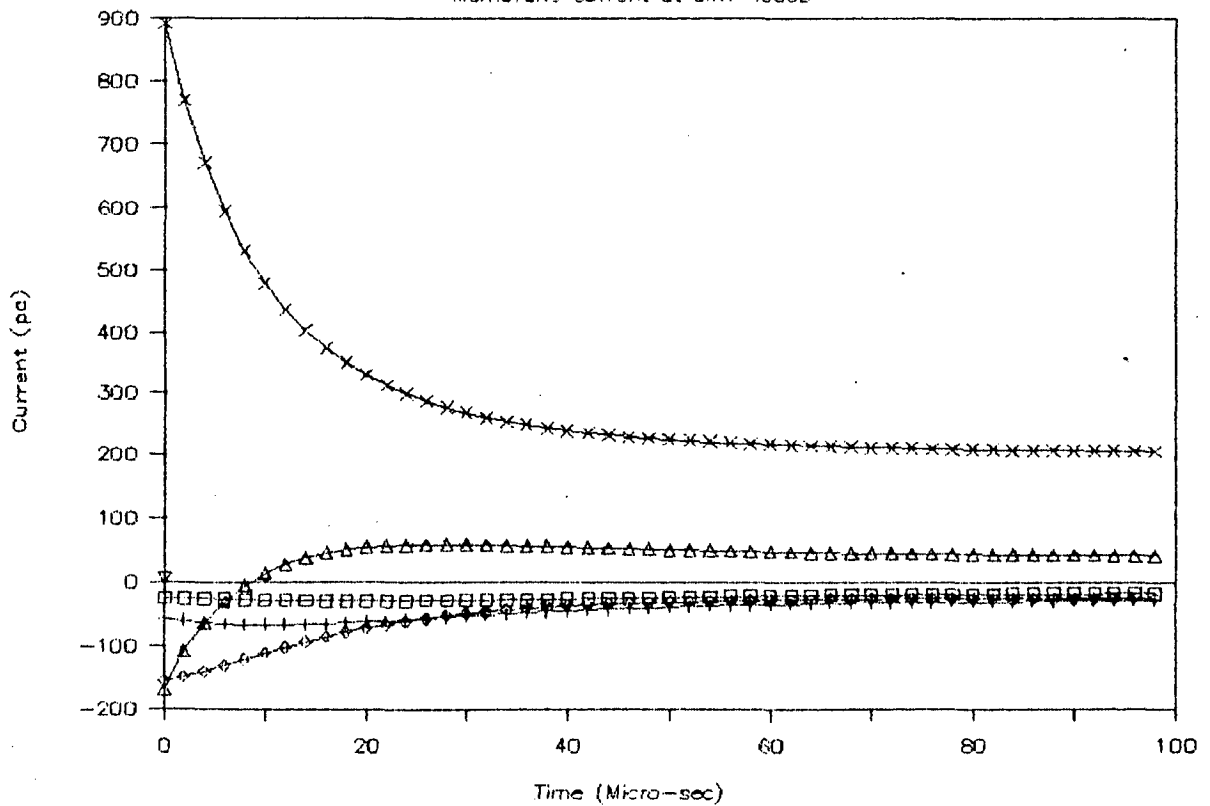X Node 0; Δ Nodes -1,1; ◊ Nodes -2,2; + Nodes -3,3; □ Nodes -4,4

Analysis of Myelinated Nerve

Membrane potential at diff. Nodes

(a)

Membrane current at diff. Nodes

(b)

FIG.4.7 (a) Membrane potential at different nodes
(b) Membrane current at different nodes
For, L=0.2Cm, d=0.14E-2Cm, l=0.25E-3Cm, I=0.1E-3A, EDist=0.25Cm
X Node 0; △ Nodes -1,1; ◊ Nodes -2,2; + Nodes -3,3; ◻ Nodes -4,4

Analysis of Myelinated Nerve
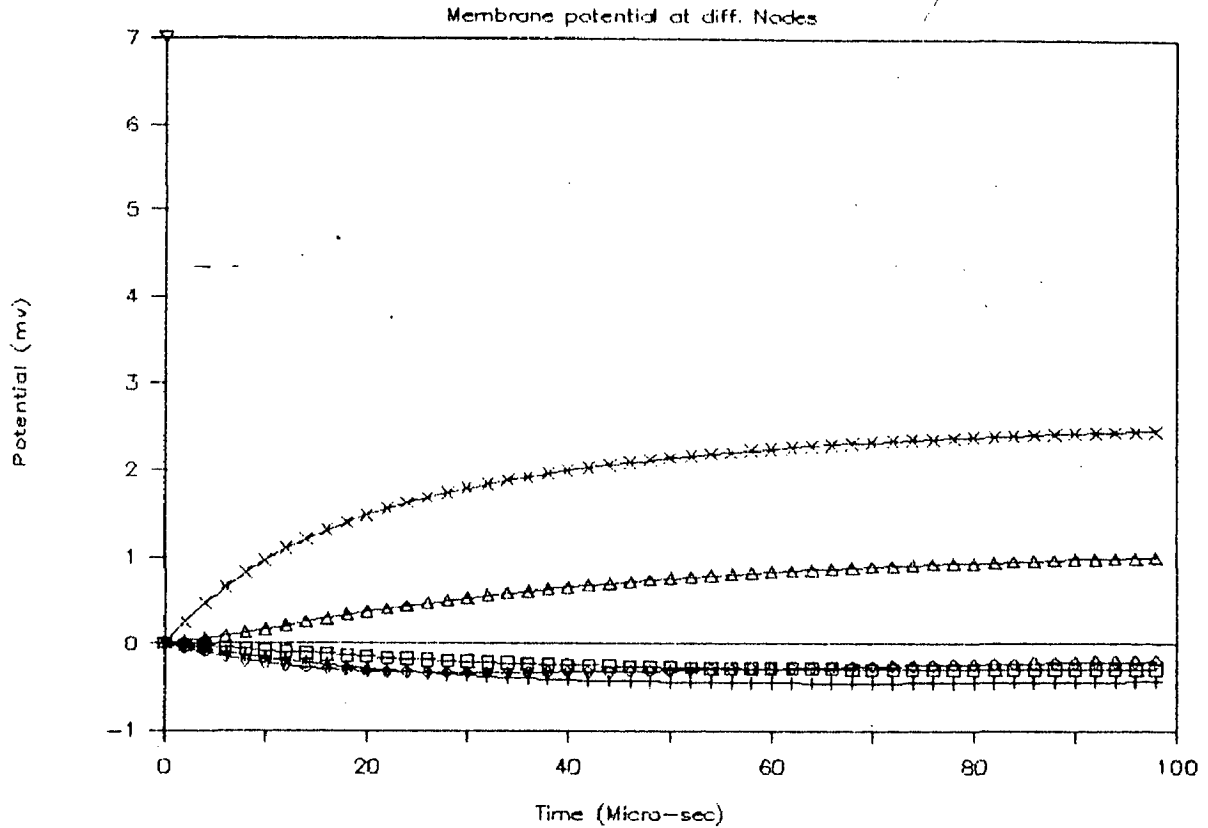
Membrane potential at diff. Nodes

(a)

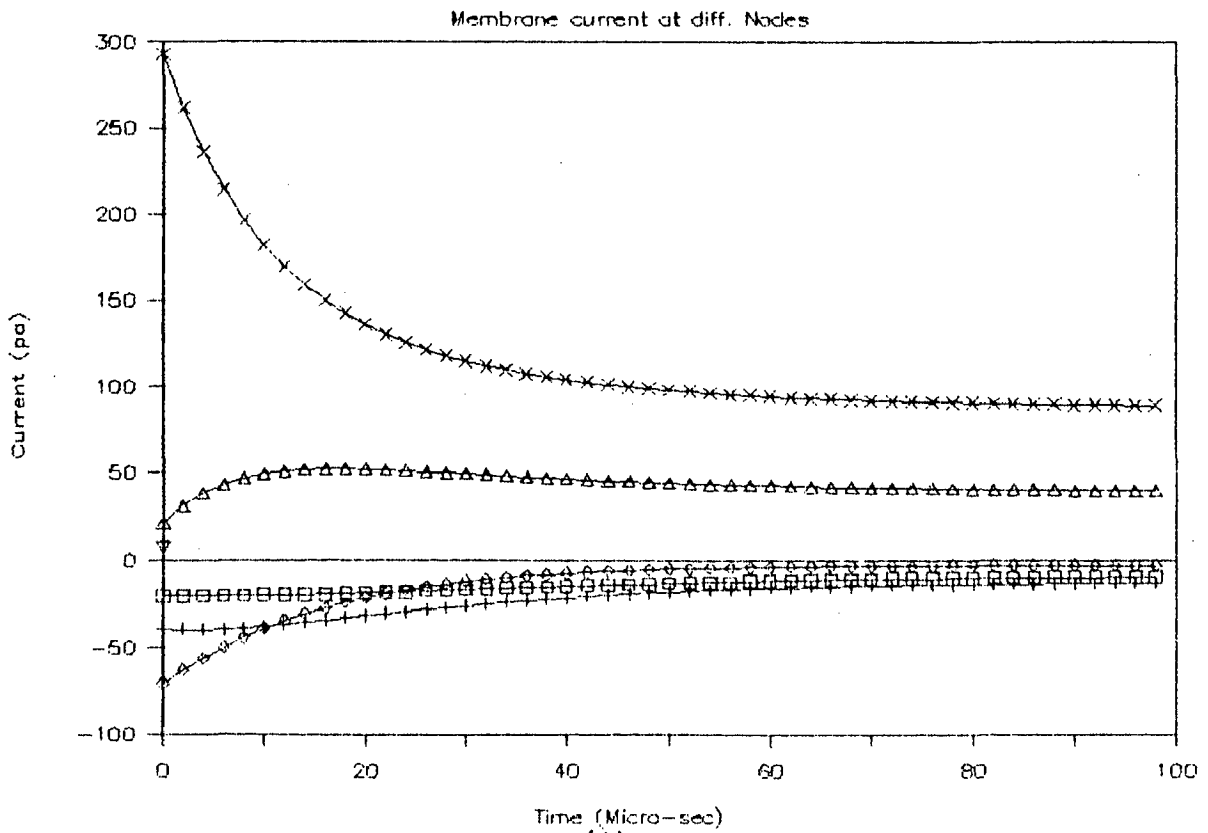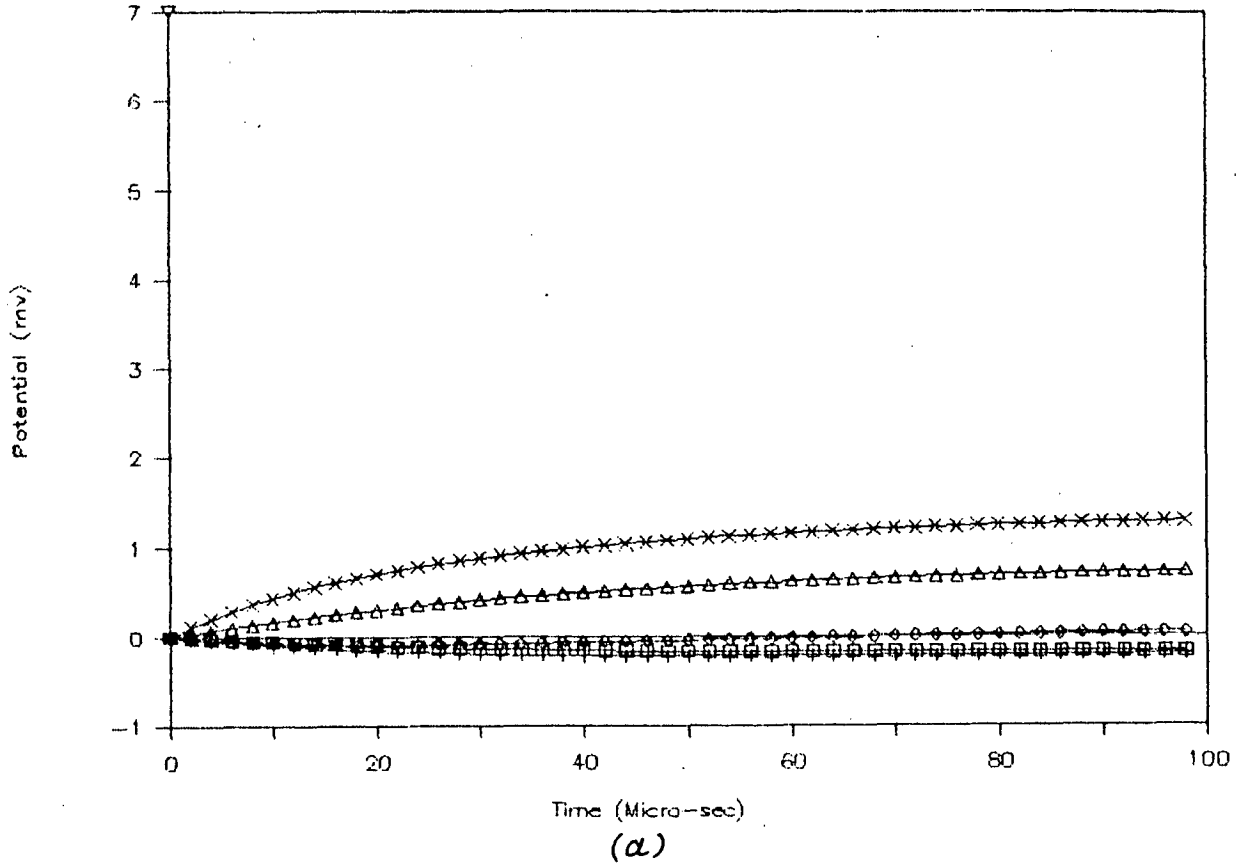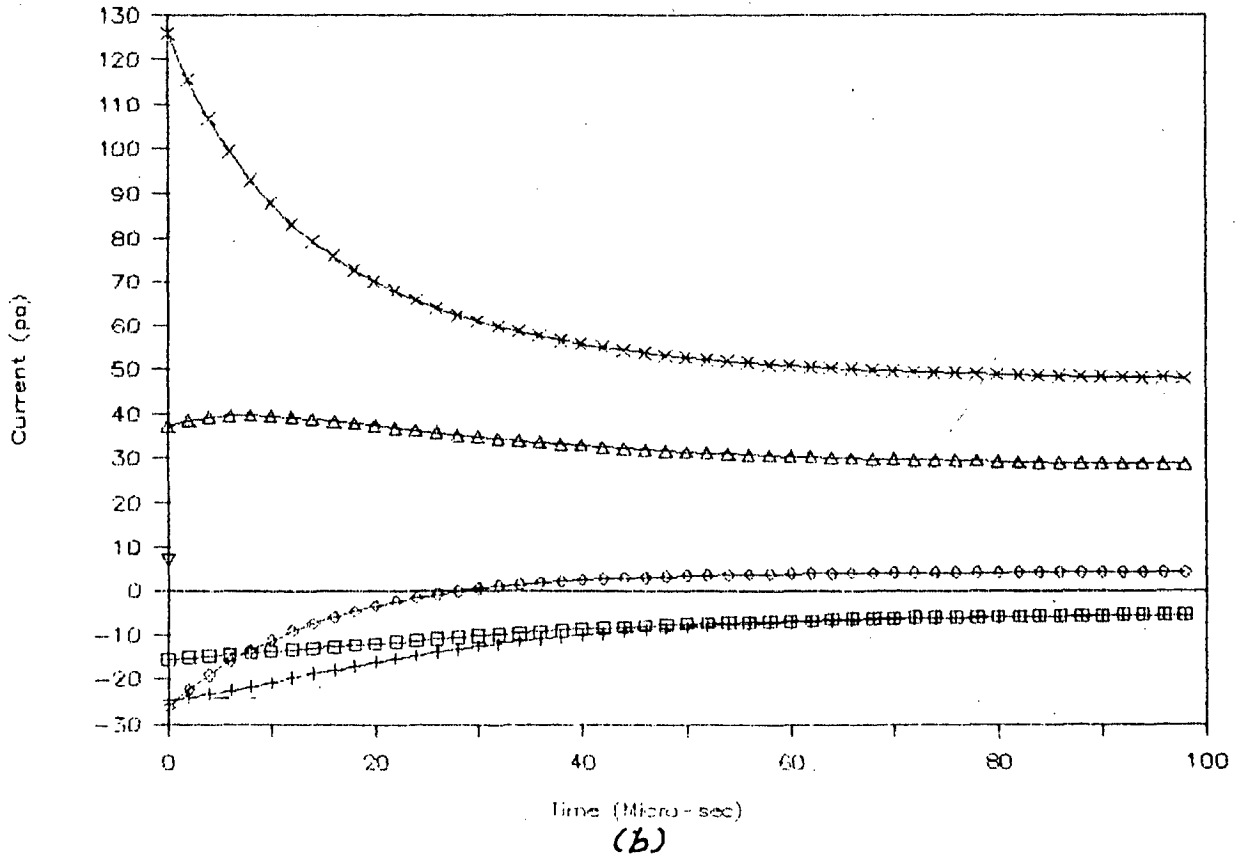### Membrane current at diff. Nodes

(b)

FIG.4.8   (a) Membrane potential at different nodes
(b) Membrane current at different nodes
For, L=0.2Cm, d=0.14E-2Cm, l=0.25E-3Cm, I=0.1E-3A, EDist=0.35Cm
X Node 0; Δ Nodes -1,1; ◊ Nodes -2,2; + Nodes -3,3; ▢ Nodes -4,4

decreases with the increase in the electrode distance from the nerve fiber, i.e. they are in inverse proportion. Here also, only node O will be excited since the depolarization at nodes 1 and -1 changes very slowly leading to accomodation.

The time response of the membrane current at these nodes is shown in Fig. 4.5(b), Fig. 4.6(b), Fig. 4.7(b) and Fig. 4.8(b). In all these cases the membrane current at node O falls off rapidly with time even though the stimulus current is constant. The initial value of the membrane current decreases sharply with the increase in the electrode distance. In Fig. 4.5(b) the membrane current at nodes 1 and -1 increases over the first 20 μsec and remains almost constant there after. In Fig. 4.6(b) the membrane currents at nodes 1 and -1 is initially negative, but becomes positive after 10 μs accounting for the eventual reversal of the membrane potential at these nodes [Fig. 4.6(a)]. In Fig. 4.7(b) the membrane currents at nodes 1 and -1 is positive from the begining and increases to twice it's initial value in 10 μsec and is constant afterwards. In Fig. 4.8(b) the membrane current at nodes 1 and -1 is positive and is constant upto 40 μs and decreases stightly at 40 μs and remains constant thereafter. The membrane current at nodes 2 and -2 increases gradually [Fig. 4.6(b)], [Fig. 4.7(b)], [Fig. 4.8(b)] initially being negative becomes positive at 30 μsec, causing the membrane potential at those nodes to reverse the sign [Fig. 4.6(b)]. All the graphs in Fig. 4.4 to Fig. 9.8 are summarized in TABLE - II.

TABLE - II

L = 0.2 cm, d = 0.14E-2, cm., L = 0.25E-3 cm, excitation
current I = 0.1 E-3A.

Electrode distance cm.	Voltage graphs	Current graphs
0.1	Fig. 4.4(a)	Fig. 4.4(b)
0.05	Fig. 4.5(a)	Fig. 4.5(b)
0.15	Fig. 4.6(a)	Fig. 4.6(b)
0.25	Fig. 4.7(a)	Fig. 4.7(b)
0.35	Fig. 4.8(a)	Fig. 4.8(b)

4.4.2 Effects Of Variation Of The Neuron Geometries And Stimulus Current :

In Fig. 4.9(a) to 4.11(b), the electrode distance is
kept constant at 0.05 cm but the stimulus current is changed
from 0.05 to 0.25 mA. Fig. 4.9(a), Fig. 4.10(a) and
Fig. 4.11(a) show the change in membrane potential at the
node below the electrode and at the four adjacent nodes and
Fig. 4.9(b), Fig. 4.10(b) and Fig. 4.11(b) show the time
course of the membrane current at these same nodes for the
stimulus currents of 0.05, 0.15 and 0.25 mA respectively. As
seen from Fig. 4.9(a), Fig. 4.10(a) and Fig. 4.11(a) only
node 0 is depolarized from the initiation of the stimulus,

Analysis of Myelinated Nerve

Membrane potential at diff.Nodes

(a)

Membrane current at diff.Nodes

(b)

FIG.4.9   (a) Membrane potential at different nodes
(b) Membrane current at different nodes
For, L=0.1Cm, d=0.05E-2Cm, l=0.1E-3Cm, EDist=0.05Cm, I=0.05E-3A
X Node 0; △ Nodes -1,1; ◊ Nodes -2,2; + Nodes -3,3; ☐ Nodes -4,4

FIG.4.10 (a) Membrane potential at different nodes
(b) Membrane current at different nodes
For, L=0.1Cm, d=0.05E-2Cm, l=0.1E-3Cm, EDist=0.05Cm, I=0.15E-3A
X Node 0; Δ Nodes -1,1; ◊ Nodes -2,2; + Nodes -3,3; □ Nodes -4,4

Analysis of Myelinated Nerve

Membrane potential at diff.Nodes

(a)

Membrane current at diff.Nodes

(b)
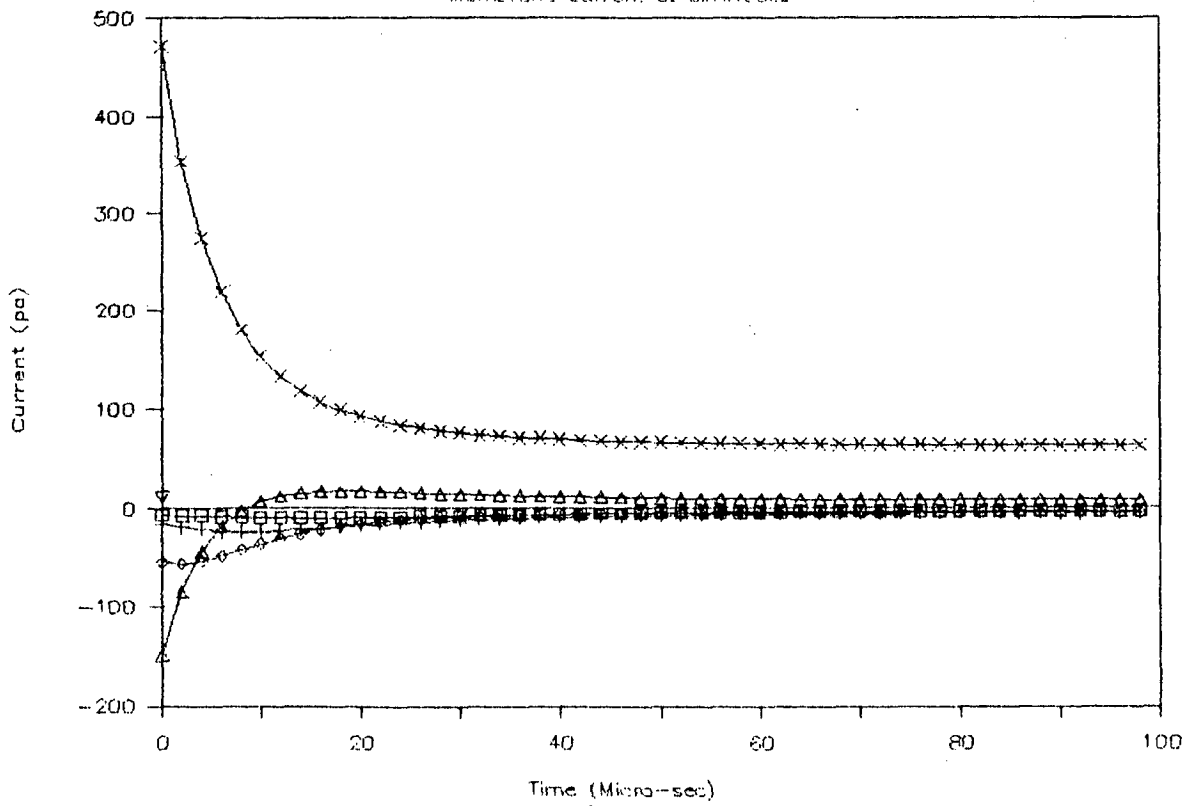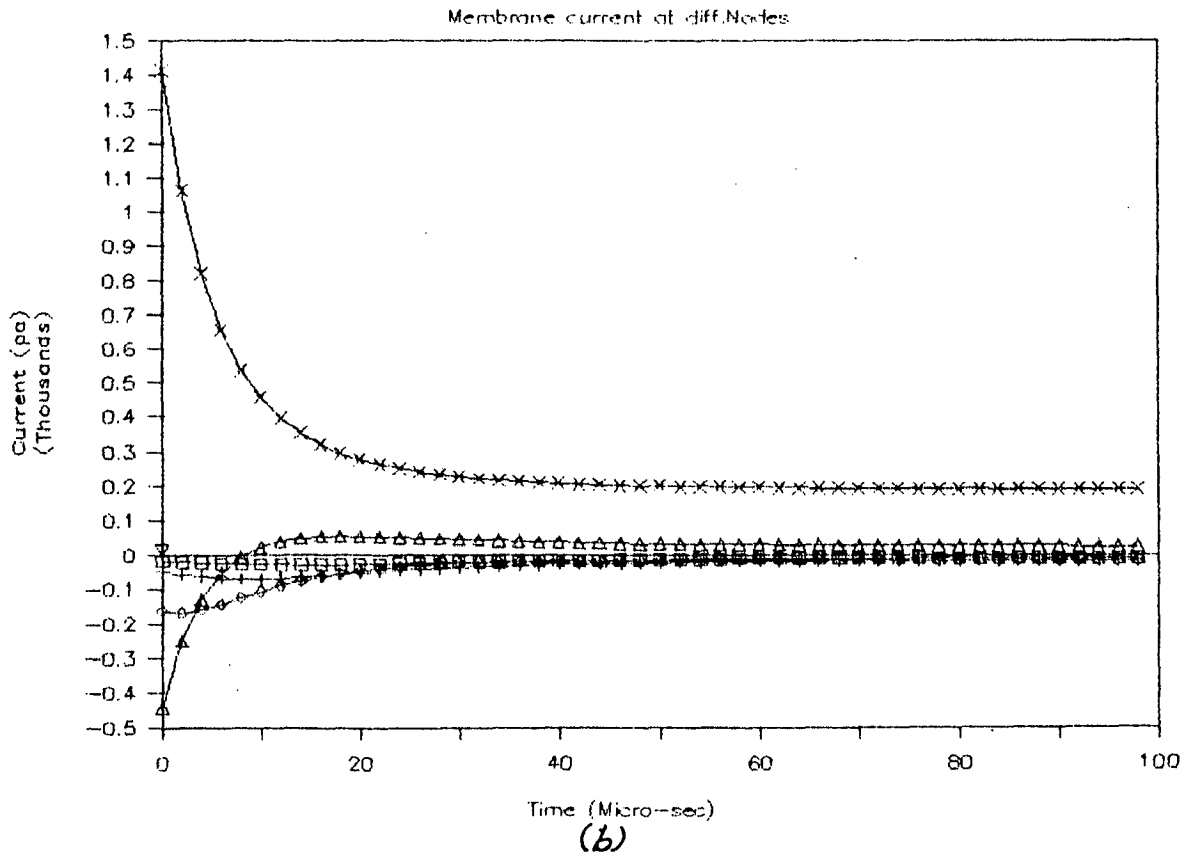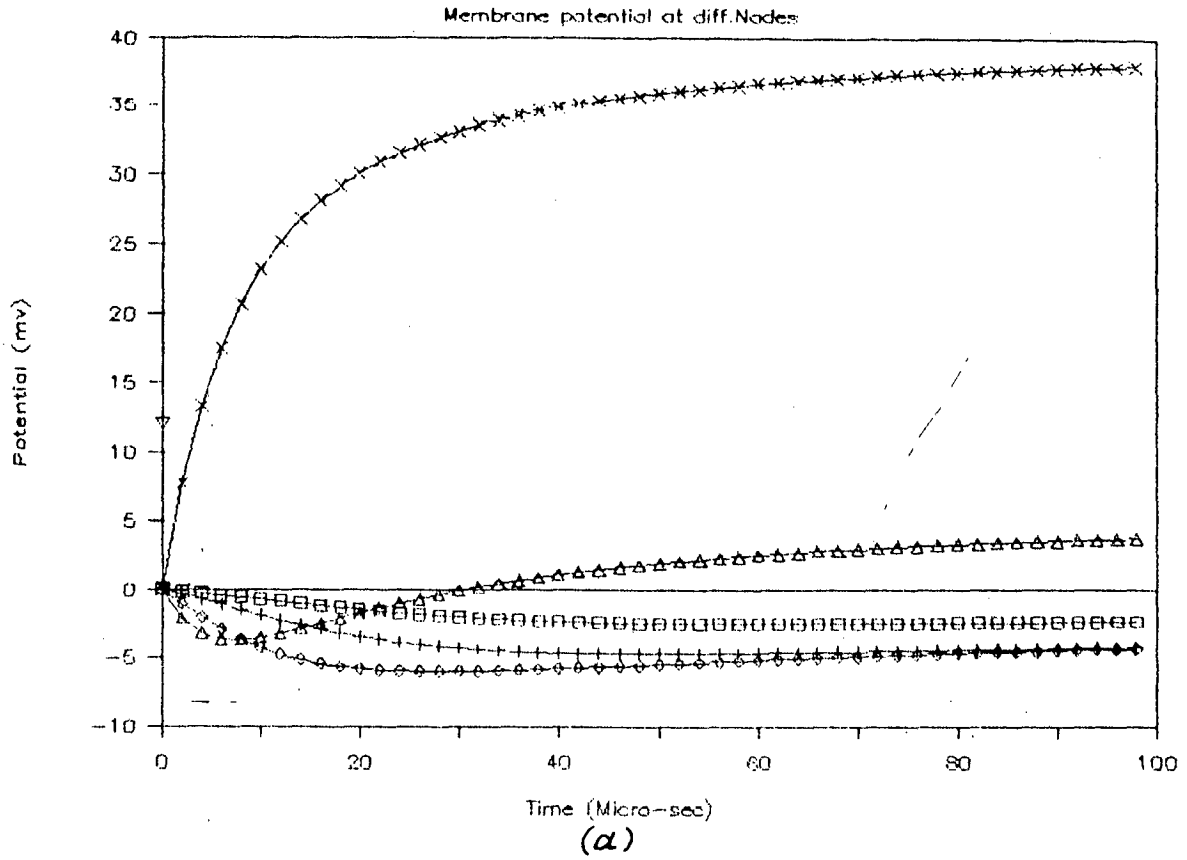
FIG.4.11 (a) Membrane potential at different nodes
(b) Membrane current at different nodes
For, L=0.1Cm, d=0.05E-2Cm, l=0.1E-3Cm, EDist=0.05Cm, I=0.25E-3A
✗ Node 0; △ Nodes -1,1; ◊ Nodes -2,2; + Nodes -3,3; ▢ Nodes -4,4

nodes 1 and -1 are hyperpolarized initially and reverse
sign at 30 µs, and remain depolarized there after. All the
other nodes are hyperpolarized. As the stimulus current is
increased the depolarization and hyperpolarization level
reached by the respective nodes progressively increases,
where as the signs remain the same.

As seen from Fig. 4.9(b), Fig. 4.10(b) and Fig. 4.11(b)
the membrane current at node 0 decreases rapidly from a initi-
ally high value to a steady-state lower value and remain
almost constant. The current at node 1 and -1 is initially
negative but becomes positive after 10 µsec and remains
positive there after causing the reversal of membrane potential
sign at those nodes. The currents at all the other nodes is
negative. The magnitude of the positive and negative currents
at the respective nodes increases with the increase in the
stimulus current as expected. In this case only node 0 is
excited as it under goes steep change in depolarization, but
nodes 1 and -1 are not excited as the change in membrane
potential at these nodes is very slow. The graphs are summ-
erized in TABLE - III.

TABLE - III

L = 0.1 cm, d = 0.05 E-2 cm, l = 0.1 E-3 cm, electrode distance = 0.05 cm.

Stimulus current Amperes	Voltage graphs	Current graphs
0.05E-3	Fig. 4.9(a)	Fig. 4.9(b)
0.15E-3	Fig. 4.10(a)	Fig. 4.10(b)
0.25E-3	Fig. 4.11(a)	Fig. 4.11(b)

The change in membrane potential and membrane current at node below the electrode and four adjacent nodes for electrode currents of 0.05, 0.15 and 0.25 mA and electrode distance = 0.25 cm are shown in Fig. 4.12(a), Fig. 4.13(a), Fig. 4.14(a) and Fig. 4.12(b), Fig. 4.13(b), Fig. 4.14(b) respectively. From Fig. 4.12(a), Fig. 4.13(a) and Fig. 4.14(a) it is seen that node 0, nodes 1 and -1 and nodes 2 and -2 are depolarized with the node 0 undergoing the highest level of depolarization and nodes 2 and -2 undergoing the lowest level of depolarization. The potential at nodes 3 and -3 are hyperpolarized initially but become depolarized after 74 μs and remain depolarized there after. All the other nodes are hyperpolarized. As the stimulus current is increased the level of depolarization and hyperpolarization at respective nodes increases.

The time response of the membrane current at these nodes is shown in Fig. 4.12(b), Fig. 4.13(b) and Fig. 4.14(b)

Analysis of Myelinated Nerve
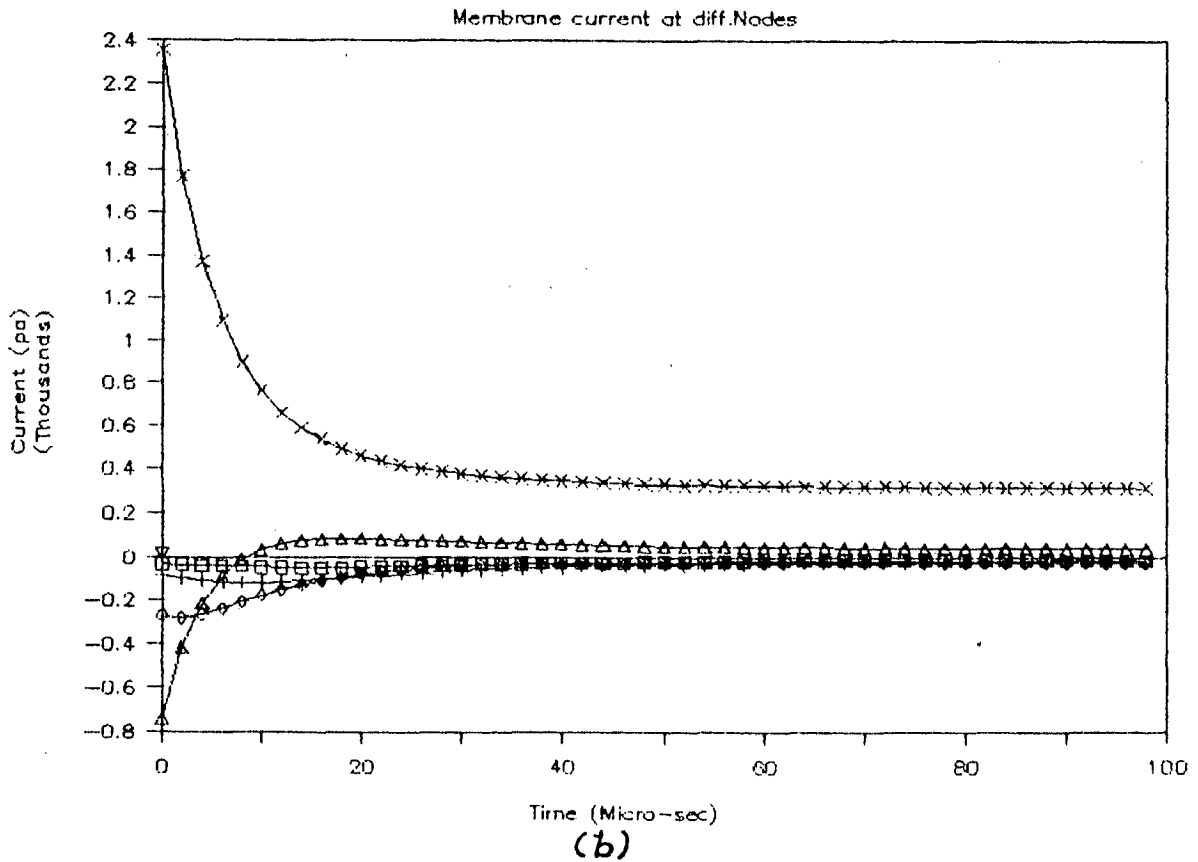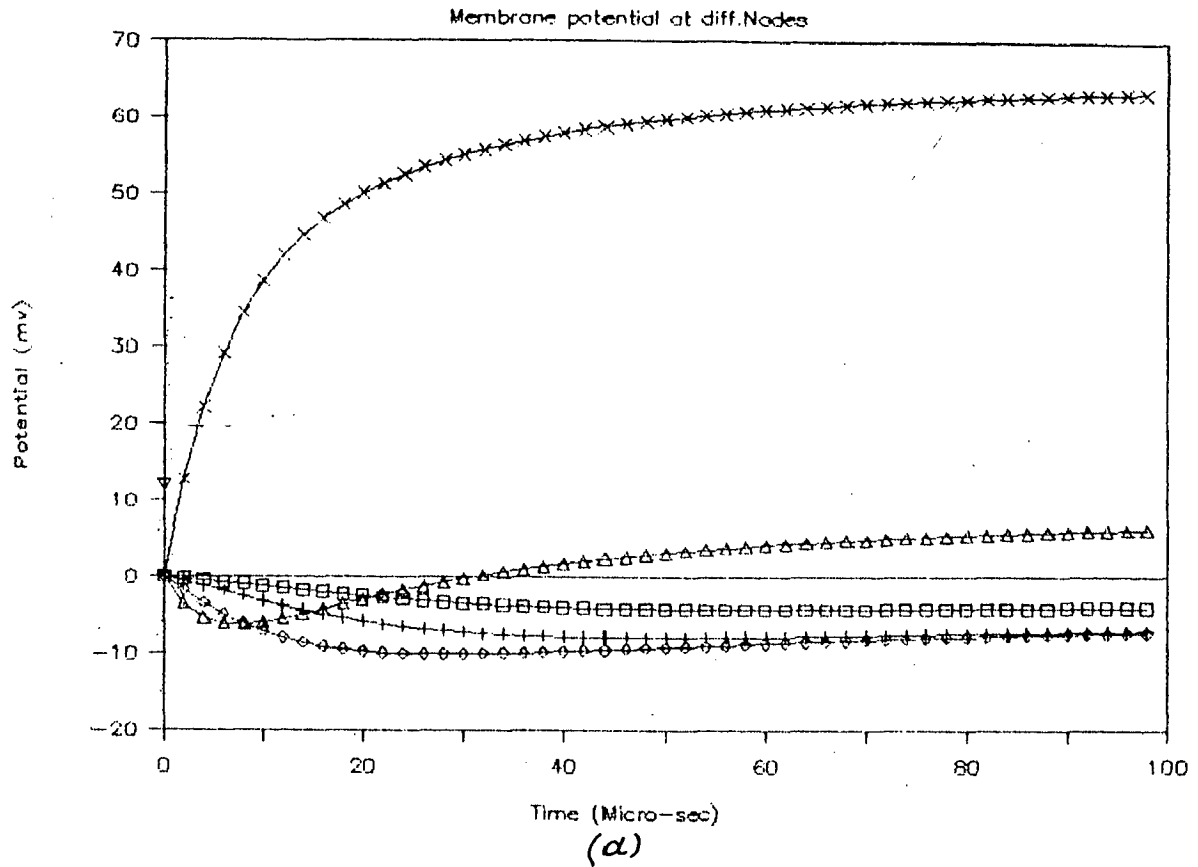
Potential at diff. Nodes

(a)
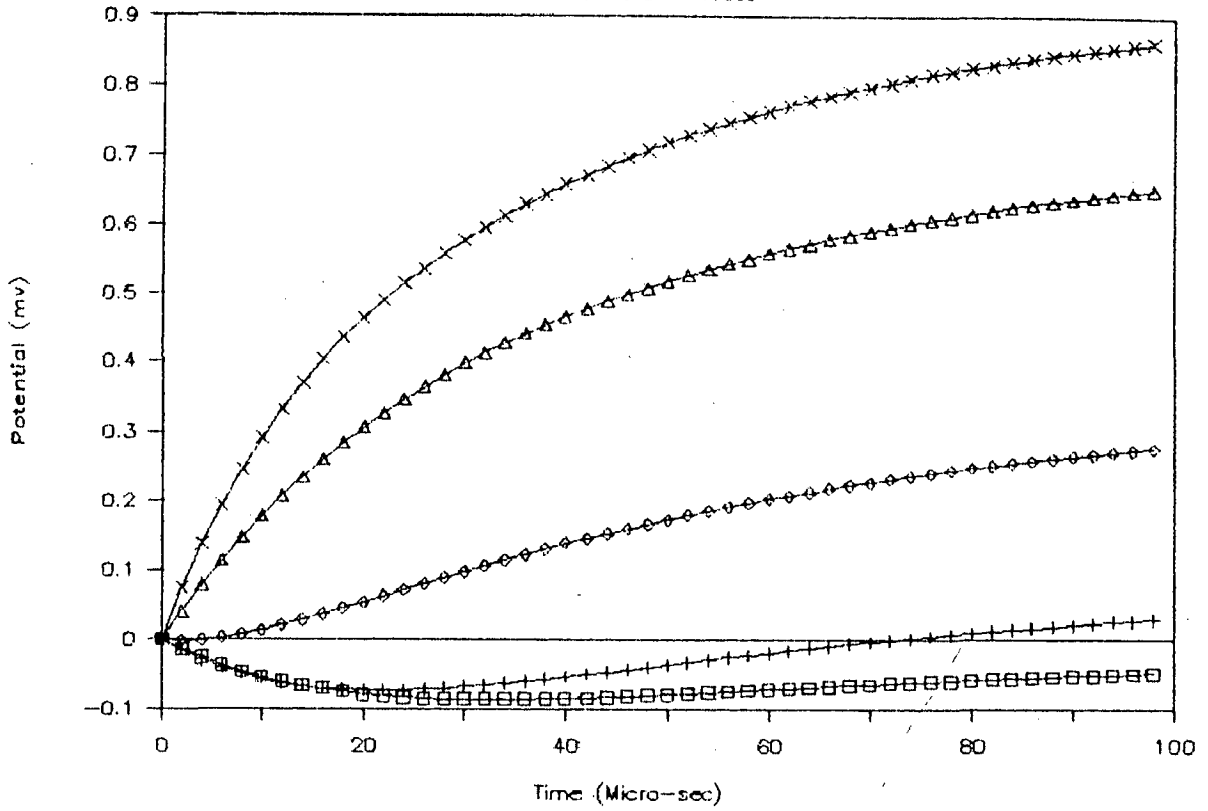
Membrane current at diff. Nodes

(b)

FIG. 4.12 (a) Membrane potential at different nodes
(b) Membrane current at different nodes
For, L=0.1Cm, d=0.05E-2Cm, l=0.1E-3Cm, EDist=0.25Cm, I=0.05E-3A
X Node 0; △ Nodes -1,1; ◊ Nodes -2,2; + Nodes -3,3; □ Nodes -4,4

FIG.4.13 (a) Membrane potential at different nodes
(b) Membrane current at different nodes
For, L=0.1Cm, d=0.05E-2Cm, l=0.1E-3Cm, EDist=0.25Cm, I=0.15E-3A
X Node 0; Δ Nodes -1,1; ◊ Nodes -2,2; + Nodes -3,3; □ Nodes -4,4

Analysis of Myelinated Nerve

Membrane potential at diff. Nodes

(a)

Membrane current at diff. Nodes

(b)

FIG.4.14 (a) Membrane potential at different nodes
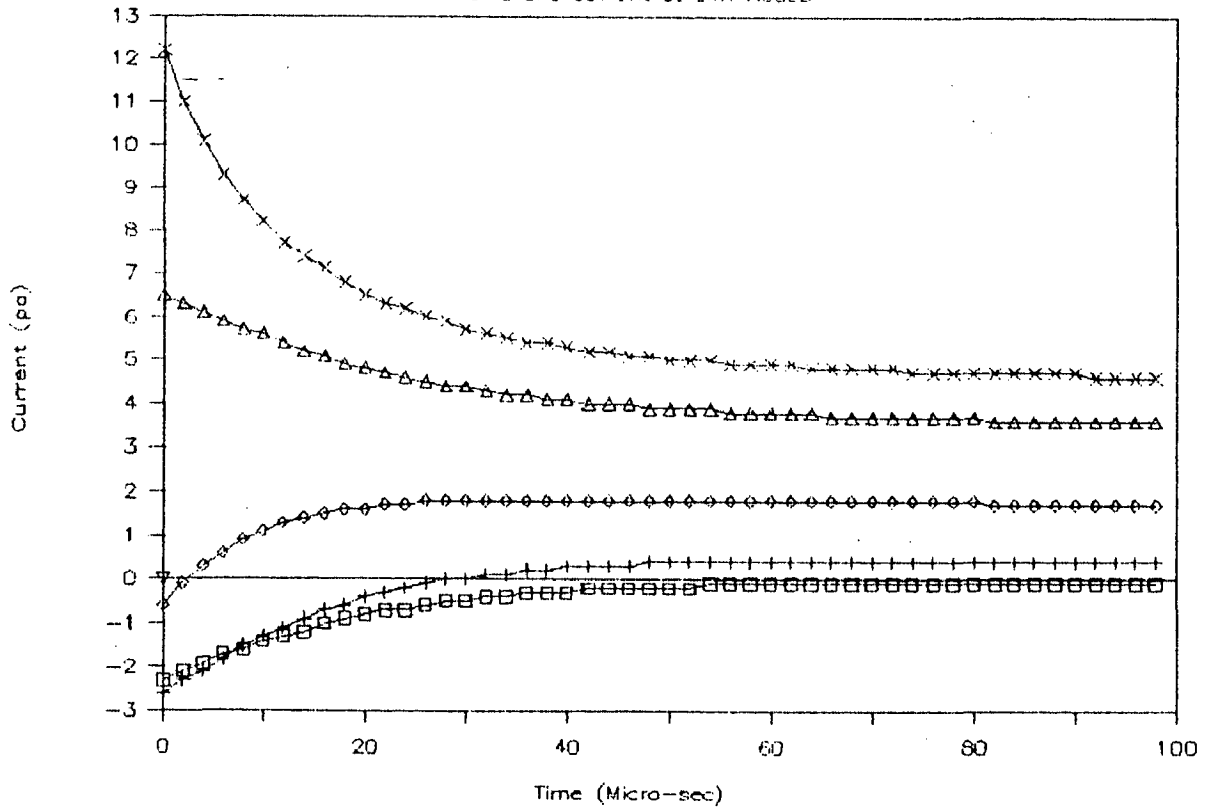(b) Membrane current at different nodes
For, L=0.1Cm, d=0.05E-2Cm, l=0.1E-3Cm, EDist=0.25Cm, I=0.25E-3A
X Node 0; △ Nodes -1,1; ◇ Nodes -2,2; + Nodes -3,3; □ Nodes -4,4

As seen the rate of decrease of the membrane current at node
0 and nodes 1 and -1 is on a slower pace compared to earlier
cases and so also is the rate of increase of the membrane
potentials at these conditions. The membrane current at
nodes 2 and -2 is negative initially but becomes positive
after 3 µsec and remains positive there after accounting for
the eventual reversal of membrane potential at these nodes.
So also the membrane current at nodes 3 and -3 is initially
negative and becomes positive at 28 µsec and remains positive
there after causing the membrane potential at these nodes to
reverse sign. Here only node 0, nodes 1 and -1 and nodes 2
and -2 will be excited. Nodes 3 and -3 will not be excited
since the depolarization attained at these nodes is very
low. (approximately 1 mV).

For the neuron conditions mentioned in TABLE - IV
if it is desired to excite selectively node 0 (the node below
the electrode) and two nodes on both sides of the electrode
then this electrode distance of 0.25 cm and the stimulus
current of 0.05 mA to 0.25 mA can be used effectively.

TABLE - IV

L = 0.1 cm, d = 0.05E-2 cm , 1 = 0.1E-3 cm , electrode distance = 0.25 cm.

Stimulus current Amperes	voltage graphs	current graphs
0.05E-3	Fig. 4.12(a)	Fig. 4.12(b)
0.15E-3	Fig. 4.13(a)	Fig. 4.13(b)
0.25E-3	Fig. 4.14(a)	Fig. 4.14(b)

In Fig. 4.15(a), Fig. 4.16(a) and Fig. 4.16(a) the change in membrane potential at the node below the electrode and at the four adjacent nodes is shown. Initially node 0, nodes 1 and -1, nodes 2 and -2, and nodes 3 and -3 are depolarized; however, nodes 4 and -4 are hyperpolarized initially but reverse sign at 25 μs and remain depolarized from that time on. The level of depolarization reached by node 0 is the highest and the depolarization reached by nodes 3 and -3 is the lowest. A striking feature of these curves is that the rate of rise of depolarization is relatively low compared to those in the earlier cases, Fig. 4.9(a), Fig. 4.10(a), Fig. 4.11(a) and Fig. 4.12(a), Fig. 4.13(a) and Fig. 4.14(a). From this it is evident that, under these conditions the increase in stimulus current upto 0.25 mA is effective only to excite nodes 0, nodes 1 and -1, nodes 2 and - 2 and nodes 3 and -3. Nodes 4 and -4 will not excited since rise of depolarization at these nodes is quite slow

Analysis of Myelinated Nerve

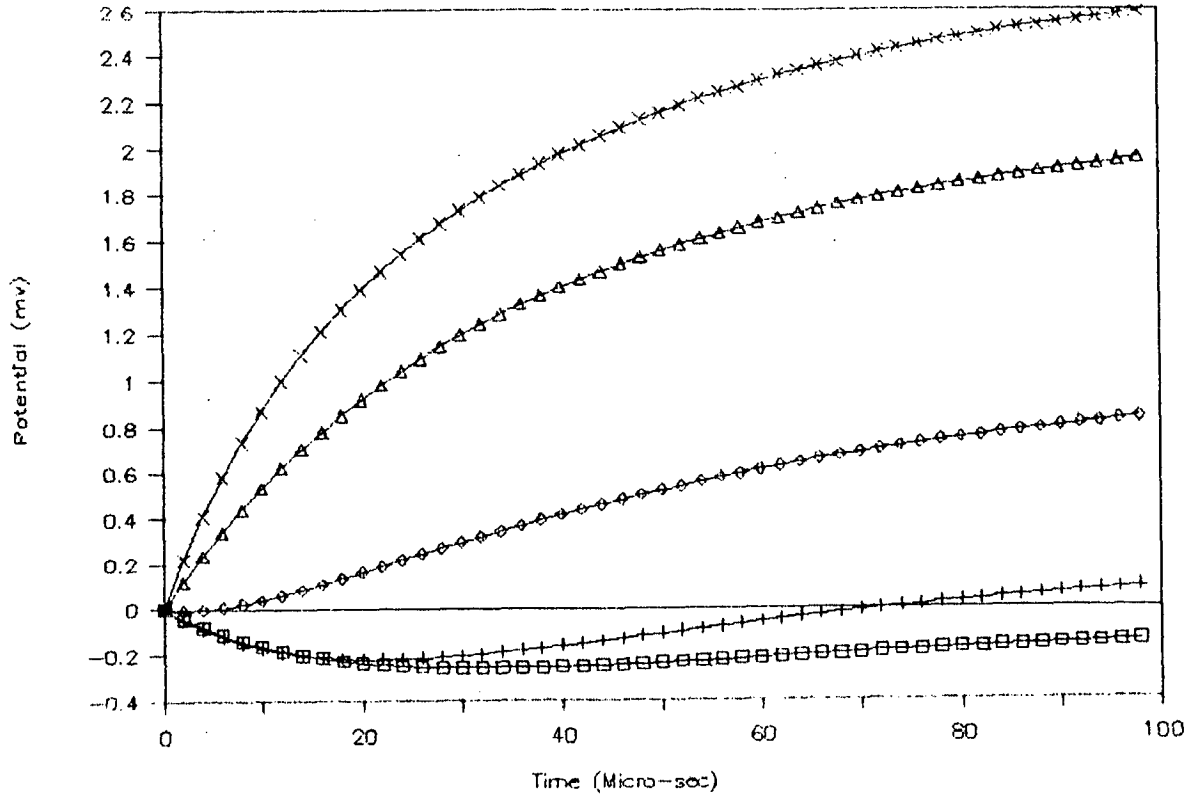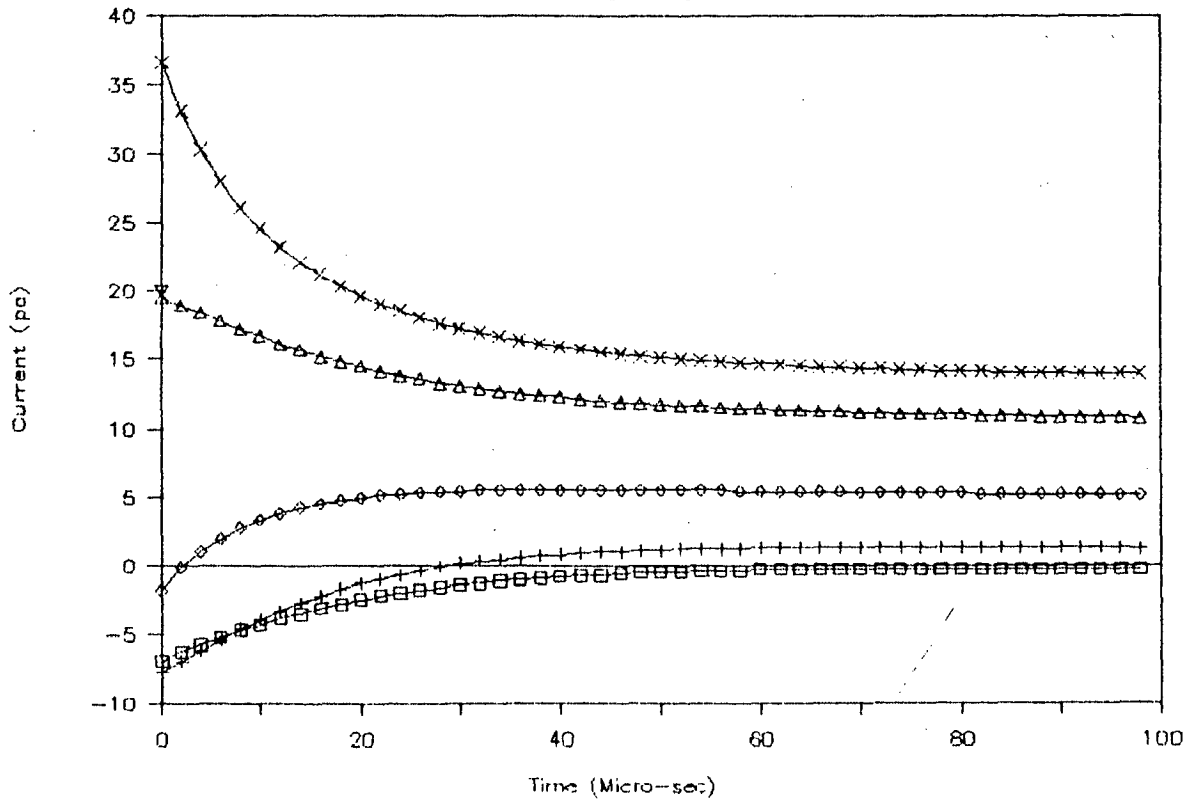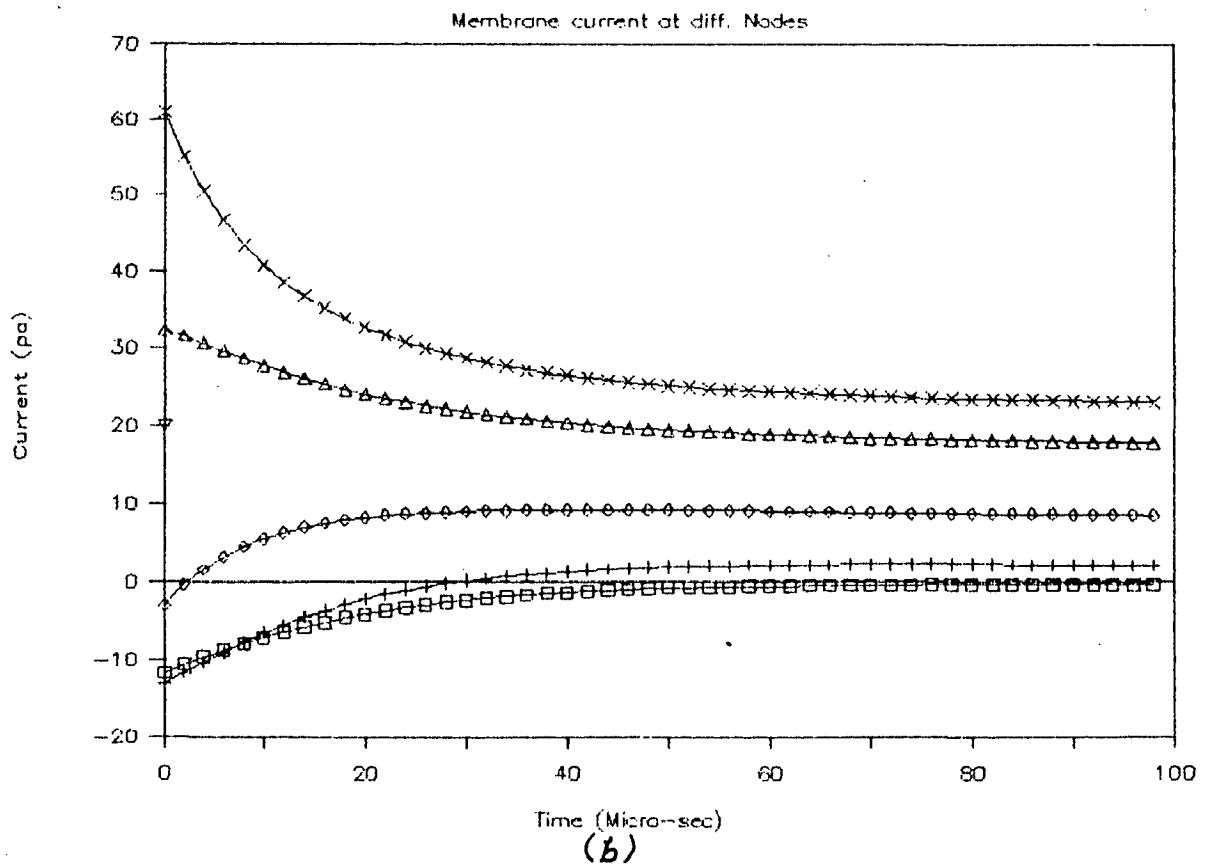## Membrane potential at diff.Nodes

(a)

Membrane current at diff.Nodes

(b)
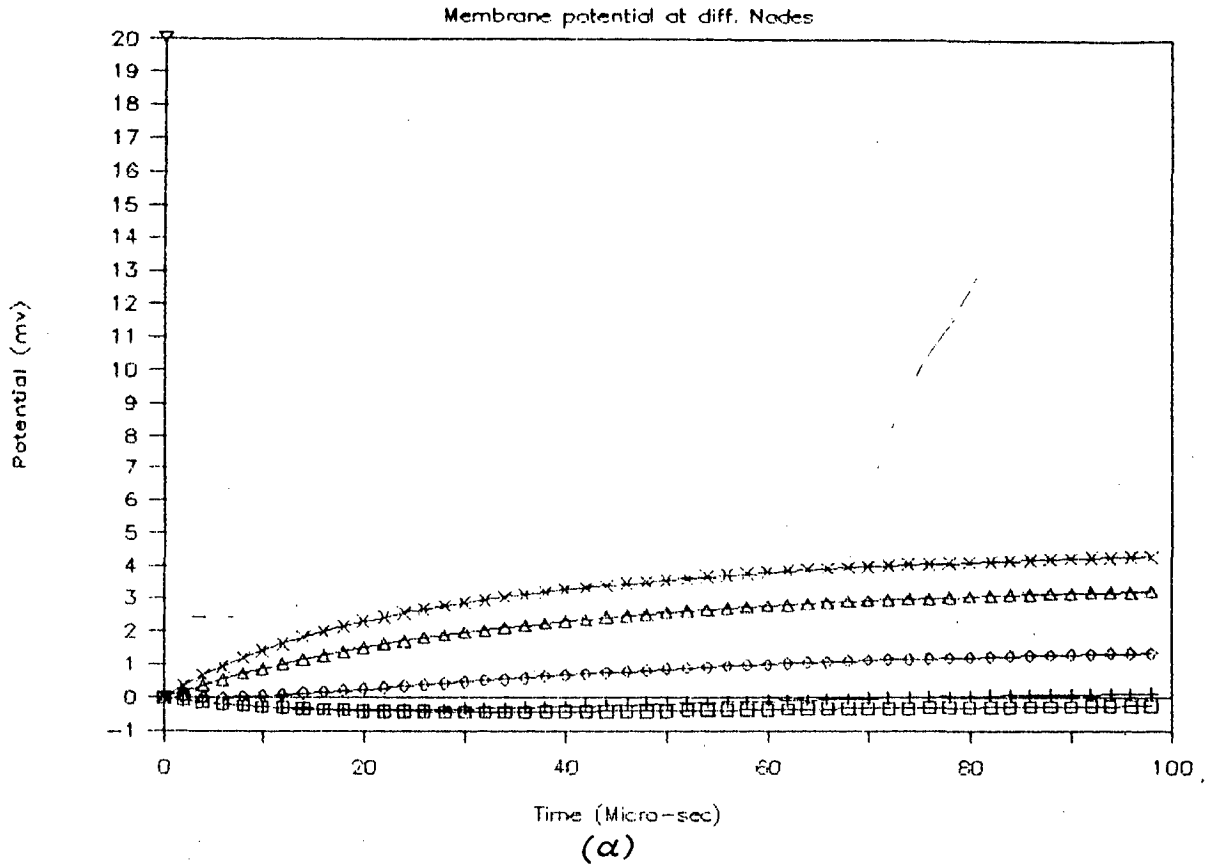
FIG.4.15 (a) Membrane potential at different nodes
(b) Membrane current at different nodes
For, L=0.1Cm, d=0.05E-2Cm, l=0.1E-3Cm, EDist=0.45Cm, I=0.05E-3A
X Node 0; △ Nodes -1,1; ◊ Nodes -2,2; + Nodes -3,3; □ Nodes -4,4

Analysis of Myelinated Nerve

Membrane potential at diff.Nodes

(a)

Membrane current at diff.Nodes

(b)

FIG.4.16 (a)Membrane potential at different nodes
(b)Membrane current at different nodes
For,L=0.1Cm,d=0.05E-2Cm,l=0.1E-3Cm,EDist=0.45Cm,I=0.15E-3A
X Node 0;△ Nodes -1,1;◊ Nodes -2,2; + Nodes -3,3;◻ Nodes -4,4

Analysis of Myelinated Nerve

Membrane potential at diff.Nodes

Potential (mv)

Time (Micro-sec)

(a)

Membrane current at diff.Nodes

Current (pa)

Time (Micro-sec)

(b)

FIG.4.17 (a) Membrane potential at different nodes
(b) Membrane current at different nodes
For, L=0.1Cm, d=0.05E-2Cm, l=0.1E-3Cm, EDist=0.45Cm, I=0.25E-3A
X Node 0; △ Nodes -1,1; ◇ Nodes -2,2; + Nodes -3,3; □ Nodes -4,4

and also the level of depolarization reached by them is very low. An important conclusion is arrived at here. That is by further increasing the dimensions of the various parts of the neuron will not even excite as many nodes on either side of node 0, since there is a minimum rate of increase and level of depolarization that a stimulus current is required to full fill for generating excitation at the neuron nodes [5,7].

Fig. 4.15(b), Fig. 4.16(b) and Fig. 4.17(b) show the time response of the membrane current at these same nodes. The membrane current for nodes 0, nodes 1 and -1 nodes 2 and -2, nodes 3 and -3 is positive. The current at nodes 0 and nodes 1 and -1 decreases slightly upto 20 μs and remains almost constant there after. The current at nodes 2 and -2 is highly stable. The current at nodes 3 and -3 increases slightly upto 20 μs and remains almost stable there after. The capacitive effect under these conditions is suppressed and the ionic component dominates in contrary to the observations made in Fig. 4.4(b), Fig. 4.5(b), Fig. 4.6(b), Fig. 4.7(b) and Fig. 4.8(b). The current at nodes 4 and -4 is initially negative, but becomes positive after 11 μs and remains positive there after accounting for the eventual reversal of membrane potential at these nodes. [Fig. 4.15(a)], [Fig. 4.17(b)]. The graphs are summarized in TABLE - V.

TABLE - V

L = 0.1 cm, d = 0.05E-2 cm., 1 = 0.01E-3 cm., electrode

distance = 0.45 cm.

Stimulus current Amperes	Voltage graphs	Current graphs
0.05E-3	Fig. 4.15(a)	Fig. 4.15(b)
0.15E-3	Fig. 4.16(a)	Fig. 4.16(b)
0.25E-3	Fig. 4.17(a)	Fig. 4.17(b)

In Fig. 4.18(a), Fig. 4.19(a) and Fig. 4.20(a), the
change in membrane potential at the node below the electrode
and at the four adjacent nodes is shown. It is seen that
only node O is depolarized and all the other nodes are
hyperpolarized. The depolarization is quite fast in the first
40 μs and is relatively slow there after. This is caused by the
decline in the response of the ionic currents to sustained
stimulus after some time, which is in turn due to the regain-
ing of the power of the sodium-potassium-pump. All the other
nodes are hyperpolarized.

The time response of the membrane current at these
nodes is shown in Fig. 4.18(b), Fig. 4.19(b) and Fig. 4.20(b).
The membrane current at node O falls off rapidly upto 20 μs
and is about one-third of the initial value at that time.

Analysis of Myelinated Nerve

Membrane potential at diff. Nodes

(a)

Membrane current at diff. Nodes

(b)
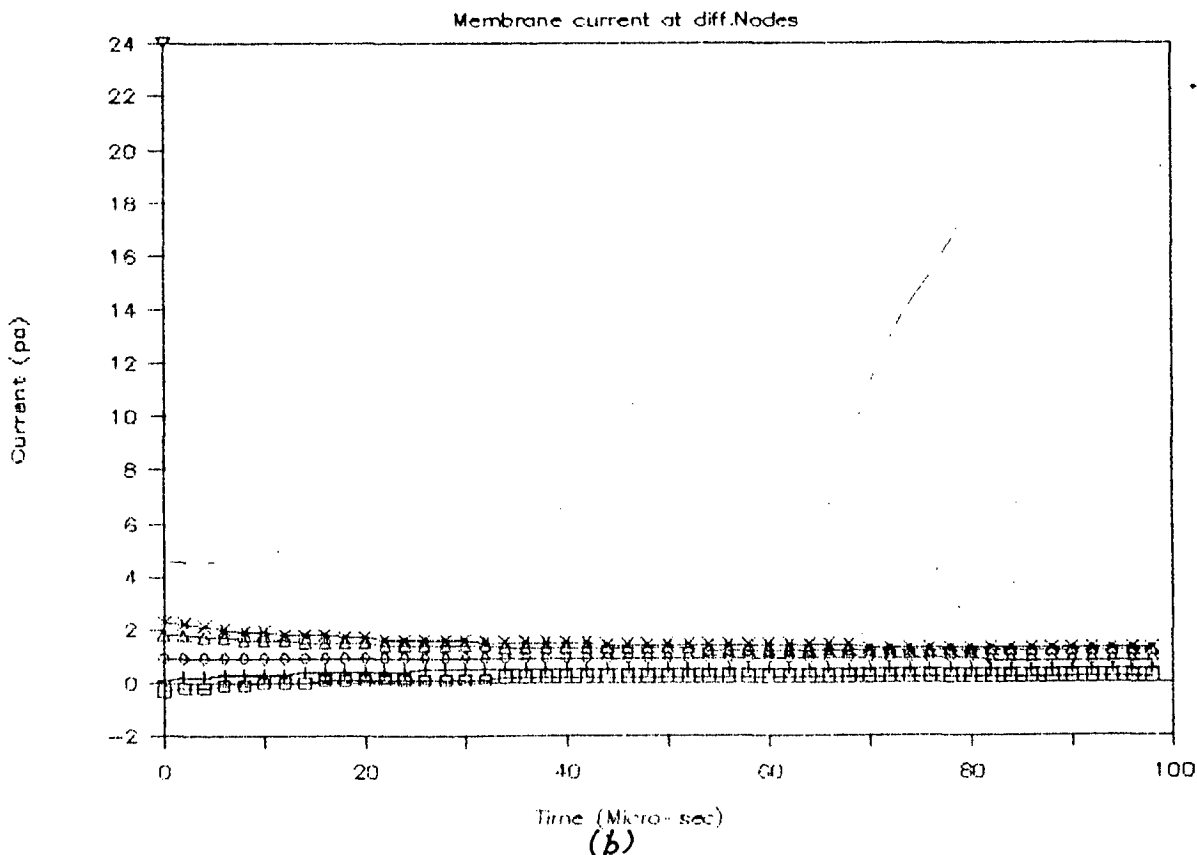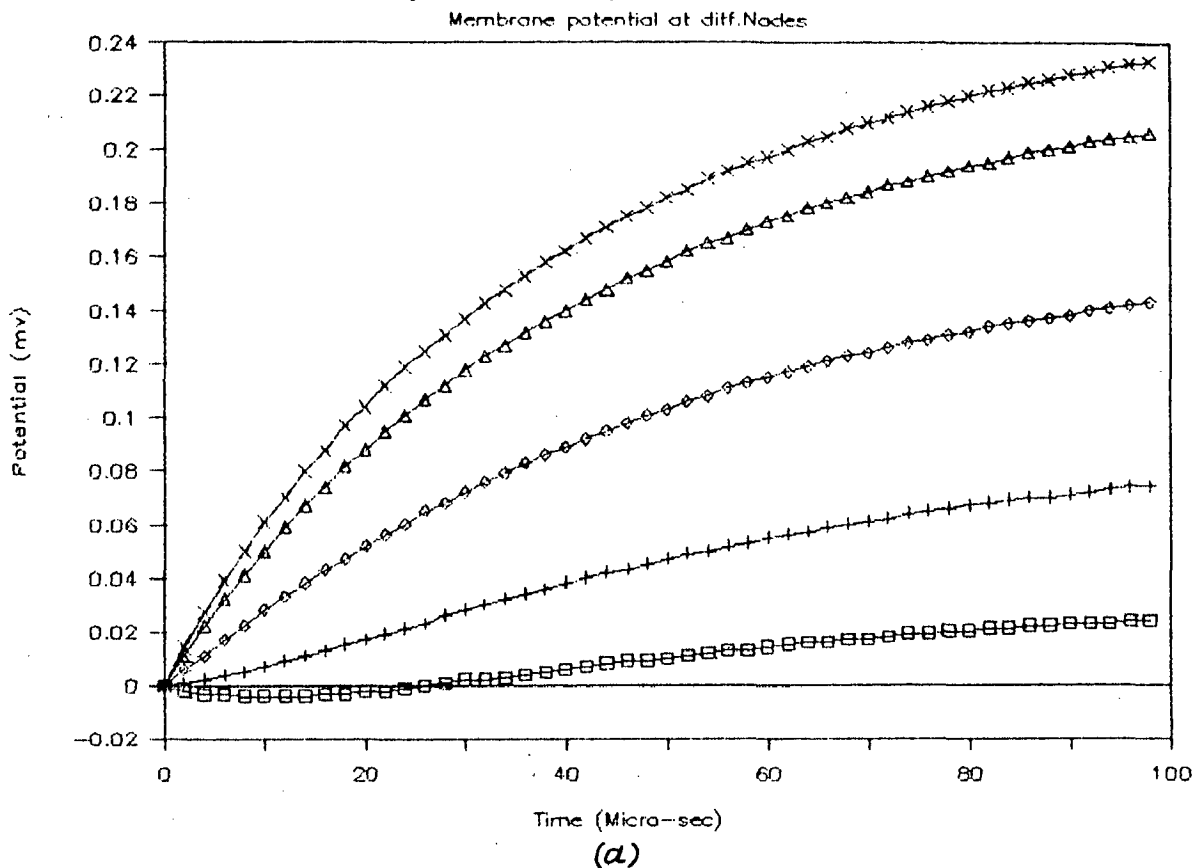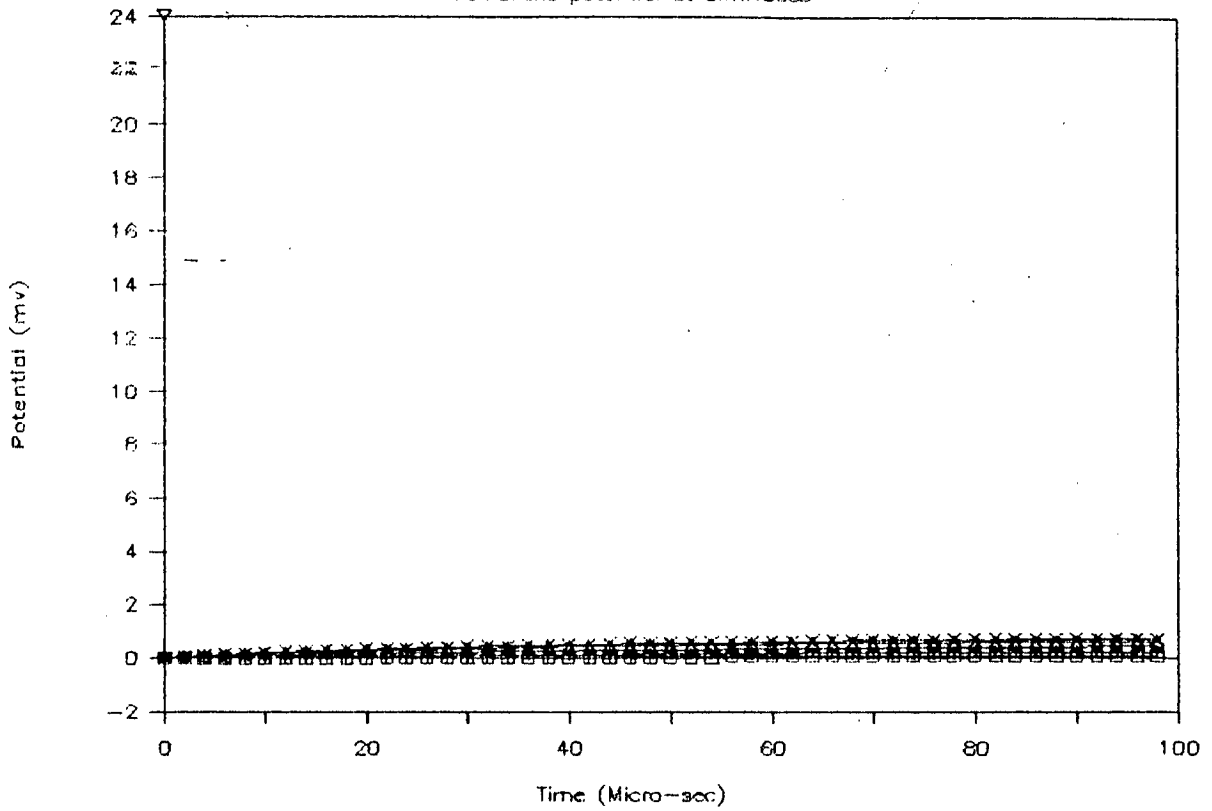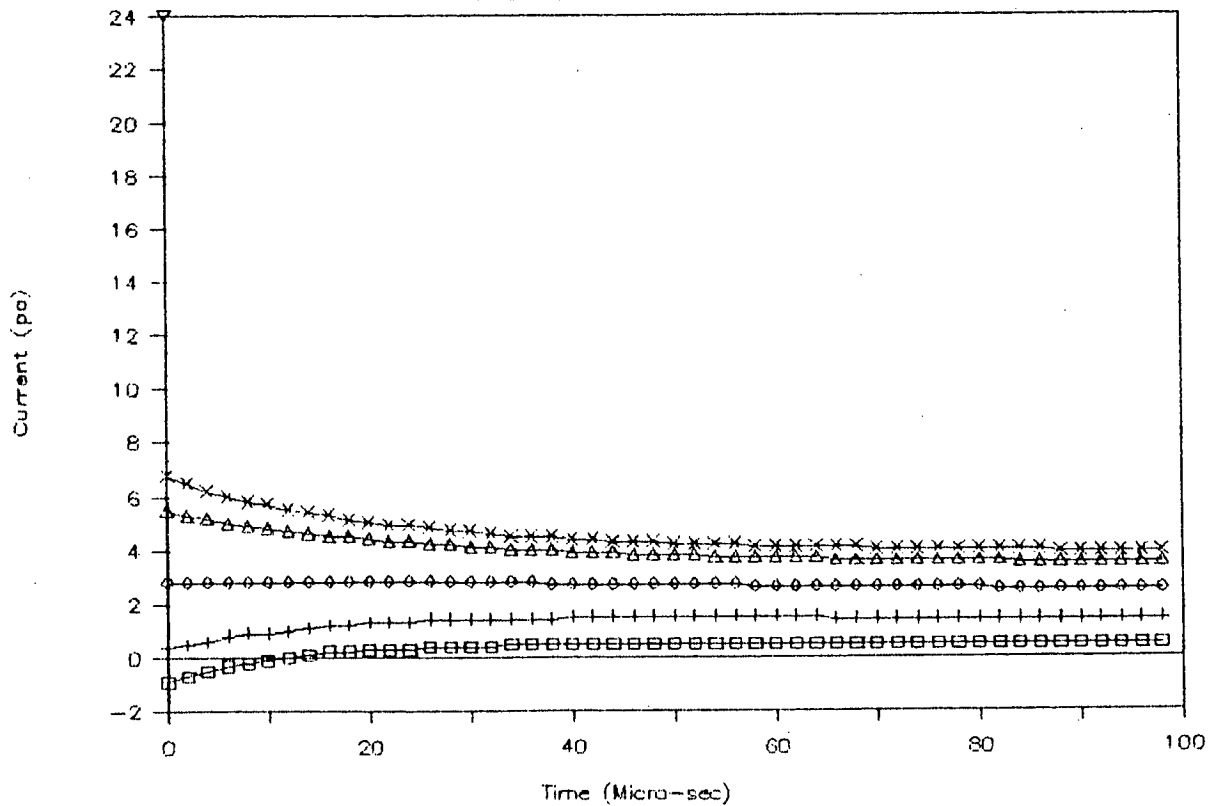
FIG.4.18 (a) Membrane potential at different nodes
(b) Membrane current at different nodes
For, L=0.3Cm, d=0.15E-2Cm, l=0.3E-3Cm, EDist=0.05Cm, I=0.05E-3A
✕ Node 0; △ Nodes -1,1; ◇ Nodes -2,2; ✚ Nodes -3,3; ⬜ Nodes -4,4

Analysis of Myelinated Nerve

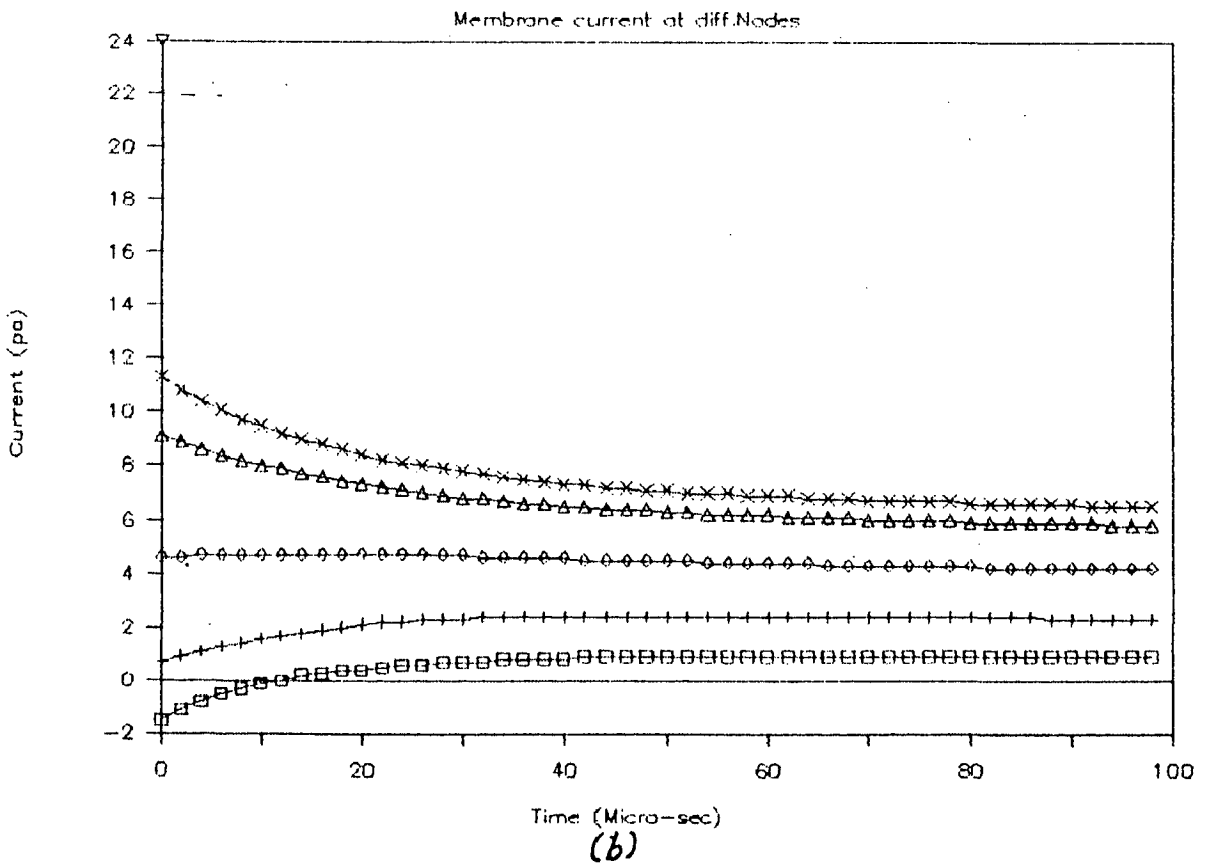### Membrane potential at diff. Nodes

(a)

Membrane current at diff. Nodes

(b)

FIG.4.19 (a) Membrane potential at different nodes
(b) Membrane current at different nodes
For, L=0.3Cm, d=0.15E-2Cm, l=0.3E-3Cm, EDist=0.05Cm, I=0.15E-3A
✕ Node 0; △ Nodes -1,1; ◊ Nodes -2,2; + Nodes -3,3; ☐ Nodes -4,4

Analysis of Myelinated Nerve

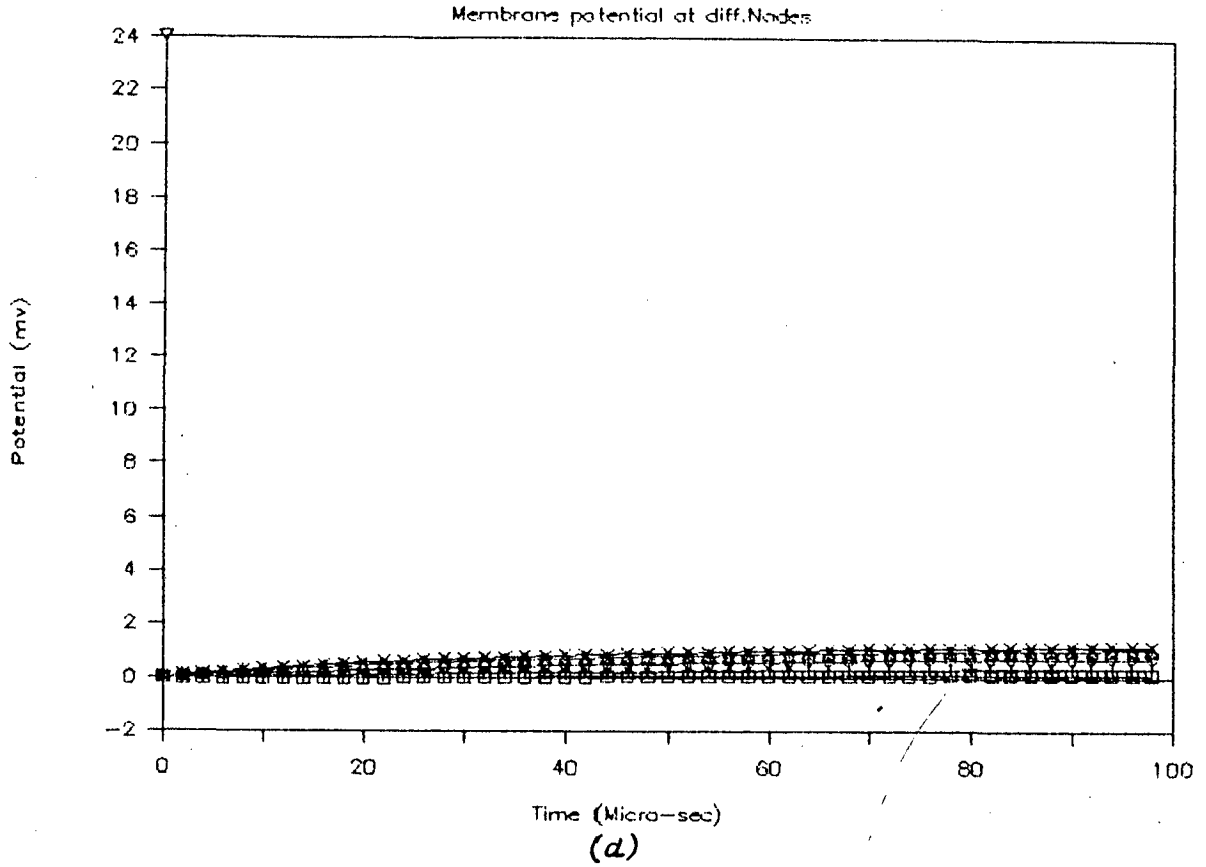## Membrane potential at diff. Nodes

(a)

Membrane current at diff. Nodes

(b)

FIG.4.20 (a) Membrane potential at different nodes
(b) Membrane current at different nodes
For, L=0.3Cm, d=0.15E-2Cm, l=0.3E-3Cm, EDist=0.05Cm, I=0.25E-3A
X Node 0; △ Nodes -1,1; ◇ Nodes -2,2; + Nodes -3,3; □ Nodes -4,4

It further continues to fall to a steady-state value that is approximately one-fifth of the initial value. Most of the initial current is capacitive, but the ionic component dominates for $t > 50$ μs. The current at nodes 1 and -1 is more negative and undergoes a transition up to 30 μs and becomes less negative; from that point onwards it remains almost stable. With the increase in the stimulus current the respective values of the membrane potentials and the respective initial values of the membrane currents progressively increase as expected. In this case only node 0 is excited. All the other nodes are not excited.

All the graphs for this neuron geometries and electrode distance are summerized in TABLE - VI.

TABLE - VI

$L = 0.3$ cm, $d = 0.15E-2$ cm., $1 = 0.3E-3$ cm., electrode distance = 0.05 cm.

Stimulus current Amperes	Voltage graphs	Current graphs
0.05E-3	Fig. 4.18(a)	Fig. 4.18(b)
0.15E-3	Fig. 4.19(a)	Fig. 4.19(b)
0.25E-3	Fig. 4.20(a)	Fig. 4.20(b)

The change in membrane potential at the node below the electrode and at the four adjacent nodes is shown in Fig. 4.21(a), Fig. 4.22(a) and Fig. 4.23(a) for the neuron conditions under consideration. Initially, only node 0 is depolarized, however, nodes 1 and -1 are initially hyperpolarized, but reverse sign at 25 μs and remain depolarized from that time on. All the other nodes are hyperpolarized. The rate of increase of the depolarization at node 0 is relatively low compared to those in TABLE - VI. Here nodes 2 and -2 are the most hyperpolarized and the nodes 4 and -4 are the least hyperpolarized.

The time response of the membrane current at these same nodes is shown in Fig. 4.21(b), Fig. 4.22(b) and Fig. 4.23(b). Here the rate of fall of the membrane current at node 0 is at slower pace compared to those in TABLE - VI. The membrane current at nodes 1 and -1 is initially negative but becomes positive after 11 μs accounting for the eventual reversal of membrane potential at these nodes. The membrane current at nodes 1 and -1 remain positive after 11 μs. The membrane current at nodes 4 and -4 is almost constant. The membrane current at nodes 2 and -2 is more negative initially but merges with the membrane current at the nodes 4 and -4 and remain equal there after. In this case only node 0 is excited, whereas nodes 1 and -1 are not excited since the rate of rise of depolarization and the final depolarization attained by these nodes is very low. All the graphs are summerized in TABLE - VII.

Analysis of Myelinated Nerve

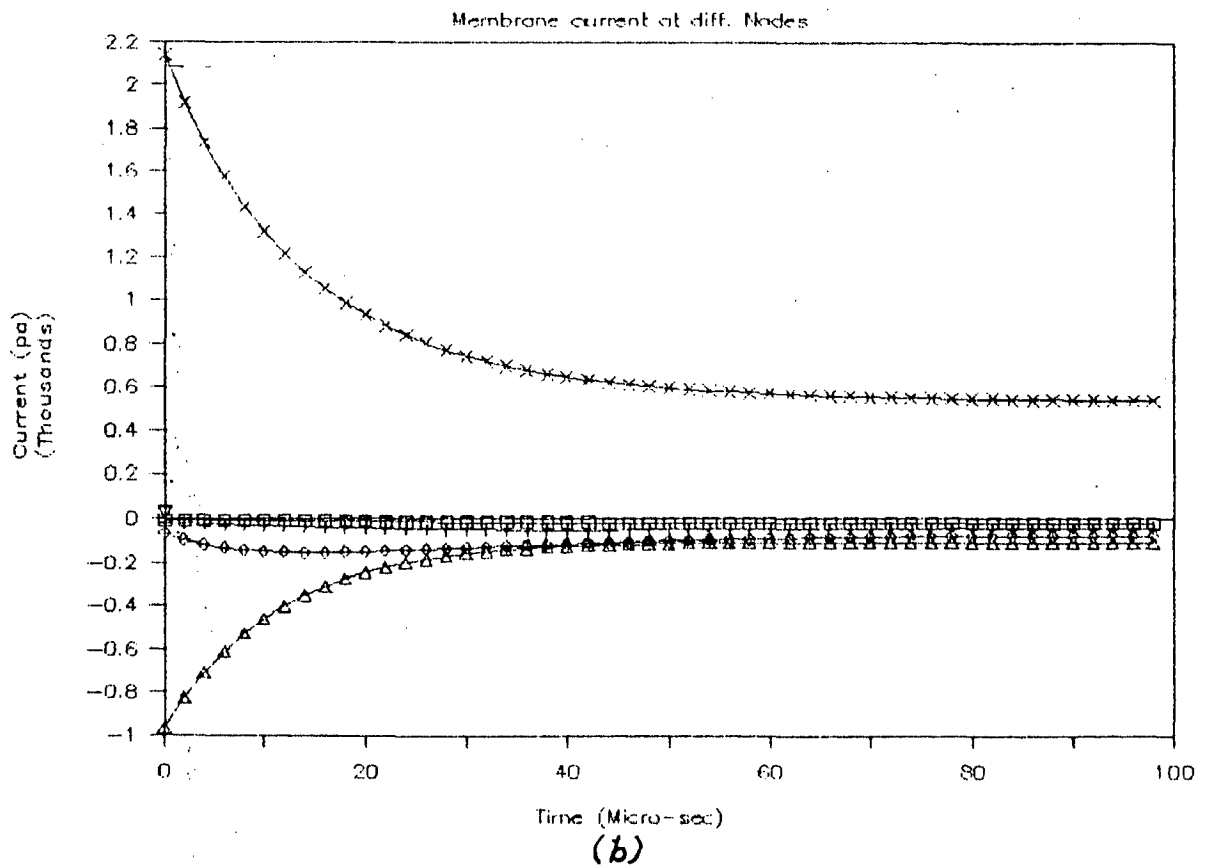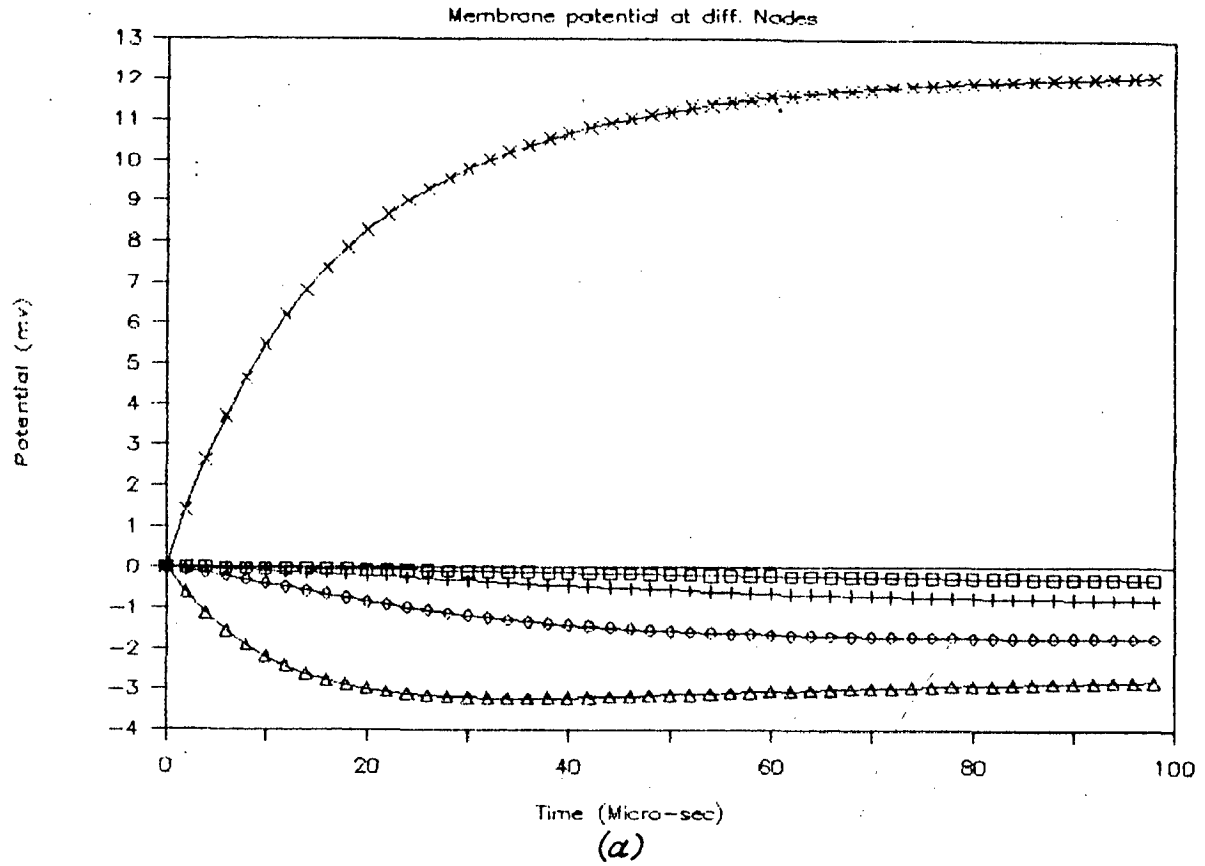## Membrane potential at diff. Nodes

(a)

Membrane current at diff. Nodes

(b)

FIG.4.21 (a) Membrane potential at different nodes
(b) Membrane current at different nodes
For, L=0.3Cm, d=0.15E-2Cm, l=0.3E-3Cm, EDist=0.25Cm, I=0.05E-3A
X Node 0; Δ Nodes -1,1; ◊ Nodes -2,2; + Nodes -3,3; □ Nodes -4,4

Analysis of Myelinated Nerve
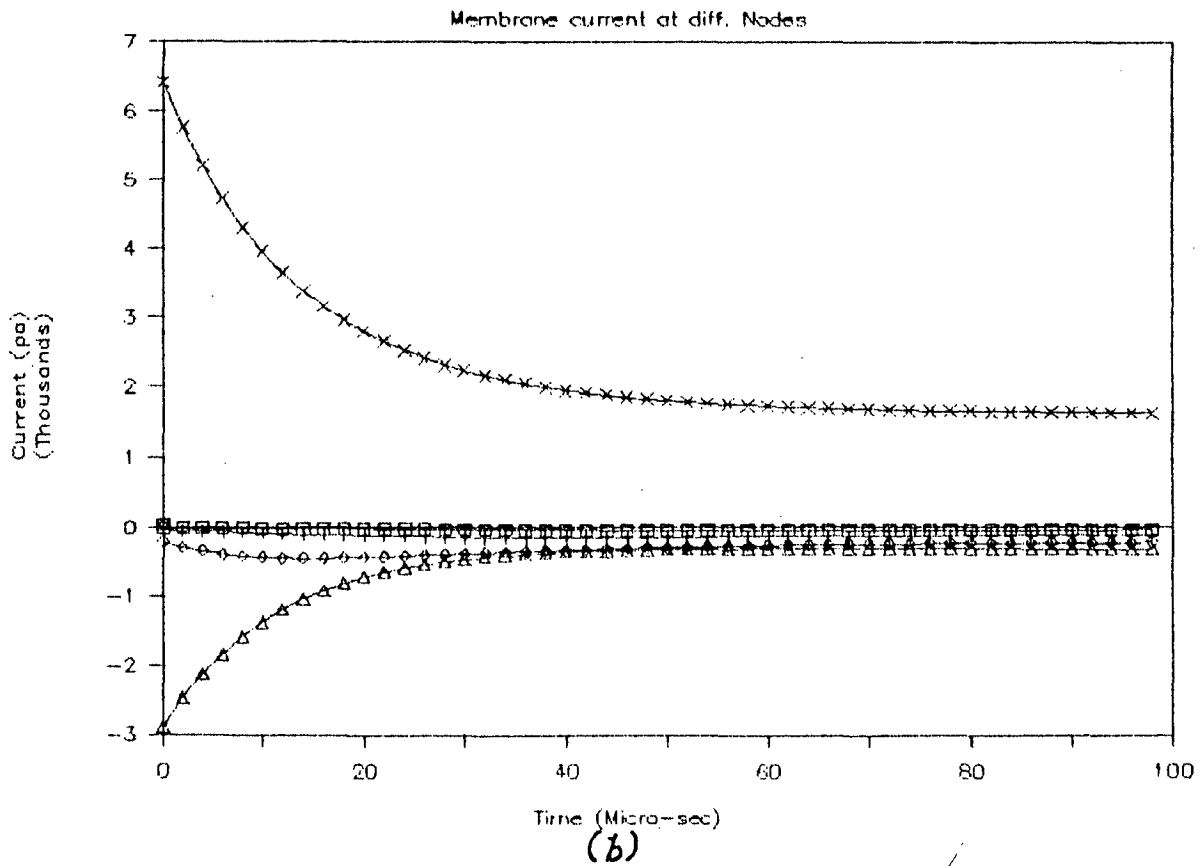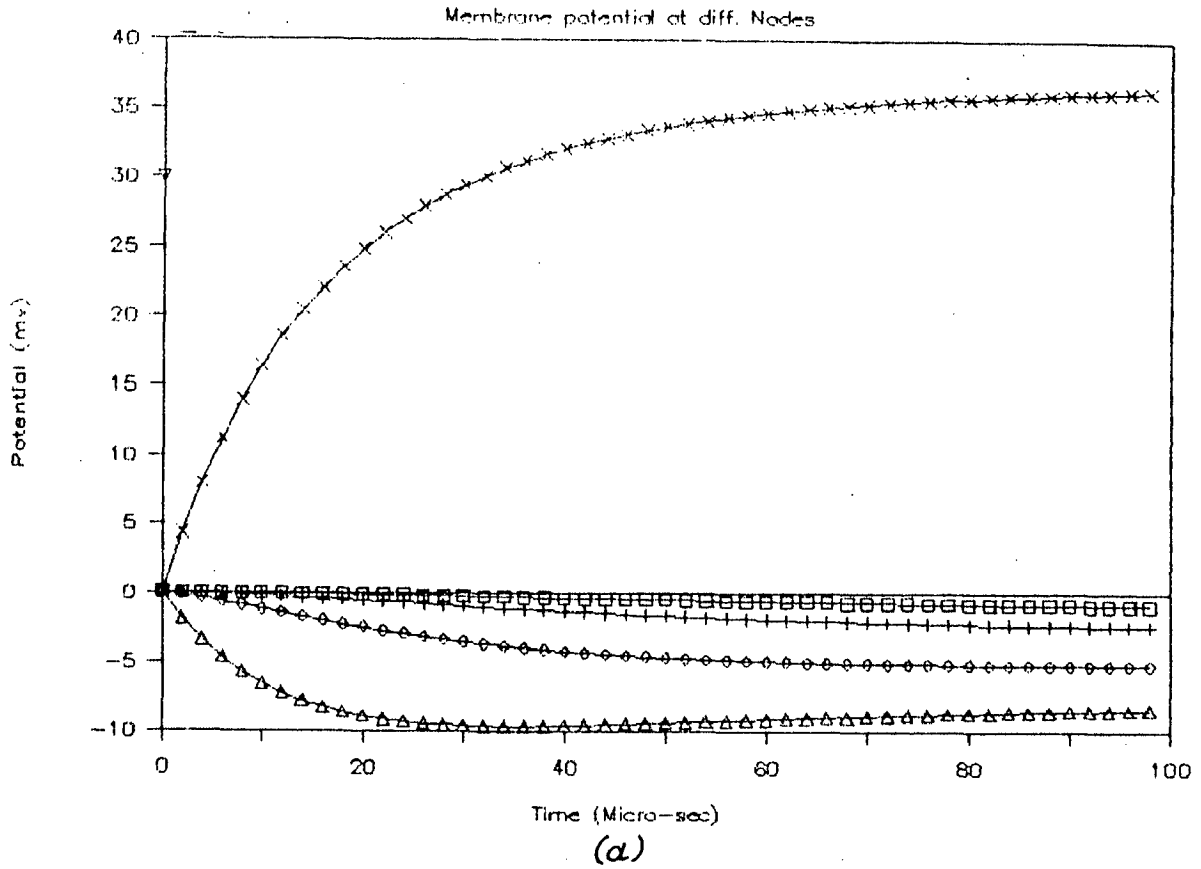
FIG. 4.22 (a) Membrane potential at different nodes
(b) Membrane current at different nodes
For, L=0.3Cm, d=0.15E-2Cm, l=0.3E-3Cm, EDist=0.25Cm, I=0.15E-3A
X Node 0; Δ Nodes -1,1; ◊ Nodes -2,2; + Nodes -3,3; □ Nodes -4,4

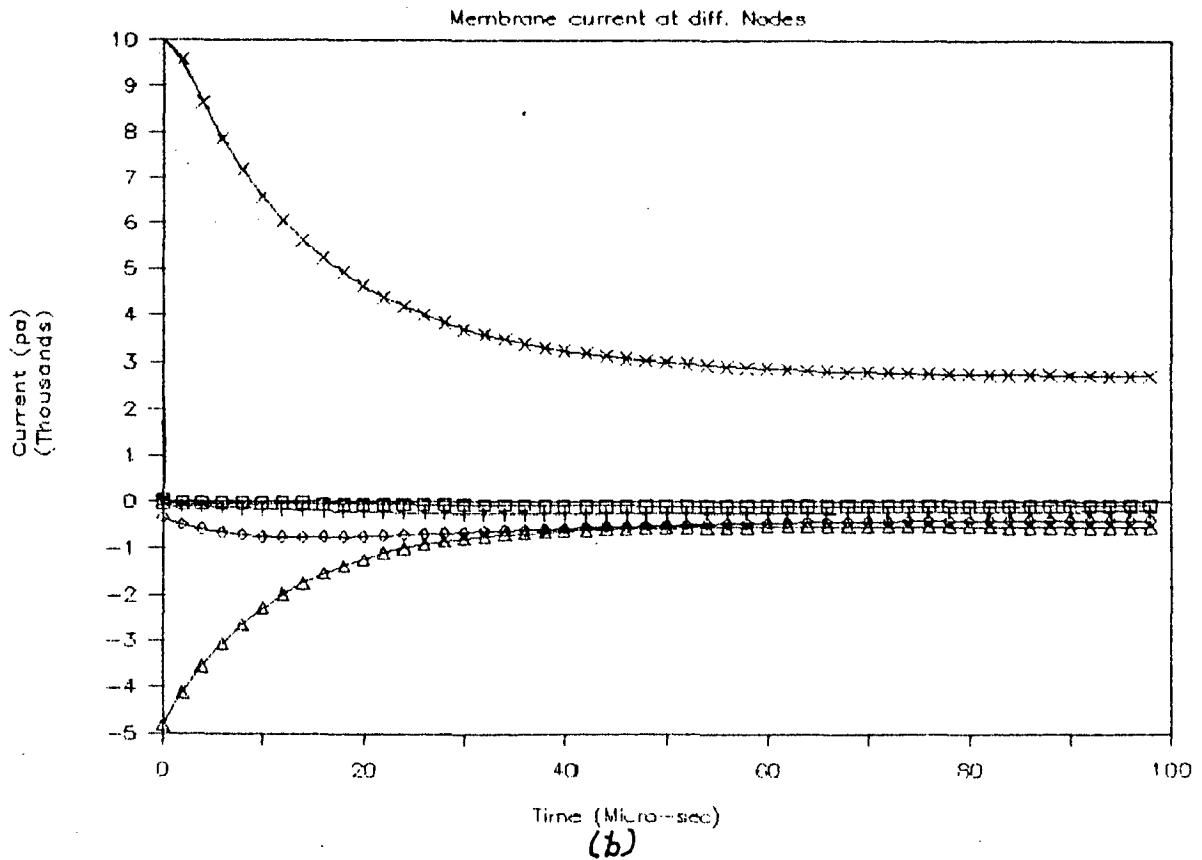## Analysis of Myelinated Nerve

Membrane potential at diff. Nodes

Membrane current at diff. Nodes
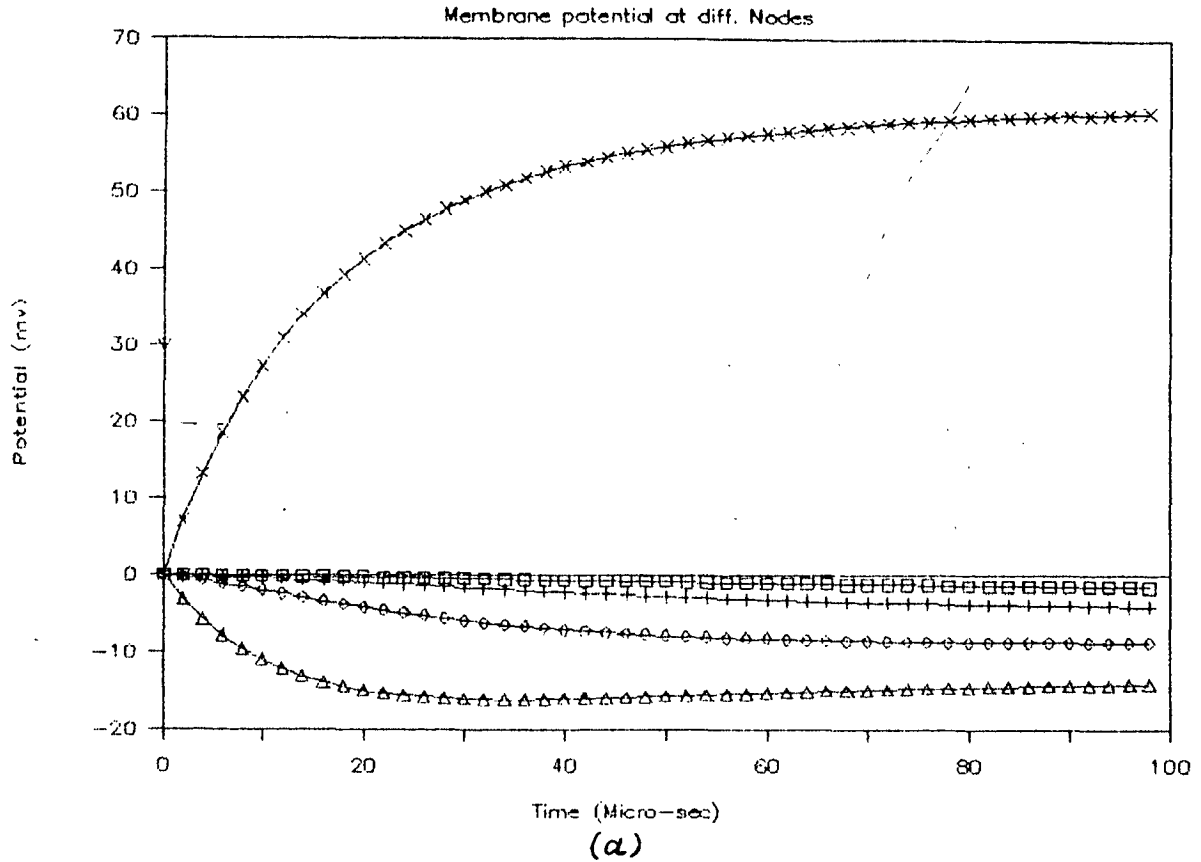
FIG.4.23 (a) Membrane potential at different nodes
(b) Membrane current at different nodes
For, L=0.3Cm, d=0.15E-2Cm, l=0.3E-3Cm, EDist=0.25Cm, I=0.25E-3A
X Node 0; △ Nodes -1,1; ◊ Nodes -2,2; + Nodes -3,3; ☐ Nodes -4,4

TABLE - VII

L = 0.3 cm d = 0.15E-2 cm,   l = 0.3E-3 cm,   electrode

distance = 0.25 cm.

Stimulus current Amperes	Voltage graphs	Current graphs
0.05E-3	Fig. 4.21(a)	Fig. 4.21(b)
0.15E-3	Fig. 4.22(a)	Fig. 4.22(b)
0.25E-3	Fig. 4.23(a)	Fig. 4.23(b)

The change in membrane potential at the node below the electrode and at the four adjacent nodes is shown in Fig. 4.24(a), Fig. 4.25(a) and Fig. 4.26(a). Node 0 and nodes 1 and -1 are depolarized and the other nodes are hyperpolarized. Nodes 3 and -3 are extensively hyperpolarized. Here only nodes 0 and nodes 1 and -1 are excited. By further increasing the dimensions of the neuron, will not even excite as many nodes on either side of node 0, as decrease in the depolarization rate further, will not be able to excite the same nodes. As the stimuls current is increased the level of depolarization and hyperpolarization reached by respective nodes progressively increases.

The time course of the membrane current at these some nodes is shown in Fig. 4.24(b), Fig. 4.25(b) and Fig. 4.26(b)

Analysis of Myelinated Nerve

Membrane potential at diff.Nodes

(a)

Membrane current at diff.Nodes

(b)

FIG.4.24 (a) Membrane potential at different nodes
(b) Membrane current at different nodes
For, L=0.3Cm, d=0.15E-2Cm, l=0.3E-3Cm, EDist=0.45Cm, I=0.05E-3A
X Node 0; △ Nodes -1,1; ◊ Nodes -2,2; + Nodes -3,3; ☐ Nodes -4,4

Analysis of Myelinated Nerve

Membrane potential at diff.Nodes

(a)

Membrane current at diff.Nodes

(b)

FIG.4.25 (a) Membrane potential at different nodes
(b) Membrane current at different nodes
For, L=0.3Cm, d=0.15E-2Cm, l=0.3E-3Cm, EDist=0.45Cm, I=0.15E-3A
✗ Node 0; △ Nodes -1,1; ◊ Nodes -2,2; + Nodes -3,3; □ Nodes -4,4

Analysis of Myelinated Nerve

Membrane potential at diff.Nodes

(a)

Membrane current at diff.Nodes

(b)
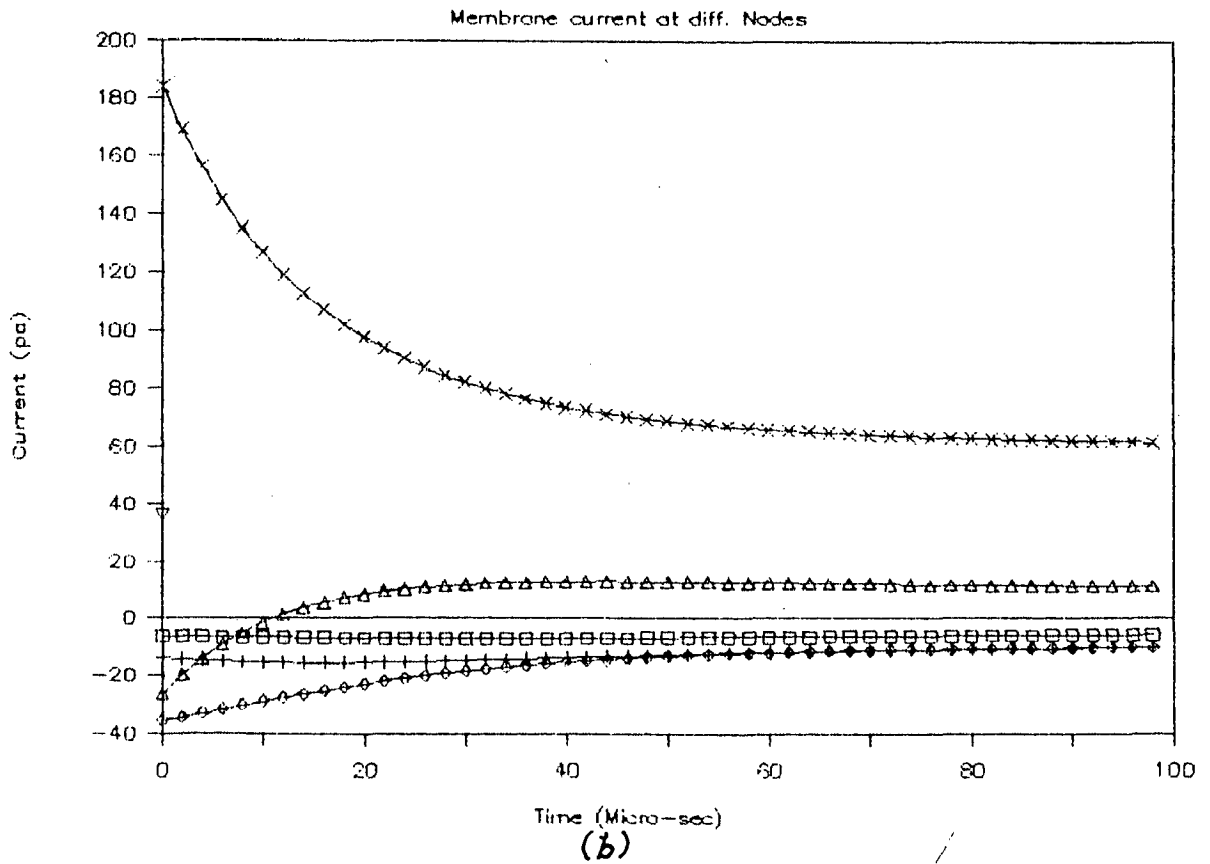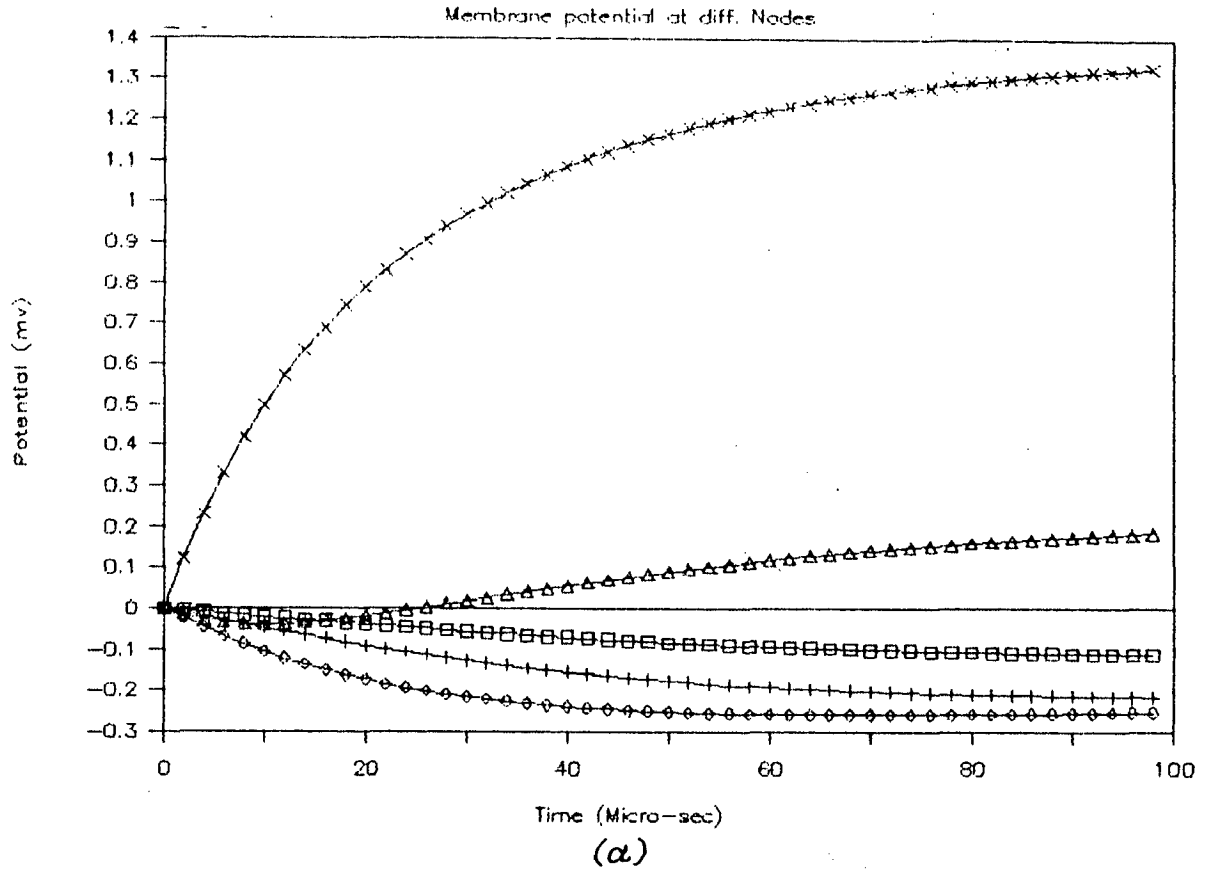
FIG.4.26 (a) Membrane potential at different nodes
(b) Membrane current at different nodes
For, L=0.3Cm, d=0.15E-2Cm, l=0.3E-3Cm, EDist=0.45Cm, I=0.25E-3A
X Node 0; △ Nodes -1,1; ◊ Nodes -2,2; + Nodes -3,3; ☐ Nodes -4,4

The rate of fall of membrane current at node 0 is at a slower pace indicating that the capacitive effect is less dominant than before [Fig.4.21b,4.22b and Fig. 4.23b].The membrane current at nodes 1 and -1 is positive, and increases slightly upto 10 µs and remains almost stable there on. The membrane current at nodes 2 and -2 is the most negative initially but becomes least negative after 30 µs on wards. The negative current at nodes 4 and -4 is almost constant. The graphs are summerized in TABLE - VIII.

TABLE - VIII

L = 0.3 cm, d = 0.13E-2 cm,   1 = 0.3E-3 cm,   electrode distance = 0.45 cm.

Stimulus current Amperes	Voltage graphs	Current graphs
0.05E-3	Fig. 4.24(a)	Fig. 4.24(b)
0.15E-3	Fig. 4.25(a)	Fig. 4.25(b)
0.25E-3	Fig. 4.26(a)	Fig. 4.26(b)

The change in membrane potential at the node below the electrode and at the four adjacent nodes, is shown in Fig. 4.27(a), Fig. 4.28(a) and Fig. 4.29(a). It is seen that only node 0 is depolarized. All the other nodes are hyperpolarized.

Analysis of Myelinated Nerve

Membrane potential at diff.Nodes

(a)
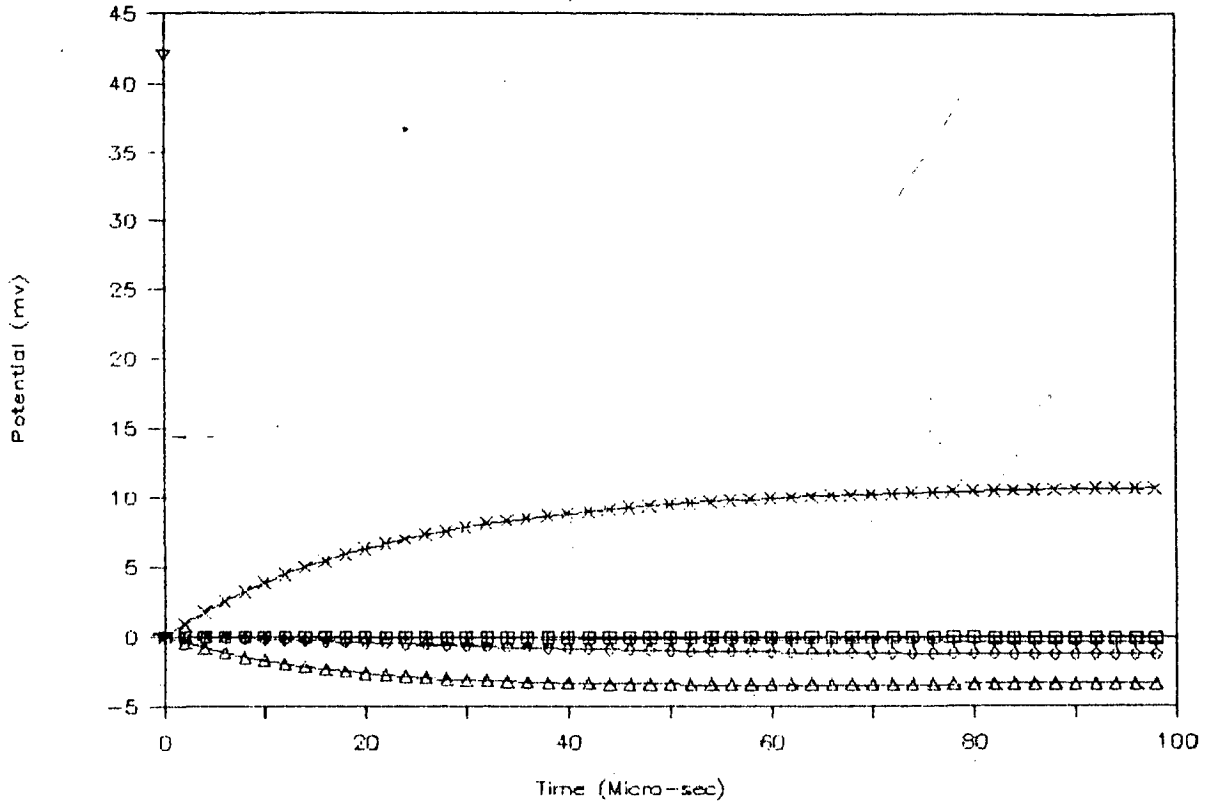
Membrane current at diff.Nodes

(b)
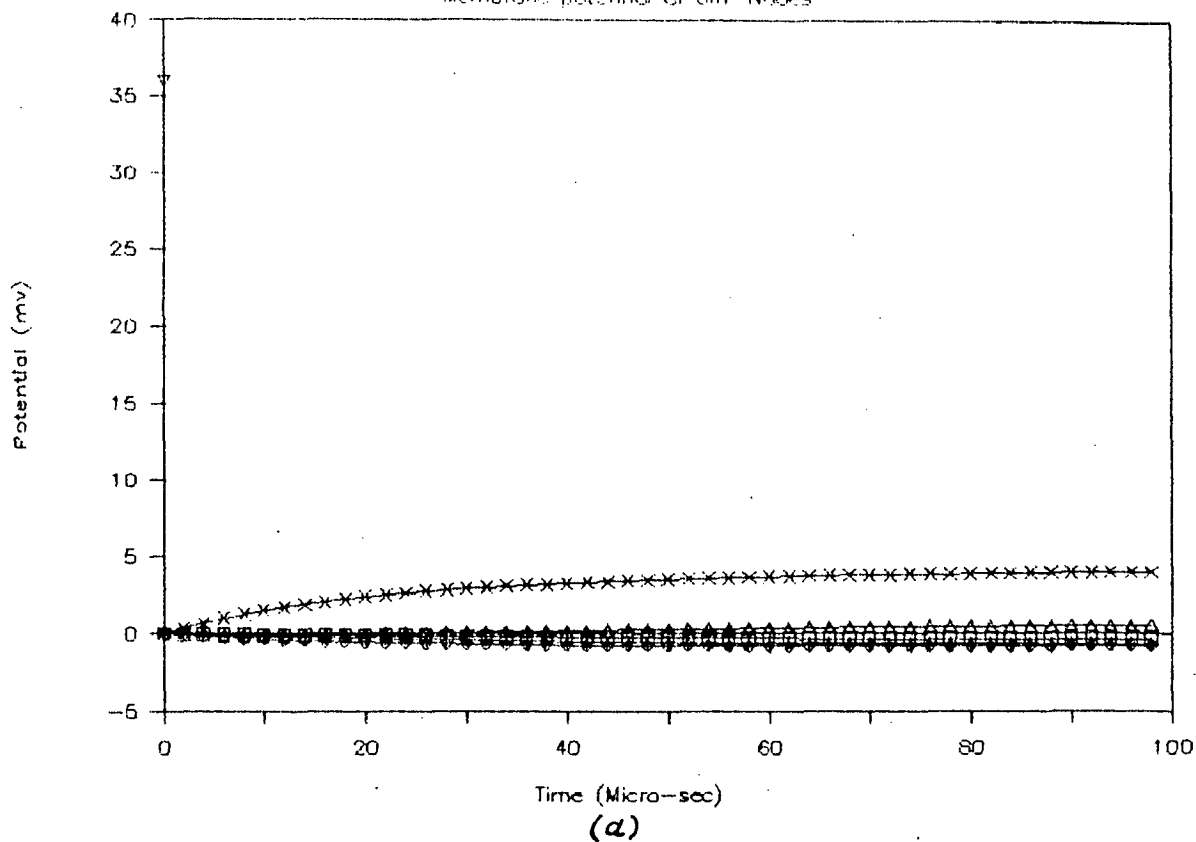
FIG.4.27 (a) Membrane potential at different nodes
(b) Membrane current at different nodes
For, L=0.5Cm, d=0.25E-2Cm, l=0.5E-3Cm, EDist=0.05Cm, I=0.05E-3A
X Node 0; △ Nodes -1,1; ◇ Nodes -2,2; + Nodes -3,3; □ Nodes -4,4

Analysis of Myelinated Nerve

Membrane potential at diff.Nodes
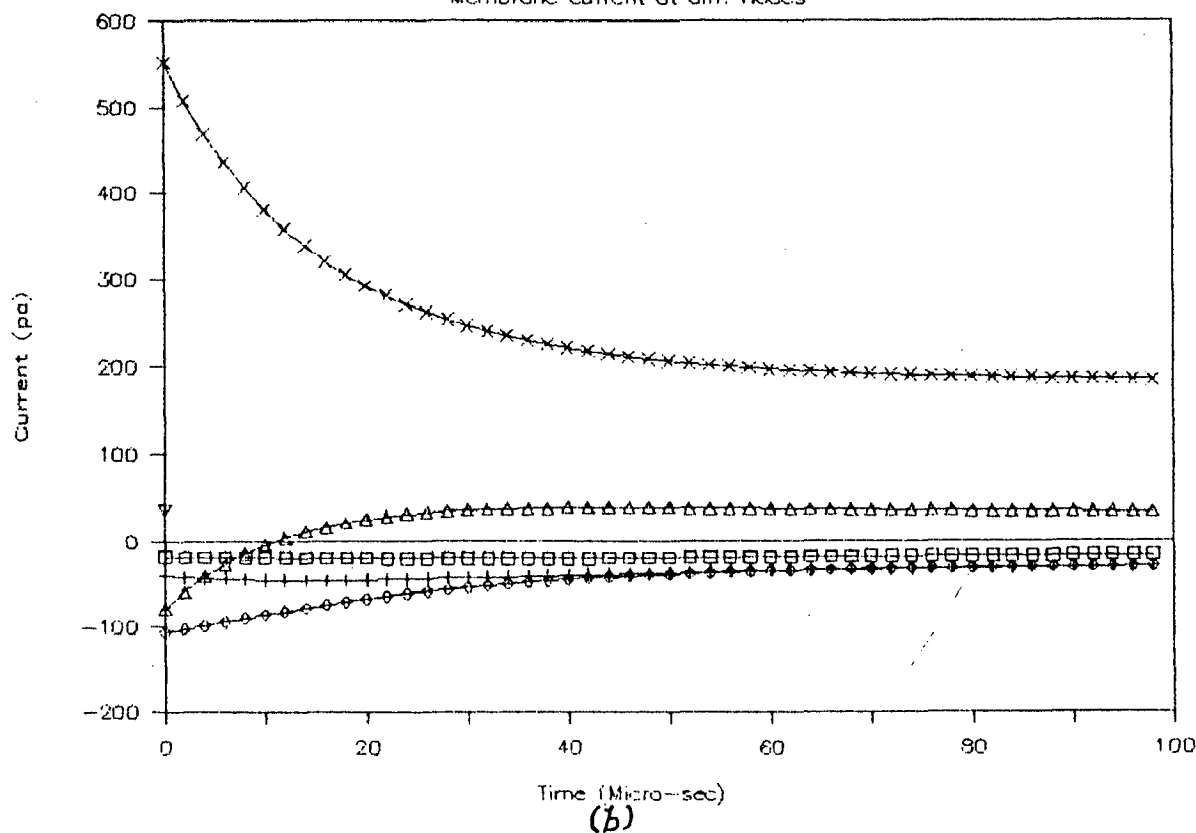

(a)

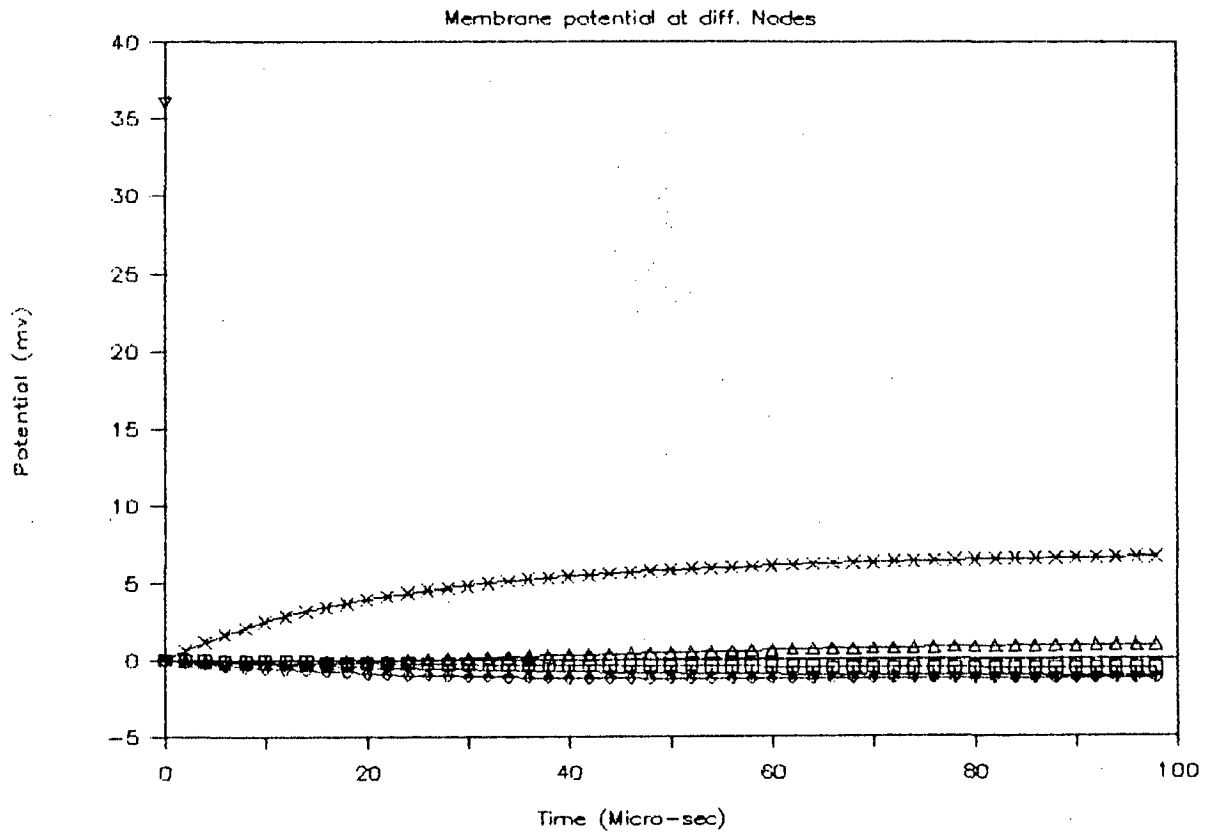### Membrane current at diff.Nodes

(b)

FIG.4.28 (a) Membrane potential at different nodes
(b) Membrane current at different nodes
For, L=0.5Cm, d=0.25E-2Cm, l=0.5E-3Cm, EDist=0.05Cm, I=0.15E-3A
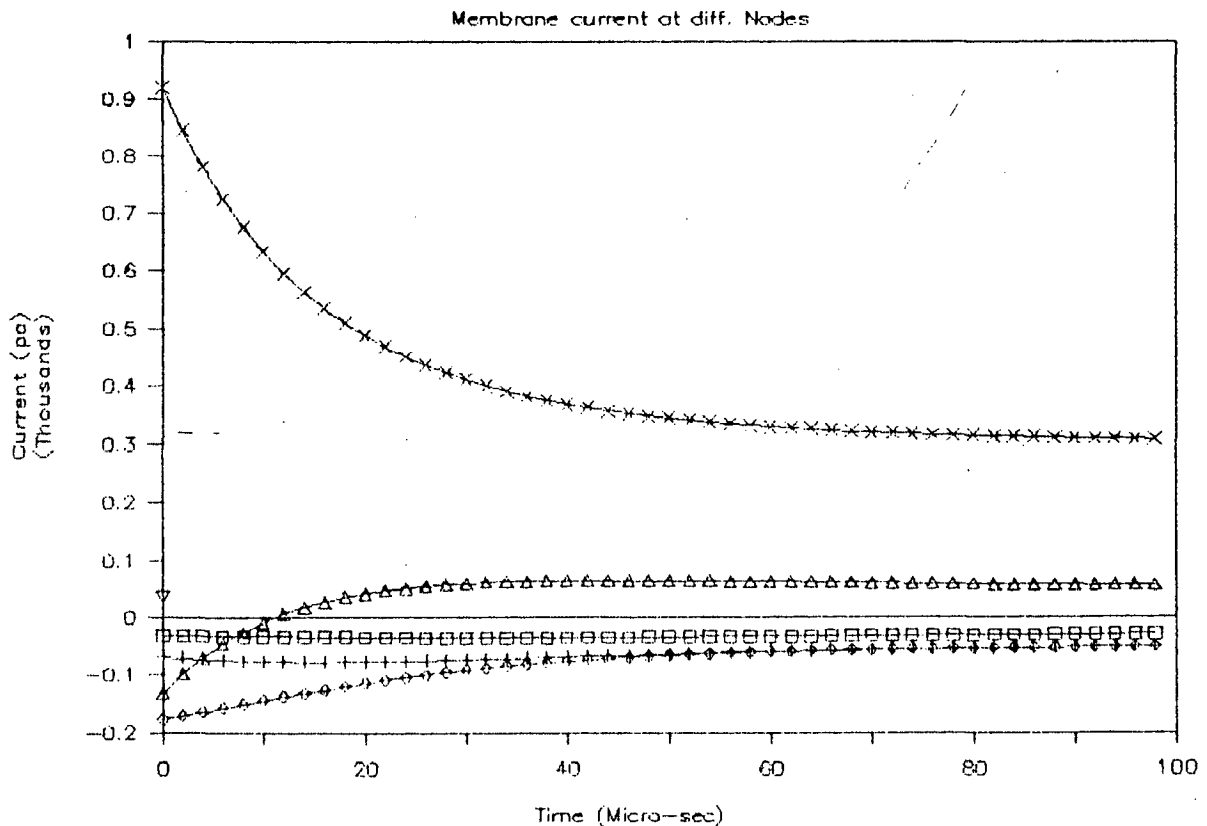X Node 0; △ Nodes -1,1; ◊ Nodes -2,2; + Nodes -3,3; □ Nodes -4,4

FIG.4.29 (a) Membrane potential at different nodes
(b) Membrane current at different nodes
For, L=0.5Cm, d=0.25E-2Cm, l=0.5E-3Cm, EDist=0.05Cm, I=0.25E-3A
X Node 0; △ Nodes -1,1; ◊ Nodes -2,2; + Nodes -3,3; □ Nodes -4,4

Nodes -4 and 4 and nodes -3 and 3 are least hyperpolarized and the hyperpolarizations are very close to zero. Nodes -1 and 1 are highly hyperpolarized and their hyperpolarization increases gradually upto 40 µs and remains constant there after. As the stimulus current is increased the magnitude of the respective depolarization and hyperpolarization progressively increases. In this case only node 0 is excited.

The time course of the membrane current at these nodes is shown in Fig. 4.27(b), Fig. 4.28(b) and Fig. 4.29(b). The membrane current at node 0 is positive. At all the other nodes the membrane current is negative. The membrane currents at nodes -4 and 4 and nodes -3 and 3 are very close to zero and stable. The membrane current at node 0 drops very slowly compared to earlier cases. Here the capacitive effect is reduced whereas the ionic component is dominant. This is because of the fact that as the dimensions of the neuron are increased the area for the exchange of ions at each node becomes proportionately large and as a result the capacitive current becomes a smaller component compared to the ionic current. The membrane current at nodes 1 and -1 is more negative initially but it increases gradually up to 60 µs and remains constant from that time and onwards. In this case only node 0 is excited. As the stimulus current is increased the initial values of the respective positive and negative currents are proportionately increased as expected. The graphs are summerized in TABLE - IX.

TABLE - IX

L = 0.5 cm, d = 0.25E-2 cm,   l = 0.5 E-3 cm,   electrode

distance = 0.05 cm.

Stimulus current Amperes	Voltage graphs	Current graphs
0.05 E-3	Fig. 4.27(a)	Fig. 4.27(b)
0.15 E-3	Fig. 4.28(a)	Fig. 4.28(b)
0.25 E-3	Fig. 4.29(a)	Fig. 4.29(b)

The change in membrane potential at the node below the electrode and at the four adjacent nodes are shown in Fig. 4.30(a), Fig. 4.31(a) and Fig. 4.32(a). It is seen that only node 0 is depolarized. All the other nodes are hyperpolarized. The nodes 4 and -4 are the least depolarized and the nodes 2 and -2 are the most depolarized. Though the hyperpolarization of nodes 2 and -2 is less negative than that of nodes 1 and -1, but after 50 µs the hyperpolarization of nodes 2 and -2 becomes more negative than that of nodes 1 and -1 and remains so. Here only node 0 is excited.

The time response of the membrane current at these same nodes is shown in Fig. 4.30(b), Fig. 4.31(b) and Fig. 4.32(b). The membrane current at node 0 is positive. At all the other nodes the membrane is negative. The membrane current at node 0 drops very slowly since for larger neurons the ionic current is in larger proportion compared to the capacitive

Analysis of Myelinated Nerve

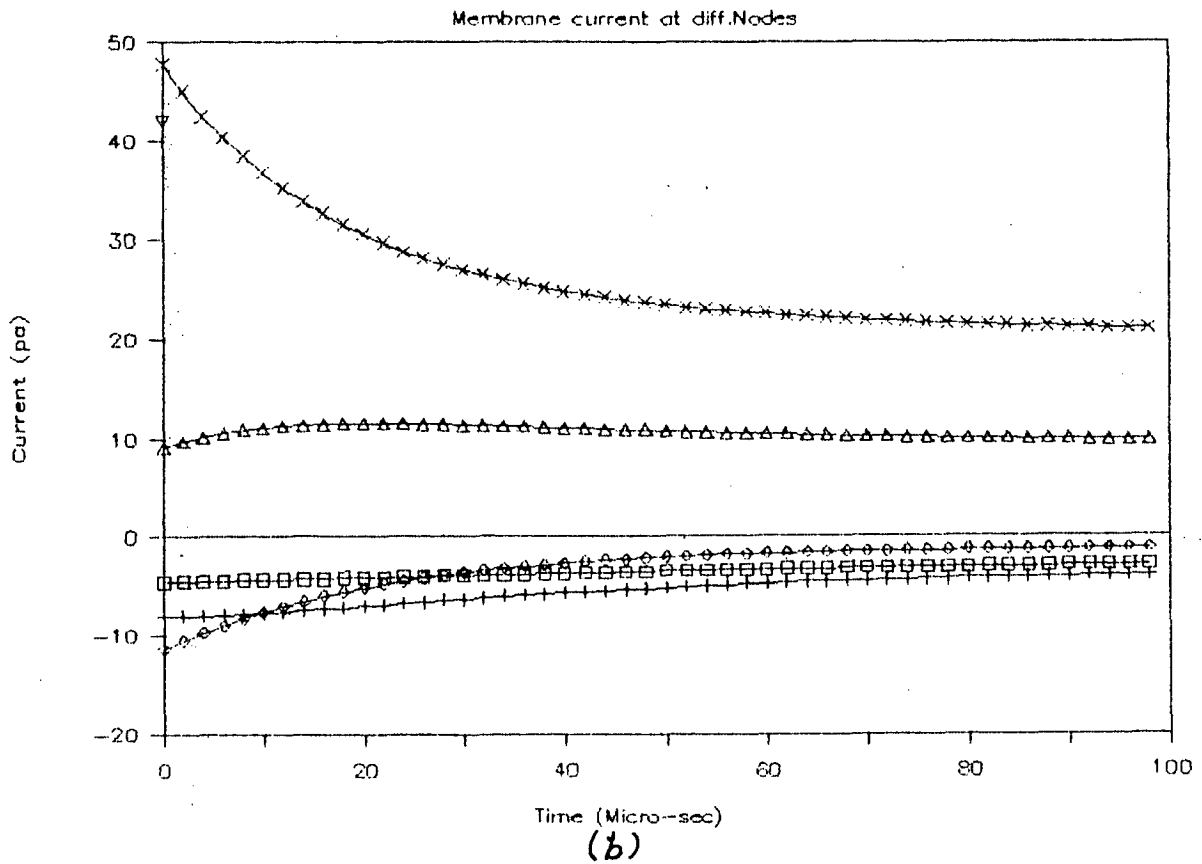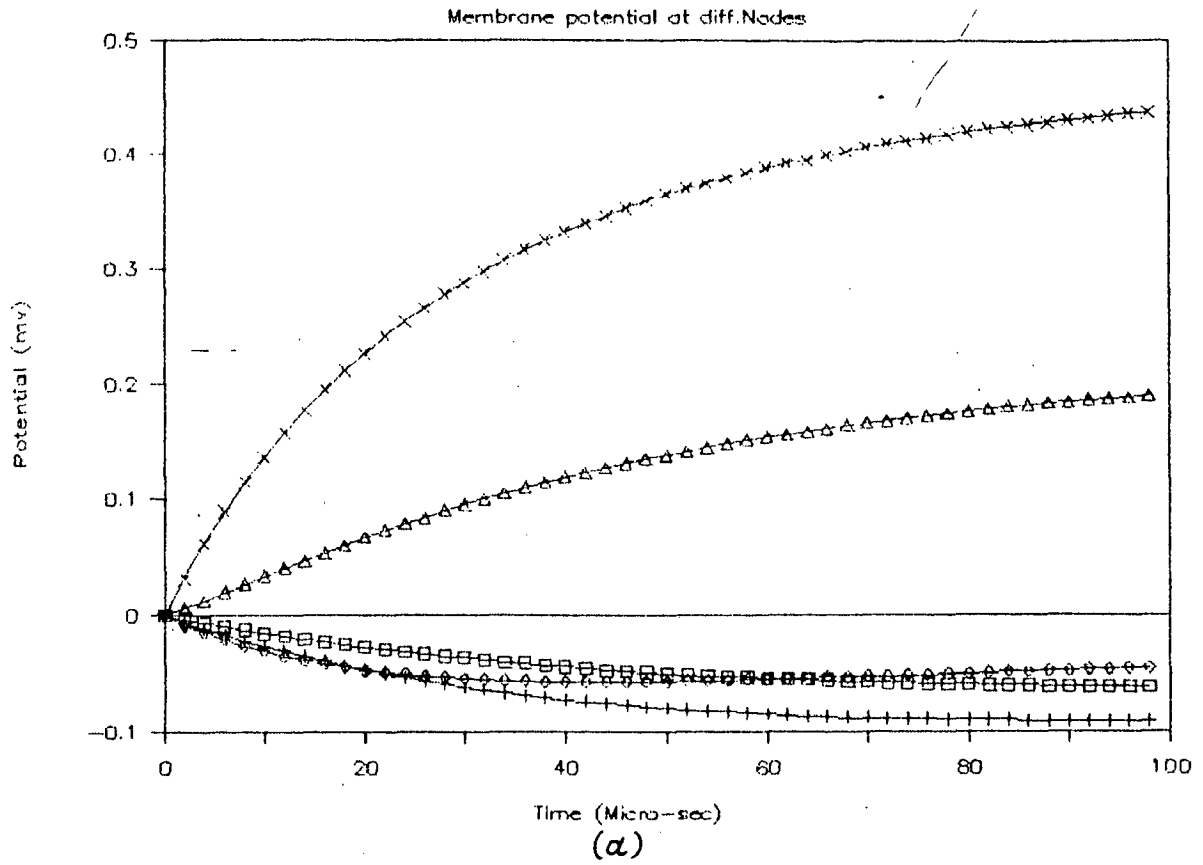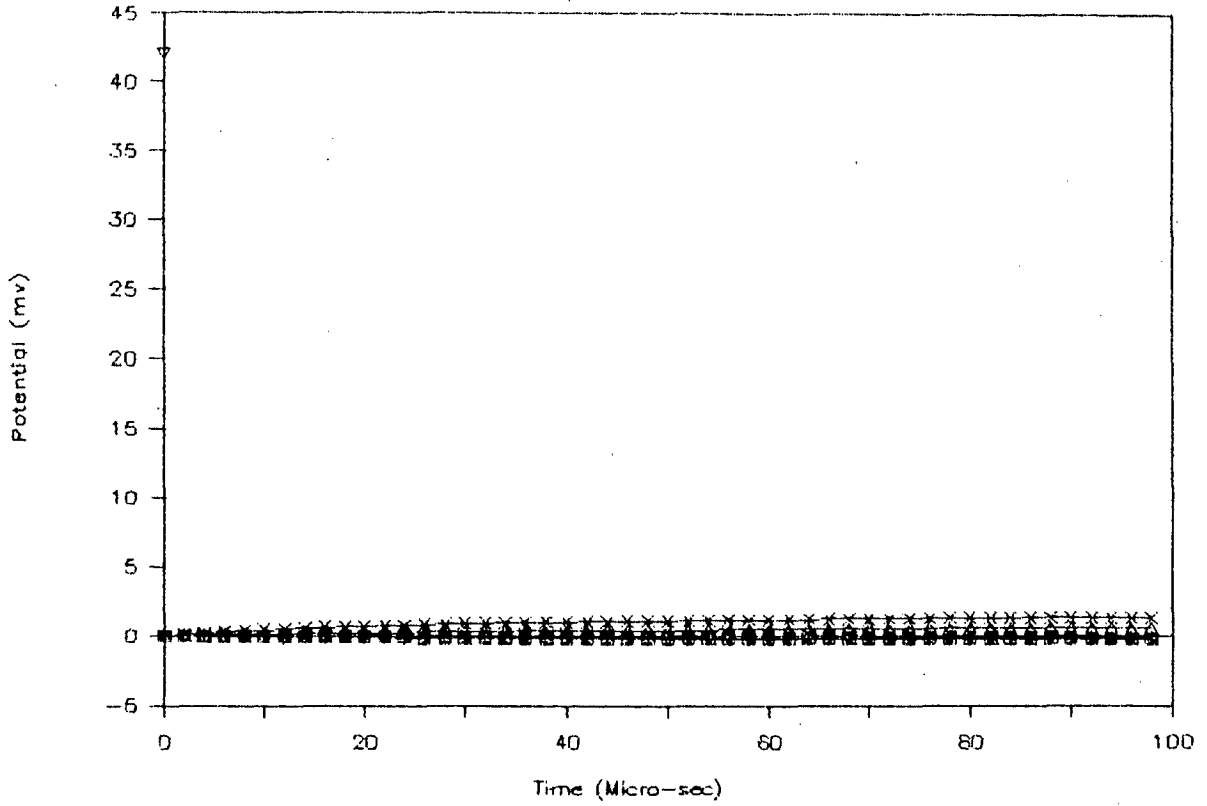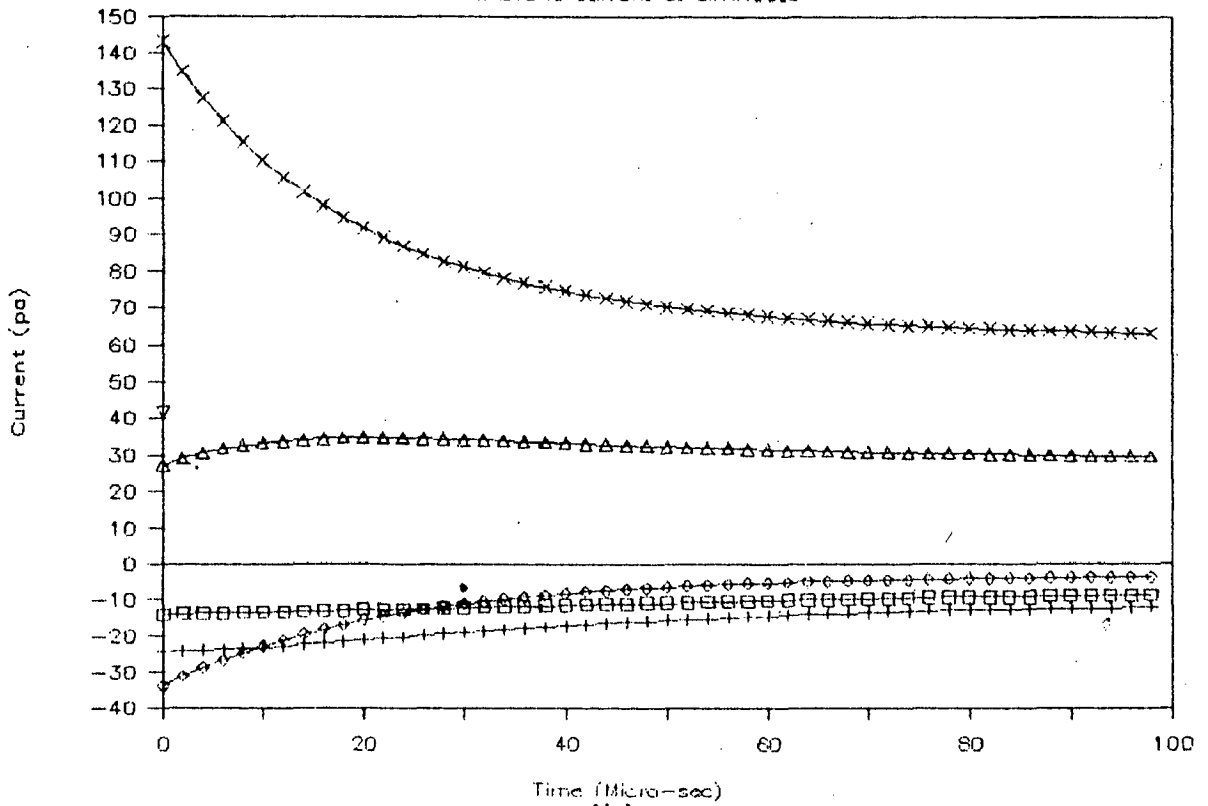### Membrane potential at diff. Nodes

(a)
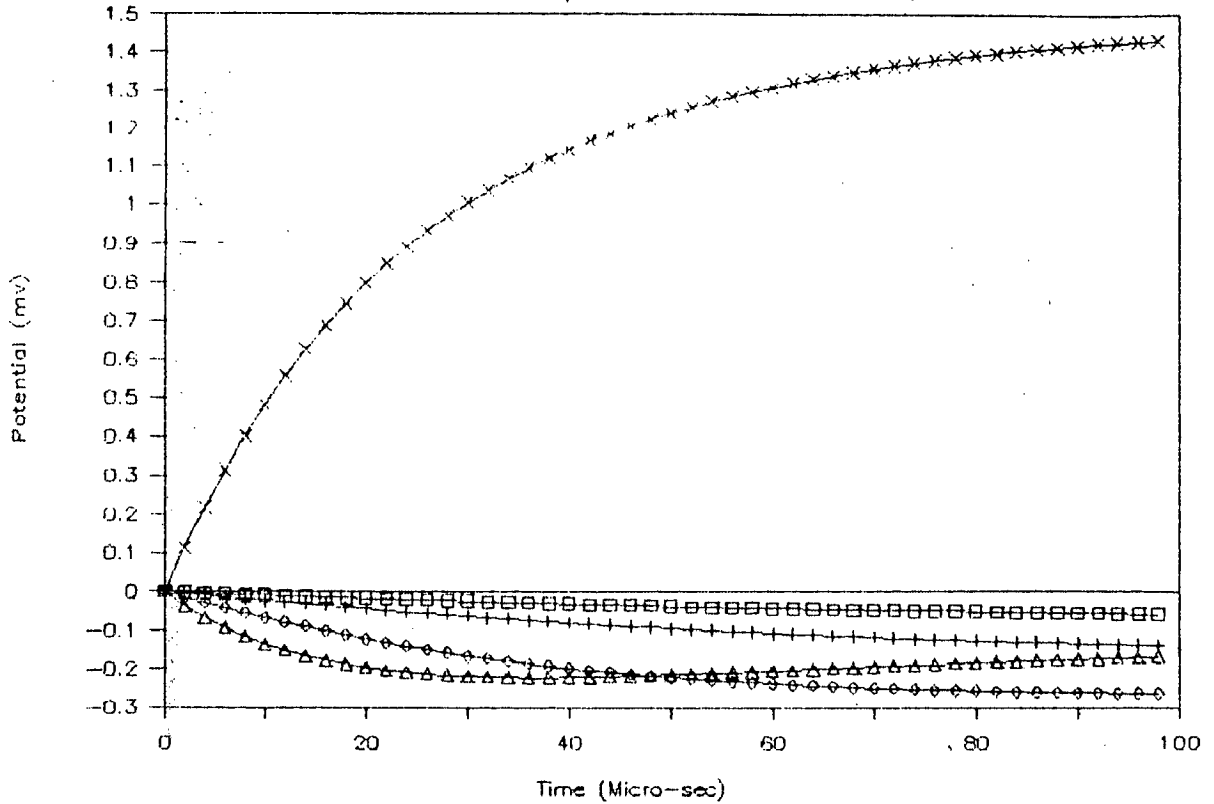
Membrane current at diff. Nodes

(b)

FIG.4.30 (a) Membrane potential at different nodes
(b) Membrane current at different nodes
For, L=0.5Cm, d=0.25E-2Cm, l=0.5E-3Cm, EDist=0.25Cm, I=0.05E-3A
X Node 0; △ Nodes -1,1; ◊ Nodes -2,2; + Nodes -3,3; ☐ Nodes -4,4

Analysis of Myelinated Nerve

Membrane potential at diff. Nodes

(a)

Membrane current at diff. Nodes

(b)

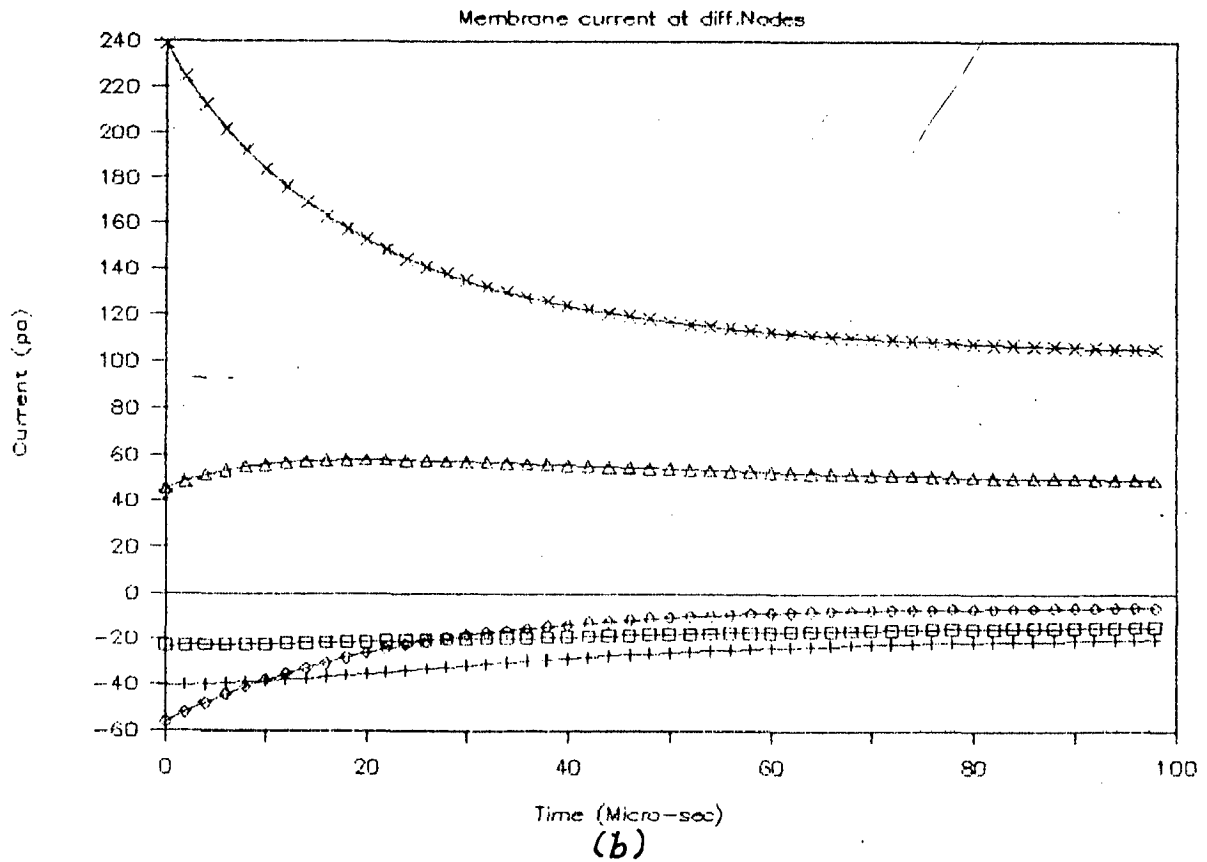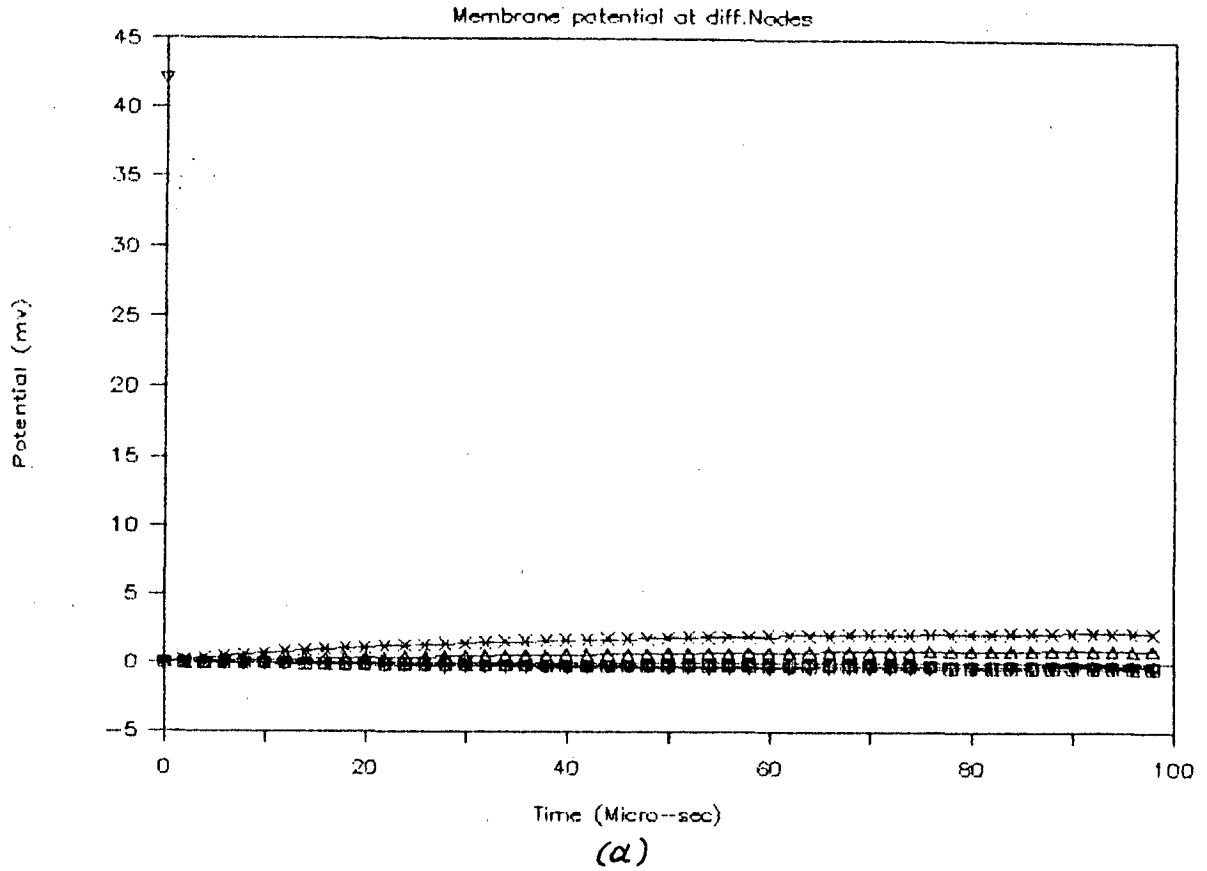FIG.4.31 (a) Membrane potential at different nodes
(b) Membrane current at different nodes
For, L=0.5Cm, d=0.25E-2Cm, l=0.5E-3Cm, EDist=0.25Cm, I=0.15E-3A
X Node 0; △ Nodes -1,1; ◇ Nodes -2,2; + Nodes -3,3; □ Nodes -4,4

FIG.4.32 (a) Membrane potential at different nodes
(b) Membrane current at different nodes
For, L=0.5Cm, d=0.25E-2Cm, l=0.5E-3Cm, EDist=0.25Cm, I=0.25E-3A
X Node 0; △ Nodes -1,1; ◊ Nodes -2,2; + Nodes -3,3; □ Nodes -4,4

component. The currents at nodes 4 and -4 is very close to zero and is almost stable. At nodes 3 and -3 and at nodes 2 and -2, the current decreases slightly up to 30 µs and later increases by the same amount upto 60 µs and remains stable from that time on. The current at node 1 and -1 is initially more negative but increases up to 60 µs and remains stable there after. In this case also only node 0 is excited. The level depolarizations and hyperpolarization reached and initial currents at the respective nodes are proportionately increased as the stimulus current is increased. All the graphs of this set of neuron geometries and electrode distance are summerized in TABLE - X.

TABLE - X

L = 0.5 cm, d=0.25E-2 cm, , 1 = 0.5E-3 cm, electrode distance = 0.25 cm.

Stimulus current Amperes	Voltage graphs	Current graphs
0.05E-3	Fig. 4.30(a)	Fig. 4.30(b)
0.15E-3	Fig. 4.31(a)	Fig. 4.31(b)
0.25E-3	Fig. 4.32(a)	Fig. 4.32(b)

The change in membrane potential at the node below the electrode and at the four adjacent nodes, are shown in Fig.4.33(a), Fig. 4.34(a) and Fig. 4.35(a). Initially only node 0 is depolarized; however, nodes 1 and -1 are initially hyperpolarized but reverse sign at 40 μs and remain depolarized that time on, the depolarization is very close to zero. All the other nodes are hyperpolarized, which is also very very close to zero. There is no significant change in membrane potential at the nodes except at node 0. Only node 0 will be excited for very low thresholds e.g., less than 1 mV.

The time response of the membrane current at these same nodes is shown in Fig. 4.33(b), Fig. 4.34(b) and Fig. 4.35(b). The current at node zero is positive and drops at slow rate to almost half the initial value and becomes stable. The effect of the capacitive current is reduced and the component of ionic current becomes dominant, because of the fact that, in larger neurons, the membrane area available for exchange of ions at each node is proportionately large. The negative membrane currents at nodes 4 and -4 and nodes 3 and -3 is almost stable. The membrane current at node 2 and -2 is more negative initially but increases almost linearly up to 60 μs and remains stable from that time on. The currents at nodes 1 and -1 are initially negative, but become positive after 15 μs accounting for the eventual reversal of membrane potential at these nodes. The magnitudes of the initial positive and negative values of the membrane currents increases
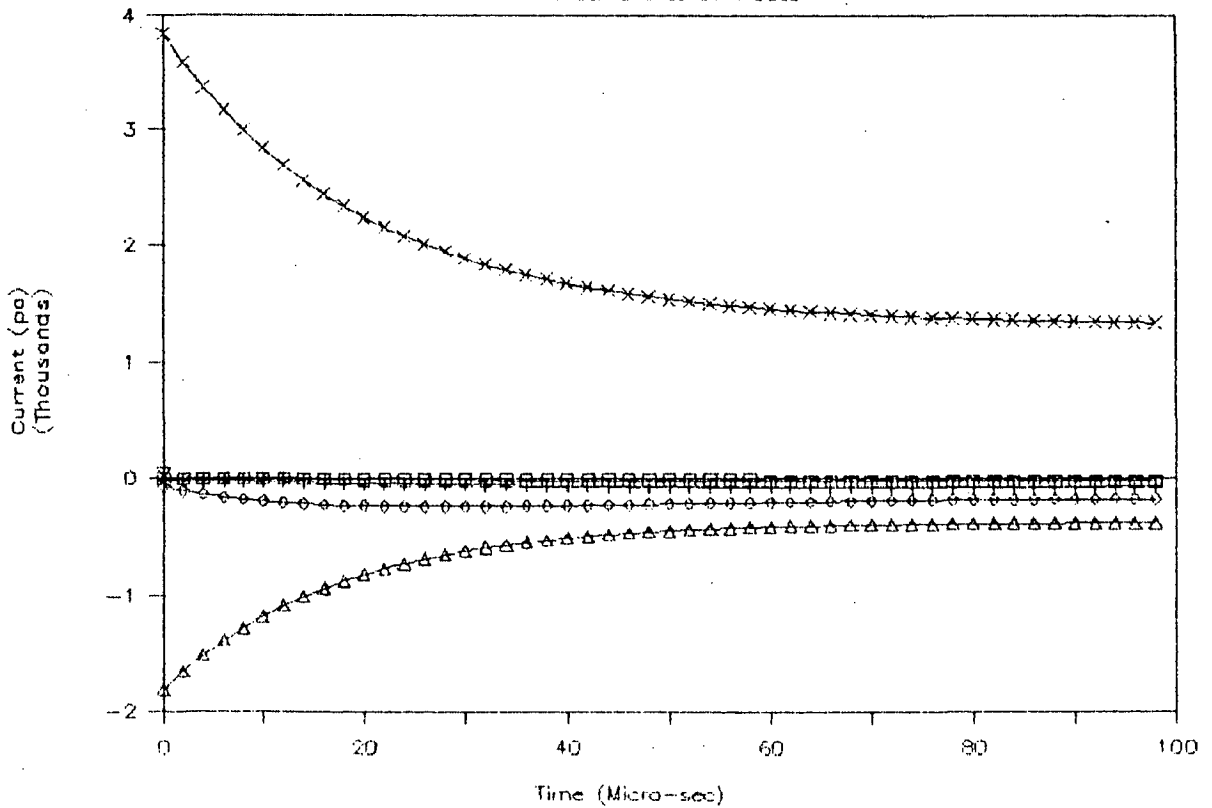
Analysis of Myelinated Nerve

Membrane potential at diff. Nodes

(a)
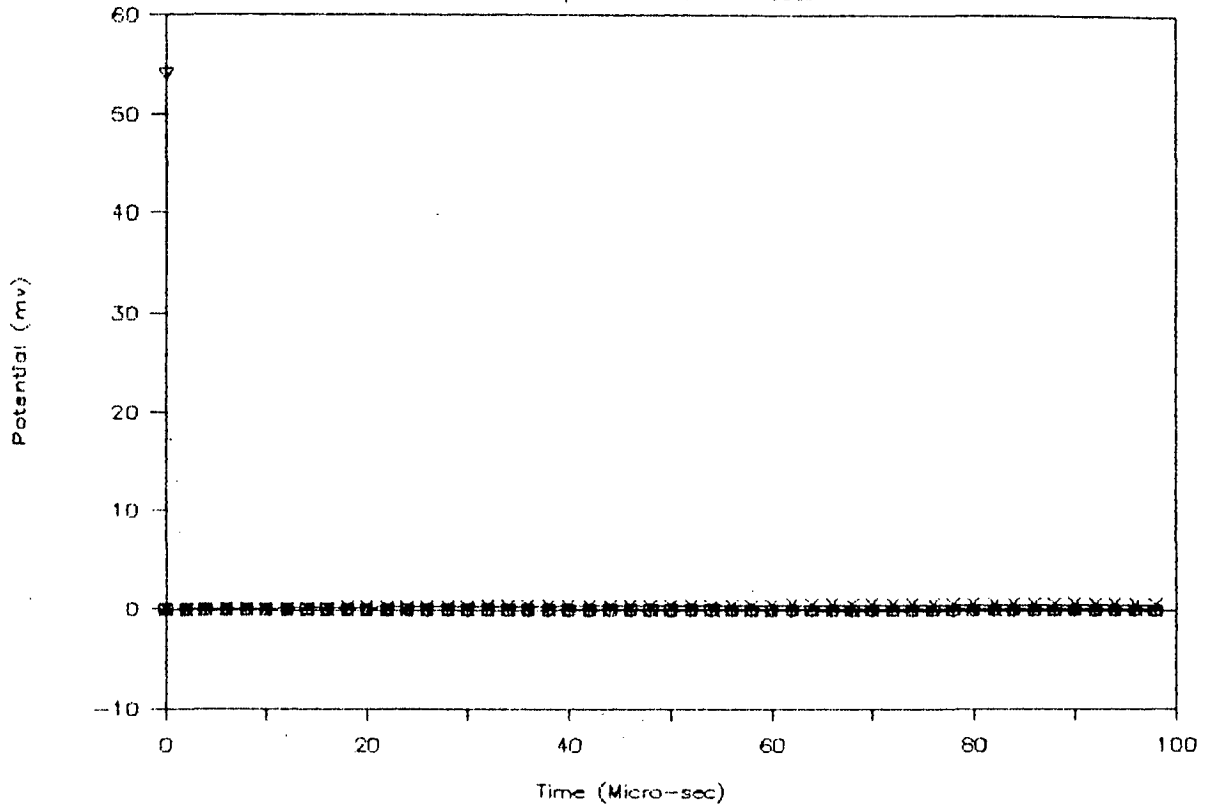
Membrane current at diff. Nodes

(b)

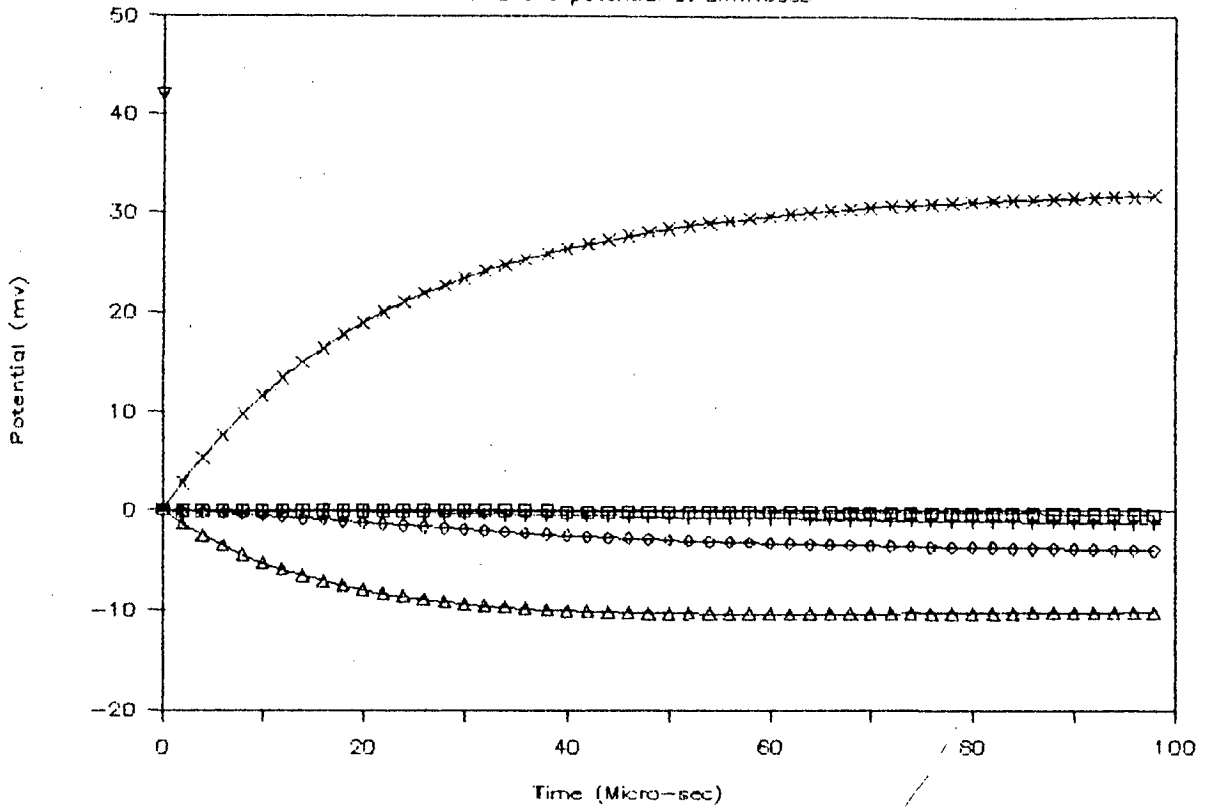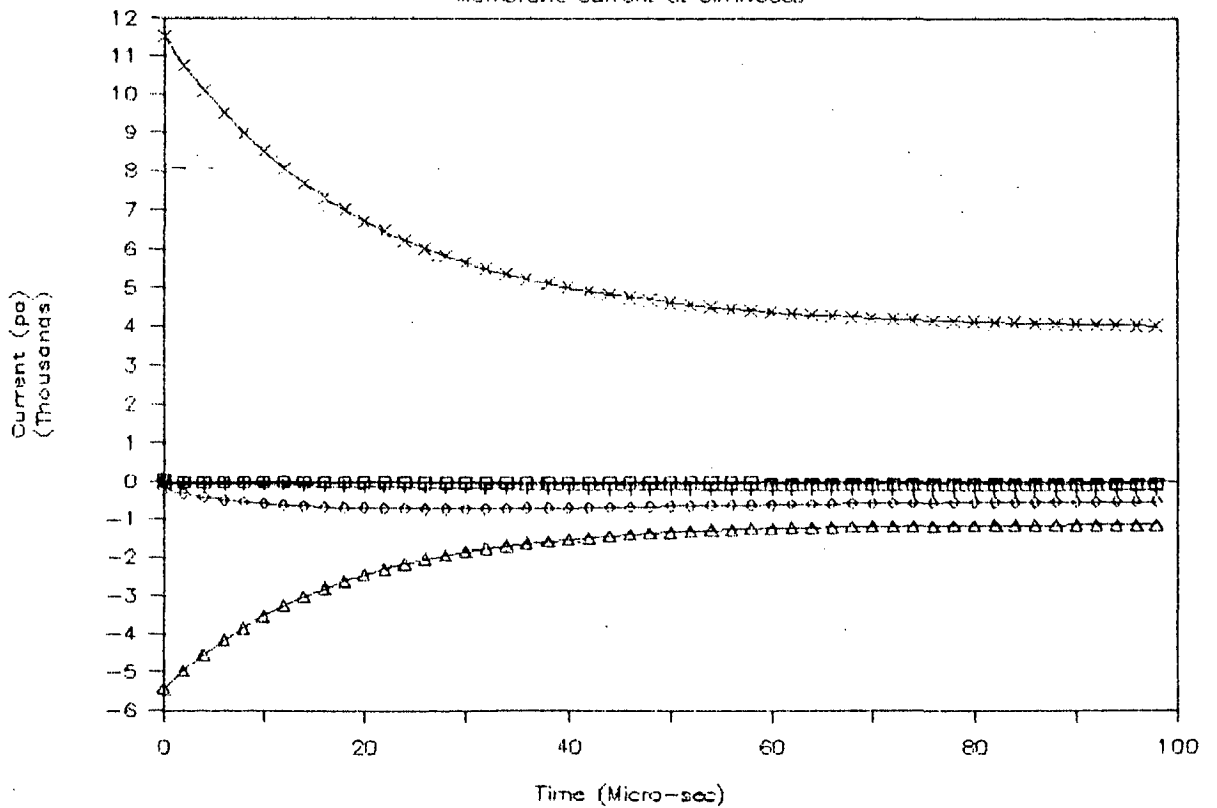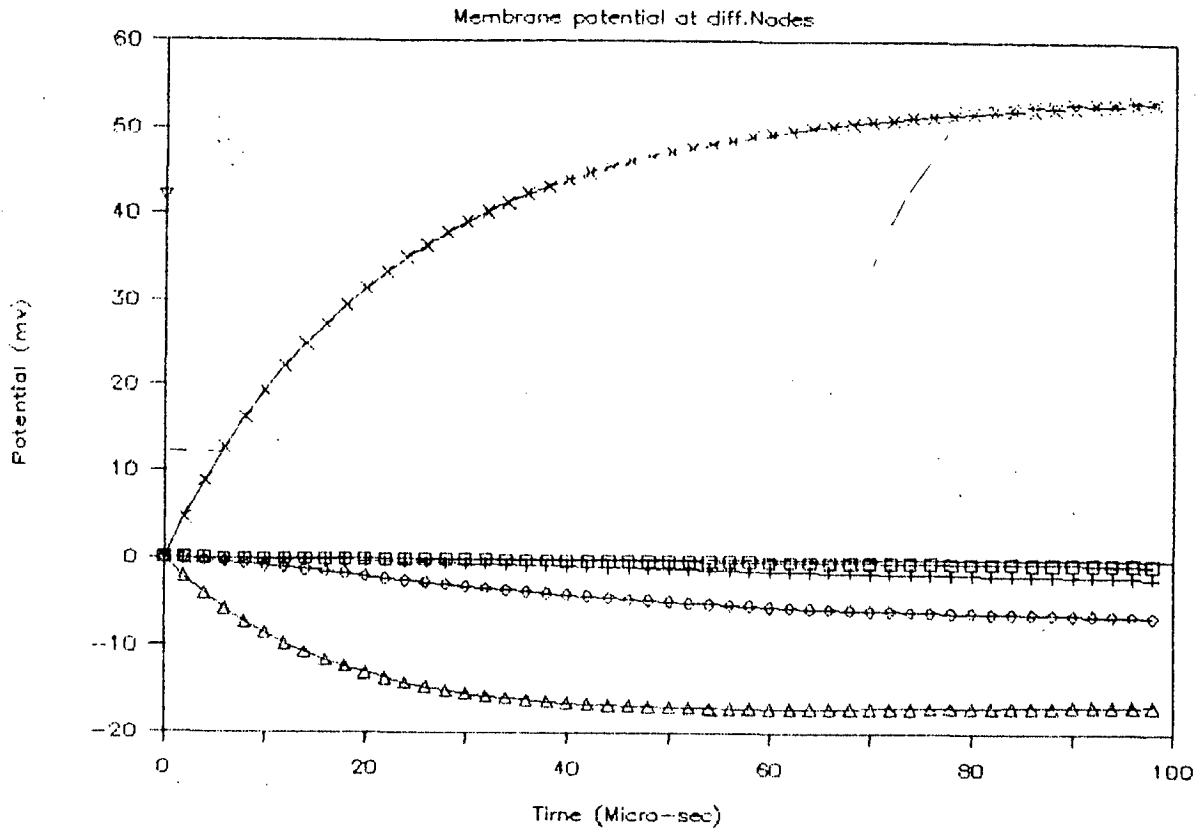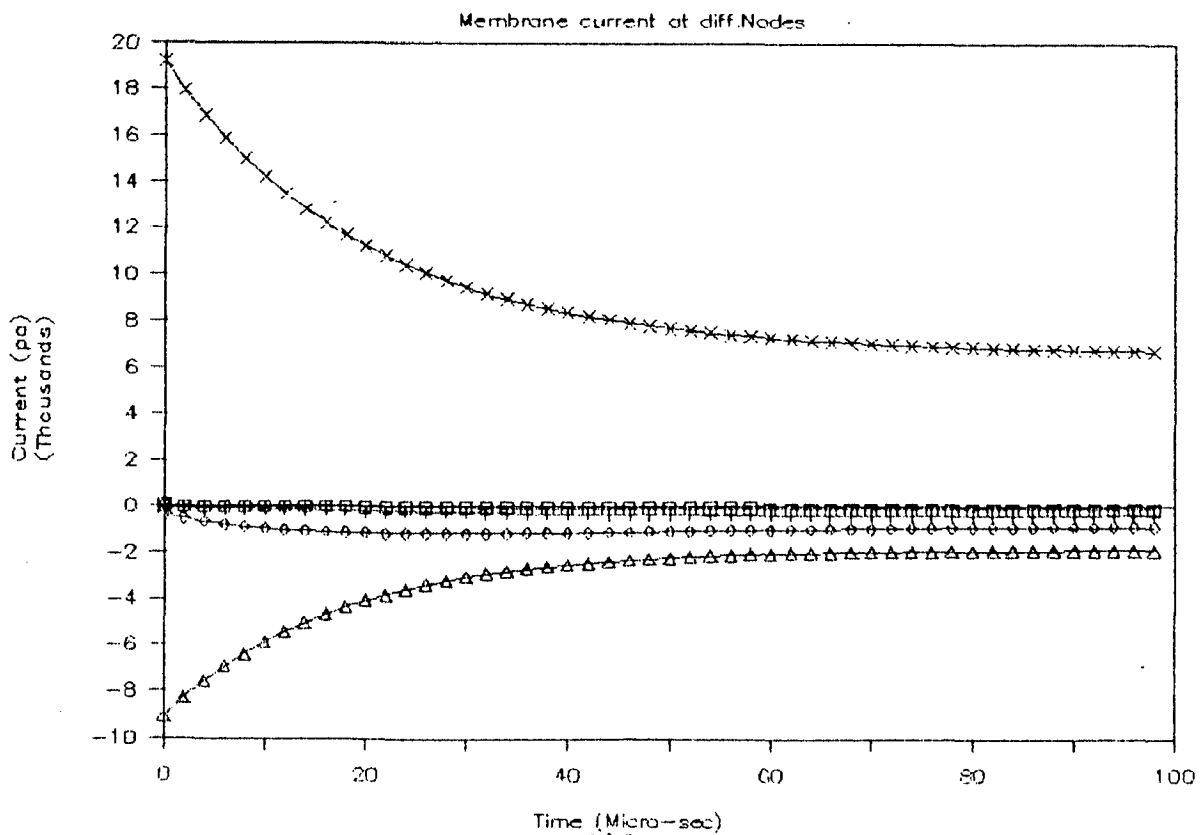FIG.4.33 (a) Membrane potential at different nodes
(b) Membrane current at different nodes
For, L=0.5Cm, d=0.25E-2Cm, l=0.5E-3Cm, EDist=0.45Cm, I=0.05E-3A
X Node 0; **△** Nodes -1,1; **◊** Nodes -2,2; **+** Nodes -3,3; **□** Nodes -4,4
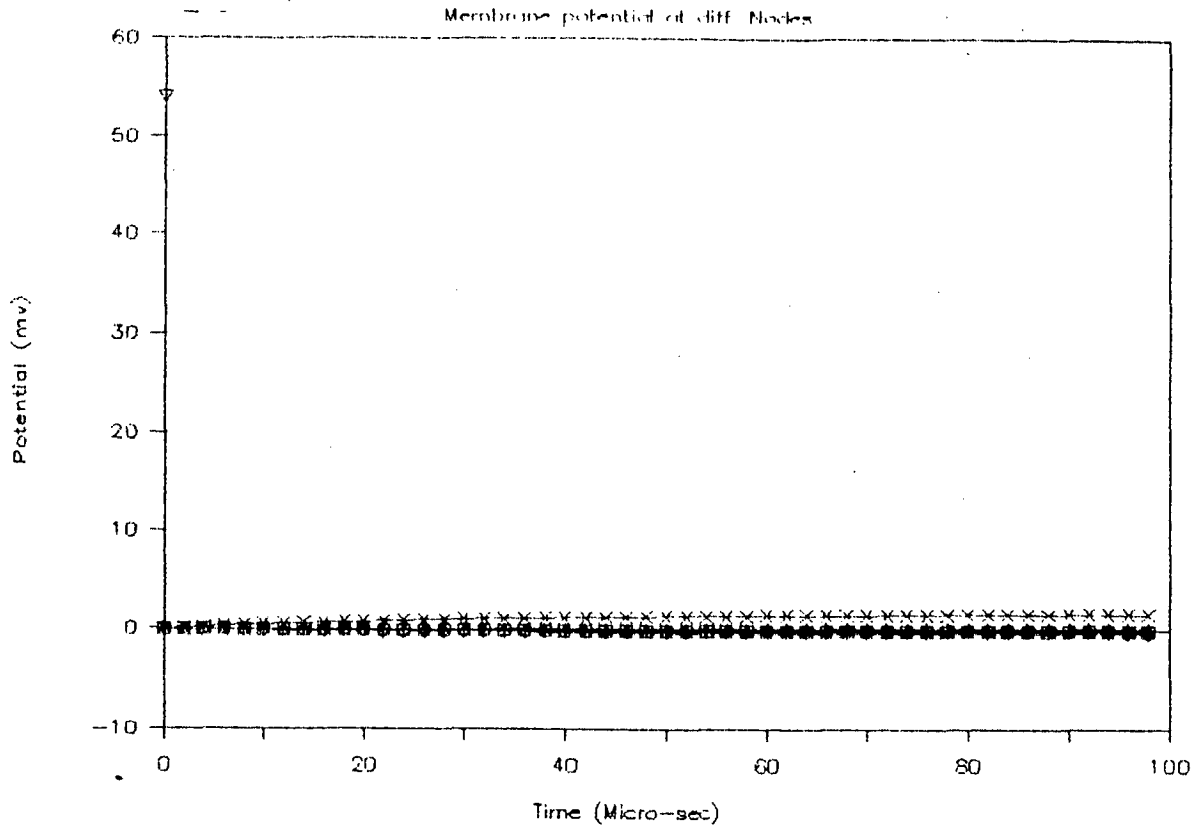
FIG.4.34 (a) Membrane potential at different nodes
(b) Membrane current at different nodes
For, L=0.5Cm, d=0.25E-2Cm, l=0.5E-3Cm, EDist=0.45Cm, I=0.15E-3A
X Node 0; △ Nodes -1,1; ◊ Nodes -2,2; + Nodes -3,3; □ Nodes -4,4

Analysis of Myelinated Nerve

Membrane potential at diff. Nodes

Membrane current at diff. Nodes

FIG.4.35 (a) Membrane potential at different nodes
(b) Membrane current at different nodes
For, L=0.5Cm, d=0.25E-2Cm, l=0.5E-3Cm, EDist=0.45Cm, I=0.25E-3A
X Node 0; △ Nodes -1,1; ◊ Nodes -2,2; + Nodes -3,3; □ Nodes -4,4

perportionately with the increase in the stimulus current. All the graphs are summerized in TABLE - XI.

TABLE - XI

L = 0.5 cm, d = 0.25 E-2 cm,   1 = 0.5 E-3 cm, electrode distance = 0.45 cm.

Stimulus current Amperes	Voltage graphs	Current graphs
0.05E-3	Fig. 4.33(a)	Fig. 4.33(b)
0.15E-3	Fig. 4.34(a)	Fig. 4.34(b)
0.25E-3	Fig. 4.35(a)	Fig. 4.35(b)

4.4.3   Effects Of Nature Of The Excitation Wave Shape :

The change in membrane potentials at the node below the electrode and at the four adjacent nodes for a triangular excitation are shown in Fig. 4.36(a). It is seen that initially, only node 0 is depolarized; however, nodes 1 and -1 reverse sign at 70 μs and remain depolarized from that time on. All the other nodes are hyperpolarized. The most striking feature of these curves is that the nodes are subject to a course of smooth variation of depolarization and hyperpolarization at the respective nodes. At node 0, the depolarization gradually increases to a peak value and then reduces with the same smoothness. All the other nodes are subject to similar
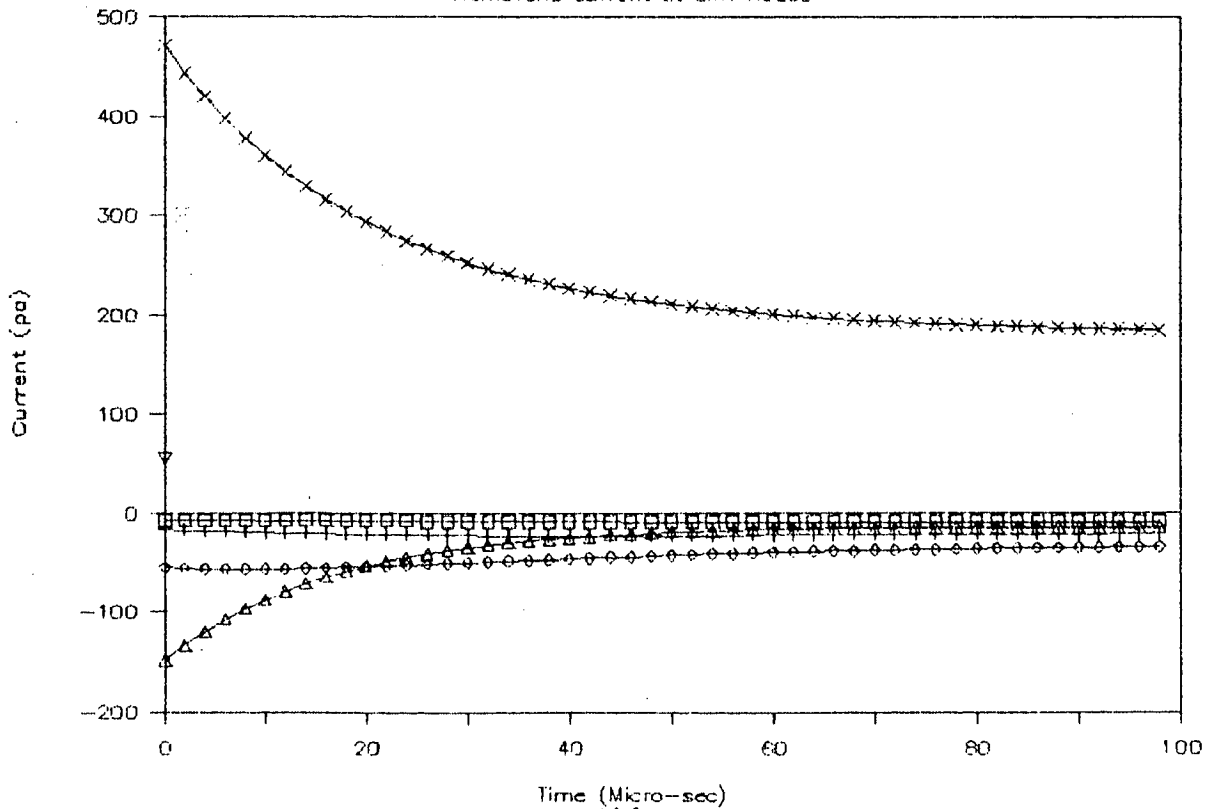
Analysis of Myelinated Nerve
Membrane potential at diff. Nodes

(a)
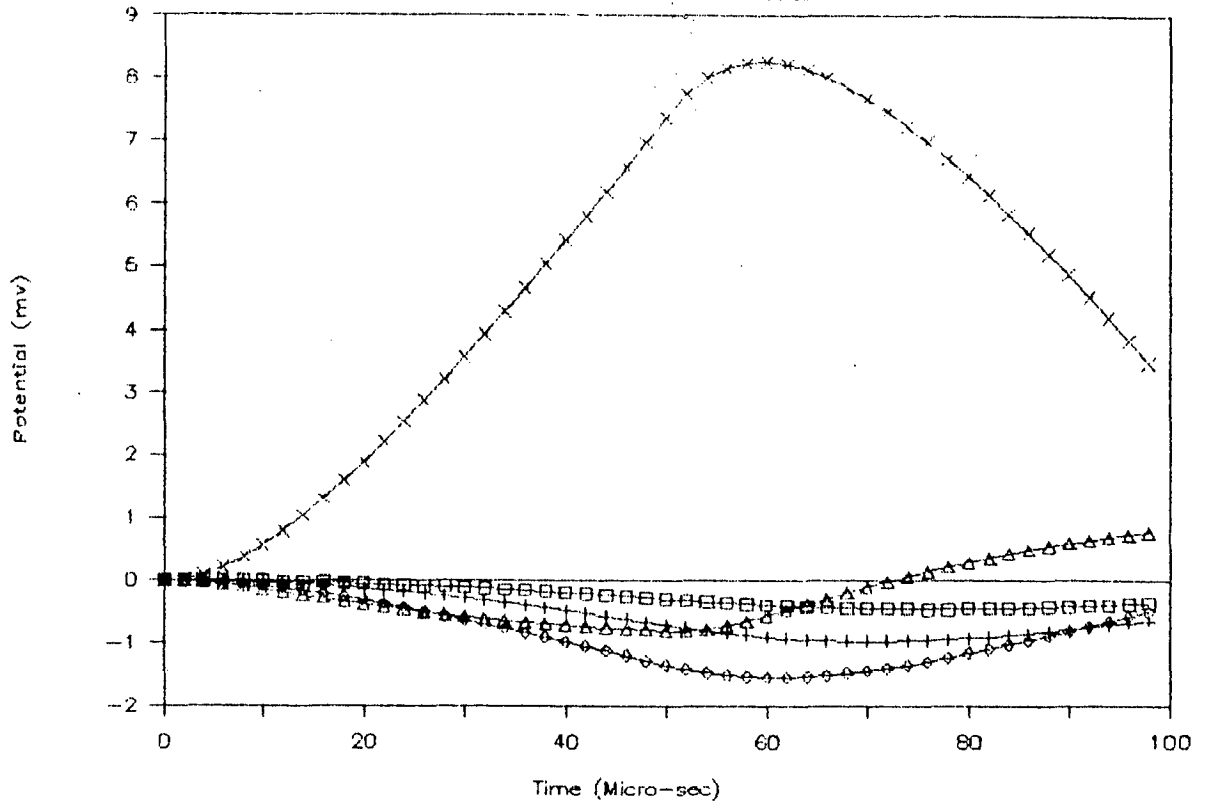
Membrane current at diff. Nodes
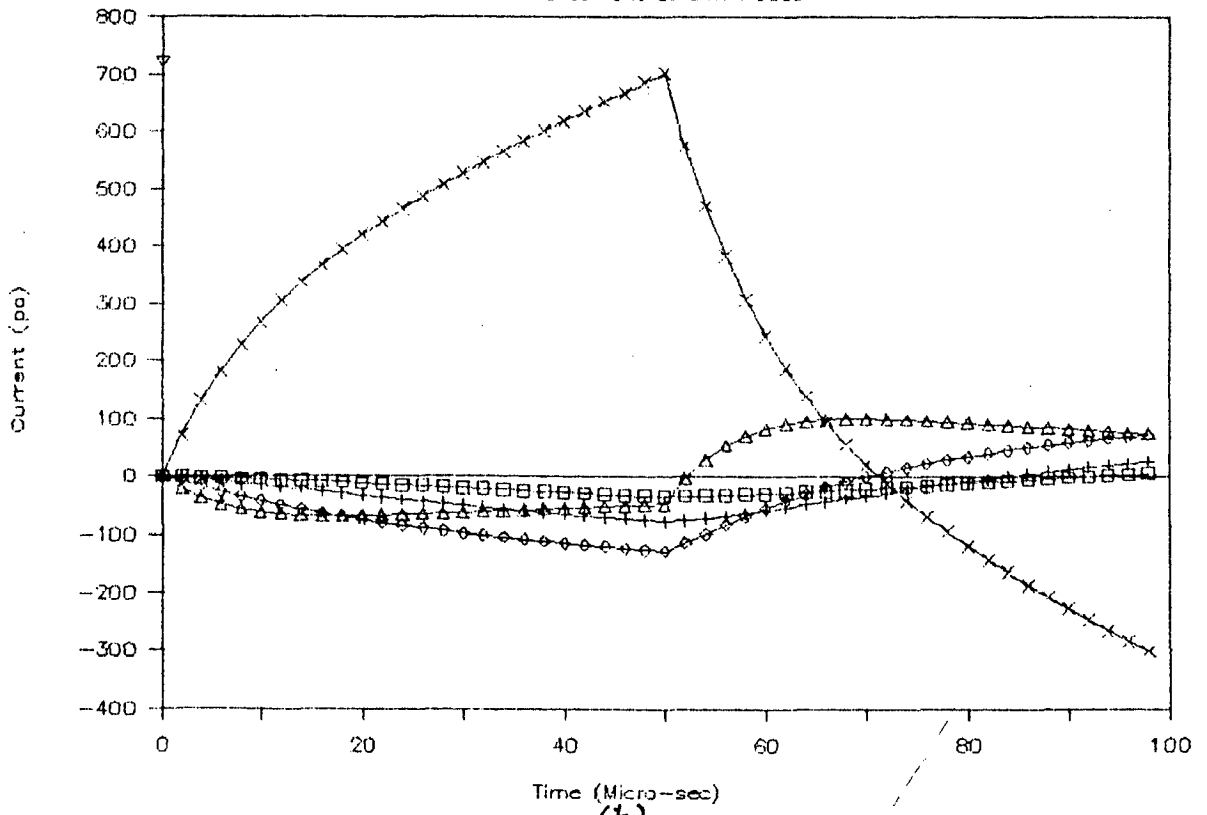
(b)

FIG.4.36 (a) Membrane potential at different nodes
(b) Membrane current at different nodes
For, L=0.2Cm, d=0.14E-2Cm, l=0.25E-3Cm, EDist=0.1Cm, I=0.1E-3A
X Node 0; △ Nodes -1,1; ◇ Nodes -2,2; + Nodes -3,3; □ Nodes -4,4
(Triangular excitation)

variation of hyperpolarization except nodes 1 and -1 which are hyperpolarized in the begining but reverse sign at 70 μs and remain depolarized from that time on. It is a highly desirable type of excitation where the various nodes are expected to be subjected to such a course of variation in and depolarization and hyperpolarization. The repetition rate of application of such variation in membrane potential at different nodes can be increased by increasing the frequency.

The time course of the membrane current at same nodes is shown in Fig. 4.36(b). The current at node 0 is initially positive but becomes negative after 70 μs accounting for the eventual reversal of membrane potential at these nodes. The membrane currents at nodes 4 and -4 and nodes 3 and -3 are negative. The membrane currents at nodes 1 and -1 and nodes 2 and -2 is initially negative but become positive after 50 μs accounting for the eventual reversal of membrane potential at these nodes. In this case only node 0 can be excited, but nodes 1 and -1 and nodes 2 and -2 will not be excited as the depolarization reached at these nodes is very low.

The change in membrane potential at the node under the electrode and at the four adjacent nodes for a ramp type of excitation is shown in Fig. 4.37(a). Here only node 0 is depolarized. All the other nodes are hyperpolarized. The maximum depolarization reached at the node 0 is 7.838 mV at t = 90 μs. The nodes 2 and -2 are subjected to the highest hyperpolarization which is -1.398 mV at t = 90 μs. The hyperpolarization

Analysis of Myelinated Nerve
Membrane potential at diff. Nodes
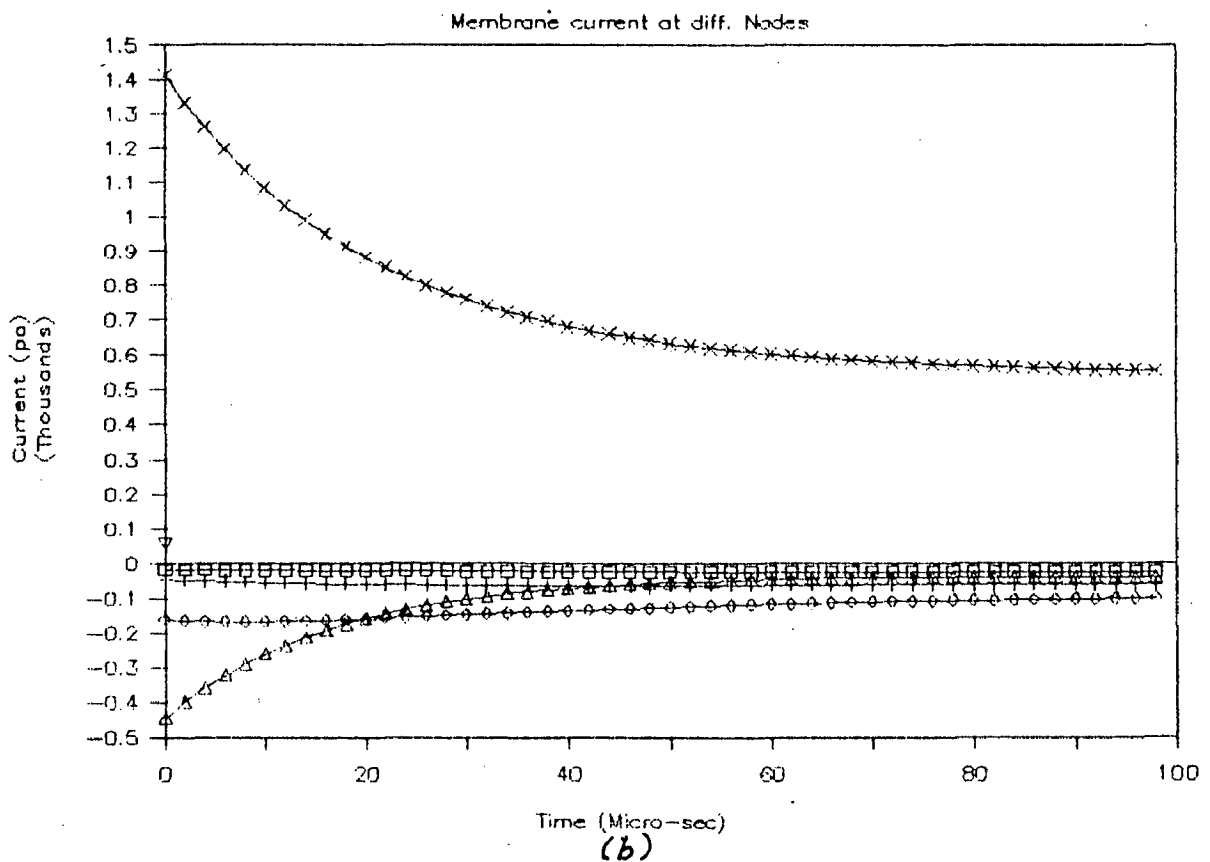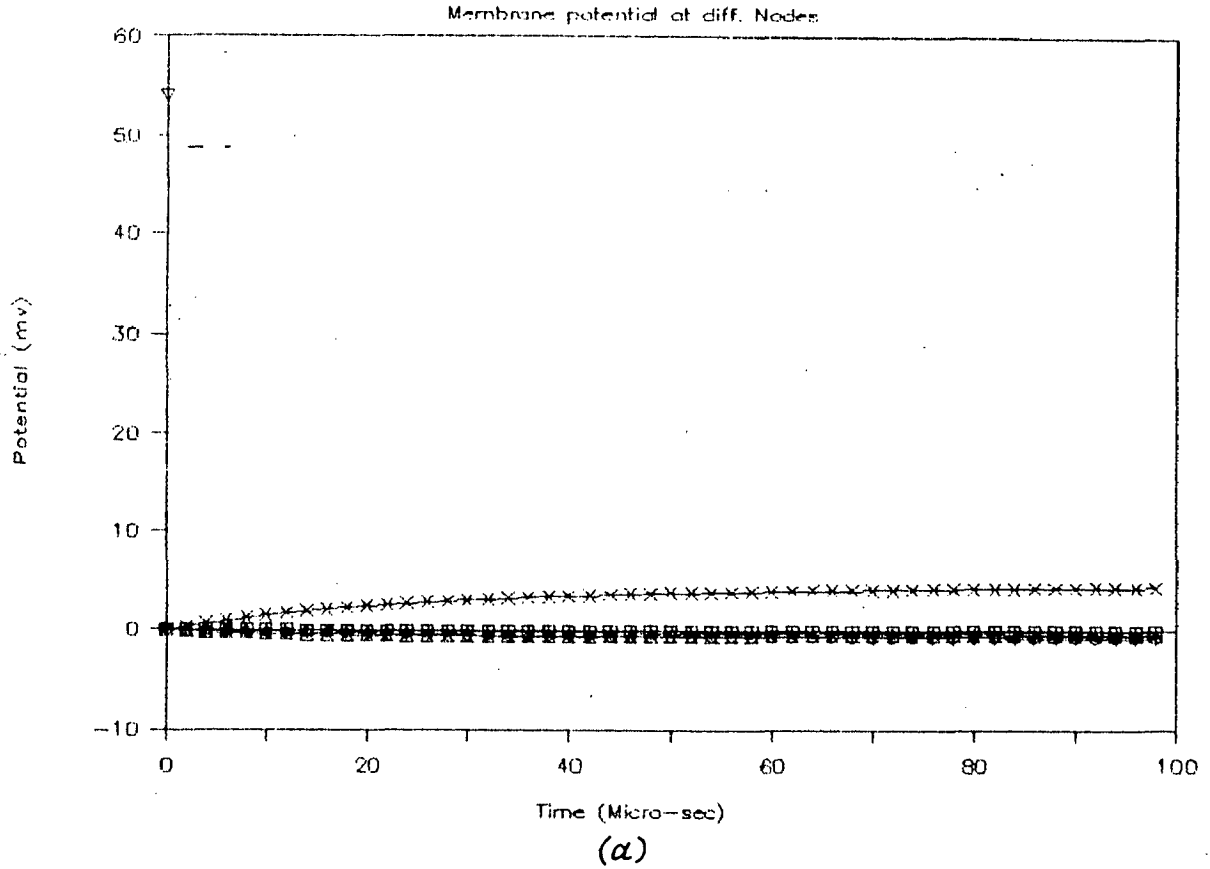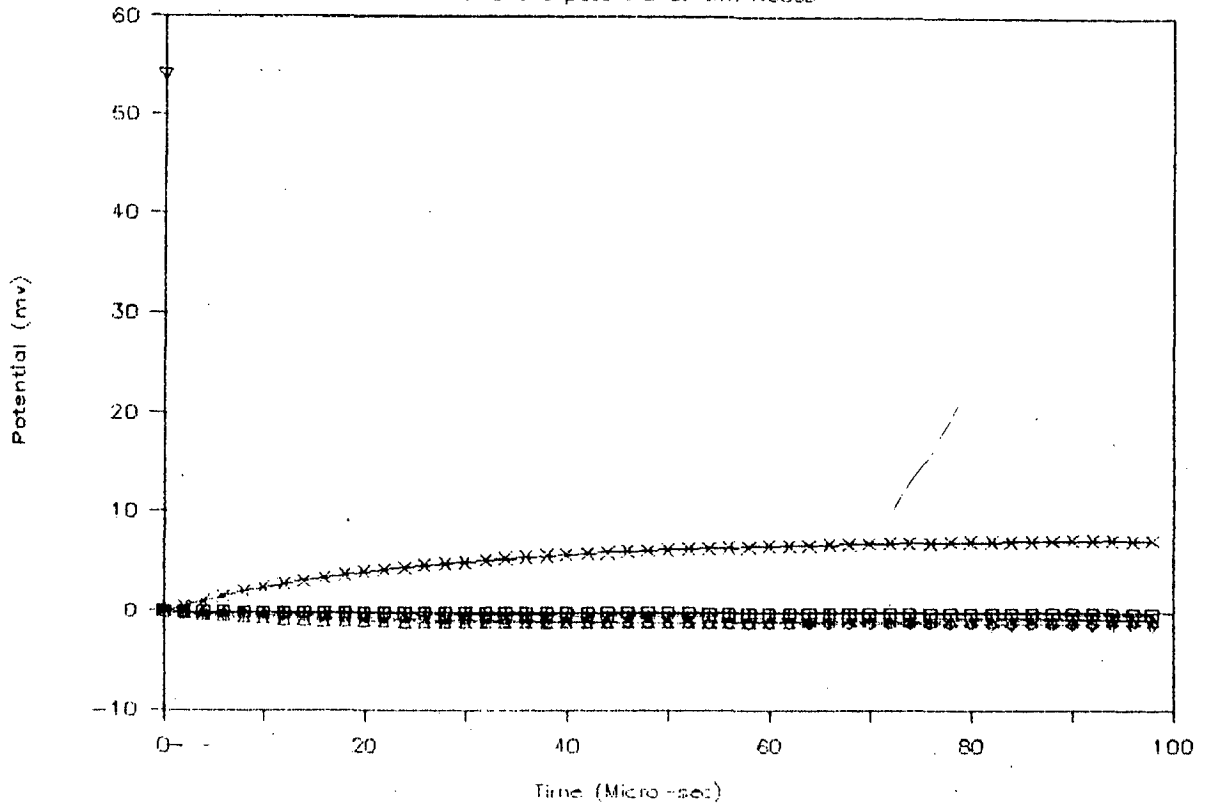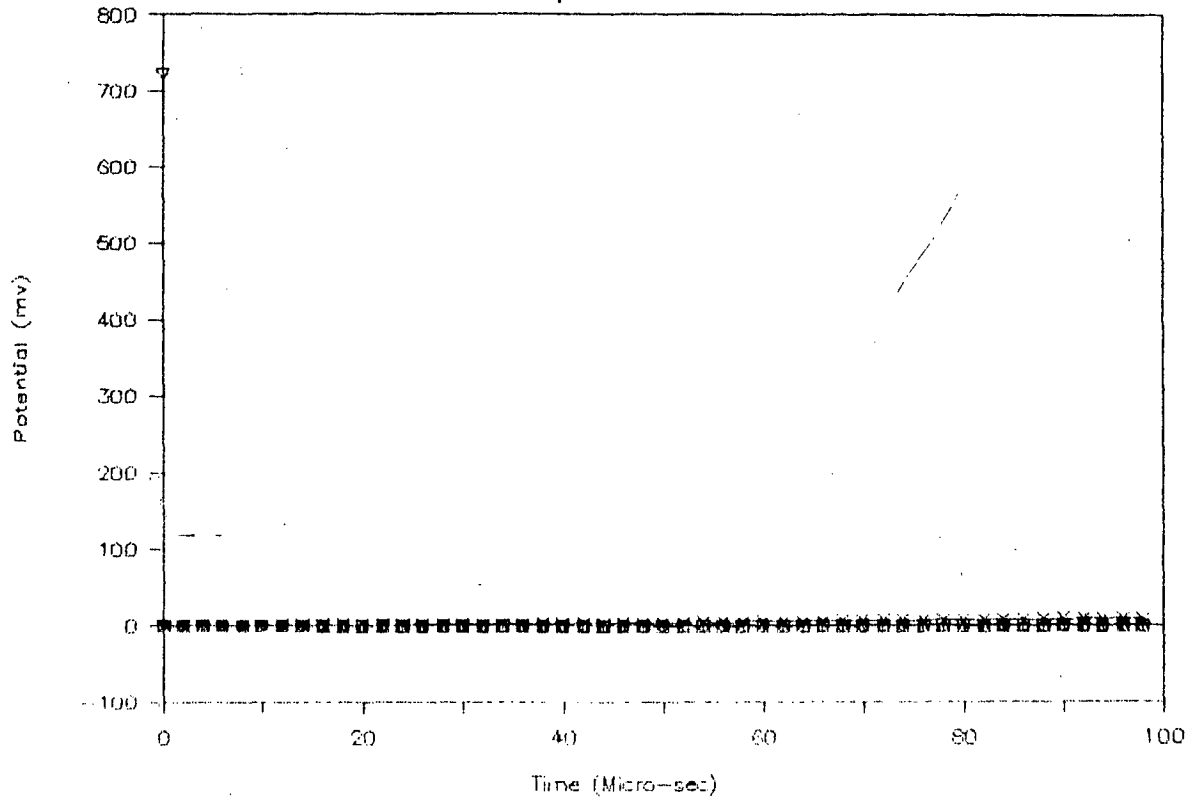
FIG.4.37 (a) Membrane potential at different nodes
(b) Membrane current at different nodes
For, L=0.2Cm, d=0.14E-2Cm, 1=0.25E-3Cm, EDist=0.1Cm, I=0.1E-3A
X Node 0; △ Nodes -1,1; ◊ Nodes -2,2; + Nodes -3,3; □ Nodes -4,4
(Ramp excitation)

reached by other nodes is very close to zero. In this case only node O can be excited. The special feature of this type of excitation is that depolarization and hyperpolarization at the respective nodes is highly linear from zero to maximum depending upon the choice of stimulus value. This stimulus function can be used where linear variation of the membrane potentials at different nodes is desired.

The time response of the membrane current at these same nodes is shown in Fig. 4.37(b). It is seen that the membrane current is positive at node O only. At all the other nodes the membrane current is negative. The increase in the membrane current at these different nodes is highly linear with increase in the stimulus. In this case also only node O can be excited. This a highly desirable function of stimulation, where only node below, the electrode i.e. node O is desired to be excited, with the variation of depolarization at that node being highly linear.

The change in membrane potential at the node below the electrode and at the four adjacent modes for pulse type of stimulation is shown in Fig. 4.38(a). It is seen that only node O is initially, depolarized, however nodes 1 and -1 and nodes 2 and -2 reverse sign at 60 and 90 μs respectively and remain depolarized from that time on. Nodes 3 and - 3 reach the maximum hyperpolarization which is - 0.248 mV at t = 90 μs and nodes 4 and -4 reach the minimum hyperpolarization which is -0.211 mV at t = 90 μs. Node O undergoes the
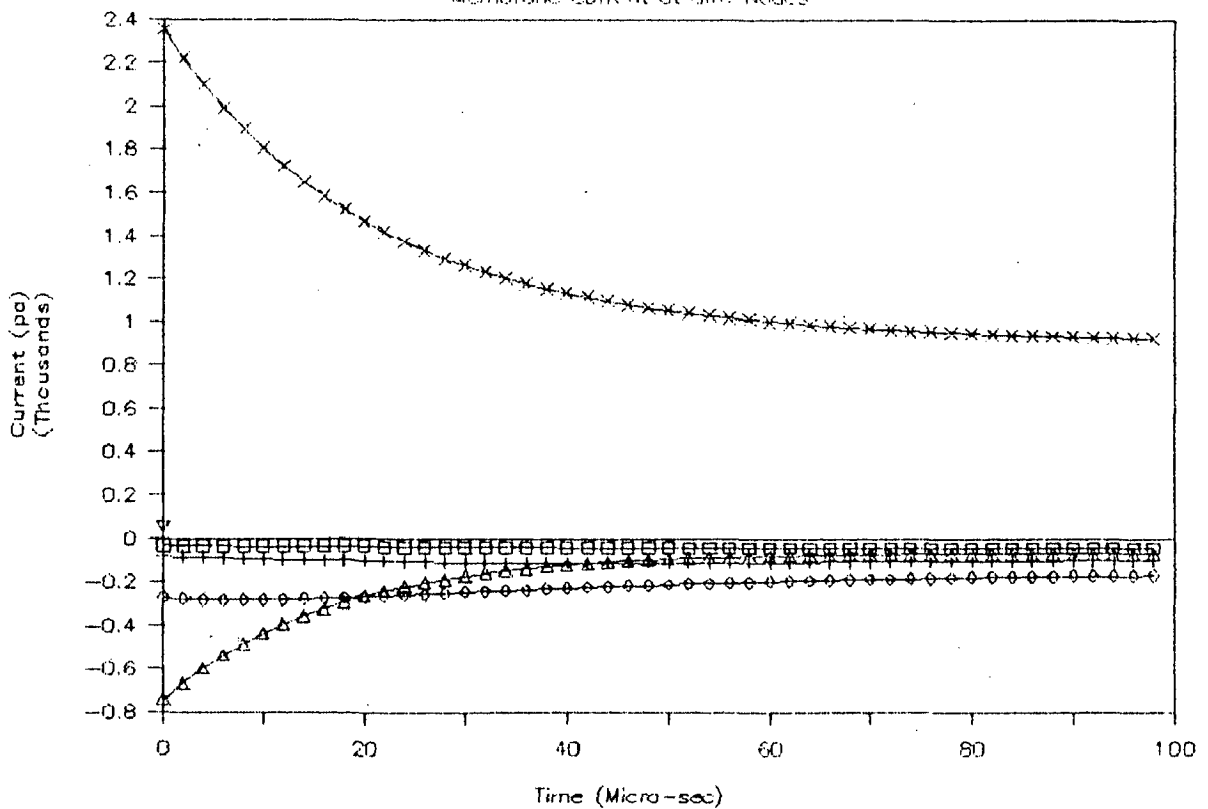
Analysis of Myelinated Nerve

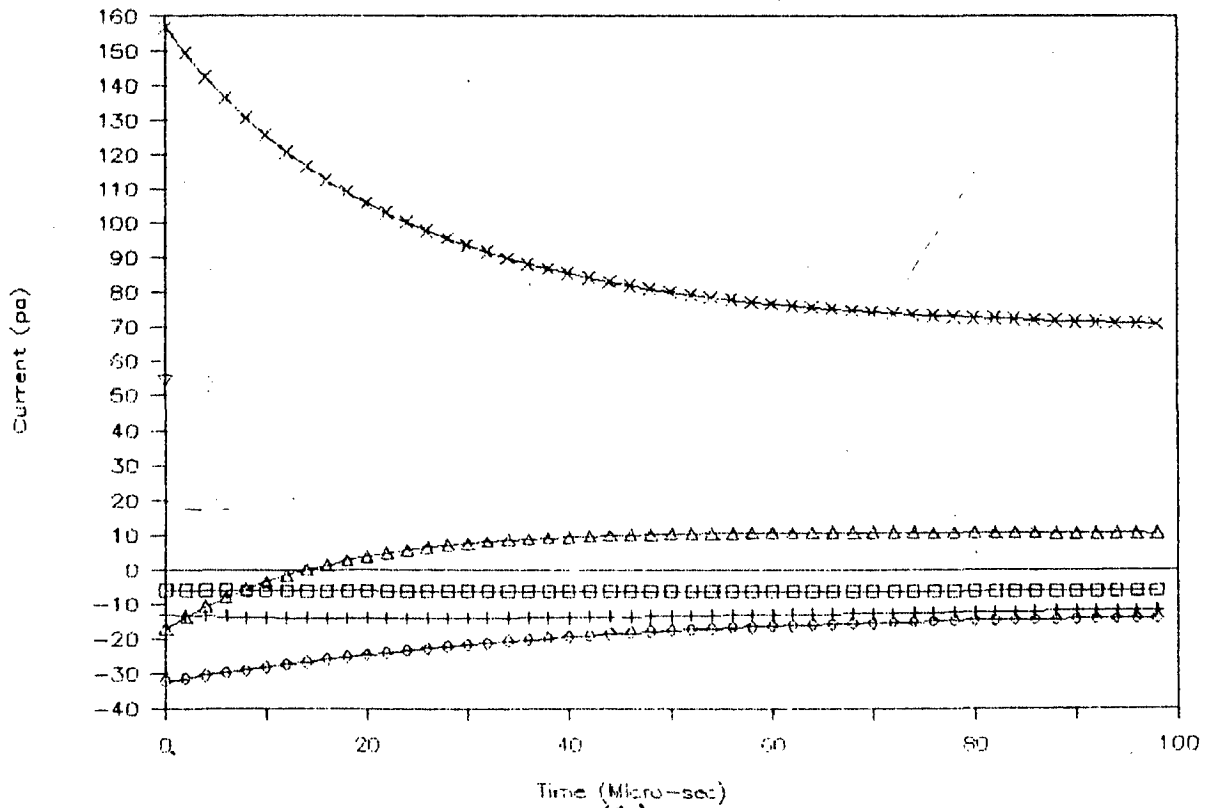### Membrane potential at diff. Nodes

(a)

Membrane current at diff. Nodes

(b)

FIG.4.38 (a) Membrane potential at different nodes
(b) Membrane current at different nodes
For, L=0.2Cm, d=0.14E-2Cm, l=0.25E-3Cm, EDist=0.1Cm, I=0.1E-3A
X Node 0; △ Nodes -1,1; ◇ Nodes -2,2; + Nodes -3,3; □ Nodes -4,4
(Pulse excitation)

maximum depolarization which is 9.976 mV at t = 50 µs.

In this case also only node 0 can be excited. This function can be used as a stimulus if it is desired that only the node below the electrode i.e.,node 0 is to be excited and nodes 1 and -1 and nodes 2 and -2 be subject to very mild depolarization and nodes 3 and -3 and nodes 4 and -4 be subjected to a very mild hyperpolarization.

The time course of the membrane current at these nodes is shown in Fig. 4.38(b). The response at node 0 to 0.1 mA pulse of duration 50 µs is also seen. At the termination of the pulse, the change in membrane current is equal and opposite to the change at t = 0. A significant negative current, therefore, flows after the stimulus has been terminated. The effect of this negative spike on the membrane potential is to drive the potential back to zero very rapidly. This fact is clearly observed from the data tables. The membrane currents at nodes 1 and -1 and nodes 2 and -2 are initially negative but become positive at 50 µs and remain positive from that time on, accounting for the eventual reversal of the membrane potential at these nodes. At 50 µs the membrane current at nodes 1 and -1 and nodes 2 and -2 experiences a sudden positive spike and decays slowly causing the membrane potential at these nodes to reverse sign suddenly at 50 µs and then gradually decay to a stable value before next pulse is applied.The membrane current at all the other nodes is negative and is very low.By increasing the frequency of the pulses, the transition rates of membrane potentials and

membrane currents can be increased. In this case also only
node 0 is excited, but nodes 1 and -1 and nodes 2 and -2 are
not excited as the depolarization reached at these nodes is
feable. This type of stimulus function is highly desirable,
in such cases where the membrane potentials and the membrane
currents at the different nodes are expected to undergo sharp
transitions at the desired time fixed by the pulse durations.
The graphs for triangular, ramp, and pulse type of excitations
are summerized in TABLE - XII.

TABLE - XII

L = 0.2 cm, d = 0.14 E-2 cm, excitation current I = 0.1 E-3A,
1 = 0.25E-3 cm, electrode distance = 0.1 cm.

Type of excit-ation	Voltage graphs	Current graphs
Trangular	Fig. 4.36(a)	Fig. 4.36(b)
Ramp	Fig. 4.37(a)	Fig. 4.37(b)
Pulse	Fig. 4.38(a)	Fig. 4.38(b)

The change in membrane potential at the node below
the electrode and at the four adjacent nodes for a sinusoidal
stimulus with ϕ = 0 is shown in Fig. 4.39(a). In this case,
initially, only node 0 is depolarized, however, nodes 1 and -1
reverse sign at 50 µs and remain depolarized from that time

Analysis of Myelinated Nerve
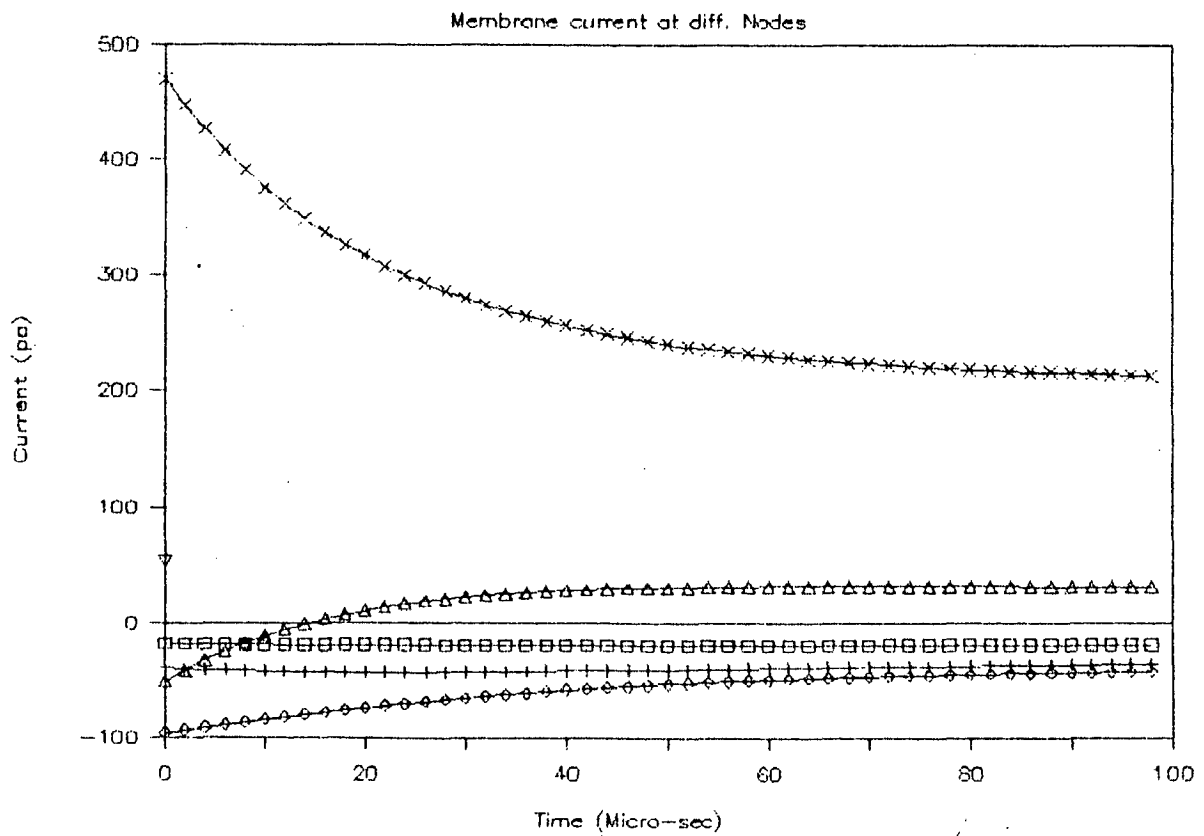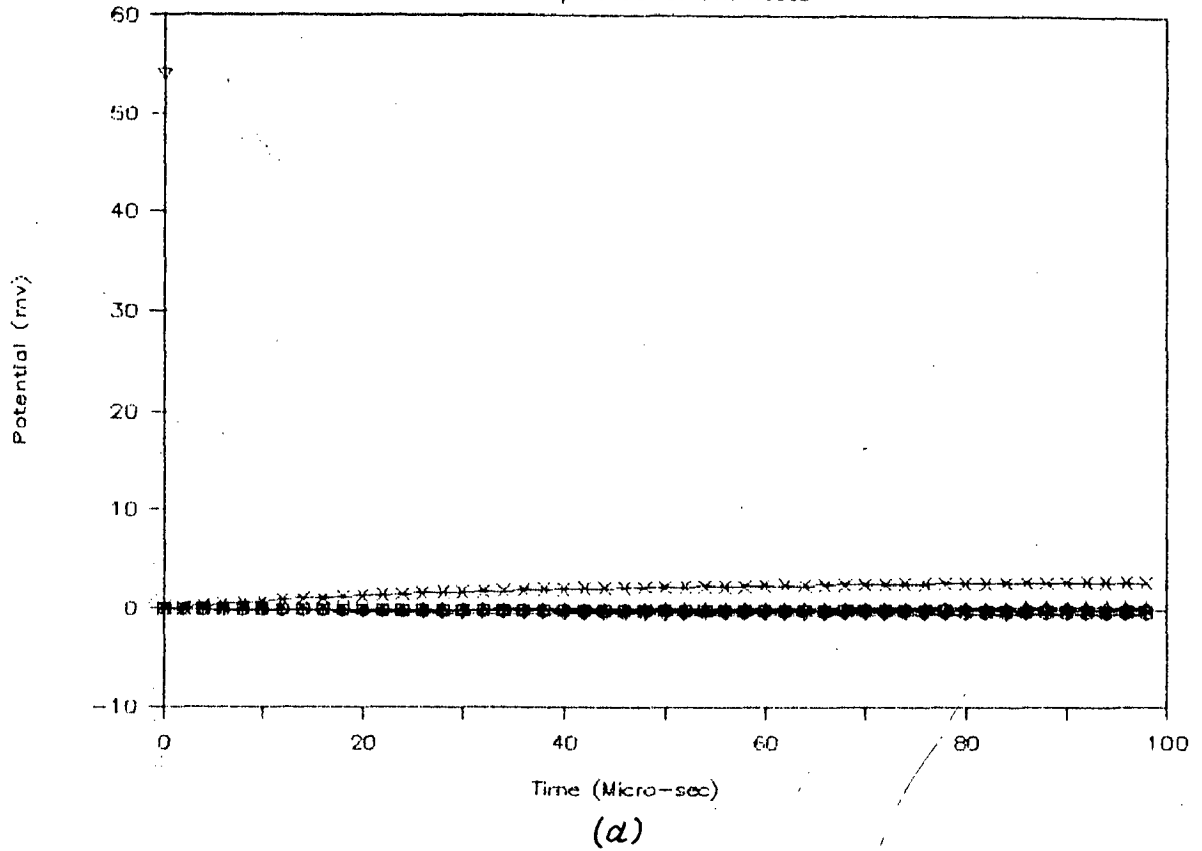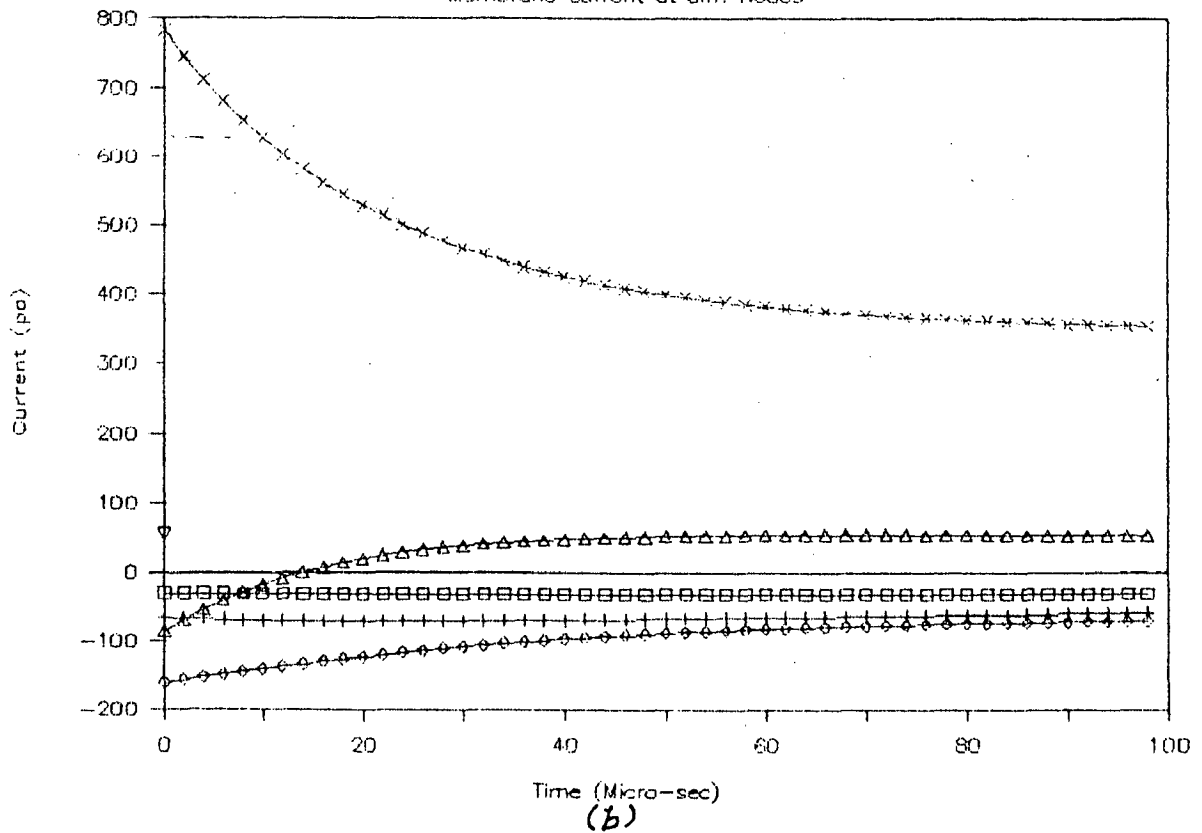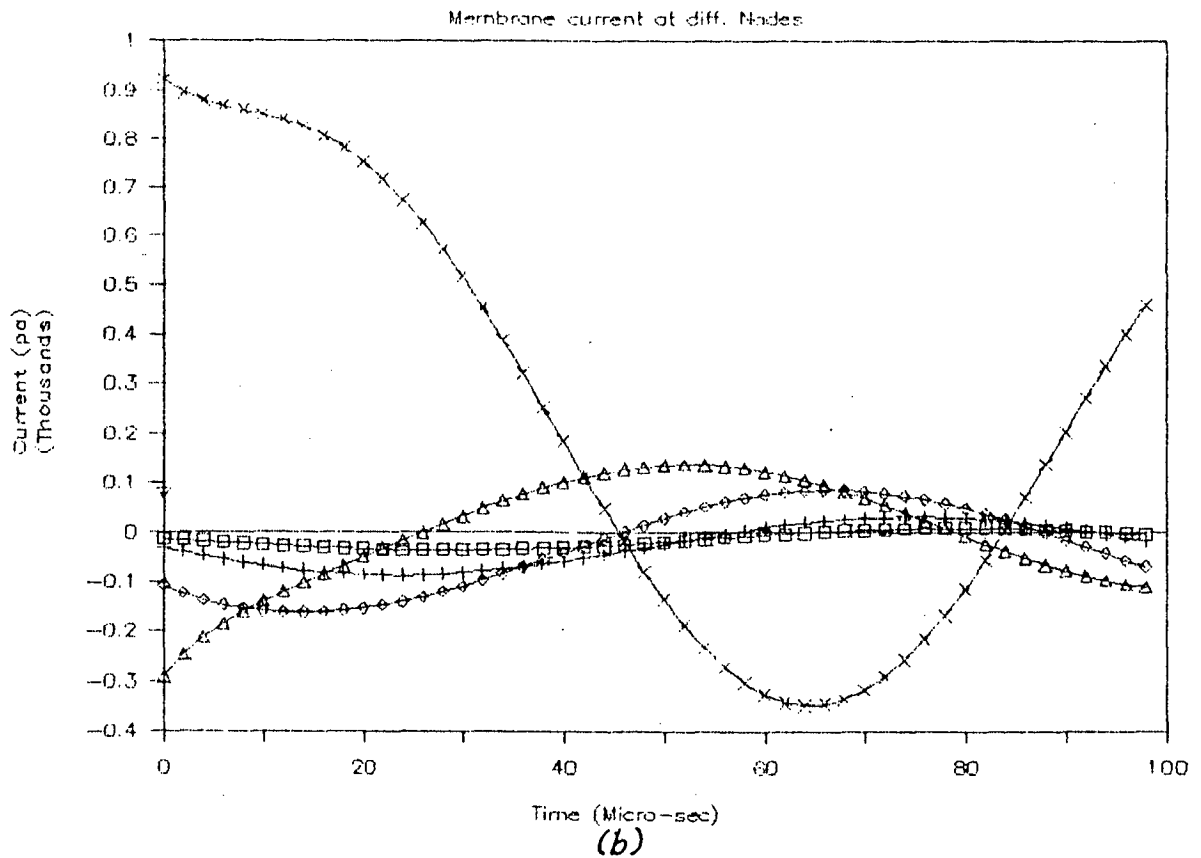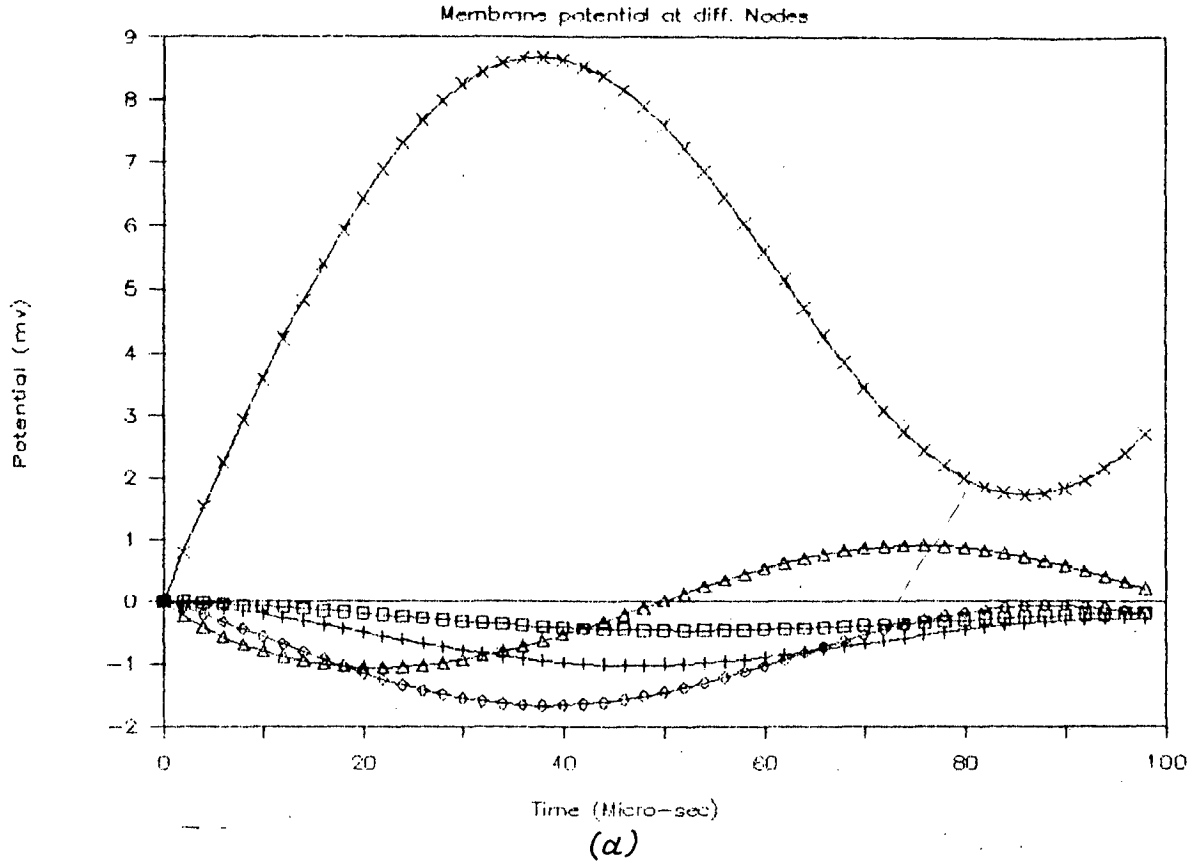

FIG.4.39 (a) Membrane potential at different nodes
(b) Membrane current at different nodes
For, L=0.2Cm, d=0.14E-2Cm, l=0.25E-3Cm, EDist=0.1Cm, I=0.1E-3A
✗ Node 0; △ Nodes -1,1; ◊ Nodes -2,2; + Nodes -3,3; ☐ Nodes -4,4
(Sinusoidal excitation, ∅ = 0 rad.)

on. All the other nodes are hyperpolarized. The membrane potentials (depolarizations and hyperpolarizations) at the respective nodes vary in simusoidal fashion, with only node 0 being subject to maximum depolarization. In cases where only node under the electrode i.e. node 0 be excited and the membrane potential at all the nodes be varied sinusoidally, then this type of stimulus function is highly desirable. Nodes 1 and -1 will not be excited since the depolarization reached at these nodes is low i.e., about 1 mV.

The time response of the membrane current at these same nodes is shown in Fig. 4.39(b).

The membrane current at node 0 is initially positive but becomes negative after 45 μs and again becomes positive after 85 μs. The striking feature of these curves is that, after the membrane current at node 0 becomes negative after 45 μs even before the membrane potential at this node reverse sign, the membrane current has again become positive after 85 μs. Hence the membrane potential at node 0 decreases to 2 mV and again starts to increase. The membrane currents at nodes 1 and -1 and nodes 2 and -2 are initially negative but become positive after 25 μs and after 45 μs and again become negative after 75 μs and after 85 μs respectively, accounting for the eventual reversals of the membrane potentials at these nodes. The membrane currents at all the nodes vary in a sinusoidal manner.

The change in membrane potential at the node below the electrode and at the four adjacent nodes for a sinusoidal

stimulus with ϕ = 31416 rad., corresponding to a delay of 5 µsc.,is shown in Fig. 4.40(a). Here initially, only node 0 is depolarized, however, nodes 1 and -1 reverse sign at 50 µs and remain depolarized from that time on. All the other nodes are hyperpolarized. The depolarizations and the hyperpolarizations reached by the respective nodes is slightly less in this case than those at ϕ = 0 [Fig. 4.39(a)]. The membrane potentials change in a simusoidal fashion at all the nodes. In this case also only node 0 is excited. Hence in cases where only node below the electrode is to be excited and all the other nodes be subjected to a feable sinusoidally varying depolarizations and hyperpolarizations [Fig. 4.40(a)], then this type of stimulus is highly desirable.

The time course of the membrane current at these nodes is shown in Fig. 4.40(b). The membrane current at node 0 is initially positive but becomes negative after 40 µs, but even before the membrane potential at this node reverse sign, the membrane current again becomes positive after 80 µs. Hence the membrane potential at node 0 decreases to 1.707 mV at 80 µs and again starts to increase. The membrane currents at nodes 1 and -1 and nodes 2 and -2 are initially negative but become positive after 20 and 40 µs and again become negative after 70 and 80 µs respectively, accounting for the eventual reversal of membrane potentials at these nodes [Fig. 4.40(a)].

The change in membrane potential at the node below the electrode and at the four adjacent nodes for sinusoidal type

Analysis of Myelinated Nerve

Membrane potential at diff. Nodes

(a)

Membrane current at diff. Nodes

(b)
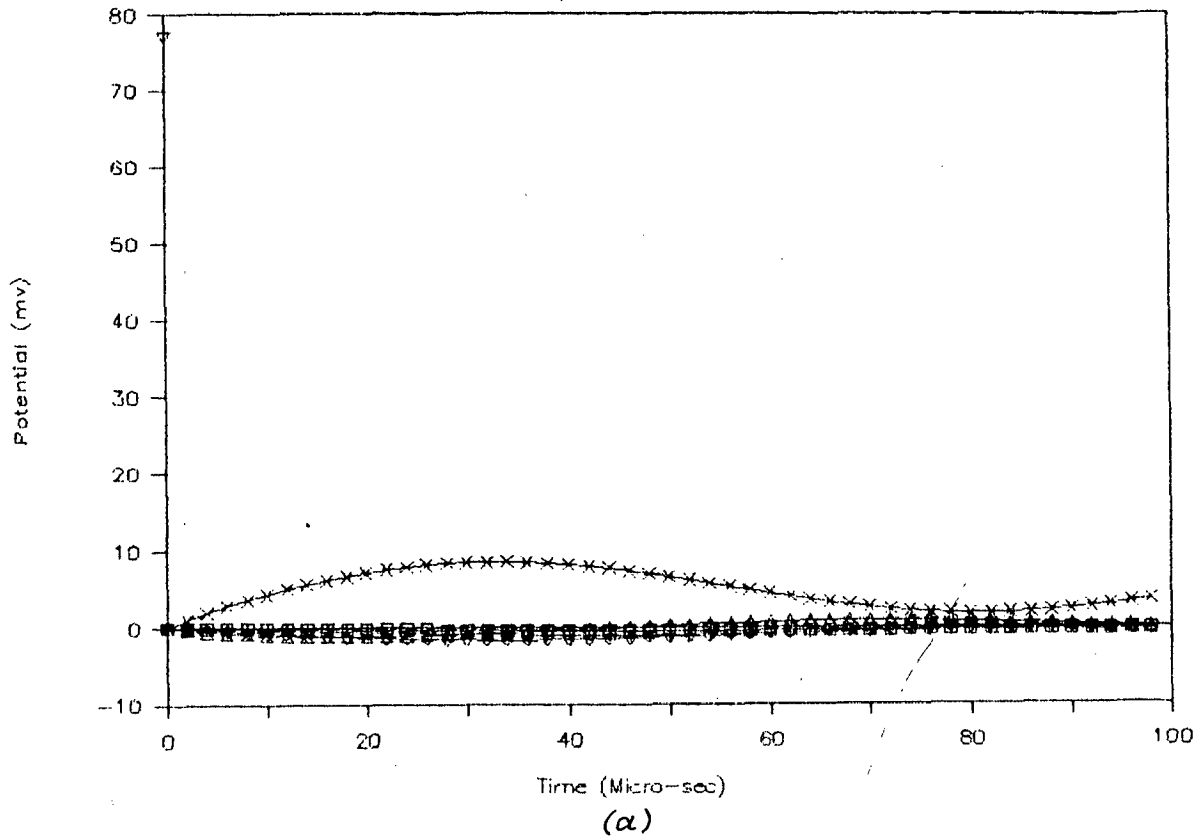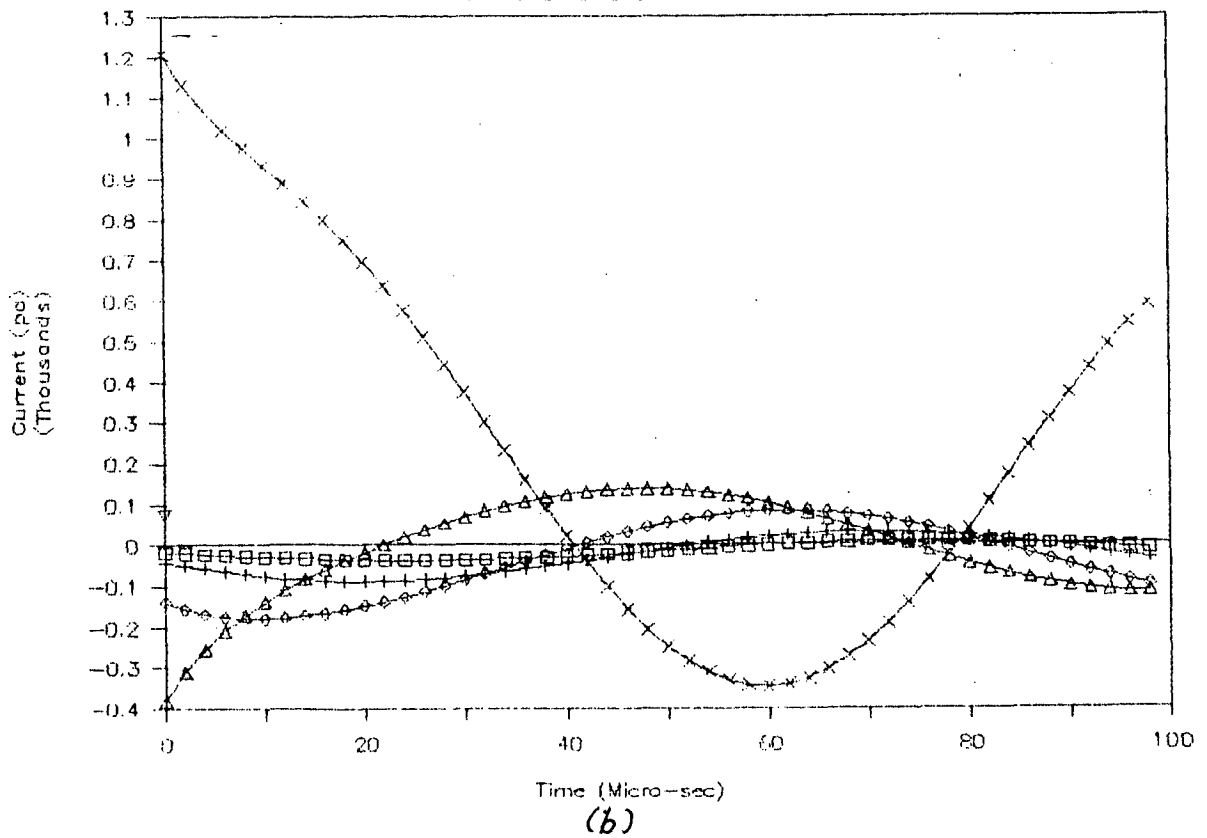
FIG.4.40 (a) Membrane potential at different nodes
(b) Membrane current at different nodes
For, L=0.2Cm, d=0.14E-2Cm, l=0.25E-3Cm, EDist=0.1Cm, I=0.1E-3A
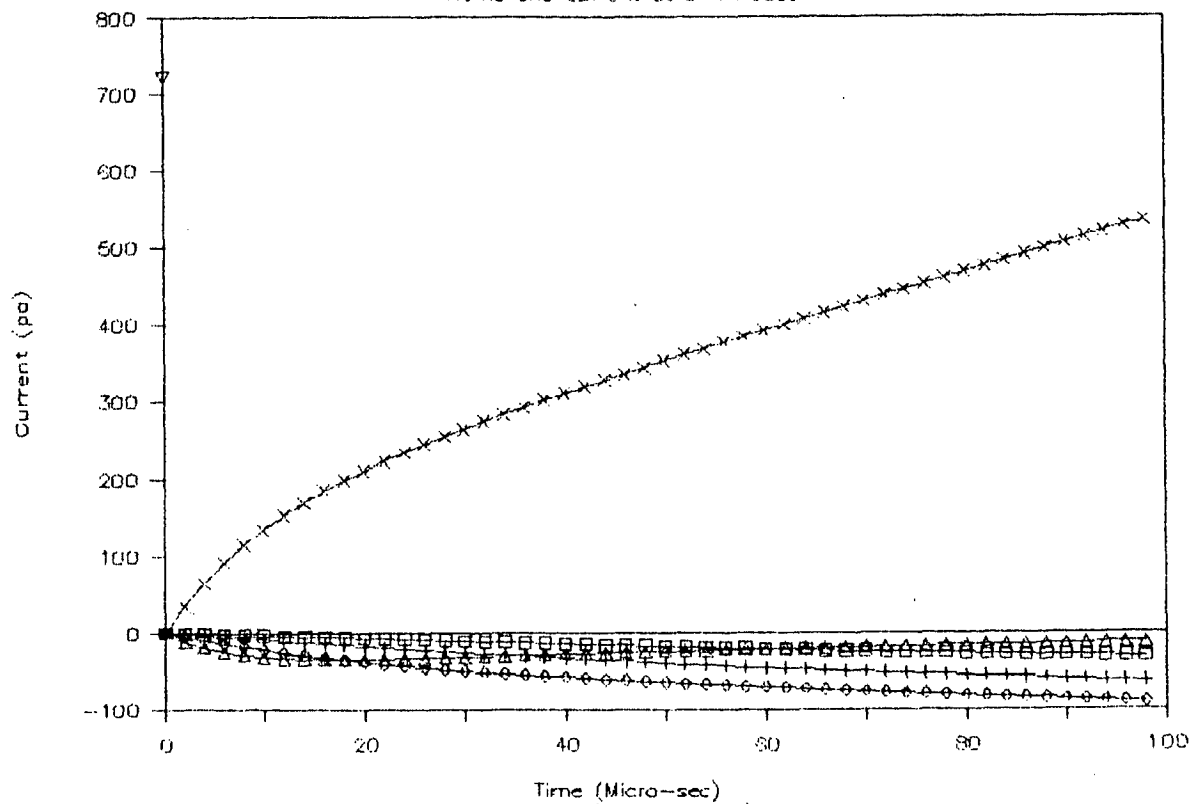X Node 0; △ Nodes -1,1; ◇ Nodes -2,2; + Nodes -3,3; ☐ Nodes -4,4
(Sinusoidal excitation, ∅ =0.314159 rad.)

of stimulus with ϕ = 0.62832 rad., corresponding to a delay of 10 μs is shown in Fig. 4.41(a). Here initially, only node 0 is depolarized, however, nodes 1 and -1 are initially hyperpolarized but reverse sign at 40 μs and again become hyperpolarized from 85 μs time on. All the other nodes are hyperpolarized. The membrane potentials (depolarizations and hyperpolarizations) at the respective nodes [Fig. 4.41(a)] is still less in this case than those at ϕ = 0.31416 rad. Only node 0 can be excited in this case. Hence such stimuations where it is desired that only node below the electrode be excited and all the respective nodes be subject to feable sinusoidally varying depolarizations and hyperpolarizations [Fig. 4.41(a)] then this type of stimulus function is highly desirable. The repitition rate of the variations of membrane potentials (depolarizations and hyperpolarizations) can be increased by increasing the frequency of the stimulus as desired.

The time response of the membrane current at these nodes is shown in Fig. 4.41(b). The membrane current at node 0 is initially positive but become negative at 45 μs, but even before the membrane potential at this node reverse sign the membrane current becomes positive at 75 μs. Hence the membrane potential at node 0 decreases to 1.766 mV at 80 μs and again starts to increase [Fig. 4.41(a)]. The membrane currents at nodes 1 and -1 and at nodes 2 and -2 are initially negative but become positive after 15 μs and after 25 μs and

Analysis of Myelinated Nerve

Membrane potential at diff. Nodes

(a)

Membrane current at diff. Nodes

(b)
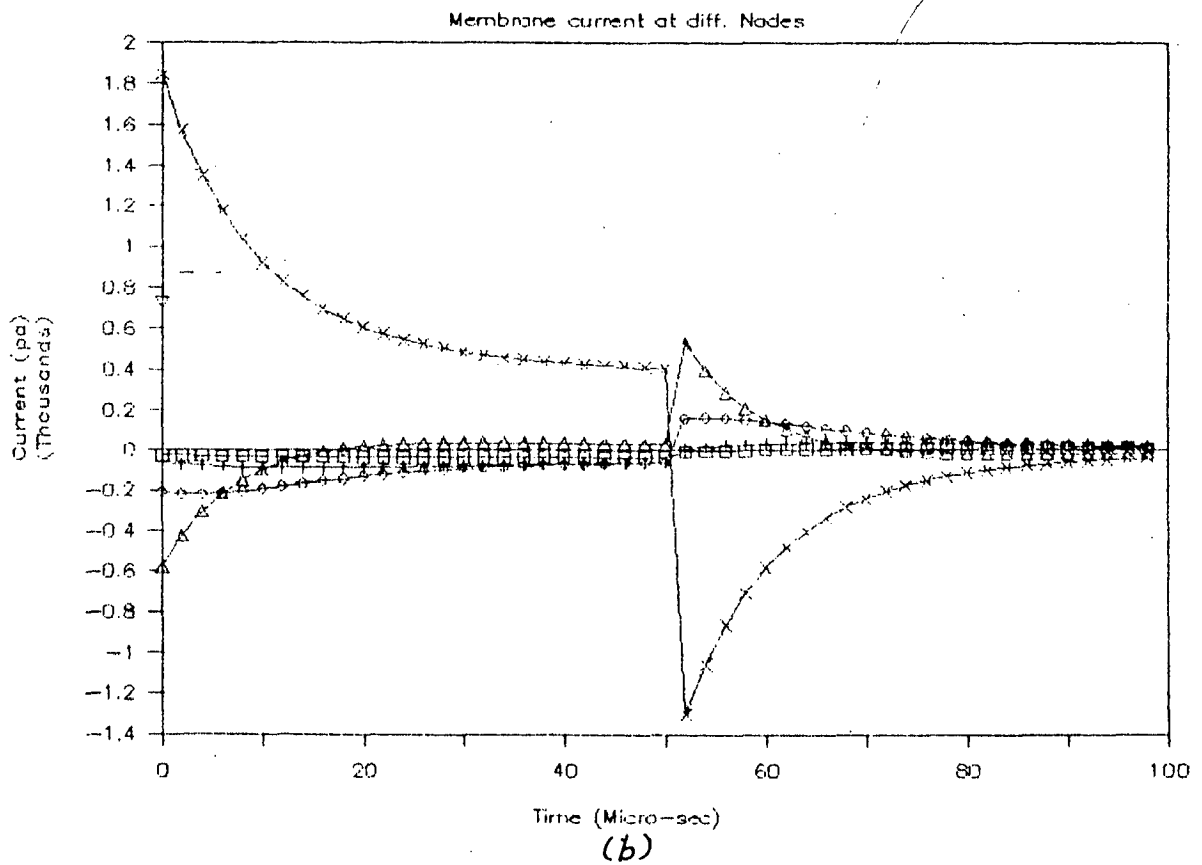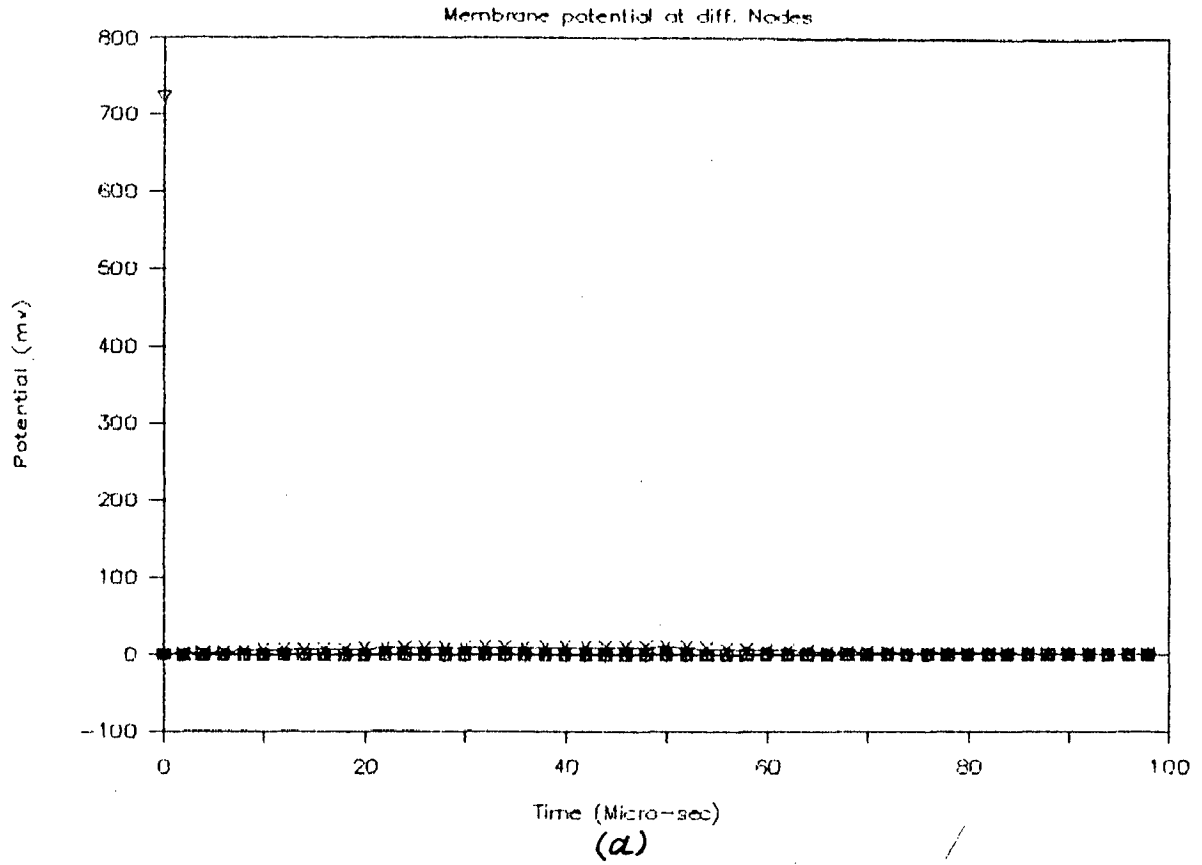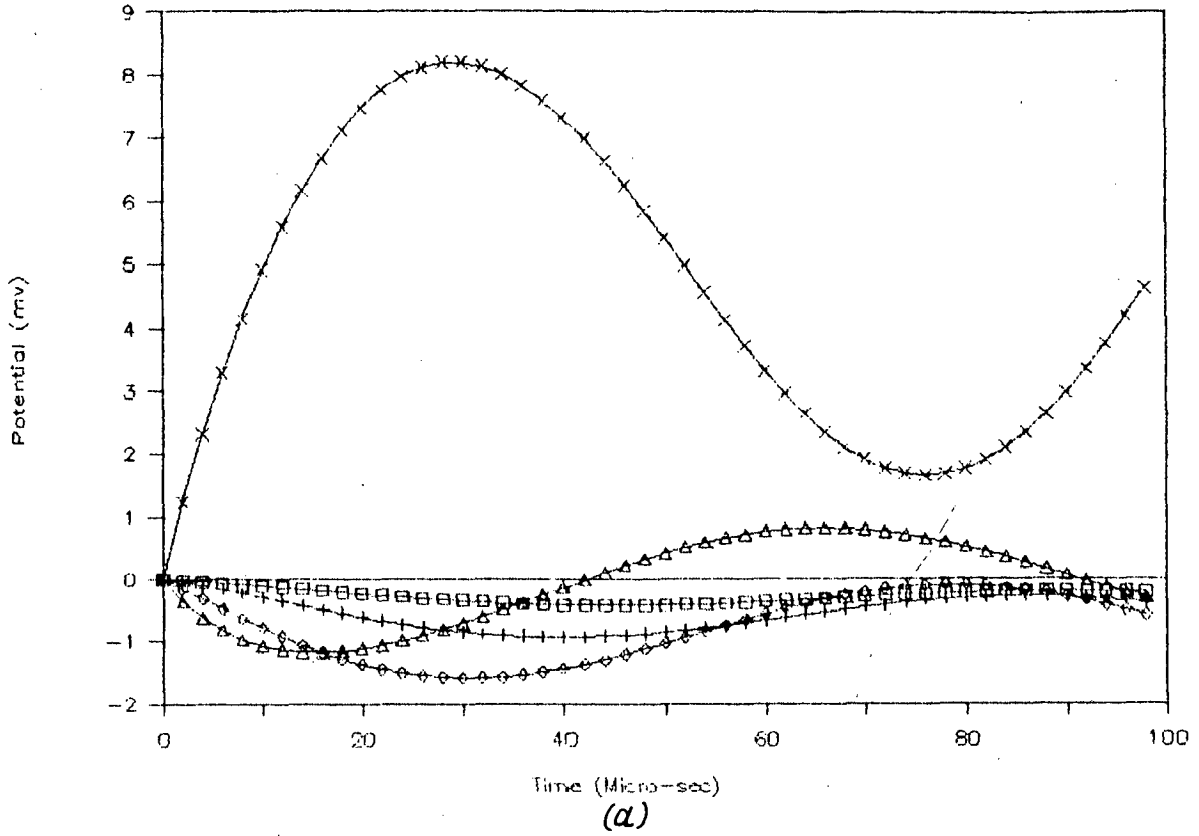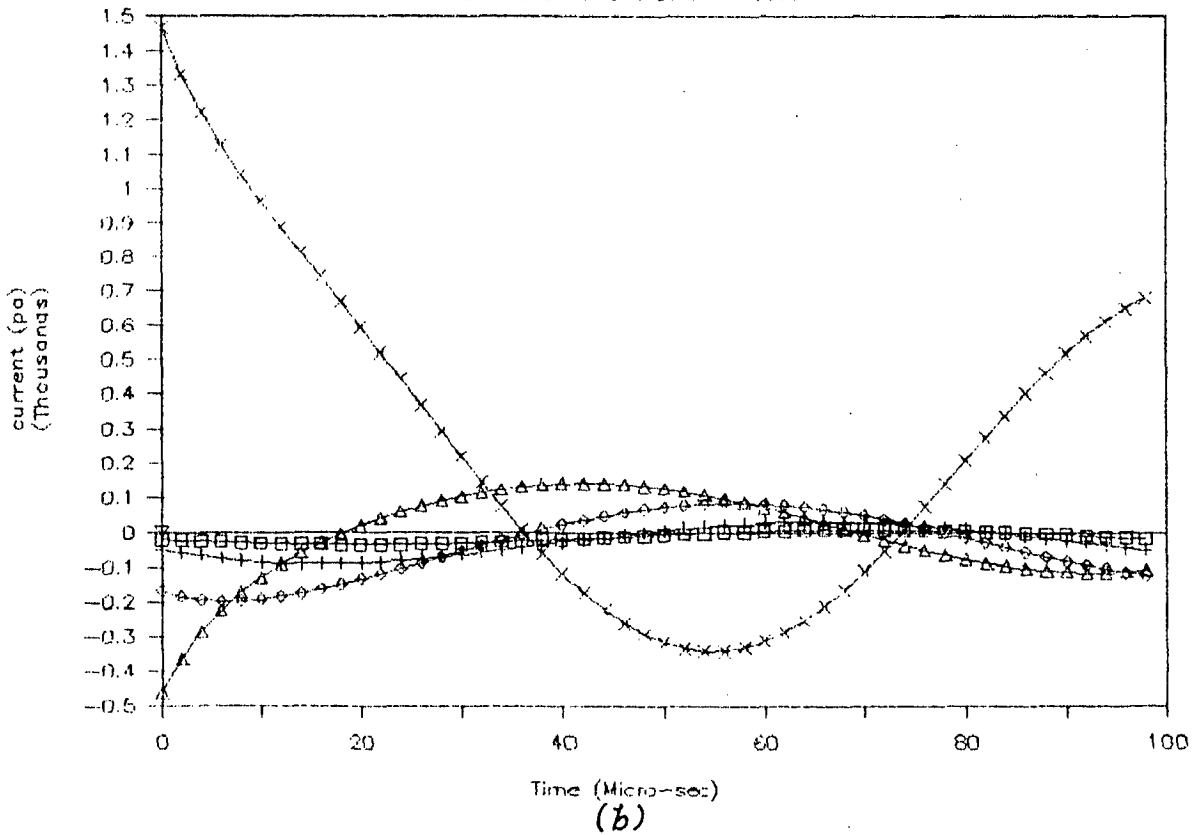
FIG.4.41 (a) Membrane potential at different nodes
(b) Membrane current at different nodes
For,L=0.2Cm,d=0.14E-2Cm,l=0.25E-3Cm,EDist=0.1Cm,I=0.1E-3A
X Node 0; △ Nodes -1,1; ◊ Nodes -2,2; + Nodes -3,3; ▢ Nodes -4,4
(Sinusodial excitation, Ø = 0.62831 rad.)

again become negative after 65 µs and after 75 µs respectively, accounting for the eventual reversals of the membrane potentials at these nodes [Fig. 4.41(a)]. The positive and negative currents at the different nodes vary in a sinusoidal fashion [Fig. 4.41(b)]. All the graphs for sinusoidal excitation are summerized in TABLE - XIII.

TABLE - XIII

$L = 0.2$ cm, $d = 0.14E-2$ cm,   excitation current $I = 0.1$ E-3A, $1 = 0.25E-3$ cm,   , electrode distance $= 0.1$ cm.

Type of excitation	Phase shift ϕ radians	Voltage graphs	Current graphs
Sinusoidal	0	Fig. 4.39(a)	Fig. 4.39(b)
Sinusoidal	0.314159 (5 µsec. delay)	Fig. 4.40(a)	Fig. 4.40(b)
Sinusoidal	0.62831 (10 µsec delay)	Fig. 4.41(a)	Fig. 4.41(b)

4.5 DISCUSSIONS :

Here the modal membrane conductance G_m is assumed to be constant for the subthreshold stimuli at the nodes in the analysis. It is also assumed that the nodal membrane conductance G_m is constant prior to the initiation of the action

potential at all the nodes. But as the threshold is appro-
ached the membrane conductance, for sodium ions suddenly
increases, thus allowing the sodium ions to flood from the
outside of the axon to the inside and it decays thereafter
at a equally faster rate. This results in further decrease in
the membrane potential so that the membrane potential reaches
zero and becomes positive by 30 mV. It does not reach the
equilibrium. Due to the slowly moving potassium ions from ins-
ide to outside of the cell, the membrane potential reverts to
the resting state. Thus the change in membrane conductance for
different ions causes the action potential [6]. This is also
confirmed by the marked difference in the potential curves
at and prior to excitation to that before the threshold is
reached [42]. Hence the assumption of constant membrane
conductance is no longer valid. This assumption is however,
fairly reasonably for subthreshold stimuli, which are 80 percent
or less than the threshold. At 80 percent of the threshold,
the response obtained by assuming that the membrane conduct-
ance is constant, is within 3 percent of the responses pred-
icted by more exact representation of the variation in the
membrane conductance [42, 43, 31].

It is necessary that the modal membrane conductance
variation should be taken into consideration at such nodes
where the excitation is taking place as explained in the
previous paragraph. But at the remaining nodes the membrane

conductance may still be considered constant, because the
membrane potential remains very low at those nodes till the
initiation of action potential at the excitation node.

We have seen in the preceding section, that the
excitation is taking place at more than one nodes. Therefore
the number of nodes, at which the variation of membrane
conductance should be taken into consideration can be deter-
mined from the subthreshold response curves, say for example
the membrane potential at any node 'n' is above 80 percent
of the membrane potential of the node of maximum depolariz-
ation then it is essential that the variation of membrane
conductance at that node be taken into consideration.

In the analysis it has also been assumed that the
surface of the membrane at nodes is at the same external
potential which is represented by $V_{e,n}$. This external potential
$V_{e,n}$ is the potential at the point occupied by the node 'n'.
And this is calculated by assuming that the whole of the
external potential is due to the stimulus current. That is to
say that it is assumed that the fiber is not present, though
it is physically present, and as such the effect of the fiber's
inherent potential on the external potential is not taken
into consideration. But in the actual neuron due to the
finite size of the fiber, there will of course be some varia-
tion in the external potential over the nodal surface. It is
very difficult to calculate this variation, because of the

distortion of the external potential in the neighbourhood of the fiber. However, the variation in the external potential over the modal surface will not differ significantly from that $V_{e,n}$, at least in comparison with the difference between the external potential at node n and the adjacent nodes. By giving a similar interpretation we can say that the inner membrane potential, $V_{i,n}$, will vary significantly in comparison with the difference in the membrane inner potential at any node n and it's adjacent nodes.

From this above analysis, without any ambiguity, the axial currents flowing into any node 'n' and the total membrane current can be given approximately by $G_a(V_{i,n-1} - 2V_{i,n} + V_{i,n+1})$. There is one more component of current that exists, which is not taken into consideration in the present analysis. This component of current is due to the currents flowing in the external medium because of the applied stimulus current. With the fiber present, some of the current will flow through the node O entering from the read end and exiting from the front side. But the precise calculations of this current requires a highly complex three dimensional analysis of the volume conductor.

The nerve fibers are also capable of changing the extracelluler potential by their own cellular activity and the inherent mechanisms. This change is not more than 1 mV where as the contribution of the intracellular voltage is high [42]. Since the threshold of the nerve fiber for the

extracellular stimulation is about 30 mV [6], the contribut-
ion to this by fiber's activity is very small and hence it's
influence is not taken into consideration.

As it can be seen from the electrical analog equivalent
circuit of the nerve fiber [Fig. 4.1a] that the nodes on the
outside surface of the membrane are isolated, assuming that
the myelin sheath is a perfect insulator. Serious error is
introduced in the model by this assumption, since the myelin
sheath has a finite resistance and capacitance. It has been
found by Tasaki [42,9] that resistance and capacitance of
the myelin sheath is about 290 $M\Omega$.mm and 1.6 $\mu\mu F$/mm, respect-
ively. It is very difficult to assess the effect of the
current leaking through the myelin sheath on the results
presented in this work. For doing the same it is necessary
to resort a highly complex simulation. Such a complex
simulation would call for a most complex expressions to describe
the variation of the membrane potential and current along
the internodal region and at the nodes. Because of such a
complexity this feature has not been incorporated in the
model and it's analysis. Since all the current is not flowing
through the nodes alone due to the leakage current through
the myelin sheath, the efficiency of the stimulation is
decreased. Qualitatively it can easily be assumed the curves
presented in this analysis will be shifted up by a small
amount, since all the current is not passing through the
nodes. But it is very difficult to predict as to how this
shift varies with the pulse duration and the different types
of excitation functions.

Even with this error introduced by the assumption that the myelin steath is a perfect insulator, it is felt that the model developed and analyzed here presents an adequate representation of the myelinated nerve fiber prior to excitation. It is therefore hoped that litle more insight could be gained by a more complex simulation. But at the same time much would be lost in terms of the enormous increase in the computational complexity and the time required for the analysis of such a complex model.

A more realistic model in terms of anisotropic medium and finite volume conductor can be developed and analyzed with some more additional complexity [61,62].

In the present analysis there have been many values of variables and for the nerve fiber constants [TABLE - I], pertaining to the relationships between the fiber diameters and axon diameters, and that with the internodal spacing, and also the approximation of the membrane surface [42,43]. All these assumptions and datas have been based on the information available at the present [29,43,63] on the modelling and analysis of the myelinated nerve fibers. None of the assumptions made in the present analysis are critical to the model presented here.

4.6 CONCLUSIONS OF ANALYSIS :

The model for a myelinated nerve fiber developed and analyzed in the present work permits us to compute the

threshold for neurons of a wide range of geometries. Also the time history of the variation of the membrane potential and membrane current at nodes below the electrode and close to the electrode and at the adjacent nodes for the threshold and subthreshold stimulations have been presented and analyzed. Constant magnitude stimulation as well as stimulations by triangular, ramp, pulse and sinusoidal excitations have also been considered in this analysis. The strength-duration data can readily be obtained by comparing the membrane potential curves for different neurons. The data relating the threshold to the fiber diameter can also be derived from the membrane potential curves for the different neurons which have been considered here.

The model allows us to study the influence of parameters to reach threshold, e.g., the dependence of the stimulus current of the electrode needed for excitation on it's distance from an axon or the influence of fiber diameter on threshold current. No attempt has yet been made to experimentally confirm the model, but the results presented in this analysis are consistent with available data [42,43]. The model also predicts an increase in threshold with decreasing fiber diameter, which is a well-known phenomenon. Unfortunately, there is a searcity of experimental data available to compare with the computed curves. The model can be updated in the future as more precise data become available.

Finally the conclusions are drawn as :

1. If only node 0 is to be excited, then, the electrode distance of 0.05, 0.1, and 0.25 cm, and an excitation current of 0.05, 0.1, 0.15, 0.25 mA is highly desirable [Fig. 4.4(a)], Fig. 4.5(a), 4.9(a), 4.10(a), 4.11(a), 4.18(a), 4.19(a), 4.20(a), 4.27(a), 4.28(a), 4.29(a), 4.30(a), 4.3o(a), 4.32(a)].

2. If it is desired that node 0 and nodes -1 and 1 are to be depolarized then the electrode distance of 0.15, 0.25, 0.35, and 0.45 cm and a stimulus current of 0.1 mA can be used effectively [Fig. 4.6(a), 4.7(a), 4.8(a), 4.24(a), 4.25(a), 4.26(a), 4.33(a), 4.34(a), 4.35(a)].

3. Node 0, nodes -1 and 1, and nodes -2 and 2 can be effectively excited by using an electrode distance of 0.25 cm, and an excitation current of 0.05, 0.15 and 0.25 mA [Fig. 4.12(a), 4.13(a), 4.14(a)].

4. If it is required that the node 0, nodes -1 and 1, nodes -2 and 2 and nodes -3 and 3 are to be excited, than an electrode distance of 0.45 cm and an excitation current 0.05, 0.15, and 0.25 mA is well suited [Fig. 4.15(a), 4.16(a) and Fig.4.17(a)].

Figs. 4.36(a), 4.37(a), 4.38(a), 4.39(a) and Fig. 4.40(a), 4.41(a) give the effect of various types of excitation functions on the neuron response.

If it is desired that the depolarization at node O should increase almost linearly except in the first 10 μs and then decrease after 50 μs, and nodes -1 and 1 getting depolarized after 50 μs, with all the other nodes being hyperpolarized then the triangular type of excitation is highly desirable [Fig. 4.36(a)].

For exciting only node O with the depolarization at that node increasing smoothly and linearly and for hyperpolarizing all the other nodes, ramp type of excitation function can be used effectively [Fig. 4.37(a)]. Triangular excitation is more effective than ramp excitation.

If it is required that, the node O should be subject to first increasing depolarization and then to decreasing depolarization after 50 μs, with nodes -1 and 1 depolarizing after 60 μs and nodes -3 and 3 depolarizing after 90 μs with the other nodes being at hyperpolarization then the pulse type of excitation function is suited [Fig. 4.38(a)].

Pulse excitation is more effective than both the ramp and triangular type of excitation functions, since the depolarization at node O for pulse excitation is of higher magnitude than for ramp and triangular excitations.

Fig. 4.39(a), 4.40(a) and Fig. 4.41(a) give the effect of sinusoidal type of excitation. If it is desired that, the depolarization at node O vary in a sinusoidal manner, and nodes -1 and 1 behyperpolarized for the first half cycle and get depolarized in the second half cycle, and with all the other nodes also getting hyperpolarized, again varying in a sinusoidal manner, then the sinusoidal type of excitation is highly desirable.

With the introduction of phase shift the magnitude of the depolarizations and hyperpolarizations at the corresponding nodes progressively decreases [Fig. 4.40(a), 4.41(a)].

Sinusoidal type of excitation is more effective than ramp and triangular type of excitations but is not as effective as the pulse type of excitation.

Depending on the specific requirements the type of excitation function may be chosen.

****

CONCLUSIONS AND SCOPE FOR FUTURE WORK

5.1 CONCLUSIONS :

The electronic model presented here has been fabricated and tested successfully in the laboratory. This model incorporates most of the important functional aspects of the actual biological neuron, such as threshold, accomodation, adaptation, subthreshold phenomenon, all-or-none relationship, absolute and relative refractory periods, inhibitory feedback from the Renshaw cell. One important feature of this model is that, it incorporates the patch membrane active axon analog. In the present work the model for synaptic terminal has also been developed, which produces the excitatory postsynaptic potential (EPSP) and inhibitory postsynaptic potential (IPSP).

The model makes use of integrated circuit chips which are of small size, reliable and inexpensive. This model offers a very convenient means of studying the two types of neural signal processing. (1) the transmission and processing of neural information in a single nerve cell and (2) the transmission of information from one nerve cell to another at the synaptic junctions. It is also possible to study the effect of EPSP's and IPSP's individually and the interactions of EPSP's and IPSP's, at the neural inputs.

The important advantages of this model are as
follows.

(1)   Since each block in the neural analog represents a
        particular part of the actual neuron, the signals at
        various blocks can be varied and the effect can be
        studied on the behaviour of the whole neuron.

(2)   This model is very flexible in it's principle of
        operation, in that, the studies can be carried out on
        the properties of different kinds of nerve cells, by
        the simple process of changing several parameters of
        the model.

(3)   The outputs of this neural analog can be processed in
        identical fashion to that of the actual biological
        neuron, for direct comparison of the data of the two.

(4)   The effect of EPSP's and IPSP's can be studied.

        As it is very difficult, rather impossible to carry
out these detailed studies on the in-vivo neuron, the neural
analog serves as a valuable aid for the purpose of studies and
analysis by bioengineers and neurophysiologists.

        If it is possible to construct the microstructure model
of this analog, it can serve as a replacement for a neuron
which has stopped functioning in some part of the body.

        The membrane patch analog can be used to study the
non-uniform distribution of excitability over the nerve cell.

Such models can be interconnected to study the small neural systems. It may be helpful in the treatment of some paralysis cases, where only a small segment, has stopped functioning and as a result a major part of the body has stopped working. This may happen when there is no transmission of neural information from that part of the body to brain and vice-versa. Hence this model can serve as a good prosthetic aid.

In the analytical work, the myelinated nerve has been considered. The values of the variables and constants have been taken on the information currently available on myelinated nerve. The software has been developed to facilitate the selection of a variety of neoron geometries, excitation currents and electrode distances of practical interest.

Three different myelinated nerves have been studied for different electrode distances and excitation currents.

Thus this neuroelectric model provides a theoretical framework for studying a wide variety of stimulus parameters, including various excitation waveshapes, and neural geometric effects.

The model is a versatile tool for providing information, guiding and interpreting experiments, and for studying variables that may not be easily implemented in the laboratory.

Here the analysis has been carried for 100 μs., because for most clinical applications of 100 - 200 μs pulse durations are used. The same analysis can be extended upto 1000 μs,

since, the results obtained are comparable at higher pulse durations for steady state models and dynamic models with the membrane conductance held constant [29].

5.2. SCOPE FOR FUTURE WORK :

In this work it is assumed that the membrane conductance G_m is constant. It's variations as per the accepted physiological standards may be considered in the future work. The effect of the inherent potentials of the nerve fiber on $V_{e,n}$ (the external potential at any node n) may be considered which is neglected in the present work. It is assumed that the myelin sheath is a perfect insulator, and the total axial current is the total nodal membrane current. But there will be some leakage current, as the myelin sheath is not a perfect insulator. This may be considered in the future work.

The model presented here could be further developed to include additional properties of the axon, such as the electrical characteristics of the internode-sheath i.e., myelin sheath. The analysis of unmyelinated fibers may be considered.

The models can be updated in the future as more precise neural data become available.

**

APPENDIX - A

The fourth-ordered classical Runge-Kutta method for the system of equations

$$\frac{du}{dt} = f(t,u)$$

$$u(t_o) = \eta$$

may be written as

$$u_{j+1} = u_j + \frac{1}{6}(K_1 + 2K_2 + 2K_3 + K_4) \qquad ...(1)$$

where

$$K_1 = \begin{bmatrix} K_{11} \\ K_{21} \\ \vdots \\ K_{n1} \end{bmatrix}, K_2 = \begin{bmatrix} K_{12} \\ K_{22} \\ \vdots \\ K_{n2} \end{bmatrix}, K_3 = \begin{bmatrix} K_{13} \\ K_{23} \\ \vdots \\ K_{n3} \end{bmatrix}, K_4 = \begin{bmatrix} K_{14} \\ K_{24} \\ \vdots \\ K_{n4} \end{bmatrix}$$

and

$$K_{i1} = hf_i(t_j, u_{1,j}, u_{2,j}, \ldots\ldots u_{n,j})$$

$$K_{i2} = hf_i(t_j + \frac{h}{2}, u_{1,j} + \frac{1}{2}K_{11}, u_{2,j} + \frac{1}{2}K_{21}, \ldots u_{n,j} + \frac{1}{2}K_{n1})$$

$$K_{i3} = hf_i(t_j + \frac{h}{2}, u_{1,j} + \frac{1}{2}K_{12}, u_{2,j} + \frac{1}{2}K_{22}, \ldots u_{n,j} + \frac{1}{2}K_{n2})$$

$$K_{i4} = hf_i(t_j + h, u_{1,j} + K_{13}, u_{2,j} + K_{23} \ldots\ldots u_{n,j} + K_{n3}),$$
$$i = 1(1)n$$

In an explicit form (1) becomes

$$
\begin{bmatrix} u_{1,j+1} \\ u_{2,j+1} \\ \vdots \\ u_{n,j+1} \end{bmatrix} = \begin{bmatrix} u_{1,j} \\ u_{2,j} \\ \vdots \\ u_{n,j} \end{bmatrix} + \frac{1}{6} \left(\begin{bmatrix} K_{11} \\ K_{21} \\ \vdots \\ K_{n1} \end{bmatrix} + 2 \begin{bmatrix} K_{12} \\ K_{22} \\ \vdots \\ K_{n2} \end{bmatrix} + 2 \begin{bmatrix} K_{13} \\ K_{23} \\ \vdots \\ K_{n3} \end{bmatrix} + \begin{bmatrix} K_{14} \\ K24 \\ \vdots \\ K_{n4} \end{bmatrix} \right)
$$

*****

APPENDIX - B

```
C*********************************************************************C
C       PROGRAM FOR STIMULATION STUDIES ON NEURON                    C
C*********************************************************************C
C       ABBREVIATIONS USED IN THIS PROGRAM ARE AS FOLLOWS :          C
C       GA    :   AXIAL INTERNODAL CONDUCTANCE                       C
C       VE    :   EXTERNAL POTENTIAL                                 C
C       VI    :   INTERNAL POTENTIAL                                 C
C       GCM   :   NODAL MEMBRANE CONDUCTANCE                         C
C       CCM   :   NODAL CAPACITANCE                                  C
C       ALC   :   INTERNODE LENGTH                                   C
C       DS    :   AXON DIAMETER (INTERNAL MYELIN DIAMETER)           C
C       EDIST:    ELECTRODE DISTANCE                                 C
C       AI    :   EXCITATION CURRENT                                 C
C       ALS   :   NODAL GAP WIDTH                                    C
C       RHOE  :   RESISTIVITY OF EXTERNAL MEDIUM                     C
C       RHOI  :   AXOPLASM RESISTIVITY                               C
C       R(K)  :   ELECTRODE RADIAL DISTANCE                          C
C       AMI   :   MEMBRANE CURRENT                                   C
C       GSM   :   MEMBRANE CONDUCTANCE PER UNIT AREA                 C
C       CSM   :   MEMBRANE CAPACITANCE PER UNIT AREA                 C
C*********************************************************************C
C       UNITS FOR                                                    C
C               LENGTH    IS    CENTIMETERS                          C
C               TIME      IS    SECONDS                              C
C               CURRENT   IS    AMPERES                              C
C*********************************************************************C
```

```
       COMMON /F1/ GA,VE(200),GCM,CCM
       DIMENSION R(200),V(200,200),AK1(200),AK2(200),AK3(200),
      1AK4(200),AMI(200,200)
C**** INTERACTIVELY ACCEPT THE REQUIRED DATA
       WRITE(5,30)
30     FORMAT(10X,'    ENTER  THE  NUMBER  OF  NODES : 's)
       READ(5,40)NODES
40     FORMAT(I4)
       TYPE 1
1      FORMAT('  ENTER THE STARTING VALUE FOR ALC      's)
       ACCEPT*,SALC
       ALC=SALC
       TYPE 2
2      FORMAT('  ENTER THE INCREMENT FOR ALC           's)
       ACCEPT*,DELALC
       TYPE 3
3      FORMAT('  ENTER THE ENDING VALUE FOR ALC        's)
       ACCEPT*,ENDALC
       TYPE 6
6      FORMAT('  ENTER THE STARTING VALUE FOR DS       's)
       ACCEPT*,SDS
       DS=SDS
       TYPE 7
7      FORMAT('  ENTER THE INCREMENT FOR DS            's)
       ACCEPT*,DELDS
       TYPE 8
8      FORMAT('   ENTER THE ENDING VALUE FOR DS        '.)
       ACCEPT*,ENDDS
9      CONTINUE
       TYPE 50
50     FORMAT('  ENTER THE STARTING VALUE FOR EDIST    's)
       ACCEPT*,SEDIST
       EDIST=SEDIST
       TYPE 51
51     FORMAT('  ENTER THE INCREMENT FOR EDIST         's)
       ACCEPT*,DEDIST
       TYPE 52
```

```
52       FORMAT('    ENTER THE ENDING VALUE FOR EDIST      '$)
         ACCEPT*,EEDIST
         TYPE 10
10       FORMAT('   ENTER THE STARTING VALUE FOR AI        '$)
         ACCEPT*,SAI
         DAI=SAI
         TYPE 11
11       FORMAT('   ENTER THE INCREMENT FOR AI             '$)
         ACCEPT*,DELAI
         TYPE 12
12       FORMAT('    ENTER THE ENDING VALUE FOR AI         '$)
         ACCEPT*,ENDAI
         TYPE 13
13       FORMAT('   ENTER THE STARTING VALUE FOR ALS       '$)
         ACCEPT*,SALS
         ALS=SALS
         TYPE 14
14       FORMAT('   ENTER THE INCREMENT FOR ALS            '$)
         ACCEPT*,DELALS
         TYPE 15
15       FORMAT('    ENTER THE ENDING VALUE FOR ALS        '$)
         ACCEPT*,ENDALS
         PI=3.1415926
         RHOI=110.0
         GSM=30.4E-3
         CSM=2.0E-6
         RHOE=300.0
         PI4=4.0*PI
5        PRINT 18,ALC,EDIST
         TYPE 18,ALC,EDIST
         AI=-DAI
         PRINT 20,AI,DS,ALS
         TYPE 20,AI,DS,ALS
         TYPE 3434
3434     FORMAT(5X,'ENTER THE NAME OF THE FILE FOR VOLTAGE :'$)
         ACCEPT3435,VOLT
         TYPE 3447,VOLT
```

```
            PRINT 3447,VOLT
3435    FORMAT(A5).
            TYPE 3436
3436__  FORMAT(5X,'ENTER THE NAME OF THE FILE FOR CURRENT :',$)
            ACCEPT3437,CURNT
            TYPE 3447,CURNT
            PRINT 3447,CURNT
3437    FORMAT(A5)
3447    FORMAT(2X,A5)
            OPEN(UNIT=1,DEVICE='DSK',FILE=VOLT)
            OPEN(UNIT=2,DEVICE='DSK',FILE=CURNT)
18      FORMAT(10X,'INTERNODE LENGTH : ',F6.3,'CM',3X,'ELECTRODE
            1  DISTANCE : ',F6.3,'CM')
20      FORMAT(5X,'ELECTRODE CURRENT : ',E14.6,'A',3X,
            1'AXON DIAMETER : ',E14.6,'CM',/20X,'NODAL GAP WIDTH : ',
            2E14.6,'CM')
            H=1.0E-6
            GA=PI*DS*DS/(4.0*RHOI*ALC)
            PIDALS=PI*DS*ALS
            GCM=GSM*PIDALS
            CCM=CSM*PIDALS
            IRSTRT=-NODES/2
C****   CALCULATE THE RADIAL DISTANCE OF ELECTRODE AND
C****   EXTERNAL VOLTAGE AT NODES
            DO 100 K=1,NODES
            ALTOT=ABS(ALC*IRSTRT)
            R(K)=SQRT(ALTOT*ALTOT+EDIST*EDIST)
            VE(K)=RHOE*AI/(PI4*R(K))
            IRSTRT=IRSTRT+1
100         CONTINUE
C****   ENFORCE THE INITIAL CONDITION
            DO 150 I=1,NODES
            V(I,1)=0.0
150         CONTINUE
C****   EVALUATE THE RUNGE-KUTTA COEFFICIENTS
            DO 600 J=1,100
            DO 200 K=2,NODES-1
```

```
         I=K
         AK1(I)=H*F(I,V(I-1,J),V(I,J),V(I+1,J))
200      CONTINUE
         DO 300 K=2,NODES-1
         I=K
         AK2(I)=H*F(I,V(I-1,J)+AK1(I-1)/2.0,V(I,J)+
        1AK1(I)/2.0,V(I+1,J)+AK1(I+1)/2.0)
300      CONTINUE
         DO 400 K=2,NODES-1
         I=K
         AK3(I)=H*F(I,V(I-1,J)+AK2(I-1)/2.0,V(I,J)+
        1AK2(I)/2.0,V(I+1,J)+AK2(I+1)/2.0)
400      CONTINUE
         DO 500 K=2,NODES-1
         I=K
         AK4(I)=H*F(I,V(I-1,J)+AK3(I-1),V(I,J)+AK3(I),V(I+1,J)+AK3(I+1))
500      CONTINUE
C****    CALCULATE THE MEMBRANE VOLTAGE
         DO 700 I=2,NODES-1
         V(I,J+1)=V(I,J)+(AK1(I)+2.0*(AK2(I)+AK3(I))+AK4(I))/6.0
700      CONTINUE
600      CONTINUE
C****    CALCULATE THE MEMBRANE CURRENT
         DO 720 J=1,100
         DO 720 I=2,NODES-1
         AMI(I,J)=GA*(V(I-1,J)-2.0*V(I,J)+V(I+1,J)+VE(I-1)-
        12.0*VE(I)+VE(I+1))
720      CONTINUE
         DO 750 I=1,NODES
         DO 750 J=1,100
         V(I,J)=1000.*V(I,J)
750      CONTINUE
         PRINT 910
         PRINT 900
         PRINT 910
         PRINT 930
         PRINT 920
```

```
      PRINT 940
      PRINT 910
      INCRMT=NODES/2+1
      DO 800 I=1,NODES
      NODE=I-INCRMT
      PRINT820,NODE,(V(I,J),J=1,100,10)
800   CONTINUE
      DO 845 J=1,100,2
      JJ=J-1
      WRITE(1,676)JJ,(V(I,J),I=2,INCRMT+1)
676   FORMAT(I3,7F10.3)
845   CONTINUE
      PRINT 910
      PRINT 910
      PRINT 1000
      PRINT 910
      PRINT 930
      PRINT 970
      PRINT 940
      PRINT 910
      DO 1050 I=1,NODES
      DO 1050 J=1,100
      AMI(I,J)=1.0E+12*AMI(I,J)
1050  CONTINUE
      DO 1200 I=1,NODES
      NODE=I-INCRMT
      PRINT820,NODE,(AMI(I,J),J=1,100,10)
1200  CONTINUE
      PRINT 910
      DO 1300 J=1,100,2
      JJ=J-1
      WRITE(2,1320) JJ,(AMI(I,J),I=2,INCRMT+1)
1320  FORMAT(I3, 7F10.2)
1300  CONTINUE
      CLOSE(UNIT=1)
      CLOSE(UNIT=2)
820   FORMAT(1X,I4,11F10.3)
```

```
900    FORMAT(30X,'MEMBRANE  VOLTAGE  IN  MILLI-VOLTS ')
910    FORMAT('  -------------------------------------------------
      1------------------------------------------------------')
920    FORMAT('     V   ------------------------------------------
      1----------------------------------------------------!)
930    FORMAT('                                        TIME
      1               MICROSECONDS      ')
940    FORMAT('                 0          10          20          30          40
      1    50          60          70          80          90          100  !)
970    FORMAT('     I   ------------------------------------------
      1-----------------------------------------------------')
1000   FORMAT(30X,'MEMBRANE  CURRENT  IN  PICO-AMPERES )
       ALC=ALC+DELALC
       IF (ALC .LE. ENDALC) GO TO 5
       ALC=SALC
       DS=DS+DELDS
       IF (DS .LE. ENDDS) GO TO 5
       DS=SDS
       EDIST=EDIST+DEDIST
       IF (EDIST .LE. EEDIST ) GO TO 5
       EDIST=SEDIST
       DAI=DAI+DELAI
       IF (DAI .LE. ENDAI) GO TO 5
       DAI=SAI
       ALS=ALS+DELALS
       IF (ALS .LE. ENDALS) GO TO 5
       ALS=SALS
       STOP
       END
```

```
C*********************************************************************C
C              DIFFERENTIAL EQUATION TO BE INTEGRATED                C
C*********************************************************************C
      FUNCTION F(N,V1,V2,V3)
      COMMON /F1/ GA,VE(200),GCM,CCM
      F=(GA*(V1-2.0*V2+V3+VE(N-1)-2.0*VE(N)+VE(N+1))-
     1GCM*V2)/CCM
      RETURN
      END
```

APPENDIX - C

```
C******************************************************************C
C     PROGRAM FOR EFFECT OF WAVEFORMS ON NEURON STIMULATION     C
C******************************************************************C
C       ABBREVIATIONS USED IN THIS PROGRAM ARE AS FOLLOWS :      C
C       GA    :    AXIAL INTERNODAL CONDUCTANCE                  C
C       VE    :    EXTERNAL POTENTIAL                            C
C       VI    :    INTERNAL POTENTIAL                            C
C       GCM   :    NODAL MEMBRANE CONDUCTANCE                    C
C       CCM   :    NODAL CAPACITANCE                             C
C       ALC   :    INTERNODE LENGTH                              C
C       DS    :    AXON DIAMETER (INTERNAL MYELIN DIAMETER)      C
C       EDIST:  -  ELECTRODE DISTANCE                            C
C       FUNC  :    NATURE OF EXCITATION CURRENT                  C
C       EC    :    EXCITATION CURRENT                            C
C       AI    :    MAXIMUM VALUE OF EXCITATION CURRENT           C
C       ALS   :    NODAL GAP WIDTH                               C
C       RHOE  :    RESISTIVITY OF EXTERNAL MEDIUM               C
C       RHOI  :    AXOPLASM RESISTIVITY                          C
C       R(K)  :    ELECTRODE RADIAL DISTANCE                     C
C       AMI   :    MEMBRANE CURRENT                              C
C       GSM   :    MEMBRANE CONDUCTANCE PER UNIT AREA            C
C       CSM   :    MEMBRANE CAPACITANCE PER UNIT AREA            C
C******            EXCITATION NATURE                    ********C
C       PLS   :    PULSE EXCITATION                             C
C       TON   :    ON TIME                                      C
C       TOF   :    OFF TIME                                     C
C       SINE  :    SINUSOIDAL EXCITATION                        C
C       OMEG  :    FREQUENCY OF EXCITATION IN RADIANS PER SECOND C
C       PHI   :    PHASE SHIFT  IN RADIANS                      C
C       RAMP  :    RAMP EXCITATION                              C
C       TRNGL:    TRIANGULAR EXCITATION                         C
C******************************************************************C
C       UNITS FOR                                              C
C                   LENGTH    IS    CENTIMETERS                C
C                   TIME      IS    SECONDS                    C
C                   CURRENT   IS    AMPERES                    C
C******************************************************************C
```

```
        COMMON /F1/ GA,VE(200,200),GCM,CCM
        COMMON /F2/ AI,FUNC,TON,TOF,TOT,NFP,OMEG,PHI
        DIMENSION R(200),V(200,200),AK1(200),AK2(200),AK3(200),
       1AK4(200),AMT(200,200)
C****  INTERACTIVELY ACCEPT THE REQUIRED DATA
        WRITE(5,514)
514     FORMAT(10X,'    ENTER   THE    NUMBER   OF   NODES : '$)
        READ(5,40)NODES
40      FORMAT(I4)
        TYPE 1
1       FORMAT('  ENTER THE STARTING VALUE FOR ALC      '$)
        ACCEPT*,SALC
        ALC=SALC
        TYPE 2
2       FORMAT('  ENTER THE INCREMENT FOR ALC           '$)
        ACCEPT*,DELALC
        TYPE 3
3       FORMAT('  ENTER THE ENDING VALUE FOR ALC        '$)
        ACCEPT*,ENDALC
        TYPE 6
6       FORMAT('  ENTER THE STARTING VALUE FOR DS       '$)
        ACCEPT*,SDS
        DS=SDS
        TYPE 7
7       FORMAT('  ENTER THE INCREMENT FOR DS            '$)
        ACCEPT*,DELDS
        TYPE 8
8       FORMAT('   ENTER THE ENDING VALUE FOR DS        '$)
        ACCEPT*,ENDDS
9       CONTINUE
        TYPE 50
50      FORMAT('  ENTER THE STARTING VALUE FOR EDIST    '$)
        ACCEPT*,SEDIST
        EDIST=SEDIST
        TYPE 51
51      FORMAT('  ENTER THE INCREMENT FOR EDIST         '$)
        ACCEPT*,DEDIST
```

```
        TYPE 52
52      FORMAT('    ENTER THE ENDING VALUE FOR EDIST        '$)
        ACCEPT*,EEDIST
        TYPE 10
10      FORMAT('  ENTER THE STARTING VALUE FOR AI        '$)
        ACCEPT*,SAI
        DAI=SAI
        TYPE 11
11      FORMAT('  ENTER THE INCREMENT FOR AI              '$)
        ACCEPT*,DELAI
        TYPE 12
12      FORMAT('    ENTER THE ENDING VALUE FOR AI         !$)
        ACCEPT*,ENDAI
        TYPE 13
13      FORMAT('  ENTER THE STARTING VALUE FOR ALS        ($)
        ACCEPT*,SALS
        ALS=SALS
        TYPE 14
14      FORMAT('  ENTER THE INCREMENT FOR ALS             ($)
        ACCEPT*,DELALS
        TYPE 15
15      FORMAT('    ENTER THE ENDING VALUE FOR ALS        ('$)
        ACCEPT*,ENDALS
        TYPE 16
16      FORMAT('    ENTER THE FUNCTION TYPE
        1(PLS,SINE,RAMP,TRNGL):'$)
        ACCEPT17,FUNC
17      FORMAT(A5)
        TYPE 19,FUNC
        PRINT 19,FUNC
19      FORMAT(5X,'   YOU HAVE CHOSEN  :',A5)
        IF (FUNC .EQ. 'PLS') GO TO 22
C****   READ THE VALUE OF ON TIME AND OFF TIME FOR PULSE EXCITATION
        GO TO 24
22      TYPE 26
        ACCEPT*,TON
        TYPE 27
```

```
          ACCEPT*,TOF
          TOT=TON+TOF
          NFP=100.E-6/TOT
          TYPE 28,TON,TOF
          PRINT 28,TON,TOF
24        CONTINUE
26        FORMAT('     ENTER THE ON TIME  : ')      /
27        FORMAT('     ENTER THE OFF TIME : ' )
28        FORMAT('      ON TIME  :',F10.5,'   OFF   TIME  :',F10.5)
          IF (FUNC .EQ. 'SINE') GO TO 30
C****  READ THE VALUE OF OMEGA AND PHASE SHIFT FOR
C****  SINUSOIDAL EXCITATION
          GO TO 37
30        TYPE 31
31        FORMAT('     ENTER THE OMEGA-ZERO   AND   PHI  : ')
          ACCEPT*,OMEG,PHI
          TYPE 33,OMEG,PHI
          PRINT 33,OMEG,PHI
33        FORMAT('    OMEGA ZERO  :',F10.5,'  PHI  :',F10.5)
37        CONTINUE
          PI=3.1415926
          RHOI=110.0
          GSM=30.4E-3
          CSM=2.0E-6
          RHOE=300.0
          PI4=4.0*PI
5         PRINT 18,ALC,EDIST
          TYPE 18,ALC,EDIST
          AI=-DAI
          PRINT 20,AI,DS,ALS
          TYPE 20,AI,DS,ALS
          TYPE 3434
3434      FORMAT(5X,'ENTER THE NAME OF THE FILE FOR VOLTAGE : ')
          ACCEPT3435,VOLT
          TYPE 3447,VOLT
          PRINT 3447,VOLT
3435      FORMAT(A5)
```

```
        TYPE 3436
3436    FORMAT(5X,'ENTER THE NAME OF THE FILE FOR CURRENT :')
        ACCEPT3437,CURNT
        TYPE 3447,CURNT
        PRINT 3447,CURNT
3437    FORMAT(A5)
3447    FORMAT(2X,A5)
        OPEN(UNIT=1,DEVICE='DSK',FILE=VOLT)
        OPEN(UNIT=2,DEVICE='DSK',FILE=CURNT)
18      FORMAT(10X,'INTERNODE LENGTH : ',F6.3,'CM',3X,'ELECTRODE
        1  DISTANCE : ',F6.3,'CM')
20      FORMAT(5X,'ELECTRODE CURRENT : ',E14.6,'A',3X,
        1,'AXON DIAMETER : ',E14.6,'CM',/20X,'NODAL GAP WIDTH : ',
        2E14.6,'CM')
        H=1.0E-6
        GA=PI*DS*DS/(4.0*RHOI*ALC)
        PIDALS=PI*DS*ALS
        GCM=GSM*PIDALS
        CCM=CSM*PIDALS
        IRSTRT=-NODES/2
C****   CALCULATE THE RADIAL DISTANCE OF ELECTRODE AND
C****   EXTERNAL VOLTAGE AT NODES
        DO 100 K=1,NODES
        ALTOT=ABS(ALC*IRSTRT)
        R(K)=SQRT(ALTOT*ALTOT+EDIST*EDIST)
        DO 90 IT=1,100
        T=(IT-1)*1.0E-6
90      VE(K,IT)=RHOE*FC(T)/(PI4*R(K))
        IRSTRT=IRSTRT+1
100     CONTINUE
C****   ENFORCE THE INITIAL CONDITION
        DO 150 I=1,NODES
        V(I,1)=0.0
150     CONTINUE
C****   EVALUATE THE RUNGE-KUTTA COEFFICIENTS
        DO 600 J=1,100
        IT=J
```

```
        DO 200 K=2,NODES-1
        I=K
        AK1(I)=H*F(IT,I,V(I-1,IT),V(I,IT),V(I+1,IT))
200     CONTINUE
        DO 300 K=2,NODES-1
        I=K
        AK2(I)=H*F(IT,I,V(I-1,IT)+AK1(I-1)/2.0,V(I,IT)+
       1AK1(I)/2.0,V(I+1,IT)+AK1(I+1)/2.0)
300     CONTINUE
        DO 400 K=2,NODES-1
        I=K
        AK3(I)=H*F(IT,I,V(I-1,IT)+AK2(I-1)/2.0,V(I,IT)+
       1AK2(I)/2.0,V(I+1,IT)+AK2(I+1)/2.0)
400     CONTINUE
        DO 500 K=2,NODES-1
        I=K
        AK4(I)=H*F(IT,I,V(I-1,IT)+AK3(I-1),V(I,IT)+AK3(I),
       1V(I+1,IT)+AK3(I+1))
500     CONTINUE
C****   CALCULATE THE MEMBRANE VOLTAGE
        DO 700 I=2,NODES-1
        V(I,J+1)=V(I,J)+(AK1(I)+2.0*(AK2(I)+AK3(I))+AK4(I))/6.0
700     CONTINUE
600     CONTINUE
C****   CALCULATE THE MEMBRANE CURRENT
        DO 720 J=1,100
        DO 720 I=2,NODES-1
        AMT(I,J)=GA*(V(I-1,J)-2.0*V(I,J)+V(I+1,J)+VE(I-1,J)-
       12.0*VE(I,J)+VE(I+1,J))
720     CONTINUE
        DO 750 I=1,NODES
        DO 750 J=1,100
        V(I,J)=1000.*V(I,J)
750     CONTINUE
        PRINT 910
        PRINT 900
        PRINT 910
```

```
          PRINT 930
          PRINT 920
          PRINT 940
          PRINT 910
          INCRMT=NODES/2+1
          DO 800 I=1,NODES
          NODE=I-INCRMT
          PRINT820,NODE,(V(I,J),J=1,100,10)
   800    CONTINUE
          DO 845 J=1,100,2
          JJ=J-1
          WRITE(1,676)JJ,(V(I,J),I=2,INCRMT+1)
   676    FORMAT(I3,7F10.3)
   845    CONTINUE
          PRINT 910
          PRINT 910
          PRINT 1000
          PRINT 910
          PRINT 930
          PRINT 970
          PRINT 940
          PRINT 910
          DO 1050 I=1,NODES
          DO 1050 J=1,100
          AMI(I,J)=1.0E+12*AMI(I,J)
  1050    CONTINUE
          DO 1200 I=1,NODES
          NODE=I-INCRMT
          PRINT820,NODE,(AMI(I,J),J=1,100,10)
  1200    CONTINUE
          PRINT 910
          DO 1300 J=1,100,2
          JJ=J-1
          WRITE(2,1320) JJ,(AMI(I,J),I=2,INCRMT+1)
  1320    FORMAT(I3,7F10.2)
  1300    CONTINUE
          CLOSE(UNIT=1)
```

```
      CLOSE(UNIT=2)
820   FORMAT(1X,I4,11F10.3)
900   FORMAT(30X,'MEMBRANE  VOLTAGE  IN  MILLI-VOLTS ')
910   FORMAT(' ------------------------------------------------------
     1----------------------------------------------------------')
920   FORMAT('    V  -------------------------------------------------
     1----------------------------------------------------------')
930   FORMAT('                                        TIME
     1                 MICROSECONDS      ')
940   FORMAT('              0         10         20         30         40
     1    50         60         70         80         90        100  ')
970   FORMAT('    I  -------------------------------------------------
     1----------------------------------------------------------')
1000  FORMAT(30X,'MEMBRANE  CURRENT  IN  PICO-AMPERES ')
      ALC=ALC+DELALC
      IF (ALC .LE. ENDALC) GO TO 5
      ALC=SALC
      DS=DS+DELDS
      IF (DS .LE. ENDDS) GO TO 5
      DS=SDS
      EDIST=EDIST+DEDIST
      IF (EDIST .LE. EEDIST ) GO TO 5
      EDIST=SEDIST
      DAI=DAI+DELAI
      IF (DAI .LE. ENDAI) GO TO 5
      DAI=SAI
      ALS=ALS+DELALS
      IF (ALS .LE. ENDALS) GO TO 5
      ALS=SALS
      STOP
      END
```

```
C*********************************************************************C
C                DIFFERENTIAL EQUATION TO BE INTEGRATED              C
C*********************************************************************C
      FUNCTION F(IT,N,V1,V2,V3)
      COMMON /F1/ GA,VE(200,200),GCM,CCM
      F=(GA*(V1-2.0*V2+V3+VE(N-1,IT)-2.0*VE(N,IT)+VE(N+1,IT))-
     1GCM*V2)/CCM
      RETURN
      END
```

```
C**************************************************************C
C          FUNCTION TO EVALUATE THE CURRENT AMPLITUDES        C
C**************************************************************C
           FUNCTION EC(T)
           COMMON /F2/ AI,FUNC,TON,TOF,TOT,NFP,OMEG,PHI
           IF (FUNC .NE. 'TRNGL') GO TO 100
           IF (T .LE. 50.0E-6) GO TO 50
           EC=-(AI*T/50.0E-6)+2.0*AI
           RETURN
50         EC=AI*T/50.0E-6
           RETURN
100        IF(FUNC .NE. 'RAMP') GO TO 200
           EC=AI*T/100.E-6
           RETURN
200        IF (FUNC .NE. 'SINE') GO TO 300
           EC=(AI/2.0)*(1.+SIN(OMEG*T+PHI))
           RETURN
300        IF (FUNC .NE. 'PLS') GO TO 400
           DO 320 IN=1,NFP
           IF((T-TOT) .LT. 0.0) GO TO 330
320        T=T-TOT
330        IF (T.LE. TON) GO TO 340
           EC=0.0
           RETURN
340        EC=AI
           RETURN
400        TYPE 450
450        FORMAT(5X,' FUNCTION DOES NOT MATCH ANY
          1OF THE FUNCTIONS PRESENT')
           RETURN
           END
```

REFERENCES

[1]   John R. Cameron and James G.S. : Medical Physics, Wiley Inter Science, John Wiley and Sons, 1978.

[2]   Erol Baser, Biophysical and Physiological Systems Analysis; Addition Wesley Publishing Company.

[3]   Eroch Callaway M.D.; Brain electrical potentials and individual physiological differences; Grume and stratton, A subsidiary of Harcourt Brace Jovanovich Publishers.

[4]   Donald M.Pace et al., Physiology and Anatomy ; The University of Nebraske (N.Y.).

[5]   Sydney Ochs; Elements of Neurophysiology ; John Wiley and Sons, Inc., (N.Y.) 1965.

[6]   Cyril A.Keele and Eric Neil ; Samson Wrights applied physiology ; Oxford University Press, 1971.

[7]   Charles F.Stevens ; Neurophysiology- A Primer ; John Wiley and Sons, Inc., (N.Y.).

[8]   Herman P. Schwan ; Biological Engineering : McGraw Hill Book Company, (N.Y.) 1969.

[9]   SID DEUTSCH, Models of Nervous System ; John Wiley and Sons, Inc., (N.Y.), 1967.

[10]   D.J.Dewhurst, An introduction to Biomedical Instrument- ation ; McGraw Hill Book Company (N.Y.).

[11]   E.Babsky et al. Human physiology Vol. I and Vol. II, MIR Publishers. (Mascow), 1982.

[12]   E.J.CASEY ; Biophysics ; concepts and Mechanisms :
         Van Nostrand and Reinhold Company, (N.Y.) 1962.

[13]   Katz Bernard, Nerve, muscle and Synapse; John Wiley
         and Sons, Inc., (N.Y.) 1966.

[14]   J.G.Graeme, et al., Operational Amplifiers, Design
         and Application; McGraw Hill Kogakusha, Ltd., (Tokyo)
         1971.

[15]   R.F.Coughlin ; et al., Operational Amplifiers and
         Linear integrated Circuits (3rd edition), PHI Pvt.,
         Ltd., (New Delhi) 1987.

[16]   Darold Wobschall, Circuit Design for electronic
         Instrumentation (2nd edition) ; McGraw Hill Book
         Company (N.Y.).

[17]   Lawrence G.Cowls ; Transistor circuit Design; McGraw
         Hill Book Company ; (N.Y.).

[18]   E.R.Hnatek ; Applications of Linear Integrated Circuits;
         DCA Reliability Laboratory Inc., John Wiley and Sons,
         (N.Y.) 1975.

[19]   J.Millman and C.Halkias ; Integrated Electronics;
         Analog and Digital Circuits and Systems; McGraw Hill,
         International student edition ; 1981.

[20]   J.Millaman and H.Tanb ; Pube, digital and switching
         waveforms ; McGraw Hill Book Company, (N.Y.) 1965.

[21]   M.K.Jain, et al.; Numerical Methods for Scientific
         and Engineering Computation; Wiley Eastern Limited,
         1985.

[22]   Alan R.Miller; Fortran Programming for Scientists and
         Engineers ; Sybex (Berkley) 1982.

[23]   S.C.Saxena et al., An electronic Model of Neuron;
         Journal of IE(I), Vol. 58, Pt - ET2, December 1977.

[24]   A.L.Hodgkin and A.F.Huxley and B.Katz ; J. Physiology;
         116-428 (1952), A.L. Hodgkin and A.F.Huxley; J.
         Physiology; 116 - 449, 473, 497 (1952).

[25]   S.C.Saxena ; Electronic Model of Neuron Processes,
         including feedback through Renshaw cell, Journal of
         IE(I), Vol. 59, Part I, 3, IDGE, June 1979.

[26]   Guy Roy ; A Simple Electronic Analog of Squid Axon
         Membrane ; IEEE Transactions on Biomedical THE
         NEUROFET Engineering, pp. 60 - 63, January 1972.

[27]   D.S.Chitore; A.K.Garg ; An electronic representation
         of neural transmission processes ; Journal of IE(I),
         ET, Vol. 67, February, 1987.

[28]   Marry Ann C.Maher et al.; Implementing neural archite-
         cture using analog VLSI circuits, IEEE Transactions
         on Circuits and Systems, Vol. 36, No. 5, May, 1989.

[29]   D.A.Teicher and D.R.McNeal; Comparison of a Dynamic
         and Steady state Model for Determing Nerve Fiber
         Threshold; IEEE Transactions on Biomedical Engineering;
         Vol. BME-25, No. 1, pp 105-107, January 1978.

[30]   L.A.Geddes and J.D.Bourland ; The Strength-Duration
         curve, IEEE Transactions on Biomedical Engineering,
         Vol. BME - 32, No. 6, pp. 458 - 459, June 1985.

[31]   D.Dean, P.D.Lawrence; Optimization of Neural Stimuli,
         Based upon a variable Threshold Potential, IEEE
         Transactions on Biomedical Engineering, Vol. BME-32,
         No. 1, January 1985.

[32]   Nelson G.Publicover ; Single Microelectrode Analysis of
         Electrically Coupled Networks; IEEE Transactions on
         Biomedical Engineering Vol. BME-32, No. 7 July 1985.

[33]   Robert Plonsey ; The active Fiber in a volume conductor;
         IEEE Transactions on Biomedical Engineering, Vol. BME-
         21, No. 5, September 1974.

[34]   E.W.Pottala   et al. A Dendritic Compartmental Model
         Neuron, IEEE Transactions on Biomedical Engineering,
         Vol. BME-20, No. 2 March 1973.

[35]   J.K.Choudhury et al., An Electronic Model for Neural
         Transmission of Information, J. of IE(I) UDC :
         621 - 38,: 681.14, IDGE Vol. 57, September 1976.

[36]   FWU TARNG DUN; The length and Diameter of the Node
         of Ranvier; IEEE Transactions on Biomedical Engineering
         Vol. BME-17, No. 1, January, 1970.

[37]   H.D.Crane, Neuristor, - A Novel Device and System
         Concept. Proceedings of the IRE; October 1962.

[38] Willium H. Brockman ; A Simple Electronic Neuron Model Incorporating Both Active and Passive Responses; IEEE Transactions on Biomedical Engineering, Vol. BME-26, No. 11, November 1979.

[39] A.S.French and R.B.Stein; A Flexible Neural Analog using Integrated Circuits; IEEE Transactions on Biomedical Engineering, Vol. BME-17, No. 3, July 1970.

[40] A.J.Thexton; A modification of the French and Stein Neural Analog; IEEE Transactions on Biomedical Engineering July 1974.

[41] Donal R. McNeal; Analysis of a Model for Excitation of Myclinated Nerve ; IEEE Transactions on Biomedical Engineering Vol. BME-23, No. 4, July 1976.

[42] Frank Rattay ; Analysis of Models for External Stimulation of Axons ; IEEE Transactions on Biomedical Engineering, Vol. BME - 33, No. 10, October, 1986.

[43] Michael J.Rosen; A Theoretical Neral Integrator; IEEE Transactions on Biomedical Engineering, Vol. BME - 19, No. 5, September 1972.

[44] Charles F.Stovens ; Synaptic Physiology; IEEE Transaction on Biomedical Engineering, Vol. BME - 56, No. 6, June 1968.

[45] R.Hallgren ; Analog Model of a Passive Myclinated Nerve Fiber ; IEEE Transactions on Biomedical Engineering, November 1973.

[46]   A.J.Cote; 'A Neuristor Prototype' Proc. IRE, Vol. 49; pp. 1430 - 1431, September 1961.

[47]   A.J.Cote; Neuristor propogation in Long-tunnel diodes Proc. IEEE, Vol. 53, pp. 164 - 165, February 1965.

[48]   Edwin R.Lewis; Using electronic circuits to model simple Neuroelectric interactions, IEEE Transactions on Biomedical Engineering; Vol. 56, No. 6, June 1968.

[49]   J.Nagumo et al.; An active pulse transmission line simulating Nerve Axon; Proc. IRE, October 1962.

[50]   R.H.Mattson; 'A Neuristor realization' Proc. IRE, Vol. 52, pp 618-619, May 1964.

[51]   W.W.L. Glenn, et al., Electrical Stimulation of excitable tissue by radio-frequency transmission 'Ann. Surg., Vol. 160, pp. 338, 1964.

[52]   R.L.Waters et al.; Experimental correction of footdrop by electrical stimulation of the peroneal nerve, J. Bone Joint Surg., Vol. 57A pp. 1047, 1975.

[53]   R.Fity Hugh, ''Computation of Saltatory Conduction'' Biophys. J., Vol. 2, pp, 11, 1962.

[54]   W.F.Pickard, On the propogation of the nervous impulse down medullated and unmedullated fiber, J. Theoret. Biol., Vo. 11, pp. 30, 1966.

[55]   B.Frankenheauser and A.F.Huxley. The action potential in the myclinated nerve fiber of Xenopus Leavis, as computed on the basis of voltage clamp data, J. Physiol. (London), Vol. 171, p. 302, 1964.

[56] J.J.Lussier and W.A.H.Rushton, 'The excitability of a single fiber in a nerve trunk' J. Physiol. (London), Vol. 117, pp. 87, 1952.

[57] S.L.BeMent and J.B.Ranck Jr., 'A model for electrical Stimulation of central myclinated fibers with mono-polar electrode' Expl. Neurol. Vol. 24, pp. 171, 1969.

[58] L.Goldman and J.S.Albus, Computation of impulse conduction in myclinated fibers' : Theoretical basis of the velocity diameter relation Biophys. J., Vol. 8, pp. 596, 1968.

[59] C.Abjug et al., 'Cervical branching of lumbar vestibu-lospinal axons' J. Physiol (London), Vol. 243, pp. 499, 1974.

[60] Charles Nicholson, Theoeretical analysis of field potentials in anisotropic ensembles of Neuronal elements; IEEE Trans. on Biomedical Engineering, Vol. BME - 20; No. 4, July 1973.

[61] A.T.Barker et al., Modelling of an active nerve fiber in a finite volume conductor, and it's application to the calculation of surface action potentials; IEEE Trans. on Biomedical Engineering, Vol. BME - 26, No. 1, January 1979.

[62] J.Patrick Reilly et al, Sensory effect of transient electrical stimulation - Evaluation with a neuro-electric model; IEEE Trans. on Biomedical Engineering, Vol. BME - 12, No. 12, December 1985.

[63]   Edwin R.Lewis; The locus concept and it's application to Neural Analogs, IEEE Transactions on Biomedical Engineering, October 1963.

*****

*****
***
*